

Exploring *Monacha cantiana* (Montagu, 1803) phylogeography: cryptic lineages and new insights into the origin of the English populations (Eupulmonata, Stylommatophora, Hygromiidae)

Joanna R. Pieńkowska¹, Giuseppe Manganelli², Folco Giusti²,
Alessandro Hallgass², Andrzej Lesicki¹

1 Department of Cell Biology, Institute of Experimental Biology, Faculty of Biology, Adam Mickiewicz University in Poznań; Umultowska 89, 61-614 Poznań, Poland **2** Dipartimento di Scienze Fisiche, della Terra e dell'Ambiente, Università di Siena, Via Mattioli 4, 53100 Siena, Italy

Corresponding author: Andrzej Lesicki (alesicki@amu.edu.pl)

Academic editor: E. Neubert | Received 10 February 2018 | Accepted 23 April 2018 | Published 6 June 2018

<http://zoobank.org/E5CAE122-33E5-436A-AA9B-B321D56A4D58>

Citation: Pieńkowska JR, Manganelli G, Giusti F, Hallgass A, Lesicki A (2018) Exploring *Monacha cantiana* (Montagu, 1803) phylogeography: cryptic lineages and new insights into the origin of the English populations (Eupulmonata, Stylommatophora, Hygromiidae). ZooKeys 765: 1–41. <https://doi.org/10.3897/zookeys.765.24386>

Abstract

Molecular analysis of nucleotide sequences of mitochondrial cytochrome oxidase subunit 1 (COI) and 16S ribosomal DNA (16SrDNA) as well as nuclear histone 3 (H3) and internal transcribed spacer 2 of rDNA (ITS2) gene fragments together with morphological analysis of shell and genitalia features showed that English, French and Italian populations usually assigned to *Monacha cantiana* consist of four distinct lineages (CAN-1, CAN-2, CAN-3, CAN-4). One of these lineages (CAN-1) included most of the UK (five sites) and Italian (five sites) populations examined. Three other lineages represented populations from two sites in northern Italy (CAN-2), three sites in northern Italy and Austria (CAN-3), and two sites in south-eastern France (CAN-4). The taxonomic and nomenclatural setting is only currently available for lineages CAN-1 and CAN-4; a definitive frame for the other two requires much more research. The lineage CAN-1 corresponds to the true *M. cantiana* (Montagu, 1803) because it is the only one that includes topotypical English populations. The relationships and genetic distances support the hypothesis of the Italian origin of this lineage which was probably introduced to England by the Romans. The lineage CAN-4 is attributed to *M. cemelelea* (Risso, 1826), for which a neotype has been designated and deposited. Its diagnostic sequences of COI, 16SrDNA, H3 and ITS2 genes have also been deposited

in GenBank. Molecular and morphological (shell and genitalia) features showed that *M. parumcincta* (Rossmässler, 1834) is a distinct taxon from the *M. cantiana* lineages.

Keywords

16SrDNA, COI, H3, ITS2, molecular features, reproductive system, Roman origin, shell, structure, species distribution

Introduction

Monacha is a diverse genus of the trochuline hygromiids widespread in the western Palaearctic from western Europe to north Africa, Iran, and Arabia. It includes a large number of nominal species and shows its highest diversity in the eastern sector of southern Europe and in Turkey (Hausdorf 2000a, 2000b, Welter-Schultes 2012, Neiber and Hausdorf 2017).

Monacha cantiana (Montagu, 1803) is one of the westernmost species. It is a medium-sized land snail living among grass in open habitats such as grasslands, pastures, cultivated and uncultivated fields or forest edges and clearings. Its geographical distribution, probably southern European in origin, was partly shaped by anthropochorous dispersal which helped the species to reach north-western Europe. For example, in the British Isles it is considered to have been introduced and this hypothesis is supported by the absence of a Holocene fossil record in England older than the third century AD (Kerney et al. 1964, Kerney 1970, 1999, Evans 1972).

The aim of the present research was: (1) to study molecular and morphological (shell and genitalia) variation of the species in order to explore its phylogeography and detect any geographical patterns; (2) to investigate relationships between molecular and morphological variability in order to characterise clades recovered by molecular study; (3) to test the hypothesis that the English populations originated from introduced propagules.

Material and methods

Taxonomic sample

Our analysis considered a number of populations of *Monacha cantiana*, mainly from Italy and England, that represent its gross morphological, geographical, and ecological variability. Some sequences deposited in GenBank were also considered for the molecular analysis. One population from the type locality of *Theba cemelelea* Risso, 1826 a taxon regarded as a junior synonym, subspecies or species, slightly distinct from *M. cantiana*, was also included. For comparison, two other *Monacha* species were used in the molecular analysis: *Monacha cartusiana* (Müller, 1774) and *M. parumcincta* (Rossmässler, 1834). The latter was also used in the morphological analysis. While

M. cartusiana is a well-established taxon, the taxonomic and nomenclatural status of *M. parumcincta* is still disputed, e.g. conspecificity of Italian and Balkan populations, authorship to Rossmässler, 1834 or Menke, 1828 (see Forcart 1965, Manganeli et al. 1995, Welter-Schultes 2012).

Material examined

Material examined is listed as follows, when possible: geographic coordinates of locality, locality (country, region, site, municipality and province), collector(s), date, number of specimens and collection in which material is kept in parenthesis (Table 1). Collection acronyms: FGC (F. Giusti collection, Dipartimento di Scienze Fisiche, della Terra e dell'Ambiente, Università di Siena, Italy); DCBC (Department of Cell Biology Collection, Adam Mickiewicz University, Poznań, Poland).

DNA extraction, amplification, and sequencing

Small foot tissue fragments of alcohol-preserved snails were used for total DNA extraction with Tissue Genomic DNA extraction Mini Kits (Genoplast) according to the manufacturer's instructions. The purified total DNA was used as template for amplification by polymerase chain reaction (PCR) of partial sequences of the following genes: mitochondrial cytochrome *c* oxidase subunit I (COI), 16S ribosomal DNA (16SrDNA), nuclear histone H3 (H3) and fragment enclosing partial sequence of 5.8SrDNA and complete sequence of internal transcribed spacer 2 of ribosomal DNA (ITS2). A 5'-end fragment of COI (often called "barcode sequence") was amplified and sequenced using two degenerate primers F01-R04 (F01 5'-CATTTTCHACTAAY-CATAARGATATTGG-3' and R04 5'-TATAAACYTCDGGATGNCCAAAAA-3'; Dabert et al. 2010). The 16SrRNA gene was amplified and sequenced using primer pair 5'-CGATTTGAACTCAGATCA-3' (LR-J-12887, Simon et al. 1994) and 5'-GT-GCAAAGGTAGCATAATCA-3' (Gantenbein et al. 1999). The DNA fragment coding H3 was amplified and sequenced using primer pair H3F-H3R (H3F 5'-ATG-GCTCGTACCAAGCAGACVGC-3' and H3R 5'-ATATCCTTRGGCATRATRGT-GAC-3'; Colgan et al. 1998). The fragment enclosing partial sequence of 5.8SrDNA and complete sequence of ITS2 was obtained for analyses using primers NEWS2 (5'-TGTGTCGATGAAGAACGCAG-3') and ITS2-RIXO (5'-TTCTATGCT-TAAATTCAGGGG-3') (Almeyda-Artigas et al. 2000).

The amplified COI fragments consisted of 650 base pairs (bp). Polymerase chain reactions were performed in a volume of 10 µl according to the modified protocol prepared by the Biodiversity Institute of Ontario for the Consortium for the Barcode of Life (http://barcoding.si.edu/PDF/Protocols_for_High_Volume_DNA_Barcode_Analysis.pdf). Reactions were carried out under the following thermal profile: 1 min at 94 °C followed by 42 cycles of 40 s at 94 °C, 40 s at 53 °C, 1 min at 72 °C,

Table 1. List of localities of the specimens of *Monacha cantiana* (CAN-1 to CAN-4), *M. parumincta* and *M. cartisiana* used for molecular and morphological (SH shell, AN genitalia) research.

No.	Localities		collector / date / no. of specimens (collection)	Clade	Revised taxonomy	COI		16SrdDNA			H3		ITS2		PCA and RDA	Figs.			
	coordinates	country and site				new haplotype	no. sps	GenBank #	new haplotype	no. sps	GenBank #	new common sequence	no. sps	GenBank #			new common sequence	no. sps	GenBank #
1.	53°31'29"N 01°27'54"W	United Kingdom, Barrow near Barnsley	R.A.D. Cameron / 10.2011 / 5 (FGC 40329) (Pienkowska et al. 2015)	CAN-1	<i>M. cartisiana</i>	UK-COI 1 4	4	KM247375 MG208884 MG208885 MG208886 MG208887	UK-16S 1 5	5	MG208966 MG208967 MG208968 MG208969 MG208970	UK-H3 1 3	3	MG209031 MG209032 MG209033	UK-ITS2 2 3	3	MH137963 MH137964 MH137965	SH, AN	20, 22- 23, 25
2.	51°30'30"N 00°15'38"W	United Kingdom, East Acton near London	M. Procków / 07.06.2010 / 3 (DCBC & FGC 42965)	CAN-1	<i>M. cartisiana</i>	UK-COI 1 3	3	MG208888 MG208889 MG208890	UK-16S 1 3	3	MG208961 MG208962 MG208963	UK-H3 2 1	1	MG209034				SH	21, 24
3.	Not available	United Kingdom, Cambridge (old material)	F. Giusti / 1981 / 3 (FGC 23773)	CAN-1	<i>M. cartisiana</i>	UK-COI 1 UK-COI 3 1	2	MG208891 MG208892	UK-16S 1 2	2	MG208972 MG208973 MG208974	UK-H3 2 1	1	MG209035	UK-ITS2 2 1	1	MH137966 MH137967	SH, AN	
4.	53°25'04.2"N 01°24'00.5"W	United Kingdom, Rotherham	R.A.D. Cameron / 07.2015 / 7 (DCBC)	CAN-1	<i>M. cartisiana</i>	UK-COI 1 UK-COI 4 1	2	MG208883 MG208893	UK-16S 1 2	2	MG208960 MG208964	UK-H3 3 1	1	MG209035	UK-ITS2 2 2	2	MH137968 MH137969		
5.	53°24'49.1"N 01°24'36.6"W	United Kingdom, Sheffield	R.A.D. Cameron / 07.2015 / 6 (DCBC)	CAN-1	<i>M. cartisiana</i>	UK-COI 1 UK-COI 7 UK-COI 9 UK-COI 10 1	1	MG208896 MG208899 MG208901 MG208902	UK-16S 2 1	1	MG208975	UK-H3 4 1	1	MG209037	UK-ITS2 2 1	1	MH137970 MH137971		

No.	Localities		Clade	Revised taxonomy	COI		16SrdDNA			H3			ITS2			PCA and RDA	Figs.
	coordinates	country and site			collector / date / no. of specimens (collection)	new haplotype	no. sps	GenBank #	new haplotype	no. sps	GenBank #	new common sequence	no. sps	GenBank #	new common sequence		
5.	53°24'49.1"N 01°24'36.6"W	United Kingdom, Sheffield	CAN-1	<i>M. cantiana</i>	UK-COI 11 UK-COI 12	1 1	MG208903 MG208904	UK-165 1	1	MG208971	UK-H3 3	1	MG209036	IT-ITS2.4	1	MH137972	SH, AN 9, 26, 28-30
6.	42°28'41.05"N 13°05'09.46"E	Italy, Latium, Gole del Velino, near-Sigillo (Posta, Rieti)	CAN-1	<i>M. cantiana</i>	IT-COI 1 IT-COI 2	4 3	MG208905 MG208906 MG208907 MG208908 MG208910 MG208911 MG208912	IT-16S 1 IT-H3 1 IT-H3 5 IT-H3 3	4 1 1 1	MG208977 MG208979 MG208980 MG208981 MG208978 MG208982 MG208983 MG208984	IT-H3 1 IT-H3 5 IT-H3 3	1 1 1	MG209039 MG209041 MG209042	IT-ITS2.4	1	MH137972	SH, AN 9, 26, 28-30
7.	Not available	Italy, Tuscany, Elba Island, Sant'Illario in Campo (Livorno)	CAN-1	<i>M. cantiana</i>	IT-COI 2	1	MG208913										SH, AN 10
8.	42°02'51.18"N 12°54'19.64"E	Italy, Latium, Valle dell'Aniene (Roccagiovine, Rome)	CAN-1	<i>M. cantiana</i>	IT-COI 3 IT-COI 4 IT-COI 5 IT-COI 6	3 1 1 1	MG208915 MG208916 MG208917 MG208918 MG208919 MG208920	IT-16S 1 IT-16S 1 IT-16S 1 IT-16S 2	3 1 1 1	MG208985 MG208987 MG208989 MG208986 MG208988 MG208995	IT-H3 6 IT-H3 7 IT-H3 8	1 1 1	MG209045 MG209046 MG209047	IT-ITS2.2 IT-ITS2.3 IT-ITS2.4	1 2 1	MH137973 MH137974 MH137975	SH, AN 8
9.	42°43'39.87"N 13°16'01.44"E	Italy, Latium, Valle del Tronto (Accumoli, Rieti)	CAN-1	<i>M. cantiana</i>	IT-COI 1 IT-COI 2 IT-COI 7	1 1 2	MG208909 MG208914 MG208921 MG208922	IT-16S 1 IT-16S 1 IT-16S 1	1 1 2	MG208992 MG208991 MG208990 MG208993	IT-H3 3	2	MG209043 MG209044	IT-ITS2.1 IT-ITS2.2	2 1	MH137976 MH137977	SH, AN 11, 27
10.	42°07'53.39"N 13°01'39.81"E	Italy, Latium, Valle del Turano, near Turania (Rieti)	CAN-1	<i>M. cantiana</i>	IT-COI 7 IT-COI 8	1 1	MG208923 MG208924	IT-16S 1	1	MG208994	IT-H3 4	1	MG209048	IT-ITS2.5	1	MH137978	SH, AN 11, 27

No.	coordinates	Localities		collector / date / no. of specimens (collection)	Clade	Revised taxonomy	COI		16SrdDNA			H3		ITS2			PCA and RDA	Figs.
		country and site	coordinates				new haplotype	no. sps	GenBank #	new haplotype	no. sps	GenBank #	new common sequence	no. sps	GenBank #	new common sequence		
11.	43°22'59.9"N 02°59'00.0"W	Spain, Sopedana, País Vasco		unknown / (SPI64) (Rozkin- <i>et al.</i> 2015; Neiber and Hausdorf 2015)	CAN-1	<i>M. capitata</i>	new haplotype	no. sps	GenBank #	new common sequence	no. sps	GenBank #	new common sequence	no. sps	GenBank #			
12.	45°11'59.85"N 10°58'49.30"E	Italy, Venetum, Sorgà (Verona)		A. Hallgass / 09.2012 / 6 (FGC 42964)	CAN-2	<i>M. capitata</i>	IT-COI 10	3	MG208928	IT-16S 4	4	MG208998	IT-ITS2 6	1	MH137980		12, 36-39	
13.	45°31'28.95"N 10°21'35.75"E	Italy, Lombardy, Rezzato (Brescia)		A. Hallgass / 07.2012 / 3 (FGC 42976)	CAN-2	<i>M. capitata</i>	IT-COI 10	2	MG208931	IT-16S 4	3	MG209002	IT-ITS2 8	1	MH137981	AN	31-35	
14.	43°15'58.76"N 11°28'26.20"E	Italy, Tuscany, Podere Grania (Asciano, Siena)		G. Manganelli & L. Manganelli / 15.10.2000 / (FGC 12960) (Manganelli <i>et al.</i> 2005)	?	<i>M. sp.</i>												
15.	44°22'09.98"N 11°15'11.28"E	Italy, Emilia Romagna, along Fiume Setta, upstream its confluence with Fiume Reno (Sasso Marconi, Bologna)		A. Hallgass / 09.2012 / 3 (FGC 42977)	CAN-3	<i>M. sp.</i>	IT-COI 11	1	MG208933	IT-16S 6	1	MG209007	IT-ITS2 9	1	MH137982	SH, AN	13, 40-42	

No.	Localities		Revised taxonomy	COI		16SrdDNA			H3			ITS2			PCA and RDA	Figs.
	coordinates	country and site		collector / date / no. of specimens (collection)	Clade	no. new haplotype	GenBank #	new haplotype	no. sps	GenBank #	new common sequence	no. sps	GenBank #	new common sequence		
22.	43°54'18.00"N 00°49'13.63"E	Italy, Tuscany, Nievole (Montecatini Terme, Pistoia)	A. Hallgass / 20.10.2013 / 2 (FGC 41562)	PAR	<i>M. parum-cincta</i>	IT-COI 18 1 IT-COI 20 1	MG208949 MG208952	IT-16S 10 IT-16S 11	1 1	MG209020 MG209024	IT-H3 12 2	MG209067 MG209063	IT-ITS2 11 2	MHI137987 MHI137988	AN	
23.	43°30'19.55"N 11°38'54.92"E	Italy, Tuscany, Autostrada A1; rest area near Ponte Romita (Pergine Valdarno, Arezzo)	A. Hallgass / 10.2013 / 6 (FGC 41561)	PAR	<i>M. parum-cincta</i>	IT-COI 19 2 IT-COI 20 1 IT-COI 21 3	MG208950 MG208951 MG208953 MG208956 MG208957 MG208958	IT-16S 12 IT-16S 11 IT-16S 12	2 1 3	MG209028 MG209029 MG209021 MG209025 MG209026 MG209027	IT-H3 12 3 IT-H3 13 1	MG209068 MG209069 MG209065 MG209070	IT-ITS2 11 2 IT-ITS2 13 1	MHI137989 MHI137990 MHI137991	SH	
24.	40°13'25.49"N 15°52'17.07"E	Italy, Basilicata, along the road from Moliterno to Fontana d'Eboli (Moliterno, Potenza)	A. Hallgass / 2012 / 5 (FGC 42962)	PAR	<i>M. parum-cincta</i>	IT-COI 14 2 IT-COI 15 1 IT-COI 16 1 IT-COI 17 1	MG208944 MG208945 MG208946 MG208947 MG208948	IT-16S 8 IT-16S 9 IT-16S 7	2 1 1	MG209017 MG209018 MG209019 MG209016	IT-H3 12 2	MG209061 MG209064	IT-ITS2 10 1	MHI137992	SH, AN	56-59
25.	46°42'10"N 17°14'38"E	Hungary, Kiskalaton, about 30 m from the Zala Canal on the underside of goldenrod leaves in the scrub-field	J.R. Pienkowska / 31.07.2011 / 8 (DCBC) (Pienkowska et al. 2015)		<i>M. car-tusiana</i>		KM247376			KM247391	HU-H3 1 1	MG209072	HU-ITS2 1 1	MHI137993		
26.	45°46'38"N 10°30'12"E	Italy, Brescia, Anfo towards Ponte Caffaro, calcareous rocks at branch towards Tte Casali	B. Hausdorf / 19.08.2009 / 1 (ZMH51710-1594) (Pienkowska et al. 2015, Neiber and Hausdorf 2015)		<i>M. car-tusiana</i>		KM247389 KX507189			KM247397 KX495378						

and finally 5 min at 72 °C. The amplified 16SrDNA fragments were of about 385 positions. The amplification reactions were conducted in a volume of 10 µl according to a previously described procedure (Manganelli et al. 2005). The amplified H3 sequences consisted of 429 bp. PCR reactions (10 µl) were performed according to the procedure described by Colgan et al. (1998). The 585 position-long sequences of regions enclosing 89 positions of 3'-end of 5.8SrDNA and 496 positions of complete sequence of ITS2 were amplified according to procedure described by Almeyda-Artigas et al. (2000).

The PCR products were verified by agarose gel electrophoresis (1% agarose). Prior to sequencing, samples were purified with thermosensitive Exonuclease I and FastAP Alkaline Phosphatase (Fermentas, Thermo Scientific). Finally, the amplified products were sequenced in both directions with BigDye Terminator v3.1 on an ABI Prism 3130XL Analyzer (Applied Biosystems, Foster City, CA, USA) according to the manufacturer's protocols.

Phylogenetic inference

All individual sequences were deposited in GenBank (Table 1). The following COI sequences from GenBank were used: HQ204502 (Duda et al. 2011), KF596907 (Cada-hia et al. 2014), KF986833 (Dahirel et al. 2015), KM247375 (Pieńkowska et al. 2015) and KX507234 (Neiber and Hausdorf 2015) of *M. cantiana*, as well as KM247376, KM247389 (Pieńkowska et al. 2015) and KX507189 (Neiber and Hausdorf 2015) of *M. cartusiana* (as an outgroup). Regarding 16SrDNA, the following sequences from GenBank were used: AY741419 (Manganelli et al. 2005), HQ204543 (Duda et al. 2011), KF596863 (Cada-hia et al. 2014), KJ458539 (Razkin et al. 2015), KM247390 (Pieńkowska et al. 2015) and KX495428 (Neiber and Hausdorf 2015) of *M. cantiana*, AY741418 (Manganelli et al. 2005) of *M. parumcincta* and KM247391, KM247397 (Pieńkowska et al. 2015) and KX49537 (Neiber and Hausdorf 2015) of *M. cartusiana* (as an outgroup). In analysis of H3 relationships the sequence KF596955 deposited in GenBank by Cada-hia et al. (2014) was used.

Sequences were edited by eye using the program BIOEDIT, version 7.0.6 (Hall 1999). The alignments were performed using the CLUSTAL W programme (Thompson et al. 1994) implemented in MEGA 7 (Kumar et al. 2016). The COI sequences and H3 sequences were aligned according to the translated amino acid sequences. The ends of all sequences were trimmed. The lengths of the sequences after cutting were 592 bp for COI, 287 positions for 16SrDNA, 315 bp for H3 and 496 positions for ITS2. The sequences were collapsed to haplotypes (COI and 16SrDNA) and to common sequences (H3 and ITS2) using the programme ALTER (Alignment Transformation EnviRonment) (Glez-Peña et al. 2010). Gaps and ambiguous positions were removed from alignments prior to phylogenetic analysis.

Maximum Likelihood (ML) analyses were performed with MEGA 7. For each alignment file best nucleotide substitution models were specified according to the

Bayesian Information Criterion (BIC): HKY+I for COI sequences (Hasegawa et al. 1985, Kumar et al. 2016), T92+I for 16SrDNA (Tamura 1992, Kumar et al. 2016), TN93+G+I for H3 (Tamura and Nei 1993, Kumar et al. 2016) and JC+G for ITS2 (Jukes and Cantor 1969, Kumar et al. 2016). In parallel, the sequences of COI and 16SrDNA obtained in the present work together with other sequences obtained from GenBank were analysed by the genetic distance Neighbour-Joining method (Saitou and Nei 1987) implemented in MEGA7 (Kumar et al. 2016) using the Kimura two-parameter model (K2P) for pairwise distance calculations (Kimura 1980). Next, mitochondrial sequences of COI and 16SrDNA, and nuclear sequences of H3 and ITS2 were combined and as two data sets subjected to ML analysis. The combined sequences were of length of 879 positions for COI+16SrDNA pair and of 811 positions for H3+ITS2. The specified best nucleotide substitution models for ML analysis according to the Bayesian Information Criterion (BIC) were: HKY+I (Hasegawa et al. 1985, Kumar et al. 2016) for COI+16SrDNA combined sequences and TN93+G+I (Tamura and Nei 1993, Kumar et al. 2016) for H3+ITS2. Finally, sequences of COI, 16SrDNA and H3 were combined for Bayesian inference. Before doing so, uncertain regions were removed from 16SrDNA alignment with the programme GBLOCKS 0.91b (Castresana 2000, Talavera and Castresana 2007) with parameters for relaxed selection of blocks. This procedure shortened alignment of 16SrDNA sequences from 287 to 271 positions. The combined sequences with a total length of 1178 positions (592 COI + 271 16SrDNA + 315 H3) were used to infer group phylogeny by Bayesian analysis conducted with the program MRBAYES 3.1.2 (Ronquist and Huelsenbeck 2003). *Monacha cartusiana* was added as an outgroup species in each analysis. Using JMODELTEST2 (Darriba et al. 2012) according to the Bayesian Information Criterion (BIC), we specified a HKY substitution model for our data set (Hasegawa et al. 1985), assuming a gamma distributed rate variation among sites. Four Monte Carlo Markov chains were run for 1 million generations, sampling every 100 generations (the first 250 000 trees were discarded as 'burn-in'). This gave us a 50% majority rule consensus tree. In parallel, Maximum Likelihood (ML) analysis was performed with MEGA7 (Kumar et al. 2016) and calculated bootstrap values were mapped on the 50% majority rule consensus Bayesian tree.

The haplotype network was inferred with NETWORK 5.0.0.1 to reflect all relationships between COI and 16SrDNA haplotypes. During the analysis, a median-joining calculation implemented in NETWORK 5.0.0.1 was used (Bandelt et al. 1999).

Morphological study

Approximately 70 specimens of five clades (four lineages of the *M. cantiana* group: CAN-1, CAN-2, CAN-3 and CAN-4; one lineage of *M. parumcincta*) were considered for shell variability (see Table 1). Shell variability was analysed randomly, choosing when possible five adult specimens from each population. Thirteen shell variables were measured to the nearest 0.1 mm using ADOBE PHOTOSHOP 7.0.1 on digital im-

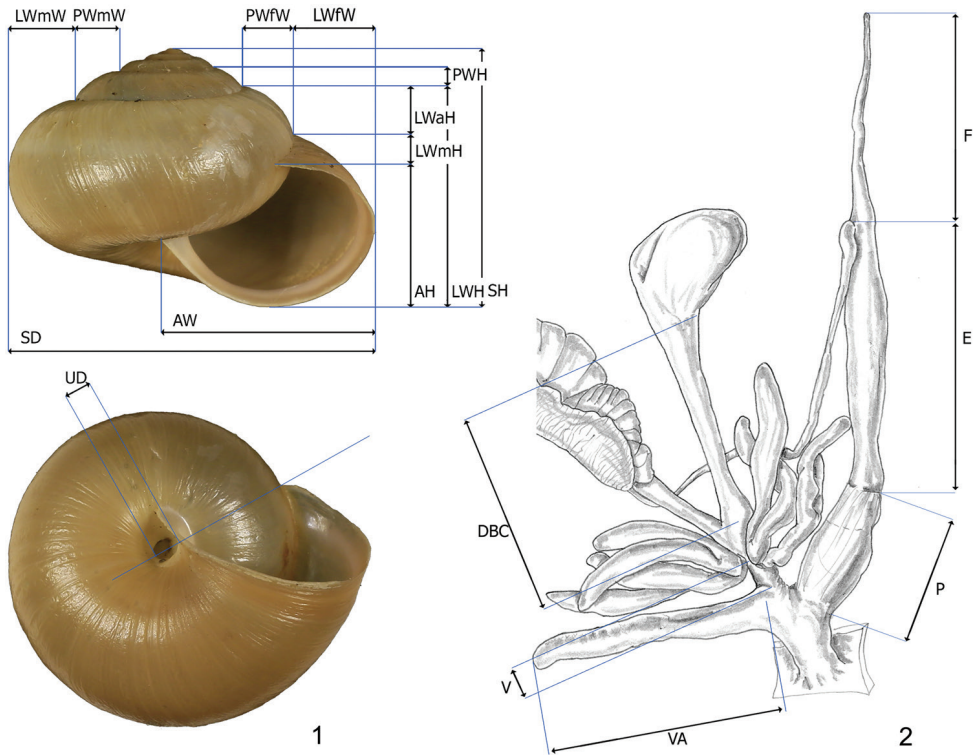
ages of apertural and umbilical standard views taken with a Canon EF 100 mm 1:2.8 L IS USM macro lens mounted on a Canon F6 camera: AH aperture height, AW aperture width, LWfW last whorl final width, LWmW last whorl medial width, LWH last whorl height, LWaH height of adapical sector of last whorl, LWmH height of medial sector of last whorl, PWH penultimate whorl height, PWfW penultimate whorl final width, PWmW penultimate whorl medial width, SD shell diameter, SH shell height, UD umbilicus diameter (Fig. 1).

Approximately 60 specimens of five clades (all lineages of the *M. cantiana* group plus one lineage of *M. parumcincta*) were analysed for anatomical variability (see Table 1). Snail bodies were dissected under the light microscope (Wild M5A or Zeiss SteREO Lumar V12). Anatomical structures were drawn using a Wild camera lucida. Acronyms: BC bursa copulatrix, BW body wall, DBC duct of bursa copulatrix, DG digitiform glands, E epiphallus (from base of flagellum to beginning of penial sheath), F flagellum, FO free oviduct, GA genital atrium, GAR genital atrium retractor, OSD ovispermiduct, P penis, V vagina, VA vaginal appendix (also known as appendicula), VAS vaginal appendix basal sac, VD vas deferens. Six anatomical variables (DBC, E, F, P, V, VA) were measured using a calliper under a light microscope (0.01 mm) (Fig. 2).

Multivariate ordination by Principal Component Analysis (PCA) was performed on shell and genitalia matrices separately in order to determine the degree of correlation between variables and their role in explaining variability. Before PCA, variables were log-transformed to obtain a linear relationship. Since variation in size is the first determinant of biometric variation (e.g., Cadima and Jolliffe 1996, Klingenberg 2016), multivariate morphometrics to distinguish size and shape components by removing isometric effects are nowadays routinely applied in shell biometry studies (Madec et al. 2003, Paquette and Lapointe 2007, Fiorentino et al. 2008, Caruso and Chemello 2009). We therefore performed two PCAs for each data set (shell, genitalia), one on the original matrices and one on the Z-matrices, the latter only consider shape components according to the methods proposed by Cadima and Jolliffe (1996).

Redundancy analysis (RDA; ter Braak 1986) was then applied to the original matrices and Z-matrices in order to detect any multivariate relationships between shell/genitalia variables and the taxonomic assignment. The factors “clade/lineage” were used as constraint factor. An ANOVA-like permutation test for constrained ordination was used to assess the significance (P -value < 0.05) of the constraint for the first two RDA axes. Vegan package (Oksanen et al. 2016) in RStudio 1.0.136 (RStudio Team 2016) was used for processing.

Differences between species for each shell and genitalia characters were assessed through box-plots and descriptive statistics. The significance of differences ($P < 0.01$) was obtained using analysis of variance (ANOVA); where the test proved significant, an adjusted a posteriori pair-wise comparison between pairs of species was performed using Tukey’s honestly significant difference (HSD) test. All variables were log transformed before analysis.



Figures 1–2. **1** Shell dimensional variables considered for statistical analysis. Abbreviations: AH aperture height, AW aperture width, LWfW last whorl final width, LWmW last whorl medial width, LWH last whorl height, LWaH height of adapical sector of last whorl, LWmH height of medial sector of last whorl, PWH penultimate whorl height, PWfW penultimate whorl final width, PWmW penultimate whorl medial width, SD shell diameter, SH shell height, UD umbilicus diameter **2** Genital dimensional variables considered for statistical analysis. Abbreviations: F flagellum, E epiphallus, P penis, DBC duct of bursa copulatrix, V vagina, VA vaginal appendix.

Results

Molecular study

Thirty-nine and 18 haplotypes of COI and 16SrDNA mitochondrial gene fragments, respectively, as well as 23 and 18 common nucleotide sequences of histone H3 and ITS2 nuclear gene fragments, respectively, were established (Table 1). As a result, 77 sequences of COI as MG208883–MG208959, 71 sequences of 16SrDNA as MG208960–MG209030, 42 sequences of H3 as MG209031–MG209072 and 31 sequences of ITS2 as MH137963–MH137993 were deposited in GenBank (see also Table 1). ML tree for combined sequences of COI and 16SrDNA (Fig. 3, Table 2) as well as Bayesian phylogenetic tree for combined sequences of COI+16SrDNA+H3 gene fragments (Fig. 4, Table 2) clustered the received combined sequences in five

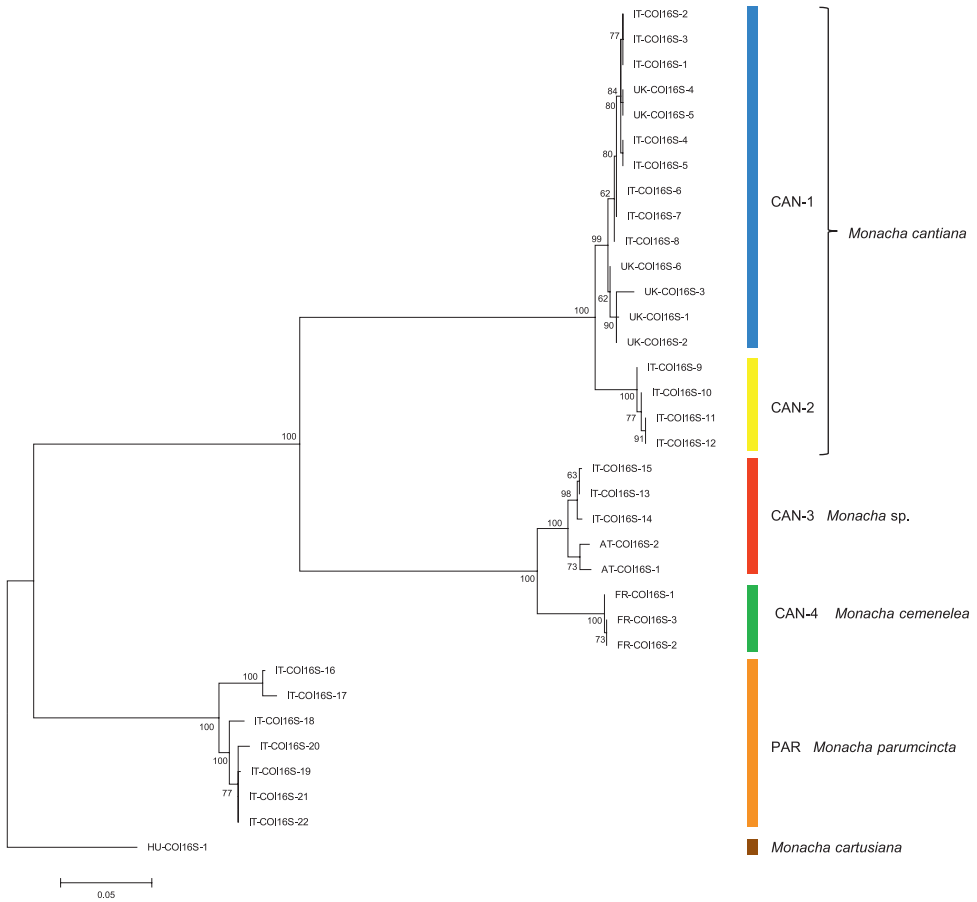


Figure 3. Maximum Likelihood (ML) tree of combined COI and 16SrDNA haplotypes of *Monacha cantiana* group (see: Table 2). Bootstrap support above 50% from maximum likelihood analysis is marked at the nodes. Bootstrap analysis was run with 1000 replicates (Felsenstein 1985). The tree was rooted with *M. cartusiana* combined sequences obtained from GenBank: KM247376 and KM247391.

clearly separate clades. ML tree of combined sequences of nuclear H3 and ITS2 gene fragments (Fig. 5, Table 2) clustered the combined sequences in three clades.

First clade CAN-1 includes 14 combined sequences in particular trees (Figs 3–4). The clade includes haplotypes and common sequences (Table 1) which have been found in specimens from the following UK populations: Barrow near Barnsley, East Acton, Cambridge, Rotherham and Sheffield, together with those found in specimens from Italian populations from Latium (Gole del Velino, Valle dell’Aniene, Valle del Tronto and Valle del Turano), as well as from Elba island (Tuscan Archipelago). It is noteworthy that sequences of haplotypes UK-COI 1 and UK-16S 1 are identical to sequences KM247375 and KM247390 deposited in GenBank for COI and 16SrDNA of *M. cantiana*, respectively (Pieńkowska et al. 2015). It is also important that UK haplotypes UK-COI 2, UK-16S 2 and UK-ITS 2 are identical to Italian IT-COI 2,

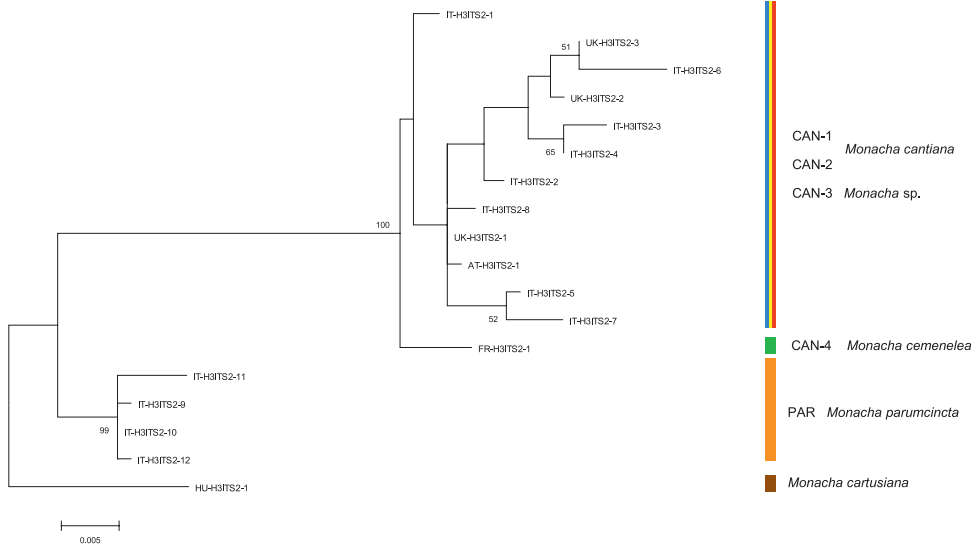


Figure 5. Maximum Likelihood (ML) tree of combined H3 and ITS2 sequences of *Monacha cantiana* group (see: Table 2). Bootstrap support above 50% from maximum likelihood analysis is marked at the nodes. Bootstrap analysis was run with 1000 replicates (Felsenstein 1985). The tree was rooted with *M. cartusiana* combined sequences MG209072 and MH137993.

This CAN-2 clade is not separated from CAN-1 and CAN-3 on the tree of combined nuclear gene sequences (Fig. 5).

Clade CAN-3 is composed of five combined sequences both in COI+16SrDNA (Fig. 3) and COI+16SrDNA+H3 (Fig. 4) trees. It is also not separated in the tree of combined sequences of nuclear H3+ITS2 gene fragments (Fig. 5). The sequences, i.e., COI, 16SrDNA, H3 and ITS2 were from specimens either from Breitenlee in Austria (in Figs 3–5, and Table 1 marked as AT-) or from northern Italy (near Bologna, marked IT-). Sequences deposited in GenBank by Duda et al. (2011), Kruckenhauser et al. (2014) (COI HQ204502, 16SrDNA HQ204543) and by Cadahia et al. (2014) (COI KF596907, 16SrDNA KF596863, H3 KF596955) for *M. cantiana* from the Carnic Alps, Friuli Venezia Giulia, also belong to the CAN-3 lineage. K2P genetic distances of haplotypes within clade CAN-3 varied in a small range (Table 3).

Clade CAN-4 (Figs 3–5) includes three COI+16SrDNA, one H3+ITS2 and three COI+16SrDNA+H3 combined sequences. All were from specimens of a French population in the Maritime Alps near Nice (Sainte Thecle, Table 1). Again K2P genetic distances in this population were small (Table 3). COI sequence KF986833 deposited in GenBank by Dahirel et al. (2015) for *M. cantiana* from Monts d’Ardèche Natural Regional Park near Jaujac (S France) seems to belong to the same clade.

The fifth clade PAR was composed of sequences from specimens identified as *M. parumcincta*. Eight COI and six 16SrDNA haplotypes, as well as two H3 and four ITS2 common sequences were recognised among specimens from four populations from central and southern Italy (Table 1). K2P genetic distances within this clade were larger than

Table 2. Combined Sequences of the following gene sequences: COI+16SrdDNA and H3+ITS2 for ML analysis and of COI+16SrdDNA+H3 for Bayesian analysis.

Combined Sequence	COI haplotype	16S haplotype	Combined Sequence	H3 sequence	ITS2 sequence	Combined Sequence	COI haplotype	16S haplotype	H3 sequence	Locality (number of specimens)
UK-COI16S-1	UK-COI 12	UK-16S 1				UK-CS_1	UK-COI 12	UK-16S 1	UK-H3 3	UK, Sheffield (1)
UK-COI16S-2	UK-COI 1	UK-16S 1	UK-H3ITS2-1	UK-H3 1	UK-ITS2 2	UK-CS_2	UK-COI 1	UK-16S 1	UK-H3 1	UK, Barrow near Barnsley (3)
UK-COI16S-3	UK-COI 4	UK-16S 1				UK-CS_3	UK-COI 4	UK-16S 1	UK-H3 3	UK, Rotherham (1)
UK-COI16S-4	UK-COI 7	UK-16S 2	UK-H3ITS2-3	UK-H3 5	UK-ITS2 2	UK-CS_4	UK-COI 7	UK-16S 2	UK-H3 5	UK, Sheffield (1)
UK-COI16S-5	UK-COI 7	UK-16S 2	UK-H3ITS2-2	UK-H3 4	UK-ITS2 2	UK-CS_5	UK-COI 7	UK-16S 2	UK-H3 4	UK, Rotherham (1)
UK-COI16S-6	UK-COI 2	UK-16S 1				UK-CS_6	UK-COI 2	UK-16S 1	UK-H3 2	UK, Cambridge (1)
IT-COI16S-1	IT-COI 3	IT-16S 1	IT-H3ITS2-3	IT-H3 7	IT-ITS2 3	IT-CS_1	IT-COI 3	IT-16S 1	IT-H3 7	Italy, Latium, Valle dell'Aniene (1)
IT-COI16S-2	IT-COI 3	IT-16S 1	IT-H3ITS2-2	IT-H3 6	IT-ITS2 2	IT-CS_2	IT-COI 3	IT-16S 1	IT-H3 6	Italy, Latium, Valle dell'Aniene (1)
IT-COI16S-3	IT-COI 3	IT-16S 1	IT-H3ITS2-4	IT-H3 8	IT-ITS2 3	IT-CS_3	IT-COI 3	IT-16S 1	IT-H3 8	Italy, Latium, Valle dell'Aniene (1)
IT-COI16S-4	IT-COI 1	IT-16S 1	IT-H3ITS2-5	IT-H3 1	IT-ITS2 4	IT-CS_4	IT-COI 1	IT-16S 1	IT-H3 1	Italy, Latium, Gole del Velino (1)
IT-COI16S-5	IT-COI 1	IT-16S 1				IT-CS_5	IT-COI 1	IT-16S 1	IT-H3 5	Italy, Latium, Gole del Velino (1)
IT-COI16S-6	IT-COI 7	IT-16S 1	IT-H3ITS2-1	IT-H3 3	IT-ITS2 1	IT-CS_6	IT-COI 7	IT-16S 1	IT-H3 3	Italy, Latium, Valle del Tronto (2)
IT-COI16S-7	IT-COI 7	IT-16S 1	IT-H3ITS2-6	IT-H3 4	IT-ITS2 5	IT-CS_7	IT-COI 7	IT-16S 1	IT-H3 4	Italy, Latium, Valle del Turano (1)
IT-COI16S-8	IT-COI 2	IT-16S 1				IT-CS_8	IT-COI 2	IT-16S 1	IT-H3 3	Italy, Latium, Gole del Velino (1)
IT-COI16S-9	IT-COI 9	IT-16S 3				IT-CS_9	IT-COI 9	IT-16S 3	IT-H3 9	Italy, Venetum, Sorgà (1)
IT-COI16S-10	IT-COI 9	IT-16S 4				IT-CS_10	IT-COI 9	IT-16S 4	IT-H3 4	Italy, Venetum, Sorgà (1)
IT-COI16S-11	IT-COI 10	IT-16S 4				IT-CS_11	IT-COI 10	IT-16S 4	IT-H3 9	Italy, Lombardia, Rezzato (1)
IT-COI16S-12	IT-COI 10	IT-16S 4	IT-H3ITS2-7	IT-H3 10	IT-ITS2 8	IT-CS_12	IT-COI 10	IT-16S 4	IT-H3 10	Italy, Lombardia, Rezzato (1)
IT-COI16S-13	IT-COI 12	IT-16S 5				IT-CS_13	IT-COI 12	IT-16S 5	IT-H3 11	Italy, Emilia Romagna (1)
IT-COI16S-14	IT-COI 11	IT-16S 6	IT-H3ITS2-8	IT-H3 2	IT-ITS2 9	IT-CS_14	IT-COI 11	IT-16S 6	IT-H3 2	Italy, Emilia Romagna (1)
IT-COI16S-15	IT-COI 13	IT-16S 5				IT-CS_15	IT-COI 13	IT-16S 5	IT-H3 1	Italy, Emilia Romagna (1)
IT-COI16S-16	IT-COI 14	IT-16S 8				IT-CS_16	IT-COI 14	IT-16S 8	IT-H3 12	Italy, Basilicata (1)
IT-COI16S-17	IT-COI 15	IT-16S 9				IT-CS_17	IT-COI 15	IT-16S 9	IT-H3 12	Italy, Basilicata (1)

Combined Sequence	COI haplotype	16S haplotype	Combined Sequence	H3 sequence	ITS2 sequence	Combined Sequence	COI haplotype	16S haplotype	H3 sequence	Locality (number of specimens)
IT-COI16S-18	IT-COI 18	IT-16S 10	IT-H3ITS2-9	IT-H3 12	IT-ITS2 11	IT-CS_18	IT-COI 18	IT-16S 10	IT-H3 12	Italy, Tuscany, Nievole (1)
IT-COI16S-19	IT-COI 19	IT-16S 12				IT-CS_19	IT-COI 19	IT-16S 12	IT-H3 12	Italy, Tuscany, Arezzo (1)
IT-COI16S-20	IT-COI 20	IT-16S 11	IT-H3ITS2-10	IT-H3 12	IT-ITS2 11	IT-CS_20	IT-COI 20	IT-16S 11	IT-H3 12	Italy, Tuscany, Arezzo and Nievole (3)
IT-COI16S-21	IT-COI 21	IT-16S 12	IT-H3ITS2-11	IT-H3 13	IT-ITS2 11	IT-CS_21	IT-COI 21	IT-16S 12	IT-H3 13	Italy, Tuscany, Arezzo (1)
IT-COI16S-22	IT-COI 21	IT-16S 12	IT-H3ITS2-12	IT-H3 12	IT-ITS2 12	IT-CS_22	IT-COI 21	IT-16S 12	IT-H3 12	Italy, Tuscany, Arezzo and La Casella (2)
FR-COI16S-1	FR-COI 1	FR-16S 1	FR-H3ITS2-1	FR-H3 1	FR-ITS2 1	FR-CS_1	FR-COI 1	FR-16S 1	FR-H3 1	France, Alpes-Maritimes, Sainte Thecle (1)
FR-COI16S-2	FR-COI 2	FR-16S 1				FR-CS_2	FR-COI 2	FR-16S 1	FR-H3 2	France, Alpes-Maritimes, Sainte Thecle (1)
FR-COI16S-3	FR-COI 2	FR-16S 1				FR-CS_3	FR-COI 2	FR-16S 1	FR-H3 3	France, Alpes-Maritimes, Sainte Thecle (1)
AT-COI16S-1	AT-COI 1	AT-16S 2	AT-H3ITS2-1	AT-H3 1	AT-ITS2 1	AT-CS_1	AT-COI 1	AT-16S 2	AT-H3 1	Austria, Breitenlee (1)
AT-COI16S-2	AT-COI 2	AT-16S 1				AT-CS_2	AT-COI 2	AT-16S 1	AT-H3 1	Austria, Breitenlee (2)
HU-COI16S-1	KM247376	KM247391	HU-H3ITS2-1	HU-H3 1	HU-ITS2 1	HU-CS_1	KM247376	KM247391	HU-H3 1	Hungary, Kis-Balaton (1)

Table 3. Ranges of K2P genetic distances for COI and 16SrDNA sequences analysed (mean values in parentheses).

Comparison	COI (%)	16SrDNA (%)
Within <i>M. cantiana</i> CAN-1	0.2–2.2 (0.9)	0.7–1.4 (0.7)
Within <i>M. cantiana</i> CAN-2	0.3 (0.3)	0.7 (0.7)
Within <i>M. sp.</i> CAN-3	0.2–1.9 (1.2)	0.4–2.6 (1.5)
Within <i>M. cemelelea</i> CAN-4	0.2–0.5 (0.3)	0.7 (0.7)
Within <i>M. parumcincta</i>	0.2–4.6 (2.8)	0.8–4.7 (2.5)
Between <i>M. cantiana</i> CAN-1 and <i>M. cantiana</i> CAN-2	3.3–5.3 (3.9)	1.8–2.9 (2.5)
Between <i>M. cantiana</i> CAN-1 and <i>M. sp.</i> CAN-3	17.6–19.3 (18.6)	17.5–18.9 (18.1)
Between <i>M. cantiana</i> CAN-1 and <i>M. cemelelea</i> CAN-4	17.1–18.9 (18)	20.4–21.9 (21.4)
Between <i>M. cantiana</i> CAN-1 and <i>M. parumcincta</i>	19.9–22.1 (20.9)	24.7–26.4 (25.5)
Between <i>M. cantiana</i> CAN-2 and <i>M. sp.</i> CAN-3	17.8–18.2 (18.1)	15.7–17.1 (16.4)
Between <i>M. cantiana</i> CAN-2 and <i>M. cemelelea</i> CAN-4	18.2–18.7 (18.4)	19.6–20.6 (20.1)
Between <i>M. cantiana</i> CAN-2 and <i>M. parumcincta</i>	19.7–20.9 (20.3)	23.0–26.5 (24.3)
Between <i>M. sp.</i> CAN-3 and <i>M. cemelelea</i> CAN-4	5.1–6.2 (5.3)	4.1–5.3 (4.8)
Between <i>M. sp.</i> CAN-3 and <i>M. parumcincta</i>	17.9–22.0 (19.7)	19.3–21.8 (20.3)
Between <i>M. cemelelea</i> CAN-4 and <i>M. parumcincta</i>	19.5–21.1 (20.1)	20.4–22.4 (20.8)

for other clades (up to 4.6% in COI haplotypes, Table 3). The clade PAR was clearly separated from other clades in each tree (Figs 3–5). Combined haplotypes IT-COI16S-16 – IT-COI16S-17 from Basilicata (S Italy) seem to form a separate subclade against haplotypes IT-COI16S-18 – IT-COI16S-21 from three other populations in Tuscany (Fig. 3).

K2P genetic distances between COI and 16SrDNA haplotypes are summarised in Table 3. The smallest distances are between haplotypes of CAN-1 and CAN-2 clades; however they are larger than distances within these clades. The largest K2P distances between COI sequences separate clade of haplotypes found in *M. parumcincta* from all other clades (by ca. 20–25 %). Very large distances also separate clade CAN-1 from clades CAN-3 and CAN-4 (COI 18.0% and 18.6%, respectively). Distances between clade CAN-2 and CAN-3 on one hand, and CAN-4 on the other, are also large. Only distances between clades CAN-3 and CAN-4 are smaller (COI 5.3%) although they are much larger than within each of these clades.

Networks of COI (Fig. 6) and 16SrDNA (Fig. 7) confirm separateness of five clades. Clades CAN-1 and CAN-2 are much closer than the others; French haplotypes of clade CAN-4 are separate from the Austrian-Italian CAN-3; clade PAR of *M. parumcincta* haplotypes is differentiated into two subgroups.

Morphological study: shell

The *M. cantiana* group (clades CAN-1, CAN-2, CAN-3, CAN-4; Figs 8–15) and that of *M. parumcincta* (clade PAR; Fig. 16) have a globose-subglobose shell, variable in colour and size, with roundish aperture and very small or closed umbilicus. The main

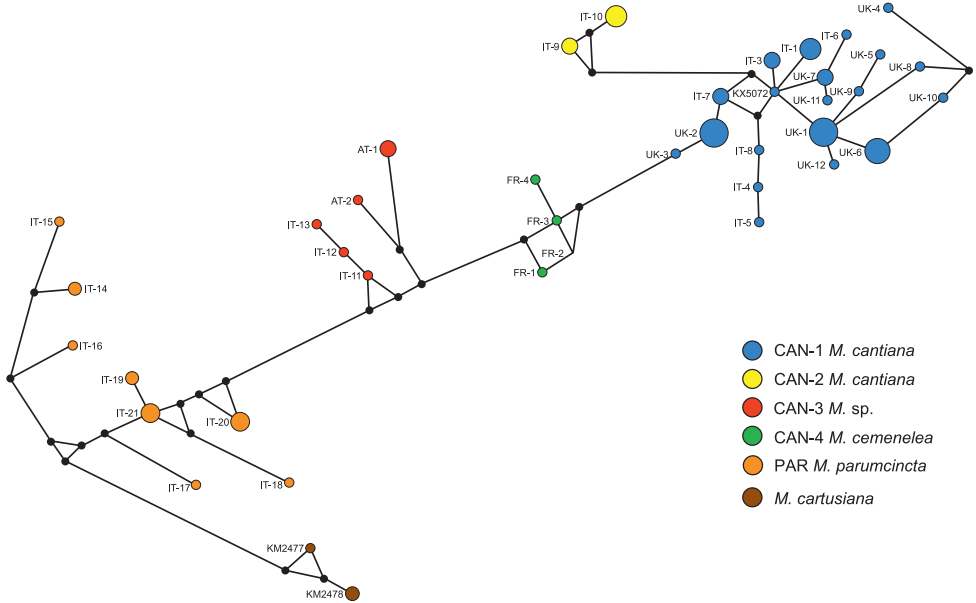


Figure 6. The median-joining haplotype network for COI haplotypes of *Monacha cantiana* group. The colours of the circles indicate *Monacha* species, and their size is proportional to haplotype frequencies. Small black circles are hypothetical missing intermediates.

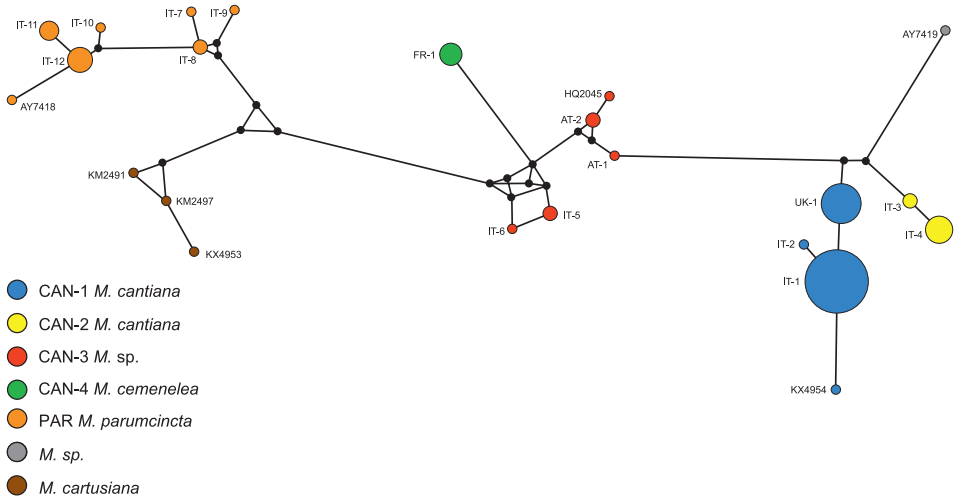
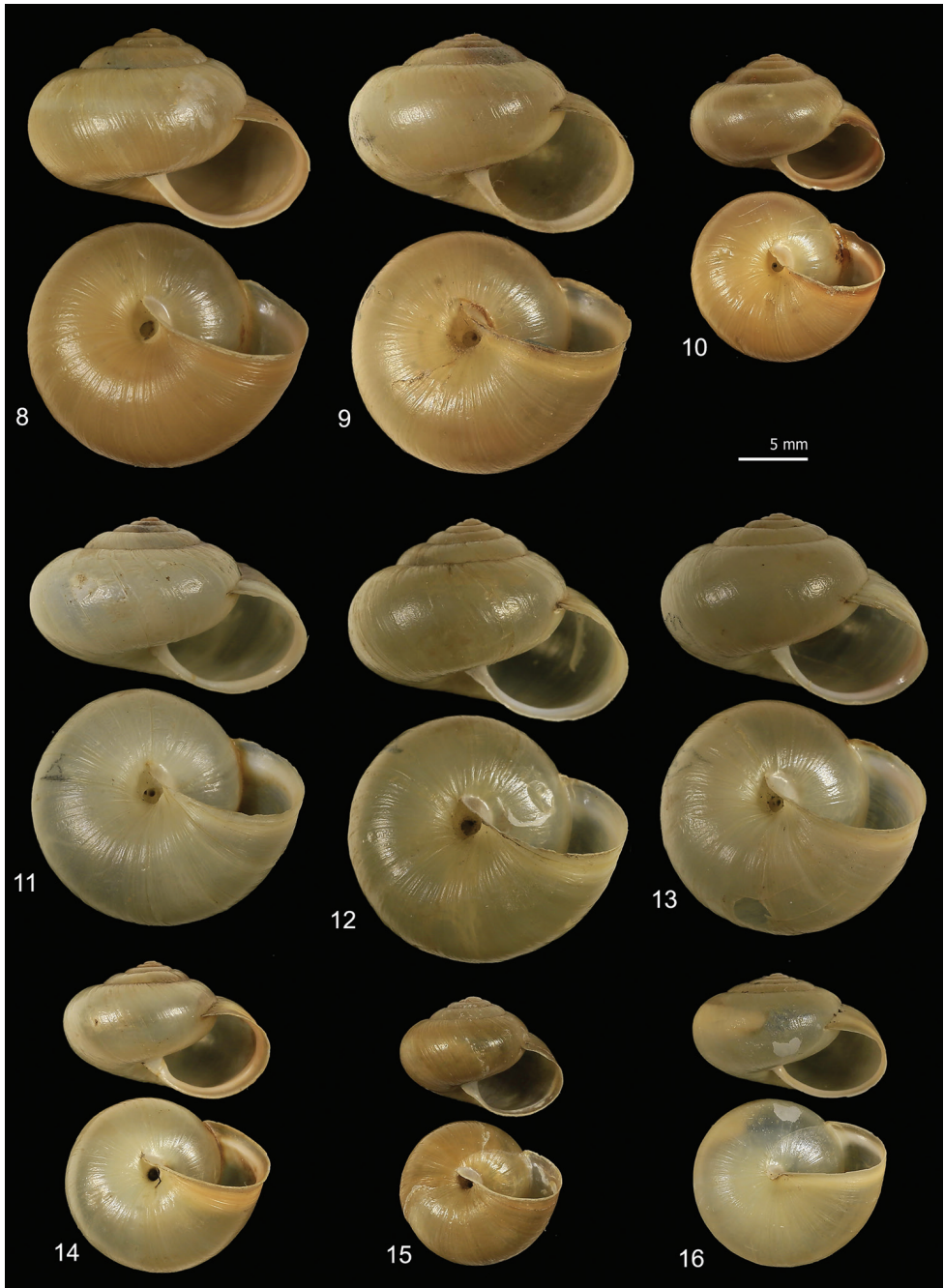
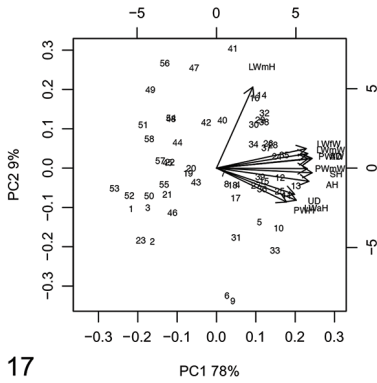


Figure 7. Haplotype network for 16SrDNA of *Monacha cantiana* group. Other explanations as in Figure 6.

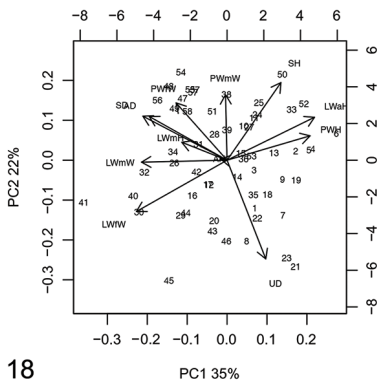
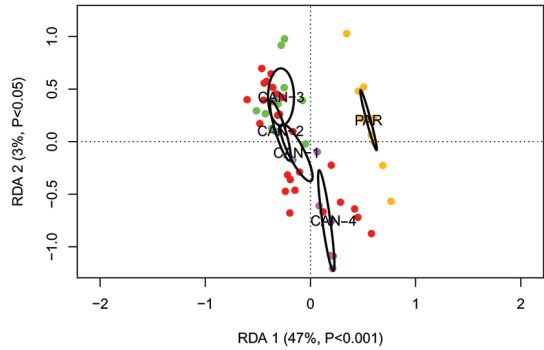
difference between the two groups consists in the umbilicus (very small, but always open in *M. cantiana* s.l.; closed in *M. parumcineta*). Some populations of *M. parumcineta* have variably evident whitish peripheral and subsutural bands (evident if the last whorl is reddish) and/or a less glossy (more opaque) shell surface.



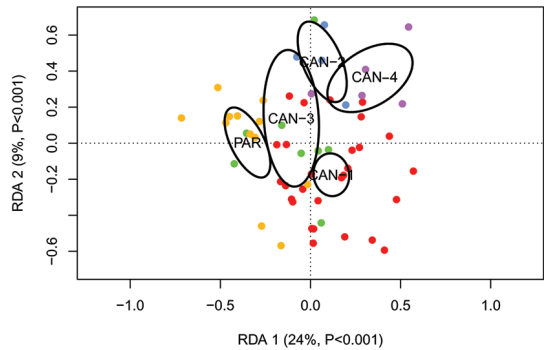
Figures 8–16. Shell variability in *Monacha cantiana* s.l. group (**8–15**) and *Monacha parumcincta* (**16**). CAN-1 from Valle dell’Aniene (FGC 42973) (**8**), Gole del Velino, near Sigillo (FGC 42960) (**9**), Elba Island, Sant’Ilario in Campo (FGC 23586) (**10**) and Valle del Turano, near Turania (FGC 42969) (**11**); CAN-2 from Sorgà (FGC 42964) (**12**); CAN-3 from Fiume Setta (FGC 42977) (**13**) and Breitenlee (FGC 44020) (**14**); CAN-4 from Vallée de Peillon, Sainte Thecle (FGC 40320) (**15**); PAR from La Casella (FGC 44077) (**16**).



17



18



Figures 17–18. Principal component analysis (PCA) and Redundancy analysis (RDA) with clade constraint applied to the original shell matrix (17) and Z-matrix (shape-related)(18). Ellipses show the 95% confidence intervals associated with each group.

RDA with “clade/lineage” constraint on the shape and size matrix (Fig. 17) showed that RDA 1 (47%, $P < 0.001$) separated the groups CAN-1, CAN-2 and CAN-3 from PAR with CAN-4 in intermediate position. The preliminary classic PCA revealed size as the first major source of morphological variation, since PC1 (78%) was a positive combination of all variables. On the contrary, RDA 2 (3%, $P < 0.05$) showed a statistically significant separation between CAN-4 and the others; no difference was found between the CAN-1, CAN-2 and CAN-3 groups. In this regard, PC2 (9%) accounted for a contrast between LWmH and LWaH / PWH variables. RDA on the shape (Z) matrix (Fig. 18) confirmed a statistically significant separation between PAR and CAN-4 with the large group CAN-1-CAN-2-CAN-3 in intermediate position. Shape-related PCA indicated that LWfW / LWmW / LWmH / SD / AD vs LWaH / PWmW vs UD on PC1 and PWmW vs UD on PC2.

Box plots (Fig. 19) prove the poor discriminating value of shell characters in distinguishing species pairs (no character distinguishes more than four clade pairs according to Tukey’s honestly significant difference test). The most recognisable pairs are CAN-1 vs. PAR, CAN-2 vs. PAR, and CAN-3 vs. PAR (11, 9, and 10 significant

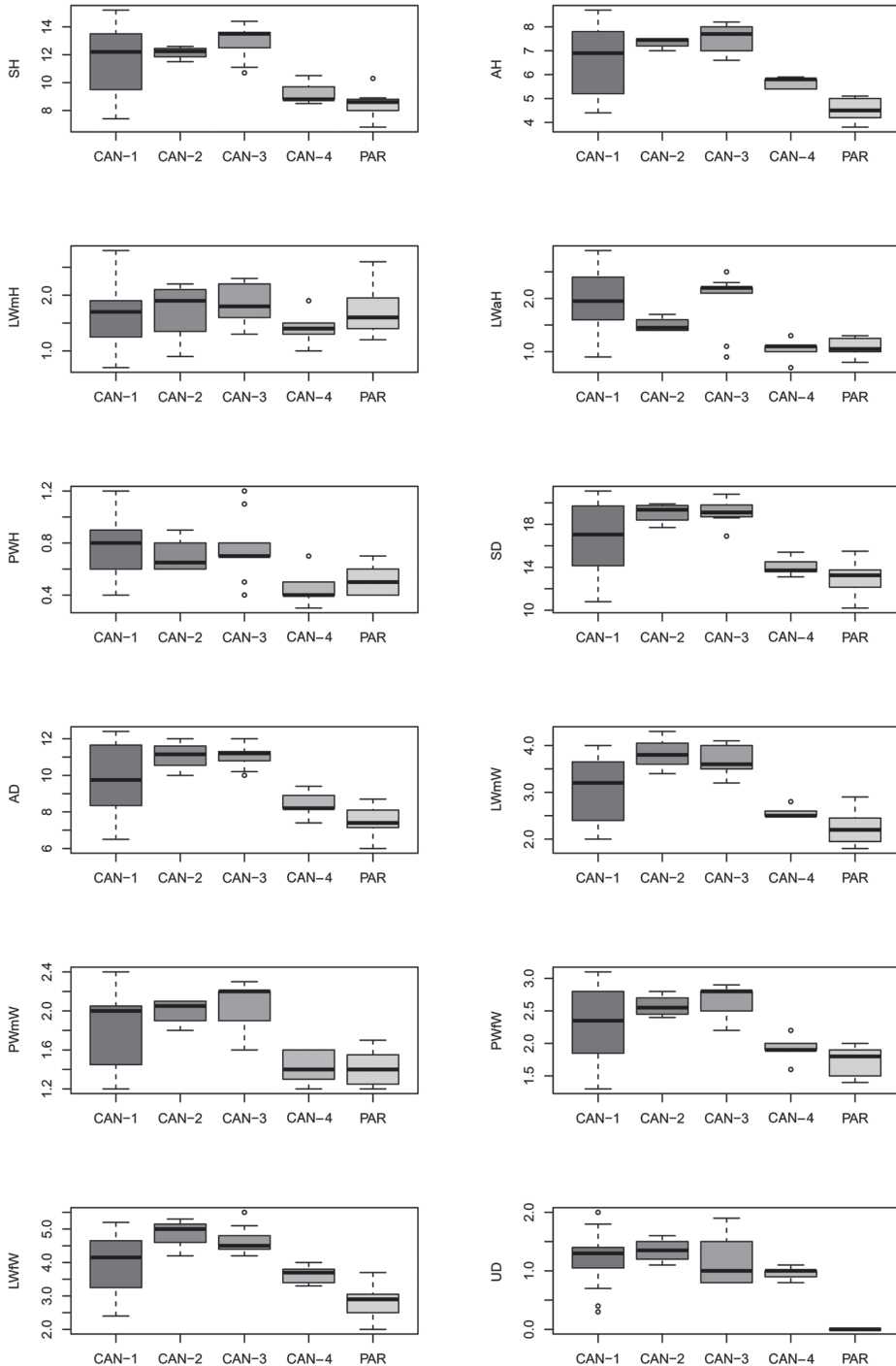


Figure 19. Box plots for shell characters of the five *Monacha* clades investigated. The lower and upper limits of the rectangular boxes indicate the 25th to 75th percentile range, and the horizontal line within the boxes is the median (50th percentile).

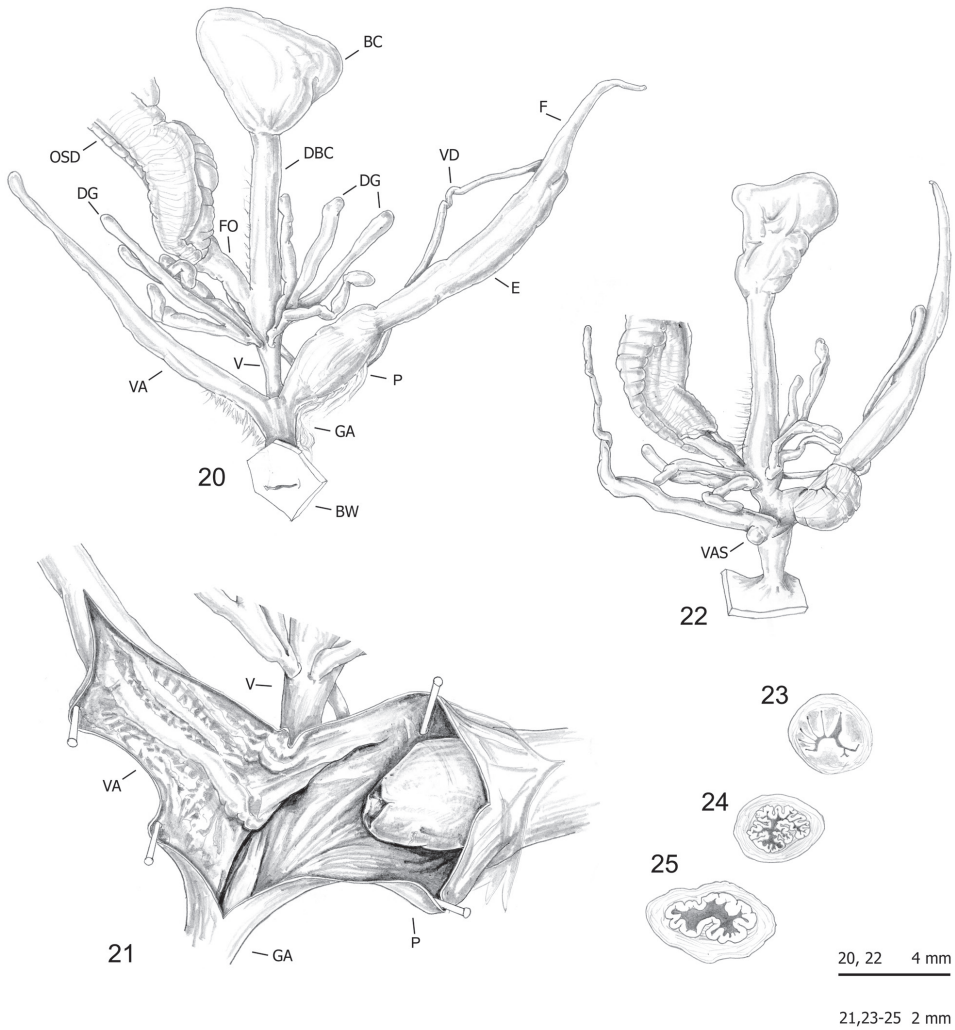
characters, respectively). Only two significant characters distinguish CAN-1 vs. CAN-4 and only one CAN-3 vs CAN-4 or CAN-4 vs. PAR. No significant character distinguishes CAN-1 vs. CAN-2, CAN-1 vs. CAN-3 or CAN-2 vs. CAN-3 (Table 4).

Morphological study: anatomy

The bodies (generally pinkish or yellowish white) and mantle (with sparse, variably numerous brown or blackish spots near mantle border or on the lung surface, one larger close to the pneumostomal opening) are very similar in the two species group, whereas the distal genitalia show some diagnostic features (Figs 20–50 vs. Figs 51–59): vagi-

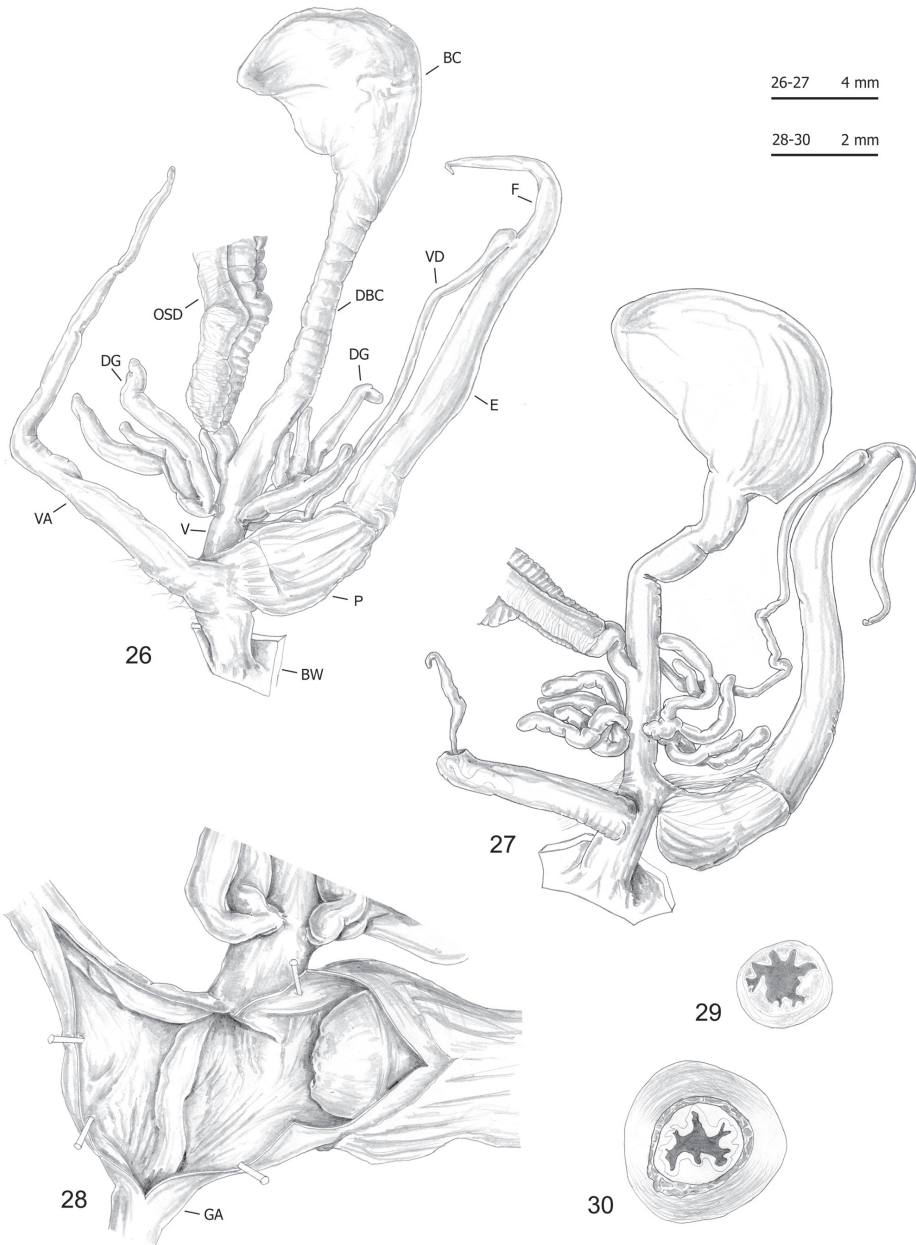
Table 4. Results of Tukey's honestly significant difference (HSD) test for shell and genitalia characters (in bold Tukey's post-hoc $P < 0.01$).

pairs	SH	AH	LWmH	LWaH	PWH	SD
CAN-1 vs CAN-2	0.97573	0.64561	0.99140	0.46817	0.95652	0.47286
CAN-1 vs CAN-3	0.39185	0.18401	0.57940	1.00000	0.99945	0.15274
CAN-1 vs CAN-4	0.05983	0.42921	0.92651	0.00065	0.00567	0.23583
CAN-1 vs PAR	0.00001	0.00000	0.97255	0.00001	0.00144	0.00030
CAN-2 vs CAN-3	0.97242	0.99963	0.98207	0.59785	0.98906	1.00000
CAN-2 vs CAN-4	0.11515	0.14765	0.87857	0.38505	0.24954	0.04877
CAN-2 vs PAR	0.00340	0.00008	1.00000	0.35237	0.39229	0.00082
CAN-3 vs CAN-4	0.00569	0.02947	0.42967	0.00414	0.03203	0.01007
CAN-3 vs PAR	0.00000	0.00000	0.92716	0.00047	0.03296	0.00001
CAN-4 vs PAR	0.84947	0.12731	0.78714	0.99908	0.96245	0.84026
pairs	AD	LWmW	PWmW	PFW	LWfW	UD
CAN-1 vs CAN-2	0.51068	0.08476	0.82369	0.68103	0.18598	0.87507
CAN-1 vs CAN-3	0.19064	0.03926	0.45194	0.22487	0.12364	0.99947
CAN-1 vs CAN-4	0.33899	0.38635	0.06390	0.44613	0.90473	0.75084
CAN-1 vs PAR	0.00010	0.00008	0.00206	0.00241	0.00002	0.00000
CAN-2 vs CAN-3	1.00000	0.99124	0.99994	0.99975	0.99254	0.86022
CAN-2 vs CAN-4	0.07939	0.01170	0.05068	0.16856	0.12920	0.48690
CAN-2 vs PAR	0.00052	0.00002	0.01253	0.00695	0.00003	0.00000
CAN-3 vs CAN-4	0.02106	0.00660	0.00750	0.03792	0.12320	0.89763
CAN-3 vs PAR	0.00000	0.00000	0.00029	0.00009	0.00000	0.00000
CAN-4 vs PAR	0.60652	0.53369	0.99999	0.86111	0.07669	0.00000
pairs	DBC	V	F	E	P	VA
CAN-1 vs CAN-2	0.04626	0.99611	0.59664	0.09790	0.14384	0.00002
CAN-1 vs CAN-3	0.87421	0.99165	0.91278	0.61442	0.07853	0.03767
CAN-1 vs CAN-4	0.99873	0.47088	0.12512	0.69751	0.65012	0.57764
CAN-1 vs PAR	0.86530	0.00445	0.00938	0.00053	0.95393	0.00000
CAN-2 vs CAN-3	0.43904	0.96413	0.97735	0.82401	1.00000	0.14098
CAN-2 vs CAN-4	0.14954	0.46577	0.02416	0.03608	0.04286	0.05841
CAN-2 vs PAR	0.01497	0.10864	0.67653	0.00001	0.07788	0.00000
CAN-3 vs CAN-4	0.89019	0.77914	0.06102	0.21675	0.02722	0.94002
CAN-3 vs PAR	0.48631	0.01053	0.24592	0.00012	0.04367	0.00000
CAN-4 vs PAR	0.99374	0.00166	0.00030	0.38095	0.93760	0.00000



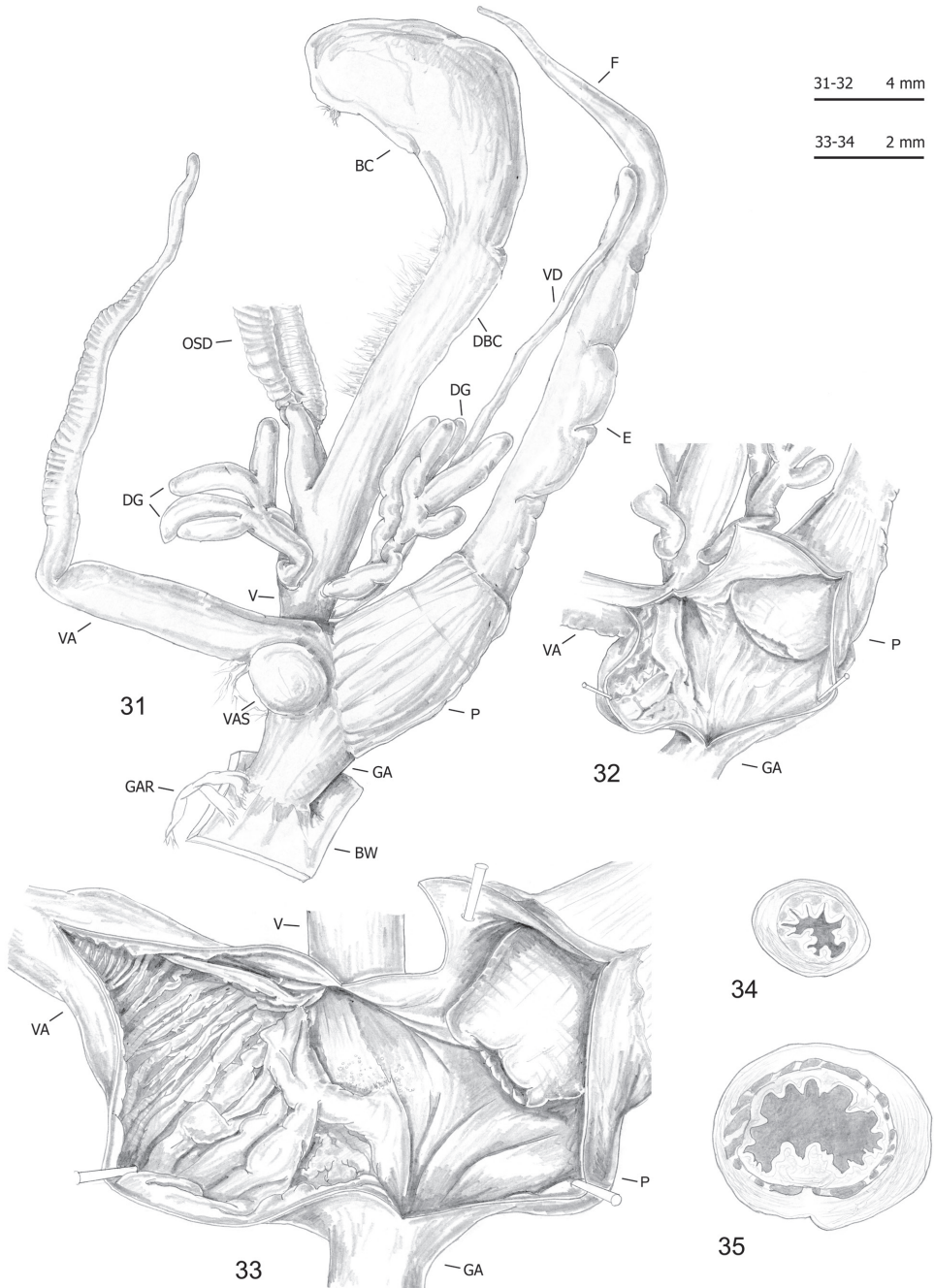
Figures 20–25. Genitalia (proximal parts excluded) (**20, 22**), internal structure of distal genitalia (**21**) and transverse sections of medial epiphallus (**23**) and penial papilla (**24–25**) of *Monacha cantiana*. CAN-1 from Barrow near Barnsley (FGC 40329) (**20, 22–23, 25**) and East Acton near London (DCBC) (**21, 24**).

nal appendix or “appendicula” rather long, always with thin walled terminal portion and with variably evident basal sac (i.e., the “sac-like diverticulum of the appendicula vaginalis” first described by Giusti and Manganelli 1987: 135, Fig. 3A, C – in “*M. cantiana*” specimens from Corsica); short, only occasionally with very short terminal portion and always without basal sac in *M. parumcincta*; the vaginal-atrial pilaster (present and variably evident in the *M. cantiana* group; absent in *M. parumcincta*); penial papilla (glans) with central canal wide, thin walled, internally irregularly jagged and with a sort of solid pilaster on one side; central canal connected to external wall of penial papilla by many muscular/connective strings in the *M. cantiana* group; penial

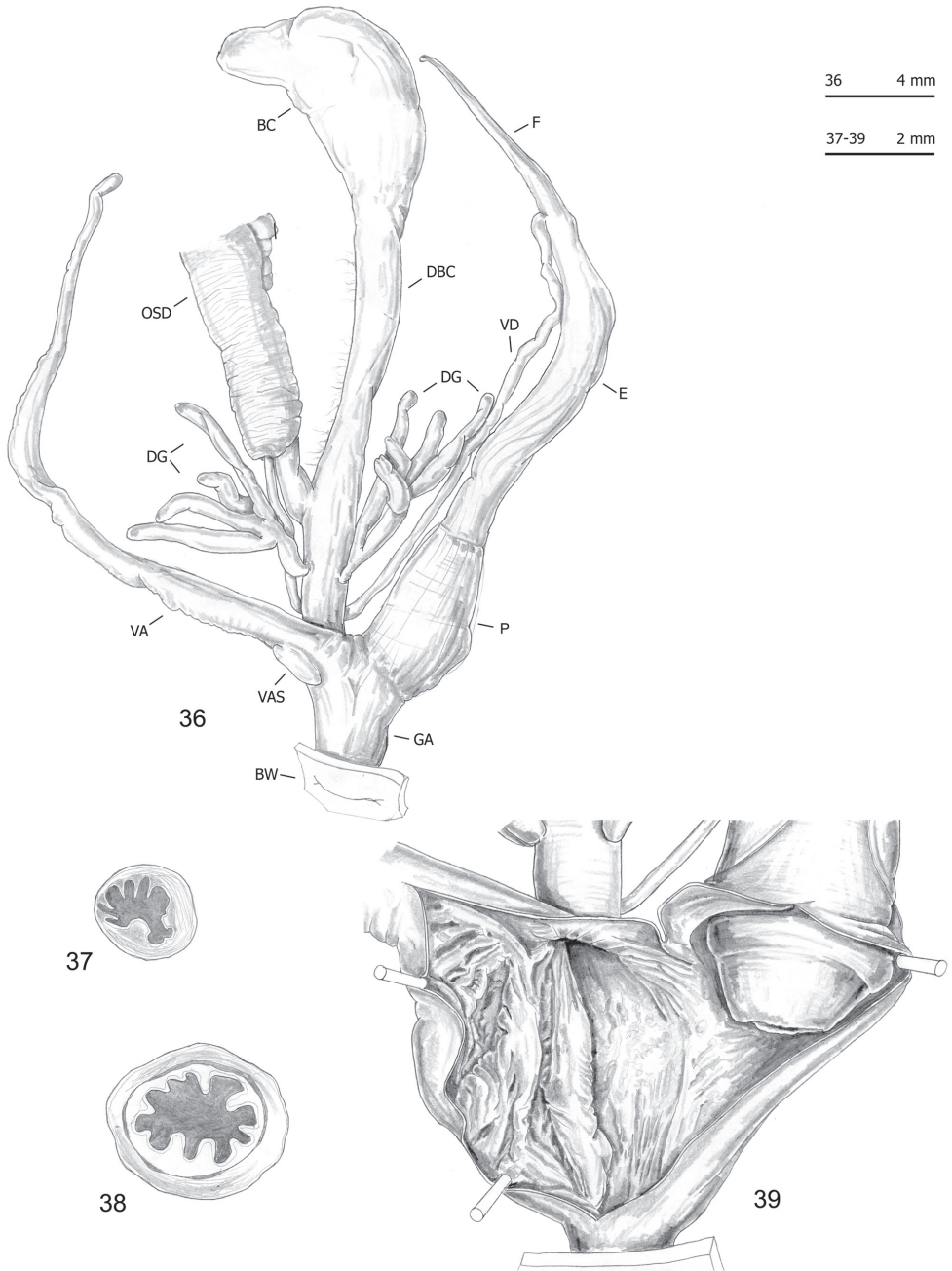


Figures 26–30. Genitalia (proximal parts excluded) (26–27), internal structure of distal genitalia (28) and transverse sections of medial epiphallus (29) and penial papilla (30) of *Monacha cantiana*. CAN-1 from Gole del Velino, near Sigillo (FGC 42960) (26, 28–30) and Valle del Turano, near Turania (FGC 42969) (27).

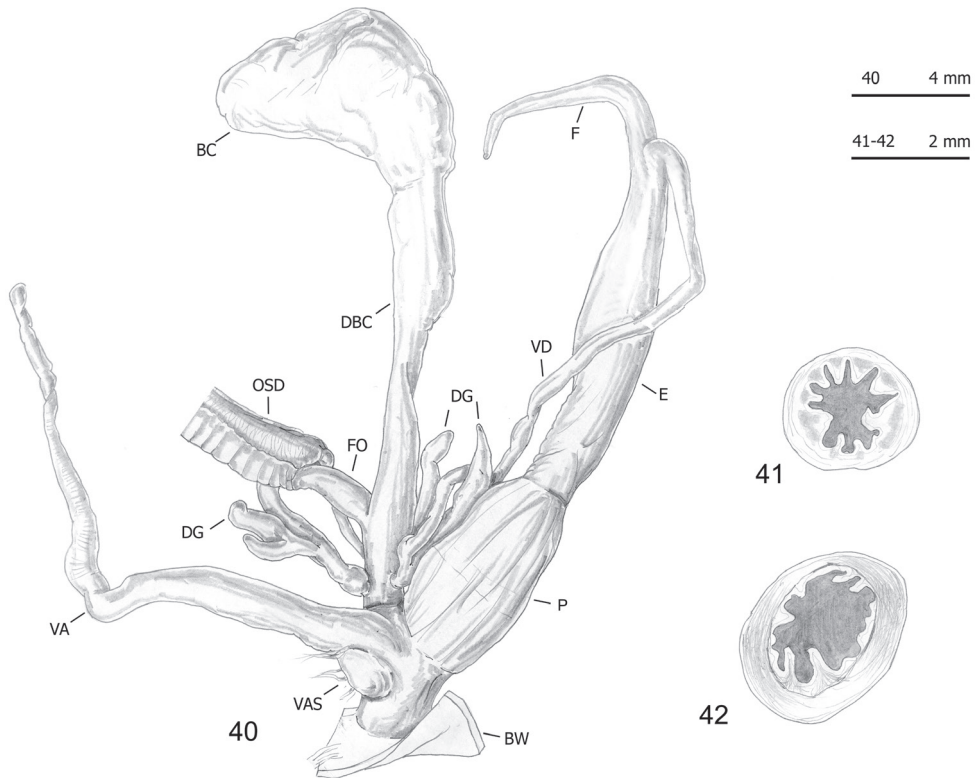
papilla with central canal thin walled, internally smooth or slightly jagged, almost completely filled by large invagination; central canal not connected to external wall of penial papilla in *M. parumcincta*.



Figures 31–35. Genitalia (proximal parts excluded) (31), internal structure of distal genitalia (32–32) and transverse sections of medial epiphallus (34) and penial papilla (35) of *Monacha cantiana*. CAN-2 from Rezzato (ex. 1: 31–32, 34–35; ex. 2: 33) (FGC 42976).



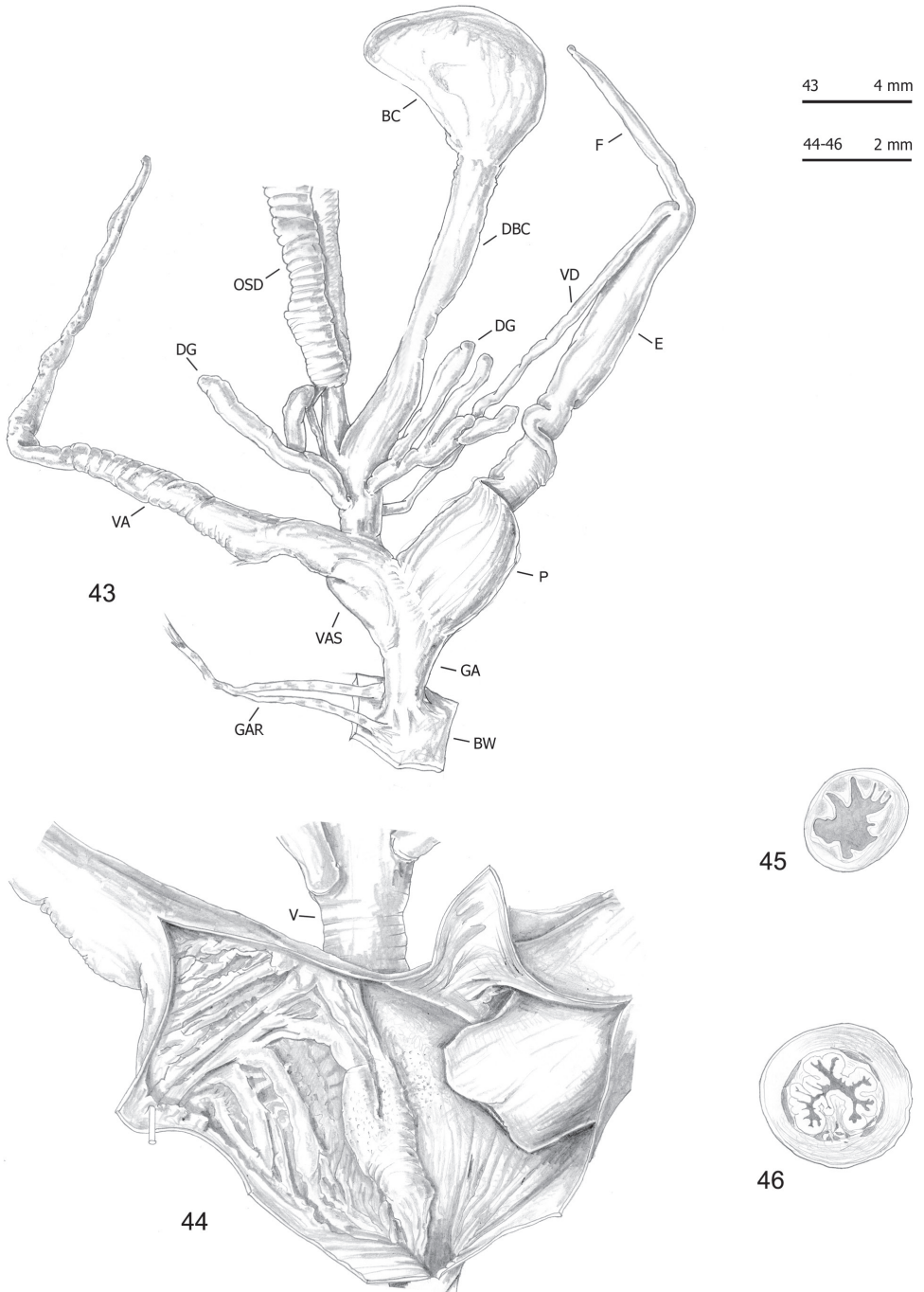
Figures 36–39. Genitalia (proximal parts excluded) (36), transverse sections of medial epiphallus (37) and penial papilla (38) and internal structure of distal genitalia (39) of *Monacha cantiana*. CAN-2 from Sorgà (FGC 42964).



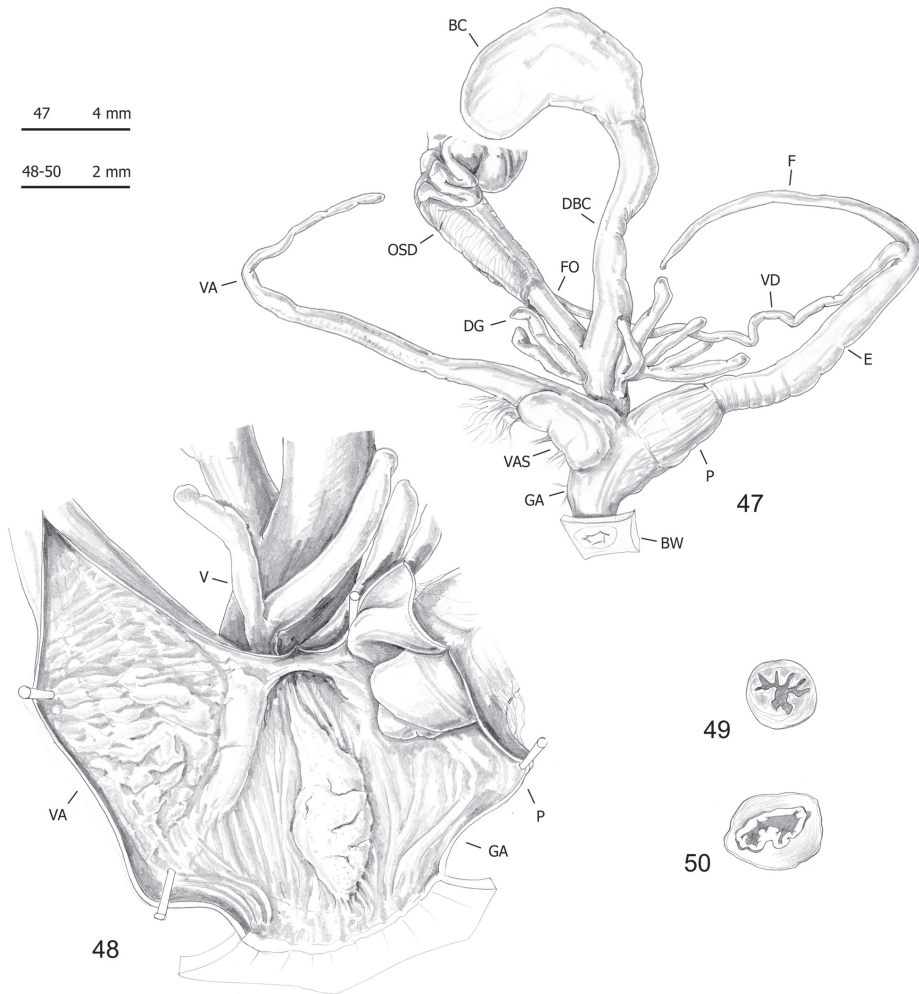
Figures 40–42. Genitalia (proximal parts excluded) (40) and transverse sections of medial epiphallus (41) and penial papilla (42) of *Monacha cantiana*. CAN-3 from Fiume Setta (FGC 42977).

RDA with “clade/lineage” constraint on the shape and size matrix (Fig. 60) showed that RDA 1 (45%, $P < 0.001$) tended to separate the group CAN-1, CAN-2, CAN-3 and CAN-4 from PAR. The preliminary classic PCA revealed size as the first major source of morphological variation, since PC1 (53%) was a positive combination of all variables. On the contrary, RDA 2 (6%, $P < 0.002$) showed statistically significant separation of CAN-1, CAN-2, CAN-3 and PAR from CAN-4. In that regard, PC2 (20%) accounted for a contrast between F and P variables. RDA with species constraint on the shape (Z) matrix (Fig. 61) showed that RDA 1 (20%, $P < 0.001$) confirmed a statistically significant separation between PAR and CAN-4, while the large group CAN-1-CAN-2-CAN-3 remained completely unexplained. Shape-related PCA indicated that VA and F vs E and P were the two principal shape determinants on PC1 and V vs BCD on PC2.

Box plots (Fig. 62) for anatomical characters showed that VA has the best discriminating value (it distinguishes five clade pairs according to Tukey’s honestly significant difference test), followed by E and V (three pairs). The most recognisable pairs are CAN-1 vs. PAR (four significant characters), CAN-2 vs. PAR, CAN-3 vs.



Figures 43–46. Genitalia (proximal parts excluded) (43), internal structure of distal genitalia (44) and transverse sections of medial epiphallus (45) and penial papilla (46) of *Monacha cantiana*. CAN-3 from Breitenlee (FGC 44020).

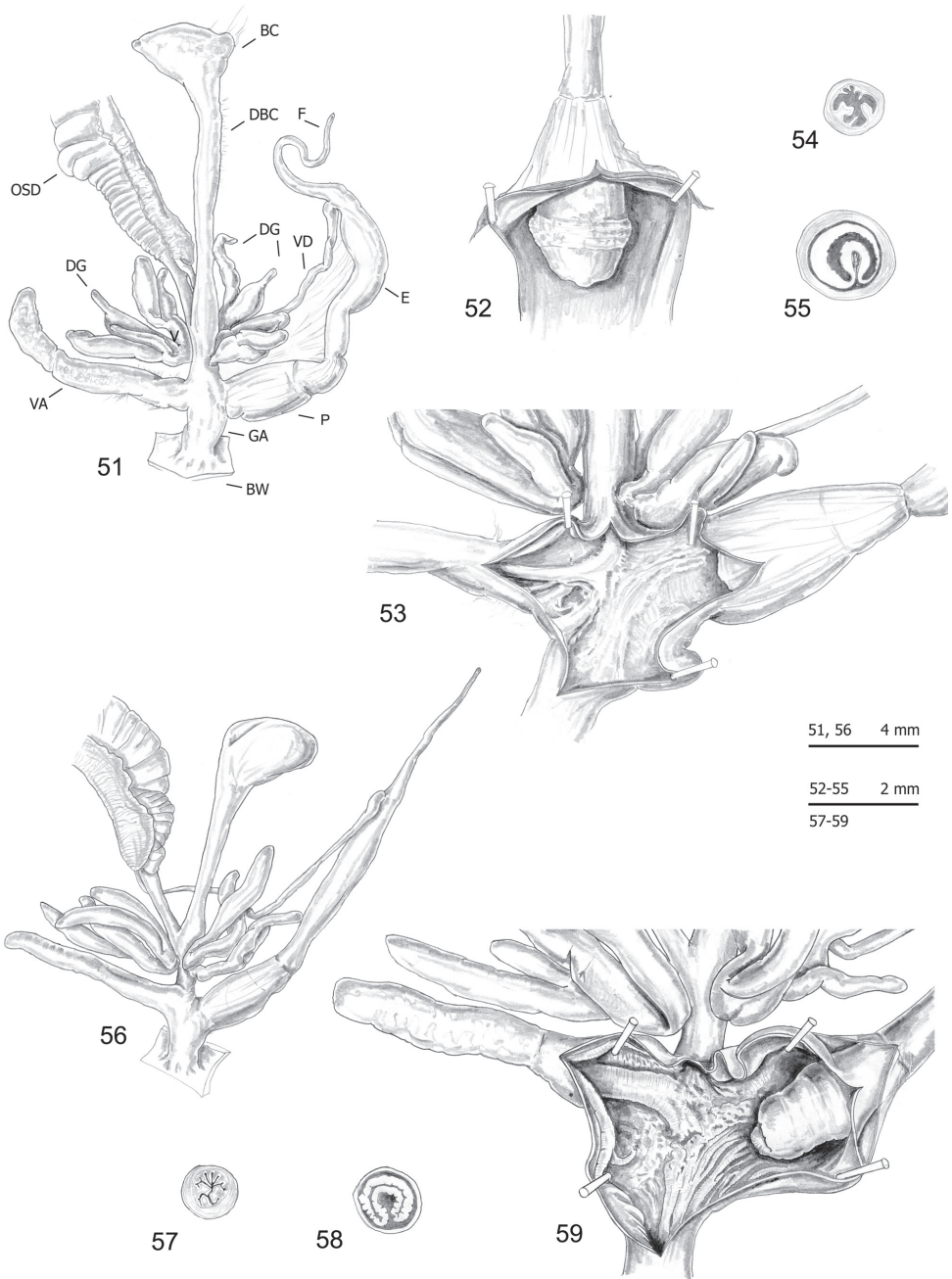


Figures 47–50. Genitalia (proximal parts excluded) (**47**), internal structure of distal genitalia (**48**) and transverse sections of medial epiphallus (**49**) and penial papilla (**50**) of *Monacha cantiana*. CAN-4 from Vallée de Peillon, Sainte Thecle (FGC 40320).

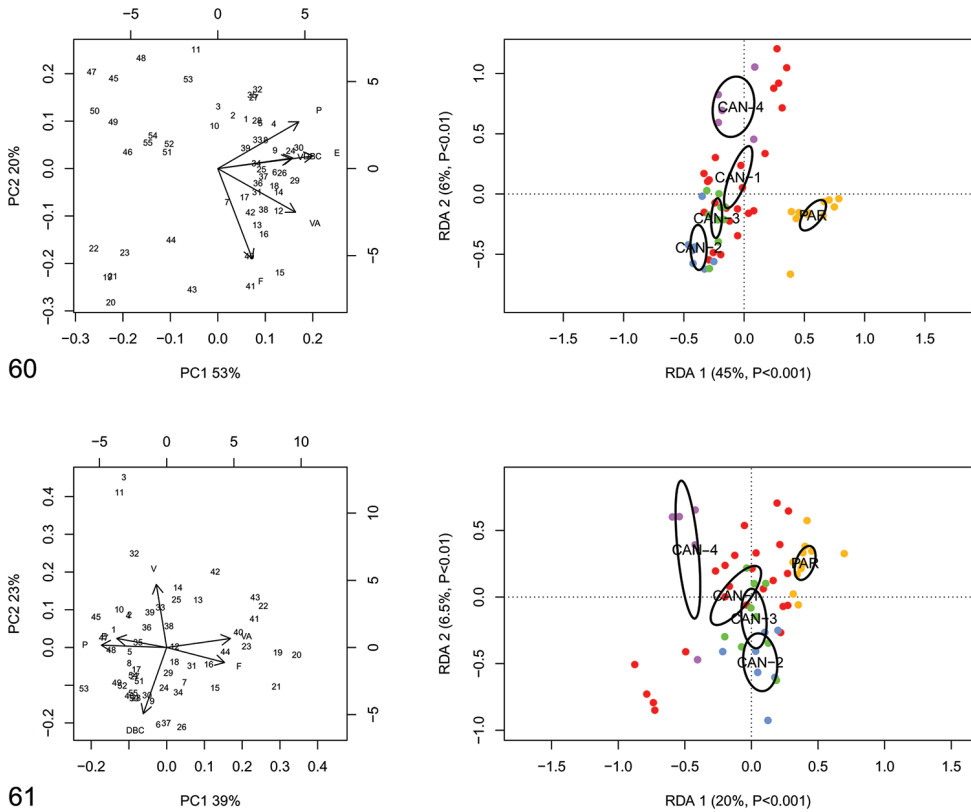
PAR, and CAN-4 vs. PAR (three significant characters). Only one significant character distinguishes CAN-1 vs. CAN-2 and none distinguish CAN-1 vs. CAN-3, CAN-1 vs. CAN-4, CAN-2 vs. CAN-3, CAN-2 vs. CAN-4, or CAN-3 vs. CAN-4 (Table 4).

Discussion

The finding that *M. cantiana*, as usually conceived, actually consists of four distinct lineages (CAN-1, CAN-2, CAN-3, CAN-4) is an absolute novelty. One of these lineages (CAN-1) included most of the populations examined (11 populations). It is widespread



Figures 51–59. Genitalia (proximal parts excluded) (**51, 56**), internal structure of distal genitalia (**52–53, 59**) and transverse sections of medial epiphallus (**54, 57**) and penial papilla (**55, 58**) of *Monacha parumcincta*. Specimens from La Casella (FGC 44077) (**51–55**) and along the road from Moliterno to Fontana d’Eboli (FGC 42962) (**56–59**).



Figures 60–61. Principal component analysis (PCA) and Redundancy analysis (RDA) with clade applied to the original genitalia matrix (60) and Z-matrix (shape-related) (61). Ellipses show the 95% confidence intervals associated with each group.

and reported from the United Kingdom, Spain and Italy. The other three lineages include only two (CAN-2 and CAN-4) or three (CAN-3) populations, respectively, and at present have a narrow distribution, being known only from two sites in northern Italy (CAN-2), three sites in northern Italy and Austria (CAN-3) and two sites in south-eastern France (CAN-4) (Fig. 63). If these lineages were treated as distinct species, a taxonomical and nomenclatural setting would only be possible for CAN-1 and CAN-4 at present (a definitive framework for the other two requires more research).

Statistical analysis of a series of shell and anatomical characters shows that at least three lineages (CAN-1, CAN-2, CAN-3) cannot be distinguished from each other based on morphology and that one lineage (CAN-4) is only marginally distinct. On the contrary, these four lineages are anatomically well distinct from the *Monacha* species used for comparison (*M. parumcincta*), and three of them (CAN-1, CAN-2, CAN-3) are also conchologically distinct on the basis of many significant characters (11, 9, and 10, respectively). The major bias of morphological analysis was the small sample available for lineages CAN-2, CAN-3, and CAN-4, which prevented a realistic account of their variability.

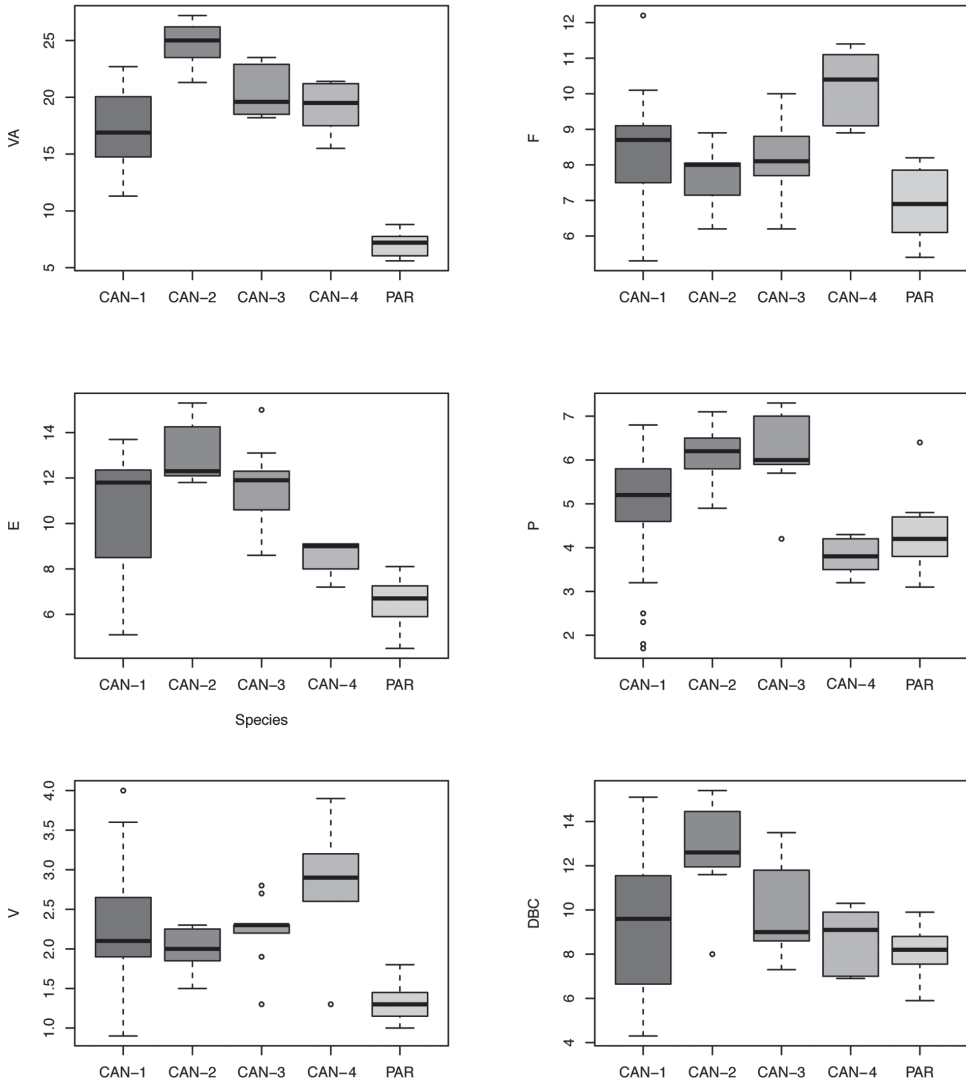


Figure 62. Box plots for anatomical characters of the five *Monacha* clades investigated. The lower and upper limits of the rectangular boxes indicate the 25th to 75th percentile range, and the horizontal line within the boxes is the median (50th percentile).

Sequences characteristic of clade CAN-1 formed a well-separated group in ML and Bayesian trees (Figs 3–5). Although they were all from UK and Italian populations, they are mixed together in the trees without separate branches for UK and Italian populations. Interestingly, three pairs of haplotypes or common sequences are identical: UK-COI 2 / IT-COI 2, UK-16S 2 / IT-16S 1 and UK-ITS2 2 / IT-ITS2 1. This and small K2P genetic distances within this clade (0.9% in COI, 0.5% in 16SrDNA) suggest that the clade represents one taxon. CAN-1 corresponds to the true *M. cantiana* because it is the only clade that includes topotypical English populations. Close rela-

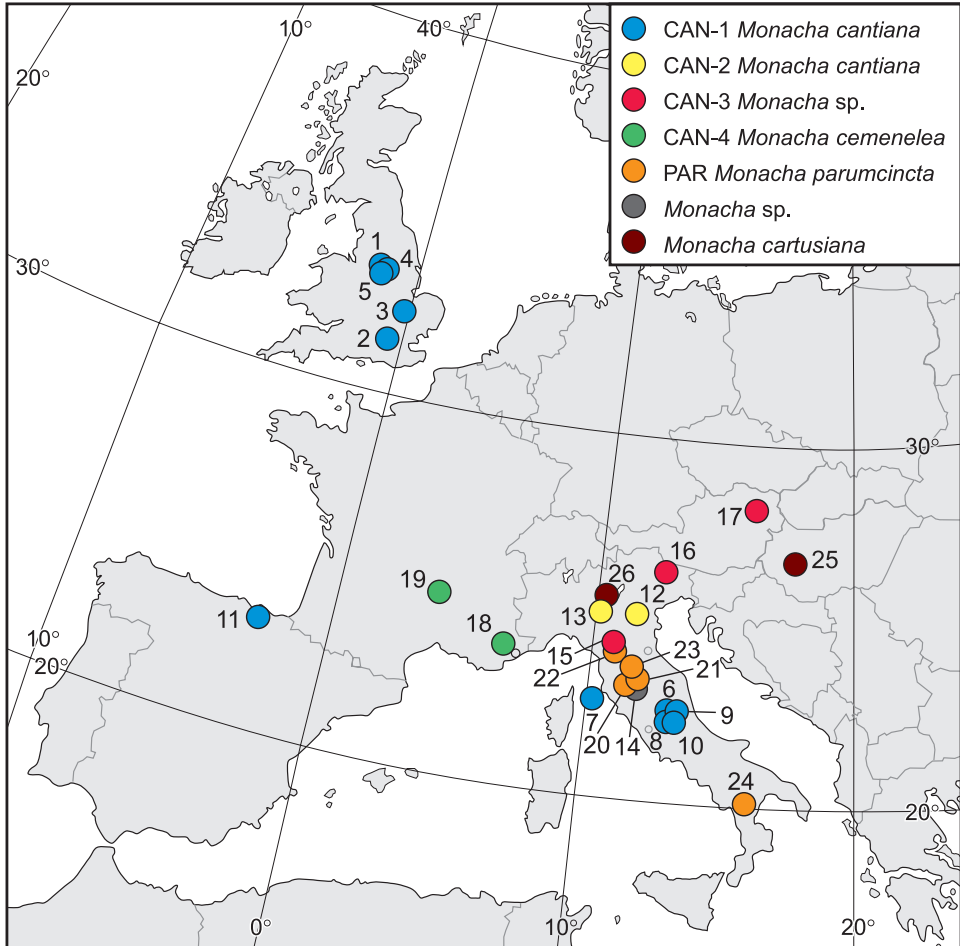


Figure 63. Localities of *Monacha cantiana*, *M. parumcincta* and *M. cartusiana* specimens where they were collected for the research (see Table 1 for locality numbers).

tions between the sequences studied (clade CAN-1 in Figs 3–5) support the conclusion that the populations have a common Mediterranean origin (Neiber and Hausdorf 2017), which in view of available fossil record (Kerney et al. 1964, Kerney 1970, Evans 1972), may be postulated to date back to the Roman conquest. The same is also true for the Spanish populations from Pais Vasco (Sopelana), whose sequences (KX507234 and KJ458539 / KX495428), deposited in GenBank for COI and 16SrDNA of *M. cantiana* (Neiber and Hausdorf 2015, Razkin et al. 2015), respectively, were located between our UK and Italian (Latium sites close to Rome) populations in our ML trees (Fig. 64). Nevertheless further studies on molecular characteristics of *M. cantiana* populations from Scotland, N France, N Germany, Belgium, and The Netherlands are necessary in order to test this hypothesis.

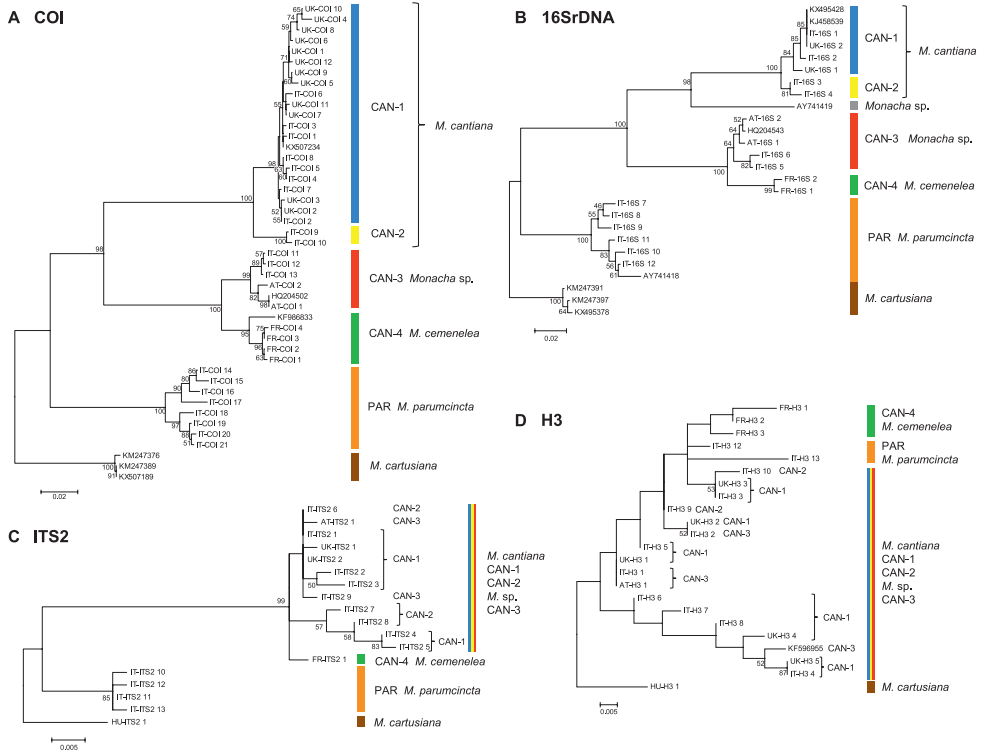


Figure 64. Maximum Likelihood trees of COI, 16SrDNA, H3, and ITS2 sequences of *Monacha cantiana* group. Bootstrap analysis was run with 1000 replicates (Felsenstein 1985). Numbers on branches represent bootstrap support above 50%. **A** the COI sequences of *Monacha cartusiana* KM247389, KM247376 and KX507189 were used as an outgroup, and those of *M. cantiana* KF986833, KX507234 and HQ204502 as reference sequences. 592-bp sequences of new COI haplotypes (Table 1) were shortened to a 556-bp fragment for alignment with the GenBank sequences used as outgroup or references **B** the 16SrDNA sequences of *Monacha cartusiana* KM247391, KM247397 and KX495378 sequences were chosen as outgroup. *M. cantiana* AY741419, HQ204543, KJ458539 and KX495428 as well as *M. parumcincta* AY741418 sequences were used as references. The final dataset contained 287 positions **C** the ITS2 tree was rooted with *Monacha cartusiana* sequence MH137993 **D** the H3 tree was rooted with *Monacha cartusiana* sequence MG209072. *Monacha cantiana* KF596955 was used as a reference.

The three percent threshold for genetic distance between COI barcode sequences was established by Hebert et al. (2003a, 2003b) as a criterion for the description of a new taxon at species level. There are many papers concerning usefulness of barcoding in taxonomy (e.g., Ebach and Holdrege 2005, Gregory 2005, Goldstein and DeSalle 2010) and showing that 3% threshold should be higher (4% or even higher) for stylummatophoran gastropods (Davison et al. 2009, Sauer and Hausdorf 2012 and references cited therein). Aware of it we think that the slightly exceeded barcode threshold in K2P distances between COI sequences of CAN-1 and CAN-2 clades together with the lack of significant differences in shell (Fig. 19) and genitalia features (Fig. 62), do

not permit to introduce a distinct taxon, even at subspecies level. Rather, the K2P distances show that some Italian populations of the *M. cantiana* group are in a process of speciation and differentiation.

The cases of the clades CAN-3 and CAN-4 are completely different, since K2P genetic distances distinguish the haplotypes of these two clades from the others (CAN-1, CAN-2, PAR) and were well above Hebert's threshold (even enlarged according to Davison et al. 2009). However, due to the lack of differences in anatomical and conchological features between CAN-3 and clades CAN-1 and CAN-2, we treat CAN-3 as mitochondrially distinct lineage only. Any taxonomic conclusion would be premature.

The situation of clade CAN-4 is distinct because this lineage includes a French population which can be considered topotypical of *Theba cemenolea*. Live specimens were collected by one of us (AH) at Sainte Thecle, Vallée de Peillon, a site located 10 km NE of Risso's original locality: Colline de Cimiez at Nice, now in the urban area of Nice. It was regarded as a junior synonym or at least a subspecies of *M. cantiana* until the early 2000s, when Falkner et al. (2002) separated it again on the basis of the presence of well evident basal sac of the vaginal appendix considered instead absent in *M. cantiana*. Since type material of *T. cemenolea* no longer exists (Chevallier 1976, Arnaud 1977), only designation of a neotype can ensure correct univocal application of Risso's name. We therefore select a specimen collected at Sainte Thecle in Vallée de Peillon as the neotype. The neotype is deposited in the malacological collection of the Museo di Storia Naturale dell'Accademia dei Fisiocritici, Siena (MOLL/3309). Its shell is illustrated in Fig. 16 and its genital anatomy in Figs 38–41. The separation of CAN-4 (*M. cemenolea*) is strongly supported by nucleotide sequence analysis of both mitochondrial and nuclear genes (Figs 3–5, 64). Therefore haplotypes of COI and 16SrDNA as well as sequences of H3 and ITS2 gene fragments characteristic of specimens from this population have been deposited in GenBank (accession Numbers for FR-COI 1–4: MG208939–MG208943; for FR-16S 1–2: MG209011–MG209015; for FR-H3 1–3: MG209058–MG209060; for FR-ITS2 1: MH137984).

Designation of the neotype is in line with the current concept of this *Monacha* species (e.g., Falkner et al. 2002) i.e., a species distinguished by a well evident basal sac of the vaginal appendix. Contrarily to what has been stated by Falkner et al. (2002), this basal sac is present but smaller or sometimes absent in *M. cantiana*. Moreover this taxonomic setting based on genitalia features is supported by molecular features of mitochondrial and nuclear genes.

A singular sequence AY741419 from Podere Grania, Asciano, Siena deposited in GenBank by Manganelli et al. (2005) for 16SrDNA (Fig. 64B, Table 1) as well as our not yet published molecular results for certain Italian populations (from Alpi Apuane, Tuscany) suggest that Italian *M. cantiana* may include other lineages.

All our results, namely shell (Figs 17–19) and genital (Figs 60–62) structures and molecular evidence of separate clades for each tree (Figs 3–5, 64), show that *M. parumcincta* and *M. cantiana* are distinct taxa. However the definitive taxonomic and nomenclatural setting of *M. parumcincta* is still unclear (see Forcart 1965, Manganelli et al. 1995, Welter-Schultes 2012). This and its infraspecific variation will be the subject of further studies.

Acknowledgements

We are grateful to Robert A.D. Cameron (University of Sheffield, UK), Michael Duda (Natural History Museum Vienna, Austria) and Małgorzata Proćków (University of Wrocław, Poland) for providing specimens. We also thank Bernhard Hausdorf (University of Hamburg, Germany) and Robert A.D. Cameron (University of Sheffield, UK) for their comments on the manuscript, Francisco Welter-Schultes (University of Göttingen, Germany) for a discussion on the nomenclatural items, Jarosław Bogucki (Poznań, Poland) for drawing the Fig. 63, Helen Ampt (Siena, Italy) for revising English, and Giovanni Cappelli (Siena, Italy) for taking photos of the shells.

References

- Almeyda-Artigas RJ, Bargues MD, Mas-Coma S (2000) ITS-2 rDNA sequencing of *Gnathostoma* species (Nematoda) and elucidation of the species causing human gnathostomiasis in the Americas. *Journal of Parasitology* 86: 537–544. <http://www.jstor.org/stable/3284869>
- Arnaud PM (1977) Revision des taxa malacologiques mediterraneens introduits par Antoine Risso. *Annales du Museum d'Histoire Naturelle de Nice* 5: 101–150. <http://paleopolis.rediris.es/benthos/TaP/Arnaud-1977.pdf>
- Bandelt H-J, Forster P, Röhl A (1999) Median-joining networks for inferring intraspecific phylogenies. *Molecular Biology Evolution* 16: 37–48. <https://doi.org/10.1093/oxfordjournals.molbev.a026036>
- Cadahia L, Harl J, Duda M, Sattmann H, Kruckenhauser L, Feher Z, Zopp L, Haring E (2014) New data on the phylogeny of Ariantinae (Pulmonata, Helicidae) and the systematic position of *Cylindrus obtusus* based on nuclear and mitochondrial DNA marker sequences. *Journal of Zoological Systematics and Evolutionary Research* 52: 163–169. <https://doi.org/10.1111/jzs.12044>
- Cadima JFCL, Jolliffe IT (1996) Size- and shape-related principal component analysis. *Biometrics* 52: 710–716. <https://doi.org/10.2307/2532909>
- Caruso T, Chemello R (2009) The size and shape of shells used by hermit crabs: a multivariate analysis of *Clibanarius erythropus*. *Acta Oecologica* 35: 349–354. <https://doi.org/10.1016/j.actao.2009.03.002>
- Castresana J (2000) Selection of conserved blocks from multiple alignments for their use in phylogenetic analysis. *Molecular Biology and Evolution* 17: 540–552. <https://doi.org/10.1093/oxfordjournals.molbev.a026334>
- Chevallier H (1976) Types des especes continentales de la collection Risso du Museum national d'Histoire naturelle (Departement de Malacologie). *Elona* 3: 38–40.
- Colgan DJ, McLauchlan A, Wilson GDF, Livingston S, Edgecombe GD, Macaranas J, Cassis G, Gray MR (1998) Histone H3 and U2 snRNA sequences and arthropod molecular evolution. *Australian Journal of Zoology* 46: 419–437. <https://doi.org/10.1071/zo98048>
- Dabert M, Witalinski W, Kazmierski A, Olszanowski Z, Dabert J (2010) Molecular phylogeny of acariform mites (Acari, Arachnida): Strong conflict between phylogenetic signal

- and long-branch attraction artifacts. *Molecular Phylogenetics and Evolution* 56: 222–241. <https://doi.org/10.1016/j.ympev.2009.12.020>
- Dahirel M, Olivier E, Guiller A, Martin M-C, Madec L, Ansart A (2015) Movement propensity and ability correlate with ecological specialization in European land snails: comparative analysis of a dispersal syndrome. *Journal of Animal Ecology* 84: 228–238. <https://doi.org/10.1111/1365-2656.12276>
- Darriba D, Taboada GL, Doallo R, Posada D (2012) jModelTest 2: more models, new heuristics and parallel computing. *Nature Methods* 9: 772. <https://doi.org/10.1038/nmeth.2109>
- Davison A, Blackie RL, Scothern GP (2009) DNA barcoding of stylommatophoran land snail: a test of existing sequences. *Molecular Ecology Resources* 9: 1092–1101. <https://doi.org/10.1111/j.1755-0998.2009.02559x>
- Duda M, Sattmann H, Haring E, Bartel D, Winkler H, Harl J, Kruckenhauser L (2011) Genetic differentiation and shell morphology of *Trochulus oreinos* (Wagner, 1915) and *T. hispidus* (Linnaeus, 1758) (Pulmonata: Hygromiidae) in the northeastern alps. *Journal of Molluscan Studies* 77: 30–40. <https://doi.org/10.1093/mollus/eyq037>
- Ebach MC, Holdrege C (2005) More taxonomy, not DNA barcoding. *BioScience* 55: 822–823. [https://doi.org/10.1641/0006-3568\(2005\)055\[0823:MTNDB\]2.0.CO;2](https://doi.org/10.1641/0006-3568(2005)055[0823:MTNDB]2.0.CO;2)
- Ellis AE (1969) *British snails. A guide to the non-marine Gastropoda of Great Britain and Ireland Pleistocene to Recent*. Clarendon Press, Oxford, 298 pp.
- Evans JG (1972) *Land Snails in Archeology. With special reference to the British Isles*. Seminar Press Inc., London, 436 pp.
- Falkner G, Ripken ThEJ, Falkner M (2002) Mollusques continentaux de France: liste de référence annotée et bibliographie. *Patrimoines naturels*, 52, Muséum national d'Histoire naturelle, Paris, 356 pp.
- Felsenstein J (1985) Confidence limits on phylogenies: an approach using the bootstrap. *Evolution* 39: 783–791. <https://doi.org/10.2307/2408678>
- Fiorentino V, Manganelli G, Giusti F (2008) Multiple scale patterns of shell and anatomy variability in land snails: the case of the Sicilian *Marmorana* (Gastropoda: Pulmonata, Helicidae). *Biological Journal of the Linnean Society* 93: 359–370. <https://doi.org/10.1111/j.1095-8312.2007.00940.x>
- Forcart L (1965) Rezenten Land- und Süßwassermollusken der süditalienischen Landschaften Apulien, Basilicata und Calabrien. *Verhandlungen der naturforschenden Gesellschaft in Basel* 76: 59–184.
- Gantenbein B, Fet V, Largiadèr CR, Scholl A (1999) First DNA phylogeny of *Euscorpius* Thorell, 1876 (Scorpiones: Euscorpiidae) and its bearing on taxonomy and biogeography of this genus. *Biogeographica (Paris)* 75: 49–65. http://www.science.marshall.edu/fet/euscorpius/fetpubl/Gantenbein%20et%20al_1999%20Euscorpius.pdf
- Giusti F, Manganelli G (1987) Notulae Malacologicae, XXXVI. On some Hygromiidae (Gastropoda: Helicoidea) living in Sardinia and in Corsica (Studies on the Sardinian and Corsican Malacofauna VI). *Bollettino Malacologico* 23: 123–206. <https://www.biodiversitylibrary.org/page/49931331#page/147/mode/1up>
- Glez-Peña D, Gómez-Blanco D, Reboiro-Jato M, Fdez-Riverola F, Posada D (2010) ALTER: program-oriented format conversion of DNA and protein alignments. *Nucleic Acids Research* 38 (Web Server issue): W14–W18. <https://doi.org/10.1093/nar/gkq321>

- Goldstein PZ, DeSalle R (2010) Integrating DNA barcode data and taxonomic practise: determination, discovery, and description. *Bioessays* 33: 135–147. <https://doi.org/10.1002/bies.201000036>
- Gregory TR (2005) DNA barcoding does not compete with taxonomy. *Nature* 434: 1067–1068. <https://doi.org/10.1038/4341067b>
- Hall TA (1999) BioEdit: a user friendly biological sequence alignment editor and analysis program for Windows 95/98/NT. *Nucleic Acids Symposium Series* 41: 95–98. <http://brownlab.mbio.ncsu.edu/JWB/papers/1999Hall1.pdf>
- Hasegawa M, Kishino H, Yano T (1985) Dating the human-ape split by a molecular clock of mitochondrial DNA. *Journal of Molecular Evolution* 22: 160–174. <https://link.springer.com/article/10.1007/BF02101694>
- Hausdorf B (2000a) The genus *Monacha* in Turkey (Gastropoda: Pulmonata: Hygromiidae). *Archiv für Molluskenkunde* 128: 61–151. <https://doi.org/10.1127/arch.moll/128/2000/61>
- Hausdorf B (2000b) The genus *Monacha* in the Western Caucasus (Gastropoda: Hygromiidae). *Journal of Natural History* 34: 1575–1594. <https://doi.org/10.1080/00222930050117495>
- Hebert PDN, Cywinska A, Ball SL, deWaard JR (2003a) Biological identifications through DNA barcodes. *Proceedings of the Royal Society B: Biological Sciences* 270: 313–321. <https://doi.org/10.1098/rspb.2002.2218>
- Hebert PDN, Ratnasingham S, deWaard JR (2003b) Barcoding animal life: cytochrome c oxidase subunit 1 divergences among closely related species. *Proceedings of the Royal Society B: Biological Sciences* 270 (Suppl. 1): 596–599. <https://doi.org/10.1098/rsbl.2003.0025>
- Jukes TH, Cantor CR (1969) Evolution of protein molecules. In: Munro HN (Ed.) *Mammalian Protein Metabolism*. Academic Press, New York, 21–132. <http://dx.doi.org/10.1016/B978-1-4832-3211-9.50009-7>
- Kerney MP, Brown EH, Chandler TJ, Carreck JN, Lambert CA, Levy JF, Millman AP (1964) The Late-glacial and Post-glacial history of the Chalk escarpment near Brook, Kent. *Philosophical Transactions of the Royal Society of London Series B, Biological Sciences* 248: 135–204. <http://www.jstor.org/stable/2416547>
- Kerney M (1970) The British distribution of *Monacha cantiana* (Montagu) and *Monacha cartusiana* (Müller). *Journal of Conchology* 27: 145–148.
- Kerney M (1999) *Atlas of the Land and Freshwater Molluscs of Britain and Ireland*. Harley Books, Colchester, 264 pp.
- Kimura M (1980) A simple method for estimating evolutionary rate of base substitutions through comparative studies of nucleotide sequences. *Journal of Molecular Evolution* 16: 111–120. <https://doi.org/10.1007/bf01731581>
- Klingenberg CP (2016) Size, shape, and form: concepts of allometry in geometric morphometrics. *Development Genes and Evolution* 226: 113–137. <https://doi.org/10.1007/s00427-016-0539-2>
- Kruckenhauser L, Duda M, Bartel D, Sattmann H, Harl J, Kirchner S, Haring E (2014) Paraphyly and budding speciation in the hairy snail (Pulmonata, Hygromiidae). *Zoologica Scripta* 43: 273–288. <https://doi.org/10.1111/zsc.12046>
- Kumar S, Stecher G, Tamura K (2016) MEGA7: Molecular Evolutionary Genetics Analysis version 7.0 for bigger datasets. *Molecular Biology and Evolution* 33: 1870–1874. <https://doi.org/10.1093/molbev/msw054>

- Madec L, Bellido A, Guiller A (2003) Shell shape of the land snail *Cornu aspersum* in North Africa: unexpected evidence of a phylogeographical splitting. *Heredity* 91: 224–231. <https://doi.org/10.1038/sj.hdy.6800301>
- Manganelli G, Bodon M, Favilli L, Giusti F (1995) Gastropoda Pulmonata. In: Minelli A, Ruffo S, La Posta S (Eds) Checklist delle specie della fauna d'Italia, Calderini, Bologna, 16: 1–60.
- Manganelli G, Salomone N, Giusti F (2005) A molecular approach to the phylogenetic relationships of the western palaeartic Helicoidea (Gastropoda: Stylommatophora). *Biological Journal of the Linnean Society London* 85: 501–512. <https://doi.org/10.1111/j.1095-8312.2005.00514.x>
- Menke CT (1828) Synopsis methodica molluscorum generum omnium et specierum earum, quae in museo Menkeano adservantur; cum synonymia critica et novarum specierum diagnosibus. Gelpke, Pyrmonti, pp. xii + 91 pp. <https://www.biodiversitylibrary.org/item/47276#page/7/mode/1up>
- Montagu G (1803) Testacea Britannica, or, Natural history of British shells, marine, land, and fresh-water, including the most minute: systematically arranged and embellished with figures. 2 vols, Romsey, London, xxxvii + 606 pp.
- Müller OF (1774) Vermium terrestrium et fluviatilium, seu animalium infusorium, helminthicorum, et testaceorum, non marinorum, succinct historia. Vol. II. Heineck & Faber, Havniae et Lipsiae, xxxvi + 214 + 10 pp.
- Neiber MT, Hausdorf B (2015) Phylogeography of the land snail genus *Circassina* (Gastropoda: Hygromiidae) implies multiple Pleistocene refugia in the western Caucasus region. *Molecular Phylogenetics and Evolution* 93: 129–142. <https://doi.org/10.1016/j.ympev.2015.07.012>
- Neiber MT, Hausdorf B (2017) Molecular phylogeny and biogeography of the land snail genus *Monacha* (Gastropoda, Hygromiidae). *Zoologica Scripta* 46: 308–321. <https://doi.org/10.1111/zsc.12218>
- Oksanen J, Blanchet FG, Kindt R, Legendre P, Minchin PR, O'Hara RB, Simpson GL, Solyomos P, Stevens MHH, Wagner HH (2016) Vegan: Community Ecology Package. R package version 2.3-3. Available online at <http://CRAN.Rproject.org/package=vegan> [Accessed 24 September 2017]
- Paquette SR, Lapointe FJ (2007) The use of shell morphometrics for the management of the endangered Malagasy radiated tortoise (*Geochelone radiata*). *Biological Conservation* 134: 31–39. <https://doi.org/10.1016/j.biocon.2006.08.022>
- Pieńkowska J, Giusti F, Manganelli G, Lesicki A (2015) *Monacha claustralis* (Rossmässler 1834) new to Polish and Czech malacofauna (Gastropoda: Pulmonata: Hygromiidae). *Journal of Conchology* 42: 79–93. <http://docplayer.net/56112556-Monacha-claustralis-rossmassler-1834-new-to-polish-and-czech-malacofauna-gastropoda-pulmonata-hygromiidae.html>
- Razkin O, Gomez-Moliner BJ, Prieto CE, Martinez-Orti A, Arrebola JR, Munoz B, Chueca LJ, Madeira MJ (2015) Molecular phylogeny of the western Palaeartic Helicoidea (Gastropoda, Stylommatophora). *Molecular Phylogenetics and Evolution* 83: 99–117. <https://doi.org/10.1016/j.ympev.2014.11.014>
- Risso A (1826) Histoire naturelle des principales productions de l'Europe méridionale et particulièrement de celles des environs de Nice et des Alpes Maritimes. Tome quatrième. Levrault, Paris, 10+439+12 pp. <https://doi.org/10.5962/bhl.title.58984>

- Ronquist F, Huelsenbeck JP (2003) MRBAYES 3: Bayesian phylogenetic inference under mixed models. *Bioinformatics* 19: 1572–1574. <https://doi.org/10.1093/bioinformatics/btg180>
- Rossmässler EA (1834) Diagnoses conchyliorum terrestrium et fluviatilium. Zugleich zu Fascikeln natürlicher Exemplare. II Heft. No. 21–40. Arnold, Dresden & Leipzig, 8 pp. <https://doi.org/10.5962/bhl.title.10380>
- RStudio Team (2016) RStudio: Integrated Development for R. RStudio, Inc., Boston, MA Available online at <http://www.rstudio.com/> [24 September 2017]
- Saitou N, Nei M (1987) The neighbor-joining method: A new method for reconstructing phylogenetic trees. *Molecular Biology and Evolution* 4: 406–425. <https://doi.org/10.1093/oxfordjournals.molbev.a040454>
- Sauer J, Hausdorf B (2012) A comparison of DNA-based methods for delimiting species in a Cretan land snail radiation reveals shortcomings of exclusively molecular taxonomy. *Cladistics* 28: 300–316. <https://doi.org/10.1111/j.1096-0031.2011.00382.x>
- Simon C, Frati F, Beckenbach AT, Crespi B, Liu H, Flook P (1994) Evolution, weighting and phylogenetic utility of mitochondrial gene sequences and a compilation of conserved polymerase chain reaction primers. *Annals of the Entomological Society of America* 87: 651–701. <https://doi.org/10.1093/aesa/87.6.651>
- Talavera G, Castresana J (2007) Improvement of phylogenies after removing divergent and ambiguously aligned blocks from protein sequence alignments. *Systematic Biology* 56: 564–577. <https://doi.org/10.1080/10635150701472164>
- Tamura K (1992) Estimation of the number of nucleotide substitutions when there are strong transition-transversion and G + C-content biases. *Molecular Biology and Evolution* 9: 678–687. <https://doi.org/10.1093/oxfordjournals.molbev.a040752>
- Tamura K, Nei M (1993) Estimation of the number of nucleotide substitutions in the control region of mitochondrial DNA in humans and chimpanzees. *Molecular Biology and Evolution* 10: 512–526. <https://doi.org/10.1093/oxfordjournals.molbev.a040023>
- ter Braak CJF (1986) Canonical Correspondence Analysis: a new eigenvector technique for multivariate direct gradient analysis. *Ecology* 67: 1167–1179. <https://doi.org/10.2307/1938672>
- Thompson JD, Higgins DG, Gibson TJ (1994) CLUSTAL W: improving the sensitivity of progressive multiple sequence alignment through sequence weighting, position specific gap penalties and weight matrix choice. *Nucleic Acids Research* 22: 4673–4680. <https://doi.org/10.1093/nar/22.22.4673>
- Welter-Schultes FW (2012) European non-marine molluscs, a guide for species identification. Planet Poster Editions, Göttingen, 679 pp.

Longizonitis, a new nemognathine genus from the Himalayas (Coleoptera, Meloidae)

Zhao Pan¹, Guodong Ren¹, Marco A. Bologna²

1 The Key Laboratory of Zoological Systematics and Application, College of Life Sciences, Hebei University, 071002, Baoding, Hebei Province, China **2** Dipartimento di Scienze, Università degli studi Roma Tre, Viale G. Marconi 446, 00146, Roma, Italy

Corresponding author: Zhao Pan (panzhao86@yeah.net)

Academic editor: W. Steiner | Received 10 February 2018 | Accepted 16 April 2018 | Published 06 June 2018

<http://zoobank.org/649C6C5B-2891-4CA7-9F7F-0095E958CC10>

Citation: Pan Z, Ren G, Bologna MA (2018) *Longizonitis*, a new nemognathine genus from the Himalayas (Coleoptera, Meloidae). ZooKeys 765: 43–50. <https://doi.org/10.3897/zookeys.765.24395>

Abstract

The new blister beetle genus *Longizonitis* Pan and Bologna is described. The genus is referred to the tribe Nemognathini, subfamily Nemognathinae, and its relationships are briefly discussed. It is distributed in southern China (Yunnan, SE Xizang, and probably Fujian) and India (Uttarakhand), in a transitional area between the Palaearctic and Oriental regions. The type species, *Longizonitis semirubra* (Pic, 1911), **comb. n.**, is re-described and illustrated.

Keywords

Blister beetles, China, India, new genus, taxonomy

Introduction

The tribe Nemognathini Laporte de Castelnau, 1840, with approximately 530 described species, belonging to 28 genera, is the second most speciose tribe of Meloidae Gyllenhal, 1810 behind the Mylabrini Rafinesque, 1815 has a cosmopolitan distribution (Pinto and Bologna 1999, Bologna and Pinto 2002, Bologna et al. 2013). No comprehensive taxonomic revision or phylogenetic studies have been published on this tribe, but its monophyly was supported in recent papers (Bologna and Pinto 2001, Bologna et al. 2008, Bologna et al. 2013). The taxonomic validity of some genera was

debated and possible new genera were highlighted by Bologna and Pinto (2002) and Bologna et al. (2013). In particular, the genus *Zonitis* Fabricius, 1775 seems to have been used as ‘dumping ground’ especially for Afrotropical, Oriental and Neotropical species (Bologna and Pinto 2002, Bologna et al. 2013, Bologna unpublished). Species of this genus have been reviewed for the Nearctic (Enns 1956) and partially for the western Palaearctic (Escherich 1897) regions, while most of the Afrotropical species referred to this genus by Kaszab (1954) actually belong to other genera such as *Palaestra* Laporte de Castelnau, 1840, *Zoltanzonitis* Bologna & Pinto (in press), *Zonitodema* Péringuey, 1909 and *Zonitoschema* Péringuey, 1909 (Bologna unpublished). The Australasian species belong to several genera (see Bologna et al. 2013).

During the study of type specimens of Meloidae housed at MNHN, it was discovered that *Zonitis semirubra* Pic, 1911 (Figs 1–3) does not belong to the genus *Zonitis*. Four other specimens were found at BMNH and HBUM (see below for the abbreviations) and, after the examination of male genitalia, it is clear that *Zonitis semirubra* belongs to a new genus, which is described here together with a re-description of the type species.

Materials and methods

The following abbreviations used in the text refer to the examined collections:

BMNH Natural History Museum, London, United Kingdom;

HBUM Hebei University Museum, Baoding, China;

MNHN Muséum National d’Histoire Naturelle, Paris, France.

Figures of antennal morphological details were drawn by hand, using a Nikon SMZ1500 stereomicroscope equipped with a camera lucida. Photographs of other morphological details were taken using a Leica M205A stereomicroscope equipped with a Leica DFC450 camera which was controlled using the Leica application suite 4.3. Habitus were taken with a Canon EOS 5D Mark III camera connected to a Canon MP-E 65 mm macro lens.

Taxonomy

Longizonitis Pan & Bologna, gen. n.

<http://zoobank.org/5781AD01-3736-48F5-BA90-BA2E4AE657E5>

Type species. *Zonitis semirubra* Pic, 1911 (originally described as *Zonitis semiruber*) by present designation.

Etymology. From the Latin adjective ‘*longus*’ and *Zonitis*. The name refers to the slender shape of body, which differs from that of several other nemognathine genera.

Diagnosis. *Longizonitis* is clearly distinguishable from other nemognathine genera by the following characters: body elongate, length-width ratio distinctly more than 3.5; antennomere II distinctly shorter than III; elytra not reduced in size, only slightly dehiscent apically; tarsal claws with ventral blade narrow, its greatest width slightly more than half the basal width of dorsal blade; female with two metatibial spurs similar in shape and size, male external metatibial spur as in female, inner one stick-liked and only half width of external one; male ventrite VI completely divided, that of female V-emarginate; aedeagus without dorsal hooks, but with two sclerotised ventral lobes, curved posteriorly; gonostyli almost completely fused, gonocoxal plate longer than gonostyli.

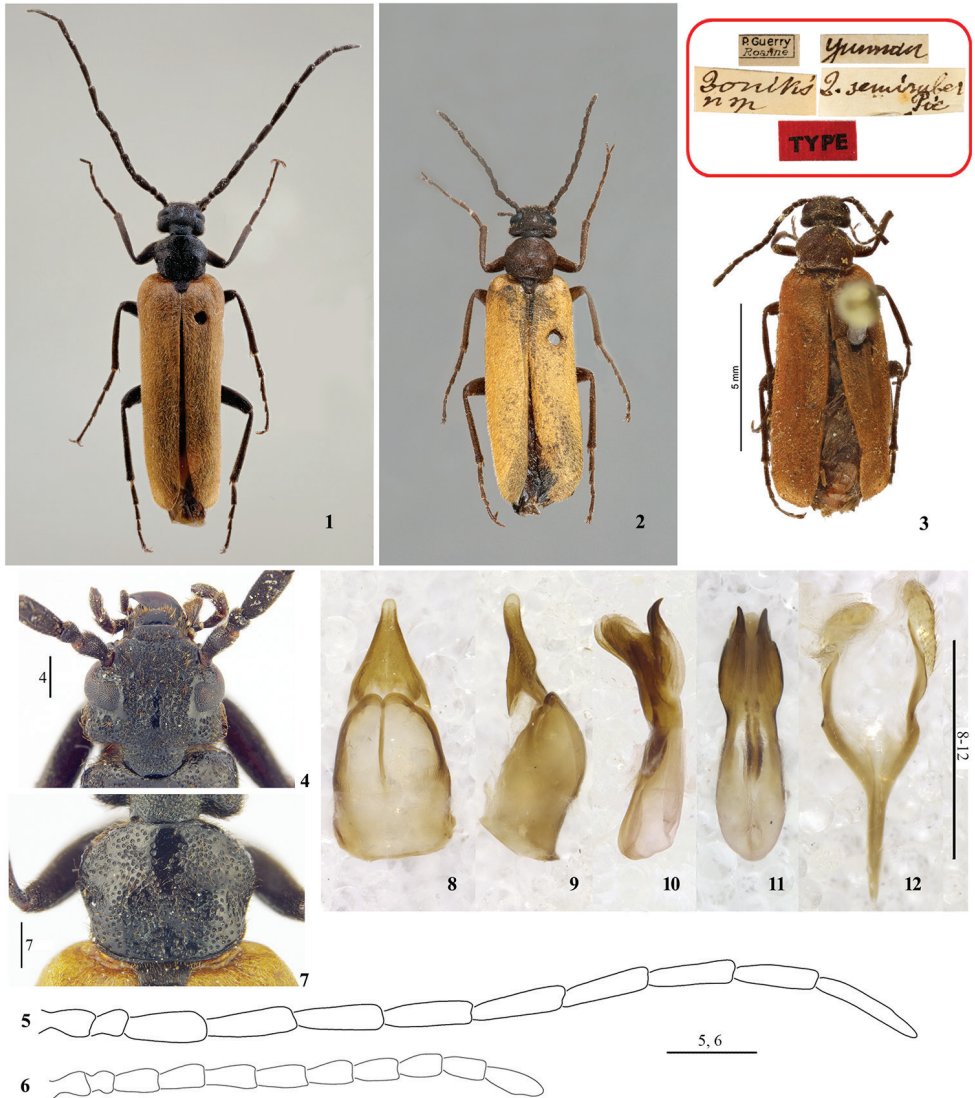
Description. Head short, subrectangular, head width at temples slightly greater than at eyes, frons not depressed, surface with dense, large and shallow punctures (Fig. 4). Eyes normal in size, only extending ventrally to outer margin of maxillae on underside of head, slightly emarginate on fore margin near base of antenna. Mandibles robust and long, extending beyond fore margin of labrum; galeae short and fringed (as in fig. 71, Bologna and Pinto 2002); maxillary palpi four segmented, palpomeres not elongate, last palpomere not widening at apex. Antennae with eleven antennomeres, filiform, elongate and slender; antennae slightly longer than elytral length in male (Figs 1, 5), and shorter in female (Figs 2, 3); male antennomere II short, subglobose, about as wide as long, apical antennomeres equal in width to basal ones; female antennomeres distinctly shorter than in male, XI almost suboval (Figs 2, 3, 6).

Pronotum wider than long, punctures as on head, slightly more scattered (Fig. 7). Elytra elongate, normal, not reduced in size, slightly dehiscent apically on inner margin; each elytron with four weak costae and with dense short setae. Hindwings present and regularly developed. Legs not modified in both sexes; both female metatibial spurs wide, spatulate and concave dorsally, similar and subequal in length and width; male external metatibial spur as in female, inner spur stick-liked and only half the width of external spur; tarsal claws with ventral blade narrow, its greatest width slightly more than half basal width of dorsal blade (as in fig. 100, Bologna and Pinto 2002); dorsal blade of claw with two rows of teeth along its ventral margin, outer row incomplete.

Male ventrite VI deeply cleft to base and completely divided longitudinally (as in fig. 105, Bologna and Pinto 2002); slightly V-emarginate in female. Male gonostyli almost completely fused, slightly separate at apex; gonocoxal plate longer than wide and longer than gonostyli, gibbous ventrally (Figs 8, 9). Aedeagus subcylindrical, without dorsal hooks, but with two sclerotised ventral lobes curved posteriorly; endophallus without hook (Figs 10, 11).

Distribution. Southern China, northwestern India.

Relationships. The new genus differs from all known Nemognathinae taxa and shows mixed distribution of character states; for this reason, their relationships remain difficult to define. It clearly belongs to the tribe Nemognathini and not to the Palaestrini Bologna, Turco & Pinto, 2013 or Horiini Latreille, 1802, due to the cylindrical shape of the aedeagus and unmodified mandibles (see Bologna et al. 2013). Among the tribe Nemognathini, the antennomere II distinctly shorter than III (typical of Palaes-



Figures 1–12. *Longizonitis semirubra* (Pic, 1911), adult **1** habitus, male, Yadong, Xizang (HBUM) **2** habitus, female, Yadong of Xizang (HBUM) **3** holotype and labels, female, Yunnan (MNHN, photographed by Dr Antoine Mantilleri) **4** head, dorsal view, male **5** antenna, male **6** antenna, female **7** pronotum, dorsal view, male **8–12** male genitalia **8** gonoforceps, ventral view **9** gonoforceps, lateral view **10** aedeagus, lateral view **11** aedeagus, ventral view **12** *spiculum gastrale*. Scale bars: 0.5 mm (**4**, **7**); 1 mm (**5**, **6**, **8–12**).

trini) is an uncommon condition, present only in a few taxa, though notably occurring in the Afrotropical genus *Zoltanzonitis* (Bologna and Pinto, in press). The shortened antennomere II is also present in the *Nemognatha*-lineage as defined by Bologna et al. (2103) (*Palaestrída* White, 1846, some Nearctic *Nemognatha* Illiger, 1807), in which, however, lack ventral sclerotized lobes of aedeagus.

Ventral sclerotised lobes are present in all New World *Zonitis*, *Pseudozonitis* Dillon, 1952 and *Gnathium* Kirby, 1818 species, and some Palearctic species of *Zonitis*; however, the short antennomere II is never represented in the American species.

In the new genus, galeae are neither penicillate nor greatly modified, a plesiomorphic condition more similar to that of Nemognathini of the sitarine lineage than that of typical lineage (see Bologna et al. 2008 for the lineages definition). Additionally, the shape of pronotum differs from that of most Nemognathini, except for some of the sitarine lineage.

***Longizonitis semirubra* (Pic, 1911), comb. n.**

Zonitis semiruber Pic, 1911: 101 (type locality: Yunnan, China; type depository: MNHN); Borchmann, 1917: 164; 1941: 23.

Zonitis semirubra: Hua, 2002: 131.

Zonitis (Zonitis) semirubra: Bologna, 2008: 411.

Diagnosis. This species, the only known member of the genus *Longizonitis*, can be diagnosed by the generic diagnosis given above. Because Pic's (1911) description is very short and provides limited morphological data, a detailed re-description of the species based on new specimens from Xizang, Yadong (China) and Uttarakhand, Kumaon (India), is provided below.

Re-description. Characters of the genus (see above) with the following details. Body (Figs 1–3) without metallic reflections, black except elytra reddish brown and last three or all abdominal ventrites yellow. Body with dense, yellow-brown, short setae. Body length (apex of mandibles – apex of elytra): 9.4–12.0 mm; body width (elytral width at widest point): 2.7–3.1 mm.

Head slightly wider than long (from fronto-clypeal suture to posterior margin of head), with maximum width at level of temples (Fig. 4). Punctures separated by less than their width, with a longitudinal impunctate area on centre of frons and around eyes (Fig. 4). Temple curved posteriorly and almost as long as length of eye. Clypeus slightly narrower than interocular width, rounded on sides, posteriorly with punctures similar to those of frons and anteriorly almost smooth and slightly sloping; labrum scarcely narrower than clypeus, rounded on sides, fore margin almost straight in both sexes, medially not depressed. Mandibles curved and progressively narrowed on apical half. Antennomere I longer than II, III–X subcylindrical and slender, similar in length, XI nearly 1.5 times as long as X, subcylindrical but narrowed in apical third; male antennomeres I and II as long as in female, III–XI considerably longer than in female (Figs 5, 6).

Pronotum slightly wider than head at temples, widest just in front of middle, rounded on sides, distinctly narrowed anteriorly and slightly posteriorly; two bulging areas behind the widest point (Fig. 7). Elytra unicolourous, elongate, approximately 2.8 times as long as wide. Legs slender; protibiae and mesotibiae with two spurs in both sexes, both slender, pointed apically and similar in length; metatibial spurs both



Figure 13. Distribution of *Longizonitis semirubra* (Pic).

spatulate in female, male external metatibial spur as similar as female, inner one stick-like and only half width of external one; tarsomeres in both sexes without pads; protarsi evidently longer than protibiae, protarsomeres longer than wide; teeth on ventral margin of dorsal blade of tarsal claws present only in basal half on outer row.

Male gonoforceps (Fig. 8) in ventral view subtriangular; *spiculum gastrale* Y-shaped (Fig. 12).

Material examined. *Type.* Holotype female, “P. Guerry // Roanne” (white, rectangular, printed), “Yunnan” (white, rectangular, handwritten), “*Zonitis* n. sp.” (white, rectangular, handwritten), “*Z. semiruber* Pic” (white, rectangular, handwritten), “TYPE” (red, rectangular, printed, added subsequently) (MNHN; as Fig. 3).

Other specimens. 1 male, 2 females, “2005-7-22 // 西藏亚东 // 石爱民 // 河北大学博物馆 [2005-7-22 // China, Xizang, Yadong // Shi Aimin // Hebei University Museum]” (white, rectangular, printed) (HBUM; as Figs 1–2). 1 male, 1 female, “2017-VI-23 // 西藏亚东下亚东 // 邱见玥、许浩 // 河北大学博物馆 [2017-VI-23 // China, Xizang, Yadong, Xiayadong // Qiu Jianyue & Xu Hao leg. // Hebei University Museum]” (white, rectangular, printed) (HBUM). 1 male, “Kumaon Ramgahr, 6000’ [= 1828 m ca.], 21–26.viii.(19)18, Fletcher coll.; ex coll. Pasa Inst., B.M. 1924–220” (BMNH).

Distribution. (Fig. 13) CHINA: Fujian? (Borchmann 1941, Hua 2002), Yunnan (Pic 1911, Borchmann 1917, Hua 2002; MNHN), SE Xizang (HBUM). INDIA: Uttarakhand (BMNH).

Remarks. The holotype and one of the female specimens from Yadong have a dark reddish body colouration that could be caused by the following reasons: 1) the curation and conservation conditions would make the colour change from black to dark reddish over time; 2) these individuals may still be somewhat teneral, and the integument was not completely sclerotized and/or pigmented.

The name of this species was emended as *semirubra* by Hua (2002) because *Zonitis* is a female genus and in Latin the adjective *ruber* is masculine and *rubra* is feminine.

Borchmann (1941) recorded three specimens from “Kwangtsch-Fukien”, which corresponds to Hangchuan in the Fujian province of China. However, this locality

is far from others Chinese recorded (Yunnan, Xizang) and it is doubtful because it is located in tropical coastal region of China, while other localities are in high mountain regions. We are not sure if this record is correct because Borchmann (1941) indicated that the identification was in doubt due to the short description published by Pic (1911). This specimen is probably housed at the Bonn Museum (Germany).

Acknowledgments

We wish to thank particularly Dr Antoine Mantilleri (MNHN) and Dr Max Barclay (BMNH) for their scientific help during the study period of two of us (ZP, MAB) on collections of Paris and London museums and took the habitus of the type. Thanks to three reviewers, Prof. John D. Pinto (University of California), Dr M. Andrew Johnston (Arizona State University), and Dr Michael Thomas (Florida Department of Agriculture and Consumer Services), for constructive comments.

This study was supported by grants from the Construction Foundation for Comprehensive Strength Promotion of Universities in Mid-western China to Hebei University, the Postdoctoral Research Foundation of Hebei Province (No. B2015003007), the Key Laboratory of Zoological Systematics and Application (No. 14967611D), and the National Natural Foundation of China (No. 31572309).

References

- Bologna MA (2008) Meloidae. In: Löbl I, Smetana A (Eds) Catalogue of Palaearctic Coleoptera (Vol. 5: Tenebrionoidea). Apollo Books, Stenstrup, 384–390.
- Bologna MA, Pinto JD (2001) Phylogenetic studies of Meloidae (Coleoptera), with emphasis on the evolution of phoresy. *Systematic Entomology* 26: 33–72. <http://dx.doi.org/10.1046/j.1365-3113.2001.00132.x>
- Bologna MA, Pinto JD (2002) The Old World genera of Meloidae (Coleoptera): a key and synopsis. *Journal of Natural History* 36: 2013–2102. <http://dx.doi.org/10.1080/00222930110062318>
- Bologna MA, Pinto JD (in press) *Zoltanzonitis* a new genus of Afrotropical Nemognathinae (Coleoptera: Meloidae). *African Entomology*.
- Bologna MA, Oliverio M, Pitzalis M, Mariottini P (2008) Phylogeny and evolutionary history of the blister beetles (Coleoptera, Meloidae). *Molecular Phylogenetics and Evolution* 48: 679–693. <http://dx.doi.org/10.1016/j.ympev.2008.04.019>
- Bologna MA, Turco F, Pinto JD (2013) The Meloidae (Coleoptera) of Australasia: a generic review, descriptions of new taxa, and a challenge to the current definition of subfamilies posed by exceptional variation in male genitalia. *Invertebrate Systematics* 27: 391–427. <http://dx.doi.org/10.1071/IS12054>
- Borchmann F (1917) Pars 69: Meloidae, Cephaloidae. W. Junk, Berlin.
- Borchmann F (1941) Über die von Herrn J. Klapperich in China gesammelten Heteromeren. *Entomologische Blätter* 37: 22–29.

- Enns WR (1956) A revision of the genera *Nemognatha*, *Zonitis* and *Pseudozonitis* (Coleoptera, Meloidae) in America North of Mexico, with a proposed new genus. The University of Kansas Science Bulletin 37: 685–909. <https://doi.org/10.5962/bhl.part.24548>
- Escherich KL (1897) Revision der palaearktischen Zonitiden, einer Unterfamilie der Meloiden. Verhandlungen des Naturforschenden Vereines in Brünn 35: 96–132.
- Hua LZ (2002) Meloidae. List of Chinese Insects (Vol. II). Zhongshan (San Yat-sen) University Press, Guangzhou, 129–131.
- Kaszab Z (1954) Die aethiopischen Arten der Gattung *Zonitis* Fabr. (Coleoptera Meloidae). Revue de Zoologie et Botanique Africaine 50: 17–28.
- Pic M (1911) Coléoptères exotiques nouveaux ou peu connus (Suite). L'Échange, Revue Linnéenne 27: 99–101.
- Pinto JD, Bologna MA (1999) The New World genera of Meloidae (Coleoptera): a key and synopsis. Journal of Natural History 33: 569–620. <http://dx.doi.org/10.1080/002229399300254>

Two new species of the genus *Dryopomorphus* Hinton, 1936 from China (Coleoptera, Elmidae)

Dongju Bian¹, Xue Dong^{1,2}, Yunfei Peng^{1,2}

1 CAS Key Laboratory of Forest Ecology and Management, Institute of Applied Ecology, Shenyang 110016, China

2 Graduate University of Chinese Academy of Sciences, Beijing 100039, China

Corresponding author: Dongju Bian (biandongju@163.com)

Academic editor: M. Michat | Received 9 February 2018 | Accepted 19 May 2018 | Published 6 June 2018

<http://zoobank.org/BEAF294C-4418-4888-BF03-B528582AC700>

Citation: Bian D, Dong X, Peng Y (2018) Two new species of the genus *Dryopomorphus* Hinton, 1936 from China (Coleoptera, Elmidae). ZooKeys 765: 51–58. <https://doi.org/10.3897/zookeys.765.24366>

Abstract

Two new species of the genus *Dryopomorphus* Hinton, 1936 are described from China: *Dryopomorphus heineri* sp. n. and *D. ruiлиensis* sp. n. Habitus photographs and detailed line drawings of the male genitalia are provided.

Keywords

Dryopomorphus, Guangdong, Riffle beetle, taxonomy, Yunnan

Introduction

The genus *Dryopomorphus* Hinton, 1936 occurs in eastern Asia, from China and Japan to Malaysia and Brunei. Fourteen species of this genus were described until now (Hinton 1971, Spangler 1985, Kodada 1993, Yoshitomi and Satô 2005, Čiampor and Kodada 2006, Čiampor et al. 2012, Yoshitomi and Jeng 2013, Jäch et al. 2016). Yoshitomi and Satô (2005) reviewed the four species of Japan. Čiampor et al. (2012) reviewed the *Dryopomorphus* species of Malaysia, from where three known species were diagnosed and five new species were described.

The presence of the genus *Dryopomorphus* in China was indicated by Jäch and Kodada (1995) based on specimens collected during the China Water Beetle Survey (CWBS), but the authors did not give detailed species information. In the catalogue of Elmidae (Jäch et al. 2016), there is no record of this genus from China, so this is the first time that the genus *Dryopomorphus* is reported from China formally. In this article, two new species of this genus, collected during the China Water Beetle Survey, are described.

Materials and methods

Specimens were examined with a Leica M205c stereomicroscope and an Olympus BX51 compound microscope. Genitalia were drawn with the aid of a drawing tube. Male genitalia were placed in concentrated lactic acid in a cavity slide for at least several hours before they were examined. Habitus photographs were made with a KEYENCE VHX-2000 – Super Resolution Digital Microscope System. Label data are cited verbatim, with separate lines on the same label indicated by a slash “/”; different labels are separated by a vertical line “|”.

Abbreviations used in the text:

BL	body length = PL+EL,	EL	elytral length,
BW	maximum width of body,	EW	maximum width of elytra,
PL	pronotal length,	CWBS	China Water Beetle Survey,
PW	maximum width of pronotum.		

The type specimens of the new species are deposited in the Institute of Applied Ecology, Chinese Academy of Sciences, Shenyang, China (**IAECAS**) and in the Natural History Museum Vienna, Austria (**NMW**).

Taxonomy

Dryopomorphus heineri sp. n.

<http://zoobank.org/A1F823DD-1B47-42F6-BED0-17172409D63F>

Figures 1–2, 5–7

Type material. Holotype, male (IAECAS): “CHINA: Guangdong, Yunfu, / Yu’nan, Tongle Mountains, | 23°11'49"N, 111°23'6"E, 278m, / 2017.11.16, Leg. Peng & Sun (10)”; Paratypes: 1 male (IAECAS), same data as holotype; 1 male (IAECAS): “CHINA: Guangdong, Maoming, / 22°16'22"N, 111°14'29"E, | 994m 2017.11.19 / Leg. Peng & Sun (17)”; 2 exs. (NMW): “CHINA: Guangdong Prov. / 38 km ENE Zengcheng / 23°16'37"N, 114°03'19"E / 11.11.2001, ca. 200 m / Komarek & Wang (CWBS 489) ”; 1 ex. (NMW): “CHINA: Guangdong Prov. / 45 km N Zengcheng / 23°37'28"N, 113°50'10"E / 13.11.2001, ca. 500 m / leg. M. Wang (CWBS 495)”.

Diagnosis. Body elongate suboval, distinctly convex, large (BL: 3.64–3.81 mm), head and pronotum dark brown, elytra brown; anterior angles of pronotum explanate, distinctly protruding, median sulcus of pronotum clearly impressed from basal 0.1 to 0.6, sublateral sulci present in basal 0.4; elytral intervals 3, 5, 7 slightly elevated in basal third. This species is similar to *D. siamensis* Kodada, 1993 by parameres being angulate at apex, but it can be distinguished by its smaller and slimmer penis, which is distinctly shorter than the parameres.

Description (holotype). Body elongate oval, BL 3.64 mm, BW 1.71 mm, distinctly convex dorsally, for habitus see figures 1–2, dorsal surface with dense short adpressed yellowish setae and sparse long semi-erect setae. Head and pronotum dark brown, elytra brown, antennae yellowish brown, frons and all legs reddish brown.

Head. Labrum short, partly concealed by clypeus, anterior margin truncate with dense yellowish long setae laterally. Clypeus approx. twice as wide as long, slightly emarginated anteriorly, densely punctate and pubescent. Frontoclypeal suture straight, distinct, but not deeply impressed. Vertex densely punctate, setose, with dark triangular area. Eyes large, slightly protruding from head outline, sub-triangular in lateral view.

Thorax. Pronotum broadest at base, PL 0.99 mm, PW 1.56 mm. Disc convex, punctures densely impressed on entire surface, lateral margin narrowly ridged, slightly converging anteriorly, anterior angles explanate, distinctly protruding. Median sulcus well impressed from basal 0.1 to 0.6, sublateral sulci present in basal 0.4. Prosternal process approx. 1.7 times as long as prosternum in front of coxae, lateral margin raised, distal 0.4 distinctly narrowed, ending with narrowly rounded apex, a pair of lateral protuberances at basal 0.6, surface covered with dense long setae. Mesoventrite distinctly constricted between coxae. Metaventrite with anterior 1/3 impressed between coxae; discrimen thin, present along entire length.

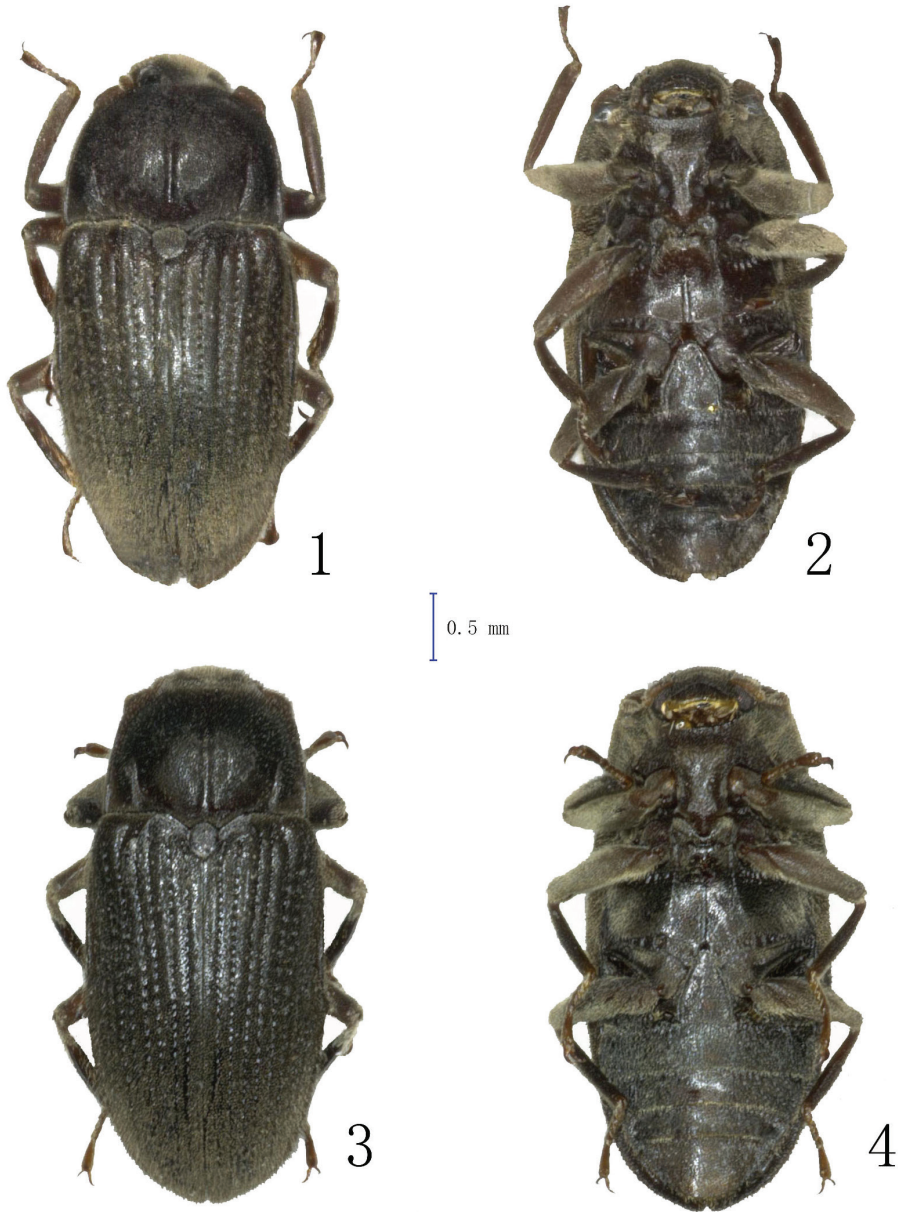
Elytra. EL 2.71 mm, EW 1.71 mm, distinctly convex, basal 1/2 subparallel, then converging to separately rounded apices, densely punctate and pubescent. Each elytron with 10 striae, punctures in discal part of striae medium-sized and in lateral part of striae larger and distinct; intervals 3, 5 and 7 slightly elevated in basal third, with dense micro-punctures. Scutellum longer than wide, sides arcuate.

Abdomen. Intercostal process of first ventrite subtriangular with rounded apex, wider than long, lateral margin raised continuously into carina reaching hind margin of ventrite 1; admedian cavities short, oblique. Posterolateral angles of ventrites 2 to 4 distinctly protruding posteriorly. Apex of ventrite 5 emarginate medially.

Aedeagus (figures 5–7). Approximately 1 mm long. In ventral view, phallobase wide, slightly shorter than penis, distinctly shorter than parameres. Distal half of penis distinctly narrowed, apices narrowly rounded; ventral sac folded, but distinctly expanding if placed in lactic acid for more than two days. Parameres distinctly longer than penis, gradually narrowed from base towards angulate apex.

Males: 3.64–3.81 mm long, 1.71–1.86 mm wide.

Females: unknown.



Figures 1–4. Habitus photographs. 1–2 *Dryopomorphus heineri* sp. n., holotype 3–4 *Dryopomorphus ruiliensis* sp. n., holotype 1, 3 in dorsal view 2, 4 in ventral view.

Distribution. CHINA (Guangdong).

Etymology. This species is dedicated to our deceased friend Heinrich (Heiner) Schönmann, Vienna, a specialist in Hydrophilidae and good collector.

***Dryopomorphus ruiliensis* sp. n.**

<http://zoobank.org/C6F85333-3817-4B4F-B6C1-3976BD6BAD09>

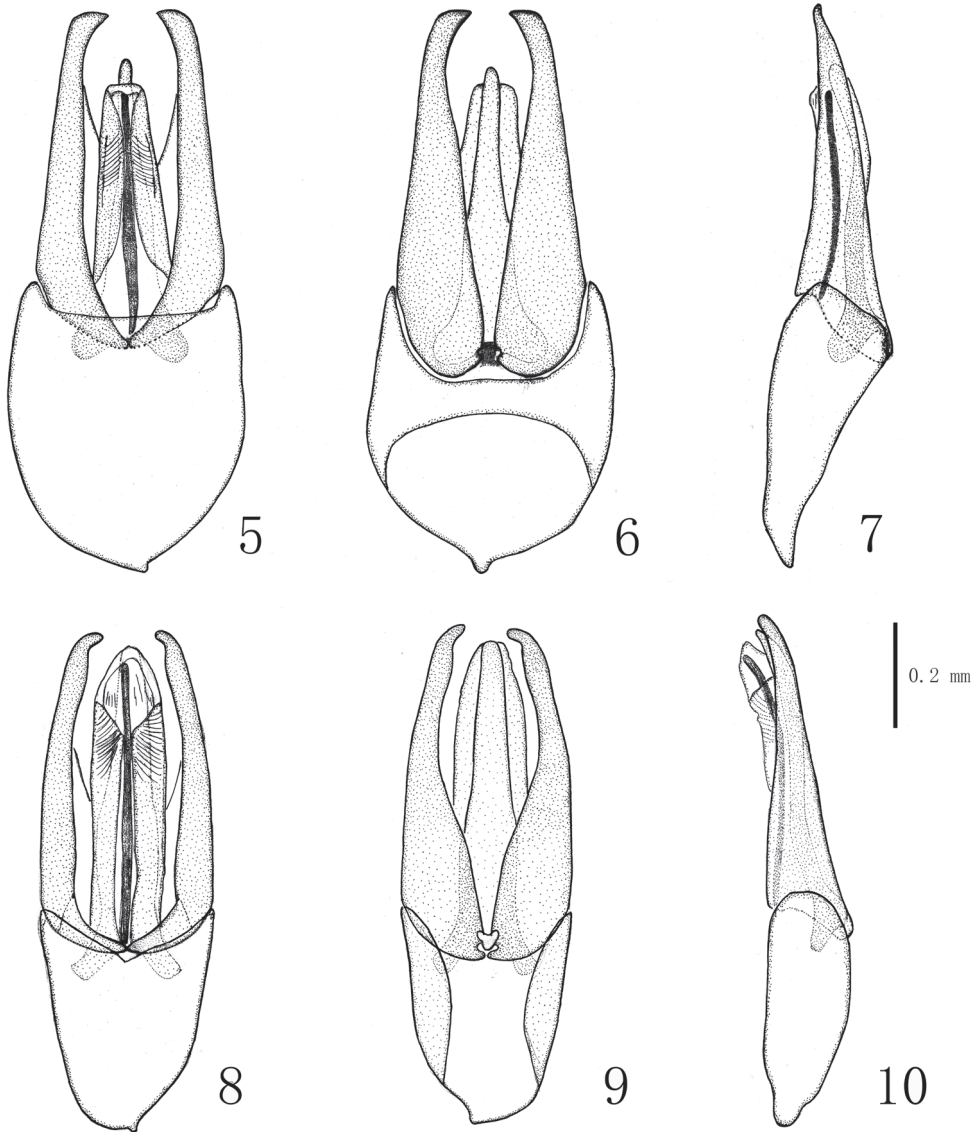
Figures 3–4, 8–10

Type material. Holotype, male (IAECAS): “CHINA: Yunnan, Ruili, / Yingjiang, ca. 830 m, | 24°6'35.634"N, 98°0'8.160"E, / 2016.10.17, Leg. Wang et al. (5)”. Paratypes: 2 males (IAECAS), 2 females (IAECAS), same data as holotype; 1 male (IAECAS): “CHINA: Yunnan, Yingjiang, / Nabang, 1308m, | 24°36'50"N, 97°35'58"E, / 2016.10.21, Leg. Peng & Sun (14)”; 1 female (IAECAS): “CHINA: Yunnan, Tengchong, / Mingguang, 1826m, | 25°28'39"N, 98°31'53"E / 2016.10.24, Leg. Peng & Sun (19)”; 1 ex. (NMW): “CHINA: Yunnan, Xishuangbanna / ca. 15km W Menglun / 5.11.1999, ca. 700–800 m / leg. Jäch, et al. (CWBS 354)”; 1 ex. (NMW): “CHINA: Yunnan, Xishuangbanna / ca. 10km NW Menglun / 7.11.1999, ca. 700 m / leg. Jäch, et al. (CWBS 359)”; 1 ex. (NMW): “CHINA: Yunnan, Xishuangbanna / ca. 10km NW Menglun / 7.11.1999, ca. 700–800 m / leg. Jäch, et al. (CWBS 360)”; 7 exs. (NMW): “CHINA: Yunnan, Xishuangbanna / ca. 6km NW Mengla / 8.11.1999, ca. 700 m / leg. Jäch, et al. (CWBS 365)”; 2 exs. (NMW): “CHINA: Yunnan, Xishuangbanna / ca. 6km NW Mengla / 9.11.1999, ca. 700 m / leg. Jäch, et al. (CWBS 367)”; 2 exs. (NMW): “CHINA: Yunnan, Xishuangbanna / pass betw. Jinghong – Mengyang / 12.11.1999, ca. 1100 m / leg. Jäch, et al. (CWBS 379)”.

Diagnosis. Body elongate, dark brown; anterior angles of pronotum explanate, slightly protruding, median sulcus of pronotum straight, present at posterior 0.7 and sublateral sulci present in posterior 0.3; elytral punctures on disc small and in lateral striae large and distinct. This species can be distinguished from *Dryopomorphus heineri* sp. n. by: 1. pronotum less convex, anterior angles less protruding; 2. elytra subparallel in basal 2/3, then gradually converging posteriorly to separately rounded apices; 3. parameres slightly extending beyond penis, with apices narrowly rounded, whereas in *D. heineri* sp. n. the parameres distinctly extend beyond penis and the apices are angulate. This species can be distinguished from all other known species of the genus by the different shape of the parameres which are gradually narrowed from the base towards the apex in ventral view, distinctly narrowed in basal half in dorsal view, with sub-distal portion slightly inflated and apices narrowly rounded.

Description (holotype). Body elongate, BL 4.14 mm, BW 1.88 mm, dorsal surface covered with short adpressed yellowish setae and long sub-erect setae which are black on the basal 3/4 and yellowish at the distal 1/4. Dorsum dark brown, anterior corners of pronotum and legs reddish brown, antennae yellowish brown, ventral surface dark brown.

Head. Partly retractable into thorax. Labrum short, densely setose, anterior margin almost truncate, with long yellowish setae, lateral angles almost rounded. Clypeus longer and wider than labrum, approx. twice as wide as long, densely setose, fronto-clypeal suture straight; surface of labrum and clypeus densely punctate. Eyes large, slightly protruding from head outline. Pubescence of frons denser on a central triangular area; frons and vertex densely punctate, punctures setose.



Figures 5–10. Male genitalia. **5–7** *Dryopomorphus heineri* sp. n. **8–10** *Dryopomorphus ruiensis* sp. n. **5, 8** in ventral view **6, 9** in dorsal view **7, 10** in lateral view.

Thorax. Pronotum widest at base, broader than long. PL 0.96 mm, PW 1.49 mm. Disc convex, densely punctate, lateral margin narrowly rimmed, slightly tilt inward, anterior angles slightly protruding. Median sulcus straight, present along posterior 0.7 of pronotum; sublateral sulci deeply impressed, present on posterior 0.3 of pronotum. Hypomeron sub-parallel, narrowed posteriorly, anterior depression developed for reception of antennae; surface coarsely punctate, densely setose. Prosternal process 1.8 times as long as prosternum in front of coxae, lateral margin distinctly raised and sub-

parallel at anterior 0.7, posterior margin distinctly produced medially; surface of prosternum densely setose and sublateral area very coarse. Mesoventrite short, mesoventral cavity for reception of prosternal process very deep. Metaventrite impressed anteriorly between mesocoxae; discrimen narrow, present from anterior impression to posterior margin; disc flat, finely and densely punctate, densely setose; sub-lateral area with two kinds of punctures, fine punctures dense, large punctures sparse.

Elytra oblong, EL 3.18 mm, EW 1.88 mm; disc convex, densely pubescent, sub-parallel in basal 2/3, then gradually converging posteriorly to separately rounded apices. Each elytron with 10 striae; punctures deeply impressed, on disc and distal striae smaller, on lateral striae large and distinct. Intervals between striae slightly convex, with dense micro-punctures. Scutellum longer than wide, subpentagonal.

Abdomen. Intercostal process of the first ventrite triangular, longer than wide, lateral margin with carina reaching posterior margin of first ventrite, admedian cavities short, oblique. Lateral portion of ventrites 1–3 with large punctures; posterolateral angles of ventrites 2–4 protruding posteriorly. Apex of ventrite 5 rounded. Surface of ventrites finely and densely punctate, densely pubescent.

Aedeagus (figures 8–10). Approximately 0.9 mm. In ventral view (figure 8), phallobase distinctly shorter than penis; parameres gradually narrowed from base towards apex, slightly extending beyond penis, sub-distal portion slightly inflated, apices narrowly rounded; penis robust, ventral sac finely sculptured in apical portion. In dorsal view (figure 9), parameres distinctly narrowed in basal half.

Males: BL 3.93–4.14 mm, BW 1.80–1.88 mm.

Females: BL 4.04–4.08 mm, BW 1.82–1.88 mm. Externally similar to males.

Distribution. CHINA: Yunnan.

Etymology. This species is named after Ruili City, Yunnan Province, China.

Habitat. A photograph of the habitat of *D. ruiliensis* sp. n. was published by Jäch and Ji (2003: figure 5).

Acknowledgements

This study was supported by the National Natural Science Foundation of China (No. 31572310/31772512).

References

- Čiampor F, Čiamporová-Zatovičová Z, Kodada J (2012) Malaysian species of *Dryopomorphus* Hinton, 1936 (Insecta: Coleoptera: Elmidae). *Zootaxa* 3564: 1–16.
- Čiampor F, Kodada J (2006) *Dryopomorphus hendrichi* sp. nov. from West Malaysia (Coleoptera: Elmidae). *Entomological Problems* 36(2): 71–73.
- Hinton HE (1936) New Dryopidae from Japan Empire (Coleoptera). *The Entomologist* 36: 164–169.

- Hinton HE (1971) The species of *Dryopomorphus* (Coleoptera, Elmidae). *The Entomologist* 104: 293–297.
- Jäch MA, Ji L (2003) China Water Beetle Survey (1999–2001). In: Jäch MA, Ji L (Eds) *Water Beetles of China*, Vol. III. Zoologisch-Botanische Gesellschaft & Wiener Coleopterologenverein, Wien, 1–20.
- Jäch MA, Kodada J (1995) Elmidae: 2. Check list and bibliography of the Elmidae of China. In: Jäch MA, Ji L (Eds) *Water Beetles of China*, Vol. I. Zoologisch-Botanische Gesellschaft in Österreich and Wiener Coleopterologenverein, Wien, 289–298.
- Jäch MA, Kodada J, Brojer M, Shepard WD, Čiampor F (2016) Coleoptera: Elmidae and Protelmidae. *World Catalogue of Insects*, Vol. 14. Brill, Leiden, 318 pp.
- Kodada J (1993) *Dryopomorphus siamensis* sp. nov., a new riffle beetle from Thailand (Coleoptera: Elmidae) and remarks on the morphology of the mouthparts and hind wing venation of *D. bishopi* Hinton. *Entomological Problems* 24(1): 51–58.
- Spangler PJ (1985) A new species of the aquatic beetle genus *Dryopomorphus* from Borneo (Coleoptera: Elmidae: Larinae). *Proceedings of the Biological Society of Washington* 98(2): 416–421.
- Yoshitomi H, Jeng ML (2013) A new species of the genus *Dryopomorphus* Hinton (Coleoptera, Elmidae, Larinae) from Laos. *Elytra (New series)* 3(1): 45–51.
- Yoshitomi H, Satô M (2005) A revision of the Japanese species of the genus *Dryopomorphus* (Coleoptera, Elmidae). *Elytra* 33(2): 455–473.

The taxonomic status of *Petropedetes newtonii* (Amphibia, Anura, Petropedetidae)

Alberto Sánchez-Vialas¹, Marta Calvo-Revuelta¹,
Santiago Castroviejo-Fisher², Ignacio De la Riva¹

1 Museo Nacional de Ciencias Naturales (MNCN-CSIC), c/ José Gutiérrez Abascal 2, 28006, Madrid, Spain
2 PUCRS, Pontificia Universidade Católica do Rio Grande do Sul, Av. Ipiranga 6681, 90619-900, Porto Alegre, Brazil

Corresponding author: Alberto Sánchez-Vialas (albertosv@mncn.csic.es)

Academic editor: A. Ohler | Received 1 March 2018 | Accepted 27 April 2018 | Published 6 June 2018

<http://zoobank.org/A6572ECF-3B4B-4014-9B7F-D84B2C4F348B>

Citation: Sánchez-Vialas A, Calvo-Revuelta M, Castroviejo-Fisher S, De la Riva I (2018) The taxonomic status of *Petropedetes newtonii* (Amphibia, Anura, Petropedetidae). ZooKeys 765: 59–78. <https://doi.org/10.3897/zookeys.765.24764>

Abstract

The taxon *Petropedetes newtonii* was described in 1895 by Bocage, from Bioko Island (Equatorial Guinea). This taxon, whose holotype is lost, has been misidentified since Boulenger's revision of the genus in 1900 and its relationships with other taxa (*P. vulpiae* and *P. johnstoni*) is confusing. Currently, *P. newtonii* is considered a synonym of *P. johnstoni*. In this work, by revising morphological characters of non-webbed *Petropedetes* of Bioko, we demonstrate the morphological singularity of these specimens with respect to *P. johnstoni* and *P. vulpiae* and their association with the name *Petropedetes newtonii*. Consequently, we provide the subsequent designation of a neotype of *P. newtonii* and revalidate this species from its synonym with *P. johnstoni*.

Keywords

Bioko, Cameroon, Equatorial Guinea, morphology, neotype, *Petropedetes johnstoni*, *Petropedetes vulpiae*, *Petropedetes newtonii*, taxonomy

Introduction

The family Petropedetidae Noble, 1931 includes three genera allopatrically distributed, *Arthroleptides* Nieden, 1911, from East Africa, the monotypic *Ericabatrachus* Largen, 1991, from Ethiopia, and *Petropedetes* Reichenow, 1874, from Central Africa (Frost 2018).

Petropedetes is distributed throughout the Gulf of Guinea, in Western Central Africa, including the island of Bioko, where the species generally inhabit the surroundings of fast-flowing streams. Reproduction takes place in land and male parental care has been described (Barej et al. 2010). Tadpoles generally present a semi-terrestrial life stage, developing in the water film covering the surface of rocks or in the water of running streams (De la Riva 1994, Barej et al. 2010). Eight species are currently recognised within the genus, namely: *P. cameronensis* Reichenow, 1874, *P. euskircheni* Barej, Rödel, Gonwouo, Pauwels, Böhme & Schmitz, 2010, *P. johnstoni* (Boulenger, 1888), *P. juliawurstnerae* Barej, Rödel, Gonwouo, Pauwels, Böhme & Schmitz, 2010, *P. palmipes* Boulenger, 1905, *P. parkeri* Amiet, 1983, *P. perreti* Amiet, 1973 and *P. vulpiae* Barej, Rödel, Gonwouo, Pauwels, Böhme & Schmitz, 2010. They are generally easy to distinguish from each other based on the development of webbing and tympanum, and in some dimorphic characters of males such as femoral glands, tympanum size, presence and position of tympanic papilla, and skin keratinised spicules (Barej et al. 2010).

The phylogenetic relationships of the genus *Petropedetes* have been recently revised by Barej et al. (2014), revealing that the species diversity of the genus is underestimated and also that the validity of the taxon *P. newtonii* (Bocage, 1895), placed in the synonymy of *P. johnstoni* by Barej et al. (2010), remains uncertain.

Bocage described *P. newtonii* in 1895 as *Tympanoceros newtonii*. Its description was based on an adult male specimen from Bioko (formerly Fernando Poo) (type locality: “L’île de Fernão do Pó dans le golfe de Guiné”) (Bocage 1895a). The holotype of *P. newtonii* is lost (Perret 1976, Barej et al. 2010) but, fortunately, a detailed illustration and an additional description were published based on a second male specimen collected from Basilé, Bioko (Bocage 1895b). Previous to the description by Bocage (1895a), two more species of *Petropedetes* had already been described: *P. cameronensis* Reichenow, 1874 (type species of the genus) and *P. johnstoni* (= *Cornufer johnstoni* Boulenger, 1888). Boulenger (1900) transferred *Tympanoceros newtonii* (misspelled “*newtoni*”) and *Cornufer johnstoni* to the genus *Petropedetes* and provided the first revision of the genus, with a synthesis of diagnosable characters for the species recognised at that time (*P. cameronensis*, *P. johnstoni*, and *P. newtonii*). The specimens of “*P. newtonii*” used by Boulenger (1900) were from mainland Cameroon and no specimens were included from Bioko (type locality of *P. newtonii*). The morphological characters considered in Boulenger’s revision to characterise *P. newtonii* were not consistent with the holotype description made by Bocage (1895a). Furthermore, Amiet (1983), following Boulenger’s description, studied more characters than those present in the original description of *P. newtonii* (e.g., relative position of tympanic papilla and femoral gland size). Boulenger’s (1900) and Amiet’s (1983) descriptions of *P. newtonii* were widely used by subsequent authors (Mertens 1968, De la Riva 1994, Lasso et al. 2002, Frétey

et al. 2012). Incongruences between the original description of *P. newtonii* and the ones using mainland populations (Boulenger 1900, Amiet 1983) have been discussed by Barej et al. (2010). According to Barej et al. (2010), the continental populations of formerly considered *P. newtonii* represent a different evolutionary unit, which was described as *P. vulpiae*. In their revision, Barej et al. (2010) placed *Petropedetes newtonii* (Bocage, 1895) in the synonymy of *P. johnstoni* (Boulenger, 1888), due to the apparent absence of morphological differences between both descriptions. Consequently, two species were considered to occur in Bioko, one of them with webbed toes (*P. cameronensis*) and the other one with non-webbed toes (*P. johnstoni*) (Barej et al. 2010). Specimens of non-webbed *Petropedetes* from Bioko studied using molecular data by Barej et al. (2014) were nested with continental *P. vulpiae*, but forming a clade, together with a few samples from nearby localities in Cameroon, sister to all other samples of *P. vulpiae* (including topotypic specimens). Barej et al. (2010, 2014) indicated that the original description of *P. newtonii* (Bocage, 1895a) does not fit with the morphological characters of *P. vulpiae* and, consequently, they kept them as separate taxa (*P. newtonii* in the synonymy of *P. johnstoni*).

The results of these studies suggest that three independent evolutionary units of *Petropedetes* might be present in Bioko. One of them, *P. cameronensis*, is diagnosable based on molecular and morphological characters and easily recognisable by having males with half-webbed toes, a very small tympanum without tympanic papilla, and metacarpal spine absent. The other two units are non-webbed and correspond to (1) the specimens morphologically assignable to *P. johnstoni* (apparently not studied with molecular data), and (2) the specimens treated as *P. vulpiae* based on molecular data (Barej et al. 2014). The problem posed by Biokoan *P. johnstoni* and *P. vulpiae* in relation to *P. newtonii* needs to be clarified.

The objective of this work is to solve the systematics of the non-webbed *Petropedetes* of Bioko by analysing the morphological characters of the available series of specimens from Bioko included in the molecular phylogeny of Barej et al. (2014) assigned by them to *P. vulpiae*. To do this, we compared the morphological characters of these specimens with (A) the original Bocage's (1895a) description of *P. newtonii*, Boulenger's (1888) of *P. johnstoni*, and Barej's et al. (2010) of *P. vulpiae*; and (B) continental specimens of *P. johnstoni* included in Barej et al.'s (2014) molecular study. As a result, we demonstrate the morphological singularity of the non-webbed *Petropedetes* from Bioko with respect to both *P. johnstoni* and *P. vulpiae* and the association of these *Petropedetes* from Bioko with the original *P. newtonii*. Consequently, we revalidate the taxon *P. newtonii* from its junior synonym with *P. johnstoni* and designate and describe a neotype of *P. newtonii* to allow its fully taxonomic recognition and facilitate future work on *Petropedetes*.

Materials and methods

We revised 14 specimens of non-webbed *Petropedetes* from several localities of Bioko (Equatorial Guinea) held at the herpetological collection of the Museo Nacional de

Ciencias Naturales (MNCN-CSIC), Madrid, Spain. Three specimens (MNCN 46703, MNCN 46708, and MNCN 46719) were collected in March 2007 and preserved in 70 % ethanol. The other 11 specimens were collected in November and December 2003, fixed in formalin 10 % and preserved in ethanol 70 %. Prior to fixation, a piece of tissue was preserved in ethanol 96 % and stored in a freezer for molecular studies. Among them, three specimens were previously included in the molecular analysis of Barej et al. (2014): MNCN 48728 (MNCN-DNA 50405), MNCN 48729 (MNCN-DNA 50465) and MNCN 48730 (MNCN-DNA 50411). Additional specimens of *Petropedetes johnstoni* stored in 70 % ethanol and housed at the Zoologisches Forschungsmuseum Alexander Koenig (ZFMK 87709, adult male, and ZFMK 87710, adult female) were studied. These specimens were collected from Nkoelon, Campo region (2°23'49.8"N, 10°02'47.4"E), Cameroon. Studied specimens and their associated data are listed in Table 1. Nomenclature used in the morphological description of the neotype follows De la Riva et al. (2012).

Measurements were taken with a digital caliper to the nearest 0.1 mm, and are given in mm. Morphometric abbreviations are as follows:

SVL (snout-vent length)	FL (femur length)
HL (head length, from rictus to point of snout)	FGL (femoral gland length)
HW (head width, at level of rictus)	FGW (femoral gland width)
IND (internarial distance)	TL (tibia length)
END (distance from eye to nostril)	FTL (foot length, from proximal border of inner metatarsal tubercle to tip of fourth toe)
TD (horizontal tympanum diameter)	THL (thenar tubercle length)
ED (eye diameter)	THBL (thumb length)
NS (distance from nostril to snout tip)	

For qualitative morphological diagnosis, we selected male specimens, which possess the most important characters to differentiate these species. These features are: tympanum size, presence of tympanic papilla and its relative position in the tympanum, presence of keratinised spicules on basis of arms, relative size of femoral glands and webbing development.

Digital photographs were taken with a reflex camera fitted with a macro lens. Micro-computed tomography (micro-CT) scans were carried out for two specimens (male and female) of non-webbed *Petropedetes* from Bioko (MNCN 48728, MNCN 48729) and in the same way for two specimens (male and female) of *P. johnstoni* (ZFMK 87709, ZFMK 87710), at the MNCN. The scans were produced using a XTH 160 Nikon Metrology, with a molybdenum target. Specimens were scanned with the following settings: 126 kV, and 47 µA over 1000 projections during 1.30 h. Raw X-ray data were processed using CTPro 3D software (Nikon Metrology) and micro-CT images were analysed using VG Studio MAX 3.0.3 (Volume Graphics, Heidelberg, Germany).

Table 1. Examined specimens of *Petropedetes*. Morphometric measurements are given in mm. Abbreviations: SVL (snout-vent length), HL (head length, from rictus to point of snout), HW (head width, at level of rictus), IND (internarial distance), END (distance from eye to nostril), HTD (horizontal tympanum diameter), ED (eye diameter), NS (distance from nostril to snout tip), FL (femur length), FGL (femoral gland length), FGW (femoral gland width), TL (tibia length), FTL (foot length, from proximal border of inner metatarsal tubercle to tip of fourth toe), THL (thenar tubercle length), and THBL (thumb length).

Species	Voucher number	Field Code	Country	Main political unit	Locality	Latitude	Longitude	Elevation (m)	Sex	SVL	HW	HL
<i>P. newtonii</i>	MNCN 46703	RC.3.1	Equatorial Guinea	Bioko Island	Campamento Smith, Río Tudela	3°18'27.34"N	8°28'15.68"E	181	FEMALE	40.4	16.8	16.3
<i>P. newtonii</i>	MNCN 46708	RC.10	Equatorial Guinea	Bioko Island	BBPP Camp, Caldera de Luba	3°20'45.34"N	8°29'48.03"E	871	INDET/JUV	28.9	12.1	12.6
<i>P. newtonii</i>	MNCN 48728	ET105	Equatorial Guinea	Bioko Island	Chopepe creek on its confluence with Río Osa	3°14'52.19"N	8°32'23.77"E	27	MALE	34.9	15.5	14.1
<i>P. newtonii</i>	MNCN 48730	ET113	Equatorial Guinea	Bioko Island	Affluent of Río Olé on right margin near camp Bite on track to Caldera de Luba	3°18'27.08"N	8°28'24.36"E	254	MALE	32.5	14.4	14.5
<i>P. newtonii</i>	MNCN 48729	ET579	Equatorial Guinea	Bioko Island	Río Sibitá, Bocooco Avendaño	3°26'46.04"N	8°26'52.39"E	33	FEMALE	41.3	16.6	15.5
<i>P. newtonii</i>	MNCN 48955	ET112	Equatorial Guinea	Bioko Island	Affluent of Río Olé on right margin near camp Bite on track to Caldera de Luba	3°18'27.08"N	8°28'24.36"E	257	FEMALE	41.3	16.2	15.5
<i>P. newtonii</i>	MNCN 48957	ET580	Equatorial Guinea	Bioko Island	Río Sibitá, Bocooco Avendaño	3°26'46.04"N	8°26'52.39"E	33	INDET/JUV	30.3	12.4	11.6
<i>P. newtonii</i>	MNCN 48956	ET107	Equatorial Guinea	Bioko Island	Chopepe creek on its confluence with Río Osa	3°14'52.19"N	8°32'23.77"E	27	FEMALE	29.7	11.3	11.6
<i>P. newtonii</i>	MNCN 48960	ET 119	Equatorial Guinea	Bioko Island	BBPP Camp, Caldera de Luba	3°20'47.32"N	8°29'48.44"E	875	INDET/JUV	16.3	6.6	7.3
<i>P. newtonii</i>	MNCN 48961	ET 108	Equatorial Guinea	Bioko Island	Chopepe creek on its confluence with Río Osa	3°14'52.19"N	8°32'23.77"E	27	INDET/JUV	14.6	6.0	6.1
<i>P. newtonii</i>	MNCN 48962	ET 84	Equatorial Guinea	Bioko Island	Stream Mukokobe. Path between Belebu and Ureka	3°24'25.81"N	8°33'3.23"E	895	INDET/JUV	10.1	4.6	4.6
<i>P. newtonii</i>	MNCN 46719	RC.19	Equatorial Guinea	Bioko Island	Río Riaco	3°20'31.83"N	8°29'59.01"E	834	INDET/JUV	14.4	5.5	5.4
<i>P. newtonii</i>	MNCN 48958	ET 103	Equatorial Guinea	Bioko Island	Chopepe creek on its confluence with Río Osa	3°14'52.19"N	8°32'23.77"E	27	INDET/JUV	17.5	7.1	7.0
<i>P. newtonii</i>	MNCN 48959	ET106	Equatorial Guinea	Bioko Island	Chopepe creek on its confluence with Río Osa	3°14'52.19"N	8°32'23.77"E	27	INDET/JUV	16.8	7.3	7.9
<i>P. johnstoni</i>	ZFMK87709	N/A	Cameroon	South Region	Nkoolon, Campo region	2°23'49.8"N	10°02'47.4"E	115	MALE	32.4	14.0	12.5
<i>P. johnstoni</i>	ZFMK87710	N/A	Cameroon	South Region	Nkoolon, Campo region	2°23'49.8"N	10°02'47.4"E	115	FEMALE	38.0	14.6	13.8

Table 1. Continued.

Species	Voucher number	IND	FL	FGL	FGW	TL	FTL	HTD	ED	END	NS	THL	THBL	Microhabitat	Date	Time
<i>P. newtonii</i>	MNCN 46703	3.6	22.1	6.7	2.6	22.4	31.1	2.8	6.4	4.3	2.8	2.0	6.3	N/A	3/7/2007	N/A
<i>P. newtonii</i>	MNCN 46708	3.2	16.1	5.0	2.0	17.5	23.6	2.1	4.1	3.4	1.8	1.5	6.5	N/A	3/10/2007	N/A
<i>P. newtonii</i>	MNCN 48728	3.7	20.8	6.9	4.8	21.3	25.9	3.2	5.7	4.6	2.4	2.2	5.7	On a leaf (20 × 15 cm) 35 cm above the ground and 1 m from water	11/22/2003	19:00
<i>P. newtonii</i>	MNCN 48730	3.0	18.6	7.1	3.9	18.5	24.5	2.5	5.4	4.0	2.1	2.1	4.2	On the shore on a rock	11/25/2003	19:30
<i>P. newtonii</i>	MNCN 48729	4.0	20.3	4.7	2.3	21.8	28.9	3.1	6.4	4.0	2.5	2.1	6.6	On a leaf (40 × 10 cm) 30 cm above water of 20 cm depth	12/3/2003	18:45
<i>P. newtonii</i>	MNCN 48955	3.7	21.7	6.9	2.8	22.0	27.7	2.6	6.8	3.9	2.1	2.4	6.5	On a rock (60 × 80 cm) in the middle of the water 20 cm above near MNCN 48730	11/25/2003	19:25
<i>P. newtonii</i>	MNCN 48957	3.2	18.1	3.9	2.0	18.9	N/A	2.0	4.6	3.5	2.1	1.8	5.2	On a dry leaf (20 × 15 cm) 7 cm above Río Sibirá of 5 cm depth	12/3/2003	18:45
<i>P. newtonii</i>	MNCN 48956	3.0	15.9	4.1	1.8	16.3	21.6	1.9	4.2	3.5	2.0	1.7	4.9	On a branch (1 cm diameter) about 1.80 m above water	11/22/2003	19:00
<i>P. newtonii</i>	MNCN 48960	2.3	8.0	N/A	N/A	8.5	7.9	1.0	3.0	1.9	1.0	N/A	2.0	On the ground of the kitchen, no vegetation and no body of water in the surroundings	11/26/2003	12:30
<i>P. newtonii</i>	MNCN 48961	2.0	7.8	N/A	N/A	8.9	6.4	0.8	2.7	1.8	0.9	N/A	2.0	On top of a leaf (20 × 10 cm), 1 m above the water, of a plant growing on a rock of the stream	11/22/2003	19:30
<i>P. newtonii</i>	MNCN 48962	N/A	6.0	N/A	N/A	6.0	5.4	1.1	2.0	N/A	N/A	N/A	N/A	On the moss covering a rock of the stream	20/11/003	9:30
<i>P. newtonii</i>	MNCN 46719	1.6	7.8	N/A	N/A	7.6	6.5	0.8	2.7	1.3	0.9	N/A	1.5	N/A	3/15/2007	N/A
<i>P. newtonii</i>	MNCN 48958	1.9	9.7	2.0	1.0	10.0	9.2	1.2	2.6	1.9	1.0	N/A	2.6	On the ground, a mix a mud and leaf-litter, 2 m from the water	11/22/2003	17:30
<i>P. newtonii</i>	MNCN 48959	2.3	9.5	2.8	1.2	10.6	8.2	1.0	2.8	1.8	1.0	N/A	2.3	Over a small leaf (7 × 4 cm) 10 cm above ground and 0.5 m from the water	11/22/2003	19:00
<i>P. johnstoni</i>	ZFMK87709	3.5	18.4	7.9	3.4	20.1	25.0	2.9	5.6	3.2	1.4	1.7	4.6	N/A	N/A	N/A
<i>P. johnstoni</i>	ZFMK87710	4.0	20.3	5.6	2.4	21.9	26.2	3.0	5.8	3.6	1.7	1.7	5.3	N/A	N/A	N/A

Results and discussion

Petropedetes johnstoni and *P. newtonii* original descriptions

Petropedetes johnstoni was described by Boulenger in 1888, based on a subadult specimen from Río del Rey, Cameroon (“Cameroons”) (= river Ndian, Western Cameroon). Despite it was treated as a female by Boulenger (1888), Parker’s (1936) revision of the holotype stated that it corresponds to an immature male (Amiet 1983).

Bocage (1895a) described *Petropedetes newtonii* from Bioko based on a single adult male specimen with well-marked sexual features.

We agree with Barej et al. (2010), which stated that morphological discrepancies between both descriptions are due to ontogeny, measurement methods (as for the tympanum size), and intraspecific variability (as for the relative position of the tibiotarsal articulation in regard to the snout tip when the leg is stretched forwards). While the holotype of *P. johnstoni* is a subadult male which lacks the typical male secondary characters, the holotype description of *P. newtonii* resembles that of a male possessing reproductive features. Barej et al. (2010) argue that both descriptions represent morphologically indistinguishable taxa and, with the evidence at hand, considered *P. newtonii* a junior synonym of *P. johnstoni*. However, we argue that this decision needs to be evaluated in the light of detailed comparisons of adult male specimens, which requires, for reasons outlined above, the study of additional specimens besides the type series. These results are presented in the following sections.

Morphological revision of *P. johnstoni*

Two specimens of *P. johnstoni* (ZFMK 87709, ZFMK 87710) were morphologically revised in order to complete the original description of the holotype made by Boulenger (1888). The selected specimens were previously characterised based on molecular data by Barej et al. (2014) and are unambiguously nested in the clade of *P. johnstoni*, which includes samples from the type locality of *P. johnstoni*.

Both specimens are characterised by: whitish posterior side of the thighs with a speckled pattern made up of brownish dots or marks (Fig. 1); ventral side whitish; lower jaw rounded, with several well marked white spots; snout slightly rounded in dorsal and ventral view (Figs 1, 2A, B); relatively small vomerine teeth (Fig. 3B); supratympanic fold distinct (Fig. 4A); palmar tubercle oval (Fig. 5B); thenar tubercles in both specimens oval (Fig. 5B), approximately $\frac{1}{4}$ of total length of Finger I; one subarticular tubercle on Finger I, placed between fingertip and centre of the finger; subarticular tubercle of Finger II centrally positioned on the finger; fingers III and IV with two subarticular tubercles; fingertips with adhesive discs of different sizes, as follows: I > II > III = IV; relative lengths of fingers: III > IV > II > I; toes not webbed or rudimentarily; outer metatarsal tubercle absent; inner metatarsal tubercle elongated, at the base of Toe I. Toes I and II with one single tubercle, toes III and V with two single tubercles and Toe III with three single tubercles; no supernumerary tubercles; relative

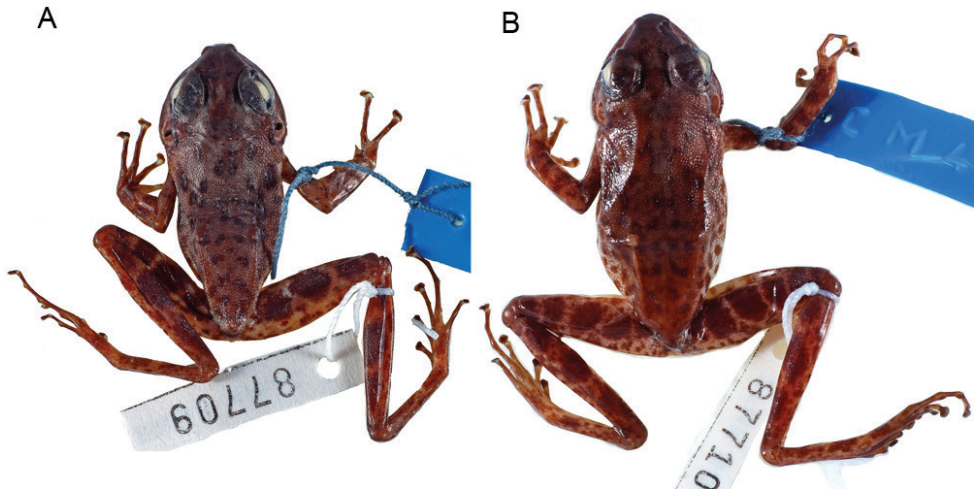


Figure 1. Dorsal view of *Petropedetes johnstoni* specimens (**A** male, ZFMK 87709 **B** female, ZFMK 87710).

lengths of toes: IV > III > V > II > I; skin with relatively small warts, especially on the anterior part of dorsum. Morphometric measurements are given in Table 1.

Male specimen ZFMK 87709 is characterised by possessing a small tympanum (relation of the TD to ED = 0.53), tympanic papilla present in the upper border of the tympanum (Fig. 4A), a big femoral gland covering most of the femoral skin (relation of femoral gland to femur length = 0.43; Fig. 2A), lack of keratinised spicules on the skin of the basis of arms (Fig. 2A), upper and lower border of tympanum round, not flattened (Fig. 4A), forearm not hypertrophied (Fig. 2A), metacarpal spines absent (Fig. 6A) and webbing rudimentary.

The study of the humerus by CT-scan analyses of a male (ZFMK 87709; Fig. 7A) and a female (ZFMK 87710) of *P. johnstoni*, shows a strong sexual dimorphism due to the presence in the male of a double crest, relatively short in length and distally divergent in the dorsal side of the bone, which is totally absent in the female.

Summary of the diagnostic characters of *P. vulpiae*

The other species involved in the taxonomic problem of *Petropedetes newtonii*, and recently suggested to be in Bioko on the basis of DNA sequences (Barej et al. 2014), is *P. vulpiae*. Before we proceed with a description of the morphology of the new material of non-webbed *Petropedetes* from Bioko, we summarised the main characters of this species to allow a clearer discussion. The diagnosis made by Barej et al. (2010) reads as follows: “medium sized *Petropedetes*; compact body shape; tympanum usually flattened on the upper and lower border; tympanum larger than diameter of eye in males, smaller in females; characters of breeding males: tympanic papilla present (broad, fleshy), papilla closer to the centre than the upper border; forearm hypertrophy well developed; carpal

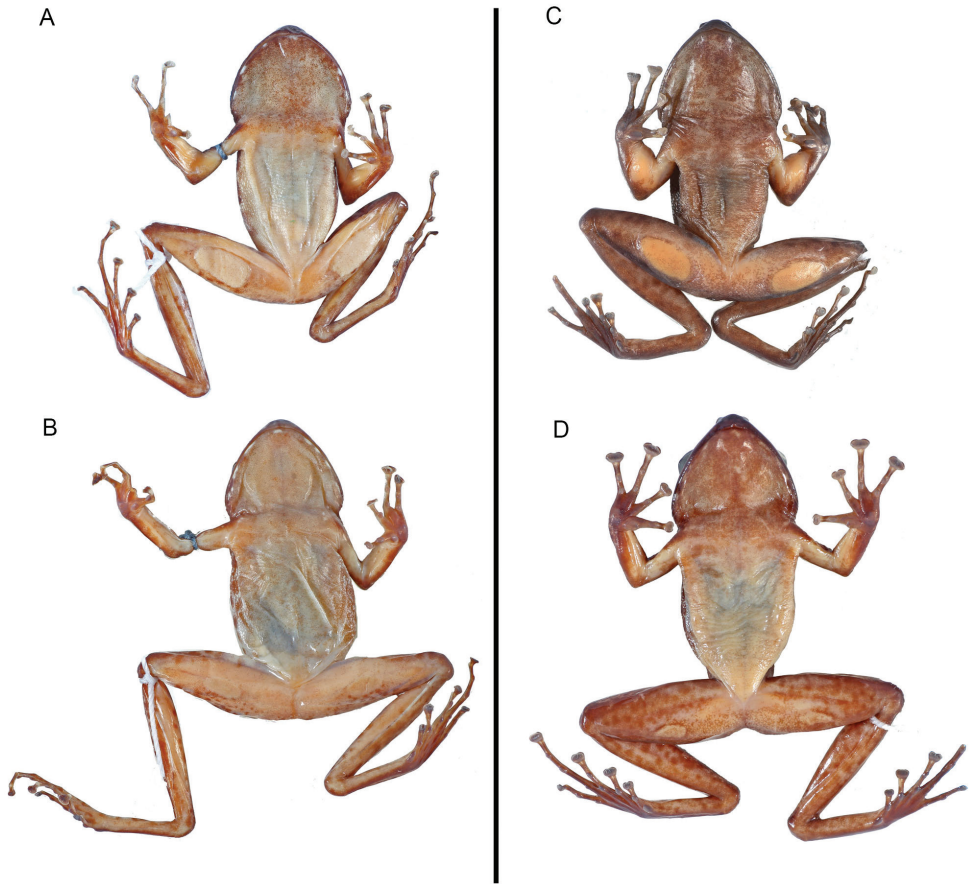


Figure 2. Ventral view of specimens of *Petropedetes johnstoni* (**A** male, ZFMK 87709 **B** female, ZFMK 87710) and *P. newtonii* (**C** male, MNCN 48730 **D** female, MNCN 48729).

spike present; spinosities on throat, forearms and on almost every wart on flanks and dorsum, even around the tympanum; femoral glands large, very prominent; webbing rudimentary”. Also, comparative drawings of some features as femoral glands and tympanum of *P. vulpiae* were included in Barej et al.’s (2010) revision, illustrating the most relevant characters and allowing indirect observations.

Description of the new material of non-webbed *Petropedetes* from Bioko

We revised the morphology of a series of 14 specimens (8 juveniles, 4 adult females, 2 adult males) collected in Bioko, including the three individuals studied in the molecular phylogeny of Barej et al. (2014). The adults have the following characteristics: Lower jaw relatively triangular; snout slightly pointed in dorsal and ventral view (Figs 2C, D, 8); relatively big vomerine teeth (Fig. 3A); supratympanic fold distinct

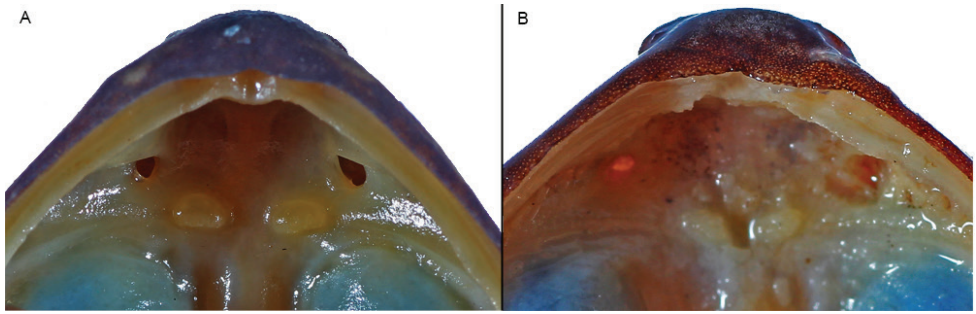


Figure 3. Mouth roof region of *Petropedetes newtonii* (A female, MNCN 48729) and *Petropedetes johnstoni* (B male, ZFMK 87709).



Figure 4. Details of the tympanum of *Petropedetes johnstoni* (A male, ZFMK 87709), *P. newtonii* (B male, MNCN 48728), and *P. vulpiae* (C male, non-collected specimen from Río Muni, Equatorial Guinea; photo by Ignacio De la Riva).

(Fig. 4B); palmar tubercle present, oval (Fig. 9). Thenar tubercle elongated, more than 1/3 of Finger I total length (Figs 5A, 9); one subarticular tubercle on Finger I, placed between fingertip and the centre of the finger; subarticular tubercle of Finger II centrally positioned on the finger; fingers III and IV with two subarticular tubercles, fingertips with adhesive discs of different sizes, as follows: I > II > III = IV; relative lengths of fingers: III > IV > II > I; toes not webbed or rudimentarily; outer metatarsal tubercle absent; inner metatarsal tubercle elongated, on the base of Toe I. Toes I and II with one single tubercle, toes III and V with two single tubercles and Toe III with three single tubercles; no supernumerary tubercles; relative lengths of toes: IV > III > V > II > I. Skin with relatively medium-sized warts, especially on the anterior part of dorsum. Morphometric measurements are given in Table 1, including two grown juveniles.

Both adult male specimens (MNCN 48728 and 48730) are characterised by sharing the following features: (1) the size of the tympanum (relation between TD and ED = 0.56 and 0.46 mm respectively), which is approximately half size of the eye diameter; (2) the position of the tympanic papilla in the upper border of tympanum (Fig. 4B); (3) the tympanum upper and lower borders round, not flattened; (4) the relatively large femoral glands (Figs 2C, 8), covering a big area of the femoral skin (relation of femoral gland to femur length = 0.33 and 0.38, respectively); (5) the presence of



Figure 5. Thenar tubercle of males of *Petropedetes newtonii* (**A** male, MNCN 48728) and *P. johnstoni* (**B** male, ZFMK 87709). Note the different shape and size and the presence of a dorsal spine on the distal edge of the metacarpal of Finger I in *P. newtonii*.

dispersed keratinised spicules on the skin of the basis of forelimb, inner surface of upper arm, lower tympanic region and supratympanic fold, and on the postcommissural region (more distinct in MNCN 48728; Fig. 9); (6) the hypertrophied, well developed forelimb (Figs 8, 9); (7) the dorsal spine on the distal edge of the metacarpal of Finger I (Figs 5A, 6B, 9); and (8) the rudimentary webbing (Fig. 9).

The study of the humerus by CT-scan of a male (MNCN 48728; Fig. 7B) and a female (MNCN 48729) shows a strong sexual dimorphism due to the presence in the male of a well-developed double crest, distally divergent in the dorsal side of the bone, which is totally absent in the female.

Comparison of *P. johnstoni*, *P. vulpiae*, and non-webbed *Petropedetes* from Bioko

Considering the descriptions provided above, the specimens from Bioko could represent: (i) a new species yet to be named under the rules of the ICZN; (ii) part of *P.*

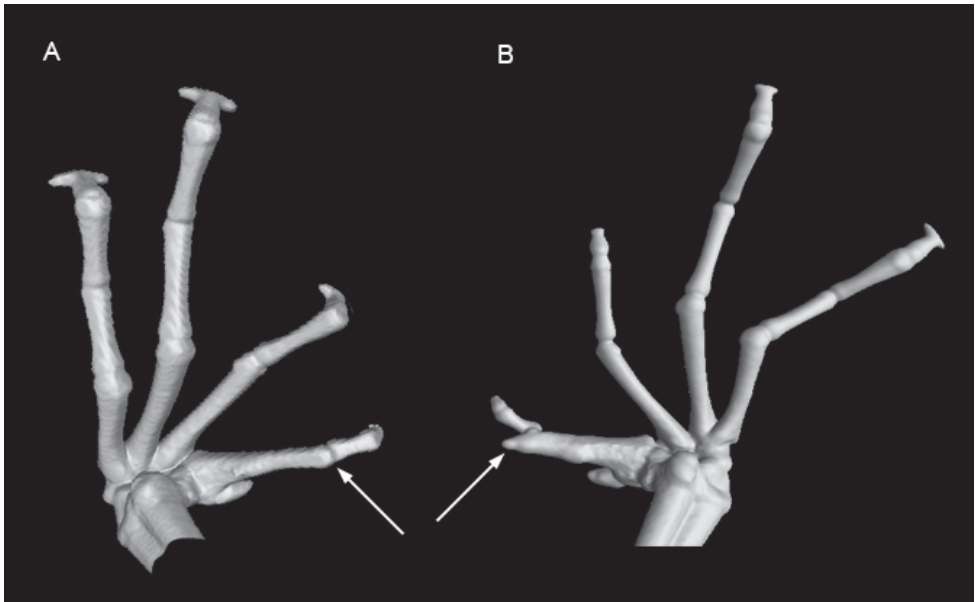


Figure 6. CT-scan image of the dorsal side of the hands of *Petropedetes johnstoni* (A male, ZFMK 87709) and *P. newtonii* (B male, MNCN 48728). No traces of metacarpal spines are detected in *P. johnstoni*.

vulpiae as suggested by the phylogenetic analyses of DNA sequences by Barej et al. (2014); (iii) part of *P. newtonii* as a synonym of *P. johnstoni*; or (iv) part of *P. newtonii* as a valid species. We argue in favour of the last scenario.

Our description of non-webbed *Petropedetes* from Bioko is fully concordant with the description of *P. newtonii*. In other words, none of the characters described in the original description of *P. newtonii* is incompatible with our own observations. Considering the geographic relationship between the specimens (both from Bioko) and their morphological similarity, we consider these specimens part of *P. newtonii*. Furthermore, our detailed study of external and internal morphology of specimens of both *P. johnstoni* and *P. newtonii* led us to discover a number of important differences (Table 2): (i) absence of keratinised spicules on the skin of the throat and on the basis of the arms in *P. johnstoni* (see also Amiet 1983), which are present in *P. newtonii*; (ii) absence of metacarpal spines in the adult male of the revisited specimen of *P. johnstoni* (Fig. 6), which are present in studied specimens of *P. newtonii*; (iii) specimens of both sexes of *P. johnstoni* present a lower jaw and a snout more rounded than specimens of *P. newtonii*; (iv) thenar tubercles are oval and distinctly smaller in *P. johnstoni* than in studied specimens of *P. newtonii*; and (v) the vomerine teeth are smaller in *P. johnstoni* than in studied specimens of *P. newtonii*, and transversally oriented (Fig. 3). Based on these differences, we consider *Petropedetes newtonii* a valid taxon and revalidate it from its junior synonym with *P. johnstoni*.

Petropedetes vulpiae is easily distinguishable from *P. johnstoni* and *P. newtonii*, sensu this work, based on the sexual dimorphic characters present in reproductive



Figure 7. CT-scan image of the dorsal side of the humerus of *Petropedetes johnstoni* (**A** male, ZFMK87709) and *P. newtonii* (**B** male, MNCN 48728). Note the differences in the development and extension of the bone crest.

Table 2. Morphological data and character states for the studied *Petropedetes* species.

Species	<i>P. vulpiae</i>	<i>P. johnstoni</i>	<i>P. newtonii</i>
Male tympanum size	Bigger than eye diameter	Smaller than eye diameter	Smaller than eye diameter
Tympanic papilla position	Close to the centre	Close to upper border	Close to upper border
Tympanum upper border shape	Flattened	Rounded	Rounded
Dorsal metacarpal spine	Present	Absent	Present
Skin keratinised spicules	Present	Absent	Present
Male humerous crest	Unknown	Relatively short	Long and well developed
Snout shape	Slightly pointed	Slightly rounded	Slightly pointed
Thenar tubercle length	Unknown	Shorter than 1/3 of the finger I	Longer than 1/3 of finger I

males (Table 2). *Petropedetes vulpiae* possesses a bigger tympanum, flattened on its upper and lower borders (Fig. 4), and the papilla is closer to the centre of the tympanum. The results of the phylogenetic analyses Barej et al. (2014) are puzzling. The Biokoan specimens studied by us and herein assigned to *P. newtonii* that are included



Figure 8. Neotype of *Petropedetes newtonii* (adult male, MNCN 48728). Left: ventral view; right: dorsal view.

in Barej et al. (2014) cluster with three purported specimens of *P. vulpiae* from nearby continental Cameroon, with nearly identical haplotypes. However, topotypic samples of *P. vulpiae* are located in the sister clade of the Biokoan specimens together with samples from other localities of Cameroon and Nigeria (Barej et al. 2014). To solve the incongruence between the morphological and molecular data at hand, we reidentified the specimens of *P. vulpiae* ZMB 78421, NMP6V 73439/1 and 73439/1 sensu Barej et al. (2014) as *P. newtonii*. Thus, *P. newtonii* and *P. vulpiae* are reciprocally monophyletic sister species.

Designation and description of the neotype of *Petropedetes newtonii*

The morphological and molecular distinctiveness of *Petropedetes* from Bioko in relation to *P. vulpiae* and *P. johnstoni* are clear. As the type material of *P. newtonii* is lost, we deem it necessary to designate a neotype.

Tympanoceros newtonii Bocage, 1895: 270, bona species. Terra typica: “L’île de Fernão do Pó dans le golfe de Guinée”.

Petropedetes newtoni –Boulenger 1900: 439 (misspelled).

Neotype. An adult male in the collection of the Museo Nacional de Ciencias Naturales (Madrid, Spain), MNCN 48728, field number ET105, collected on 22 November 2003 by Santiago Castroviejo-Fisher at Chopepe creek at its confluence with Río Osa (3°14'52.19"N, 8°32'23.77"E, 27 m a.s.l.), Bioko, Equatorial Guinea (Fig. 9).

Description. Measurements (in mm) are listed in Table 1. Adult male specimen of medium size (SVL 34.9 mm) in good state of preservation, with distant phalange of Toe IV cut for molecular analyses; body relatively robust; head slightly wider than long (head width 44.4 % of SVL; head length 40.4 % of SVL). Head moderately triangular in shape; snout relatively pointed in dorsal and ventral view; nostrils protuberant, laterally oriented and very close to tip of snout; internarial distance 3.7 mm (23.9 % of HW); nostrils closer to tip of snout than to margin of orbit; internarial region slightly concave; eye very large,



Figure 9. Ventral view of the right forelimb of *Petropedetes newtonii* (adult male, MNCN 48728). Arrows point to the dorsal spine on the distal edge of the metacarpal of Finger I and keratinised spicules along the skin surface of the upper arm and labial commissure.

40.3 % of head length; interorbital distance 2.4 mm; loreal region highly concave; tympanum distinct, rounded, not flattened in its upper side; tympanic papilla present, located in the upper margin of tympanum; supratympanic fold distinct, extending from behind the eye, bordering the tympanum, to close the level of shoulder; choanae moderately large, subcircular; vomerine teeth present, relatively big and close to each other, transversally positioned between choanae and eye orbit; tongue elongated, oval, cordiform (heart-shaped, notched posteriorly) and with a single papilla located in the middle of the anterior region.

Forelimb robust; forearm hypertrophied; paired humeral crest high, extending over most of humerus length; relative lengths of fingers III > IV > II > I; palmar webbing absent; tips of fingers flat, expanded as adhesive discs; adhesive discs heart-shaped, with

two oval plates on the dorsal side; relative width of terminal discs $IV = III > II > I$; terminal phalanges T-shaped; thenar (inner palmar) tubercle oval, more than 1/3 of Finger I total length; outer palmar tubercle distinct, rounded, bigger than thenar tubercle; one subarticular tubercle on Finger I, placed between fingertip and the centre of the finger; subarticular tubercle of Finger II centrally positioned; fingers III and IV with two subarticular tubercles; dorsal spine on the distal edge of the metacarpal of Finger I robust, whitish; keratinised spinules on humeral skin present. Hind limbs moderately robust and long (femur and tibia length 42.1 mm); femoral gland large, subcircular, 33.5 % of femur length; toes not webbed or rudimentarily; tips of toes flat, expanded as adhesive discs; adhesive discs heart-shaped, with two oval plates on the dorsal side; relative width of terminal discs: $II > I > III > IV > V$; terminal phalanges T-shaped; toes long; relative length of toes: $IV > III > V > II > I$; toes I and II with one single tubercle, toes III and V with two single tubercles and Toe III with three single tubercles; no supernumerary tubercles; outer metatarsal tubercle absent; a distinct, elongated inner metatarsal tubercle.

Skin of dorsum with scattered pustules, especially distinct in the anterior region at the level of the shoulder; keratinised spicules on inner surface of upper arm, lower tympanic region, supratympanic fold, and on postcommisural region; ventral skin smooth.

Coloration of dorsal surfaces in preservative dominated by different brown tonalities, with whitish transversal lines or marks dispersed on hind and fore limbs; posterior margin of finger and toe tips whitish. Ventral coloration white, except in the throat, palmar surfaces, and tibia, which are brownish; inner side of forearms white, external side brown; ventral side of hind legs whitish with dispersed, brown rounded spots.

Distribution of *Petropedetes newtonii*

There are few geographical records published of *P. newtonii sensu stricto*. The original type locality lacks a specific location in Bioko; however, the second known specimen was collected in Basilé, Bioko Norte province (“Bassilé”, at 527 m asl. on the grass [Bocage 1895b]). Posteriorly, other populations of *P. newtonii* were recorded within Bioko Sur province: Musola (Boulenger 1906), Rio Iladyi, at 1000 m asl. (Mertens 1965), and another in Bioko Norte province without specific locality: NW Bioko (Bocage 1903). Barej et al. (2014) provided the following specific localities: Río Osa, Río Ole, Río Sibitá and Caldera de Luba, based on specimens held at the Museo Nacional de Ciencias Naturales, all collected by SC-F in 2003 (Table 1). Additionally, Barej et al. (2014) studied populations from the southern coast of Cameroon, which are nested within the clade of Biokoan populations of *P. newtonii* (considered as *P. vulpiae* by Barej et al. [2014]).

Therefore, populations from continental Africa like those from Río Muni (Equatorial Guinea), that were formerly considered as *P. newtonii* (De la Riva 1994, Lasso et al. 2002) are now included in the taxon *P. vulpiae* (Barej et al. 2010). The distribution of *P. newtonii* would be formed by widely distributed populations throughout Bioko (both in Bioko Norte and Bioko Sur) and by continental populations on the southern coast of Cameroon (Fig. 10).

As a consequence of this validation, it must be said that the tadpole of *P. newtonii* has been described by Barej et al. (2010) (as *P. johnstoni*) based on a specimen from Musola, Bioko, which was cited by Boulenger (1906).

Natural history. Descriptions are based on the field notes of SC-F (Table 1). All specimens were collected after dusk between 18:45 and 19:30, the furthest distance from the water 2 m, in the shallower parts (20 cm depth) of streams between 22 November and 03 December 2003, which typically corresponds to the rainy season. The exceptions are three juveniles (MNCN 48960, 48962, and 48958) found during the day, one of them (MNCN 48960) in a place with no body of water in the immediate surroundings (Table 1). Two adult specimens (male MNCN 48730 and gravid female MNCN 48955) collected on a mid-elevation affluent of the right margin of the Olé River (3°18'27.08"N, 8°28'24.36"E) were found on rocks, either in the middle of the stream (the female) or on the shore (the male). The juvenile MNCN 48962 was also found on the moss covering a rock in a stream. Most of the other specimens were found on the upper side of medium-sized leaves, 7–35 cm above the water or ground levels. The adult female MNCN 48956 was perched on a thin branch (1 cm diameter) 1.80 m above the water, while juveniles MNCN 48958 and 48960 were found on the ground. No specimen was observed vocalising or engaging in reproductive behaviours such amplexus, egg deposition, or providing care to offspring.

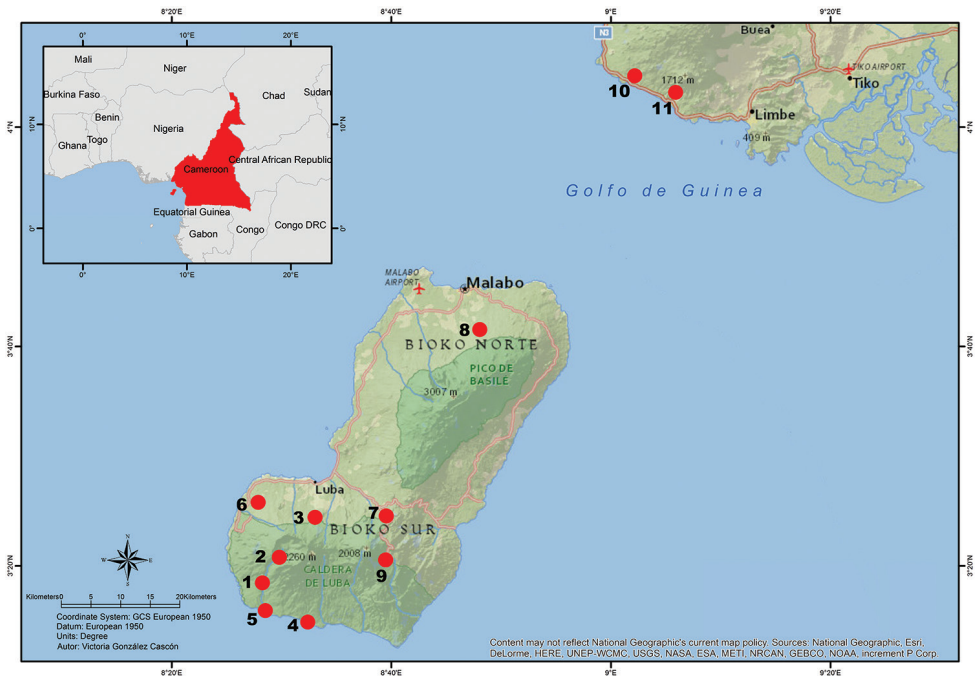


Figure 10. Distribution map of *Petropedetes newtonii* based on published records and collection data. **1** Campamento Smith, Luba, Bioko **2** Río Riaco, Caldera de Luba, Bioko **3** Stream Mukokobe, between Belebu and Ureka, Bioko **4** Río Osa, Bioko **5** Río Ole, Bioko **6** Río Sibatá, Bococo, Bioko **7** Musola, Bioko **8** Basilé, Bioko **9** Río Iladyi, Bioko **10** Bakingili, Cameroon **11** Mt. Etinde, Cameroon.

Key to adult *Petropedetes* species, modified from Barej et al. (2010)

- 1 Toes fully webbed **2**
 – Toes half or rudimentary webbed..... **3**
 2 Tympanum distinct, in males $\frac{3}{4}$ of eye diameter or larger, males with tympanic papillae and dorsal spine on the distal edge of the metacarpal of Finger I, tympanum in females up to $\frac{3}{4}$ of eye diameter, femoral glands large..... ***P. perreti***
 – Tympanum small, indistinct in both sexes, males without tympanic papillae, but with dorsal spine on the distal edge of the metacarpal of Finger I, femoral glands large to very large ***P. palmipes***
 3 Toes half-webbed **4**
 – Toes rudimentary-webbed..... **5**
 4 Tympanum distinct, males with tympanic papillae and dorsal spine on the distal edge of the metacarpal of Finger I, femoral gland line shaped in both sexes..... ***P. juliawurstnerae***
 – Tympanum indistinct, males without tympanic papillae, dorsal spine on the distal edge of the metacarpal of Finger I absent, femoral gland ovoid
 ***P. cameronensis***
 5 Tympanum small, rounded, in males smaller than eye diameter, tympanic papillae close to upper border of tympanum, femoral glands large **6**
 – Tympanum of moderate size or large, in males usually large as eye diameter or bigger than the eye **7**
 6 Males with dorsal spine on the distal edge of the metacarpal of Finger I present, keratinised spicules on arms and tympanic borders present, large thenar tubercle, male humeral crest well developed, reaching more than half of the total humeral length, snout slightly pointed..... ***P. newtonii***
 – Males with metacarpal spines absent, keratinized spicules on arms and tympanic borders absent, relatively small thenar tubercle, humeral crest reaching the half of the total length of the humerus, snout slightly rounded..... ***P. johnstoni***
 7 Femoral gland of moderate size, tympanum in males usually flattened with tympanic papillae closer to the centre than to upper border, dorsal spine on the distal edge of the metacarpal of Finger I present in males ***P. vulpiae***
 – Femoral gland small, tympanic papillae closer to upper border than to the centre, dorsal spine on the distal edge of metacarpal of Finger I present **8**
 8 Femoral gland small, in males 22% of femur length, tympanum size variable from $\frac{3}{4}$ of the eye diameter to larger than the eye, lowland species ***P. parkeri***
 – Femoral gland very small, in males 16% of femur length, tympanum in males as large as eye diameter, highland species..... ***P. euskircheni***

Acknowledgements

Fieldwork in Bioko by SC-F was possible thanks to the Asociación Amigos de Doñana (AAD) and its director Javier Castroviejo. While in Bioko, the help of Ramón Castelo (AAD) proved invaluable. We are grateful to Mario García-París for his valuable comments and to Arlo Hinkley for his English revision of the manuscript. We appreciate the kindness of Ignacio Martín for depositing in the MNCN collection specimens of several frog species collected in Bioko. We thank Ursula Bott from the Zoologisches Forschungsmuseum Alexander Koenig, Bonn (ZFMK), who kindly sent material on loan. Also, our gratitude to Cristina Paradela for generating the CT-scan image. We thank Victoria González for kindly making the map illustration. Finally, we thank Annemarie Ohler and Andreas Schmitz for their helpful reviews of the manuscript.

References

- Amiet J-L (1983) Une espèce méconnue de *Petropedetes* du Cameroun: *Petropedetes parkeri* n. sp. (Amphibia Anura: Ranidae, Phrynobatrachinae). *Revue Suisse de Zoologie* 90: 457–468. <https://doi.org/10.5962/bhl.part.81986>
- Barej MF, Rödel MO, Gonwouo LN, Pauwels OSG, Böhme W, Schmitz A (2010) Review of the genus *Petropedetes* Reichenow, 1874 in Central Africa with the description of three new species (Amphibia: Anura: Petropedetidae). *Zootaxa* 2340: 1–49.
- Barej MF, Rödel MO, Loader SP, Menegon M, Gonwouo NL, Penner J, Gvoždík V, Günther R, Bell RC, Nagel P, Schmitz A (2014) Light shines through the spindrift – Phylogeny of African torrent frogs (Amphibia, Anura, Petropedetidae). *Molecular Phylogenetics and Evolution* 71: 261–273. <https://doi.org/10.1016/j.ympev.2013.11.001>
- Bocage JVB (1895a) Sur un batracien nouveau de Fernão do Pó. *Jornal de Ciências Matemáticas, Físicas e Naturais, Academia das Ciências de Lisboa; Segunda Série* 3: 270–272.
- Bocage JVB (1895b) Reptiles et Batraciens nouveaux ou peu connus de Fernão do Pó. *Jornal de Ciências Matemáticas, Físicas e Naturais, Academia das Ciências de Lisboa; Segunda Série* 4: 16–20.
- Bocage JVB (1903) G.A. Boulenger – Batraciens nouveaux et Reptiles nouveaux. *Jornal de Ciências, Matemáticas, Physicas e Naturaes Lisboa* 7(2): 62–64.
- Boulenger GA (1888) A list of the reptiles and batrachians collected by Mr. H. H. Johnston on the Rio del Rey, Cameroons District, W. Africa. *Proceedings of the Royal Society of London* 1888: 564–565.
- Boulenger GA (1900) A list of the batrachians and reptiles of the Gaboon (French Congo), with descriptions of new genera and species. *Proceedings of the Zoological Society of London* 1900: 433–456.
- Boulenger GA (1906) Report on the batrachians collected by the late L. Fea in West Africa. *Annali del Museo Civico di Storia Naturale di Genova* 42: 157–172.

- De la Riva I (1994) Anfibios anuros del Parque Nacional de Monte Alén, Río Muni, Guinea Ecuatorial. *Revista Española de Herpetología* 8: 123–139.
- De la Riva I, Trueb L, Duellman WE (2012) A new species of *Telmatobius* (Anura: Telmatobiidae) from montane forests of southern Peru, with a review of osteological features of the genus. *South American Journal of Herpetology* 7: 91–109. <https://doi.org/10.2994/057.007.0212>
- Frétey T, Dewynter M, Blanc C (2012) Amphibiens d’Afrique centrale et d’Angola – Clé de détermination illustrée des amphibiens du Gabon et du Mbini. *Biotope, Mèze* (Collection Parthénone); Muséum national d’Histoire naturelle, Paris, 232 pp.
- Frost DR (2018) *Amphibian Species of the World: an Online Reference*. Version 6.0 (12/03/2018). Electronic Database accessible at <http://research.amnh.org/herpetology/amphibia/index.html>
- Mertens R (1965) Die Amphibien von Fernando Poo. *Bonner zoologische Beiträge* 16: 14–29.
- Mertens R (1968) Zur Kenntnis der Herpetofauna von Kamerun und Fernando Poo. *Bonner zoologische Beiträge* 19: 69–84.
- Lasso CA, Rial AI, Castroviejo J, De la Riva I (2002) Herpetofauna del Parque Nacional de Monte Alén (Río Muni, Guinea Ecuatorial). *Graellsia* 58: 21–34. <https://doi.org/10.3989/graellsia.2002.v58.i2.276>
- Parker HW (1936) The amphibians of the Mamfe Division, Cameroon. (1) Zoogeography and systematics. *Proceedings of the Zoological Society of London* 1936: 135–163. <https://doi.org/10.1111/j.1096-3642.1936.tb02284.x>
- Perret J-L (1976) Revision des amphibiens africains et principalement des types, conservés au Musée Bocage de Lisbonne. *Arquivos do Museu Bocage* 6: 15–34.

A new species of *Hyphessobrycon* Durbin from northeastern Brazil: evidence from morphological data and DNA barcoding (Characiformes, Characidae)

Erick Cristofore Guimarães^{1,5}, Pâmella Silva De Brito^{2,5}, Leonardo Manir Feitosa³,
Luís Fernando Carvalho-Costa⁴, Felipe Polivanov Ottoni^{1,2,5,6}

1 Universidade Federal do Maranhão, Programa de Pós-Graduação em Biodiversidade e Conservação. Av. dos Portugueses 1966, Cidade Universitária do Bacanga, CEP 65080-805, São Luís, MA, Brazil **2** Universidade Federal do Maranhão, Programa de Pós-Graduação em Biodiversidade e Biotecnologia da Amazônia Legal. Av. dos Portugueses 1966, Cidade Universitária do Bacanga, CEP 65080-805, São Luís, MA, Brazil **3** Universidade Federal de Pernambuco, Programa de Pós-Graduação em Biologia Animal. Av. Professor Moraes Rego 1235, Cidade Universitária, CEP: 50670-901, Recife, PE, Brazil **4** Universidade Federal do Maranhão, Departamento de Biologia, Laboratório de Genética e Biologia Molecular, Av. dos Portugueses 1966, Cidade Universitária do Bacanga, CEP 65080-805, São Luís, MA, Brazil **5** Universidade Federal do Maranhão, Laboratório de Sistemática e Ecologia de Organismos Aquáticos, Centro de Ciências Agrárias e Ambientais, Campus Universitário, CCAA, BR-222, KM 04, S/N, Boa Vista, CEP 65500-000, Chapadinha, MA, Brazil **6** Universidade Federal do Maranhão, Programa de Pós-Graduação em Oceanografia. Av. dos Portugueses 1966, Cidade Universitária do Bacanga, CEP 65080-805, São Luís, MA, Brazil

Corresponding author: Erick Cristofore Guimarães (erick.ictio@yahoo.com)

Academic editor: J. Maldonado | Received 3 February 2018 | Accepted 7 May 2018 | Published 7 June 2018

<http://zoobank.org/07277DB7-7563-4712-AC3F-E940B1B4AC27>

Citation: Guimarães EC, De Brito PS, Feitosa LM, Carvalho-Costa LF, Ottoni FP (2018) A new species of *Hyphessobrycon* Durbin from northeastern Brazil: evidence from morphological data and DNA barcoding (Characiformes, Characidae). ZooKeys 765: 79–101. <https://doi.org/10.3897/zookeys.765.23157>

Abstract

A new species of *Hyphessobrycon* is described for the upper Munim and Preguiças river basins, northeastern Brazil, supported by morphological and molecular species delimitation methods. This new species belongs to the *Hyphessobrycon sensu stricto* group, as it has the three main diagnostic character states of this assemblage: presence of a dark brown or black blotch on the dorsal fin, absence of a black midlateral stripe on its flank and the position of Weberian apparatus upward horizontal through dorsal margin of operculum. Our phylogenetic analysis also supported the allocation of the new species in this group; however, it was not possible to recover the species sister-group. *Pristella maxillaris* and *Moenkhausia hemigrammoides* were recovered as the sister-clade of the *Hyphessobrycon sensu stricto* group.

Resumo

Uma nova espécie de *Hyphessobrycon* é aqui descrita para as bacias do alto Rio Munim e Preguiças, nordeste do Brasil, sustentada por métodos morfológicos e moleculares de delimitação de espécies. Essa nova espécie é membro do grupo *Hyphessobrycon sensu stricto*, já que possui os três principais estados de caracteres diagnósticos desse agrupamento: presença de uma mancha marrom escura ou negra na nadadeira dorsal, ausência de uma faixa lateral no meio do flanco e a posição do aparelho de Weber localizado acima da horizontal da margem dorsal do opérculo. Nossa análise filogenética também apoia o posicionamento da nova espécie dentro desse grupo, entretanto não foi possível recuperar o grupo-irmão da espécie. *Pristella maxillaris* e *Moenkhausia hemigrammoides* foram recuperados com sendo o clado irmão do grupo *Hyphessobrycon sensu stricto*.

Keywords

Hyphessobrycon sensu stricto, integrative taxonomy, Pristellinae, rosy tetra clade

Palavras-chave

clado rosy tetra, *Hyphessobrycon sensu stricto*, taxonomia integrativa, Pristellinae

Introduction

Hyphessobrycon Durbin, 1908 is one of the most species-rich genera of Characidae, currently comprising approximately 150 valid species (Ohara et al. 2017). It is widely distributed along the river basins of the Neotropical region, from southern Mexico to the La Plata River basin in northeastern Argentina (Carvalho and Malabarba 2015, Teixeira et al. 2015, Garcia-Alzate et al. 2017), with highest diversity in the Amazon basin (Miquelarena and López 2006, Lima et al. 2013, Bragança et al. 2015, Carvalho and Malabarba 2015, Marinho et al. 2016, Carvalho et al. 2017, Moreira and Lima 2017).

Extensive data show that *Hyphessobrycon* is not a monophyletic group (Carvalho et al. 2017, Moreira and Lima 2017). It was diagnosed by an artificial combination of character states proposed by Eigenmann (1917), such as: the presence of an adipose fin; maxillary with few teeth or none; lateral line incomplete; third infraorbital bone not in contact with the sensory canal of the preopercle; premaxillary with two series of teeth; and caudal-fin lobes without scales at the base. Nevertheless, new species descriptions continue to follow this artificial combination (e.g., Ohara et al. 2017, Garcia-Alzate et al. 2017, Carvalho et al. 2017, Moreira and Lima 2017).

In addition, some artificial species groups of *Hyphessobrycon* were proposed based on the combination of character states (e.g., Weitzman and Palmer 1997, Zarske 2014, García-Alzate et al. 2008a, b, 2013, Carvalho and Malabarba 2015) relying mainly on coloration patterns. However, in many cases, it is not possible to assign without reasonable doubt to which group a particular species belongs (Bragança et al. 2015).

One of this species group was termed as “group F” by Géry (1977), being defined by the presence of a dark brown or black blotch on dorsal fin and no midlateral stripe on body. This group was previously termed as “*callistus* group”, with a similar composition and definition by Géry (1961). Weitzman and Palmer (1997) proposed the name “rosy tetra clade” for this assemblage, including approximately 30 species of *Hyphessobrycon*

and a few other probably closely related species belonging to other genera. These authors also confirmed the presence of the black blotch on the dorsal fin as one of the main diagnostic features of this assemblage. However, they also stated that this blotch was absent in some of its species (e.g., *H. ecuadoriensis* Eigenmann & Henn, 1914, *H. loweae* Costa & Géry, 1994 and *H. panamensis* Durbin, 1908).

After that, Carvalho (2011) and Carvalho and Malabarba (2015) proposed the group named *Hyphessobrycon sensu stricto*, diagnosed by the position of Weberian apparatus upward horizontal through dorsal margin of operculum, presence of a black blotch on dorsal fin and the absence of a midlateral black stripe on body, with a more restricted composition than the “rosy tetra clade” *sensu* Weitzman and Palmer (1997), comprising: *H. compressus* (Meek, 1904), *H. bentosi* Durbin, 1908, *H. copelandi* Durbin, 1908, *H. epicharis* Weitzman & Palmer, 1997, *H. eques* (Steindachner, 1882), *H. erythro stigma* (Fowler, 1943), *H. georgettae* Géry, 1961, *H. haraldschultzi* Travassos, 1960, *H. hasemani* Fowler, 1913, *H. khardinae* Zarske, 2008, *H. megalopterus* (Eigenmann, 1915), *H. micropterus* (Eigenmann, 1915), *H. minor* Durbin, 1909, *H. pulchripinnis* Ahl, 1937, *H. pyrrhonotus* Burgess, 1993, *H. rosaceus* Durbin, 1909, *H. roseus* (Géry, 1960), *H. simulatus* (Géry, 1960), *H. socolofi* Weitzman, 1977, *H. sweglesi* (Géry, 1961), *H. takasei* Géry, 1964 and *H. werneri* Géry & Uj, 1987. Other species recently referred to the “rosy tetra clade” such as *Hyphessobrycon dorsalis* Zarske, 2014, *H. jackrobertsi* Zarske, 2014, *H. paepkei* Zarske, 2014 and *H. pando* Hein, 2009 share these traits, but their taxonomic status is uncertain (Carvalho and Malabarba 2015). The key point is that the remaining species of *Hyphessobrycon* included in the other groups will probably need to be assigned to other genera or new genera (*Hyphessobrycon sensu lato*) (Carvalho and Malabarba 2015).

One way to overcome the confusing taxonomy of problematic groups, to have accurate species identifications and species diversity estimates of groups is to use different operational criteria for species delimitation (Goldstein and Desalle 2010, Padial et al. 2010). Any operational criteria (species delimitation methods) may separately provide evidence about the species limits and identity independently from other criteria (de Queiroz 2005, 2007), but evidence corroborated from multiple operational criteria is considered to produce stronger hypotheses of lineage divergence (de Queiroz 2007, Goldstein and Desalle 2010), converging to the proposal for an integrative taxonomy (Goldstein and Desalle 2010, Padial et al. 2010). Gathering morphological and molecular data has become a common practice to identify and delimit species of fish (Teletchea 2009), mainly in groups including cryptic or morphologically similar species. The most widespread molecular method used in taxonomy has been the DNA barcoding, which consists on the use of a single gene from mitochondrial DNA (cytochrome oxidase subunit I – COI) as a proxy for species differentiation (Hebert et al. 2003). In fact, several studies have been carried out using molecular markers and new species have been delimited and/or described, in most cases, based both on molecular and morphological evidence (e.g., Costa and Amorim 2011, Costa et al. 2012, Roxo et al 2012, Villa-Verde et al. 2012, Castro-Paz et al. 2014, Costa et al. 2014, Benzaquem et al 2015, Mattos et al. 2015, Costa et al. 2017).

A new species of *Hyphessobrycon*, member of the *Hyphessobrycon sensu stricto* Carvalho and Malabarba, 2015 is herein described from the Munim and Preguiças river basins, two coastal river basins of the Maranhão State, northeastern Brazil, based on both morphology and molecular data.

Materials and methods

Morphological analysis

Measurements and counts were made according to Fink and Weitzman (1974), with exception for the scale rows below lateral line, which were counted to the insertion of pelvic fin. Horizontal scale rows between the dorsal-fin origin and lateral line do not include the scale of the median predorsal series situated just anterior to the first dorsal-fin ray. Counts of supraneurals, vertebrae, procurrent caudal-fin rays, unbranched dorsal and anal fin rays, branchiostegal rays, gill-rakers, premaxillary, maxillary, and dentary teeth were taken only from cleared and stained paratypes (C&S), prepared according to Taylor and Van Dyke (1985). The four modified vertebrae that constitute the Weberian apparatus were not included in the vertebra counts and the fused PU1 + U1 was considered as a single element. Osteological nomenclature follows Weitzman (1962). Institutional abbreviations follow Sabaj-Pérez (2016), with addition of **CICCAA** Coleção Ictiológica do Centro de Ciências Agrárias e Ambientais and **CPUFMA** Coleção de Peixes da Universidade Federal do Maranhão.

Comparative material examined

All specimens are from Brazil.

Hyphessobrycon amandae Géry & Uj, 1987: UFRJ 1557, 5 spcms, Goiás State, Jussara municipality. *H. bentosi*: CICCAA 00849, 2 spcms, aquarium trade. *H. cf. bentosi*: CICCAA 00701, 1 spcm, Pará State, Paragominas municipality. CICCAA 00702, 2 spcms, Pará State, Paragominas municipality. CICCAA 00703, 1 spcm (C&S), Pará State, Paragominas municipality. *H. bifasciatus* Ellis, 1911: UFRJ 0068, 6 spcms, Espírito Santo State, Marataízes and Guarapari municipality. *H. copelandi*: CICCAA 00722, 2 spcms, Pará State, Marabá municipality. *H. diancistrus* Weitzman, 1977: UFRJ 2166, 55 spcms, Tocantins State, Ilha do Bananal municipality. *H. eques*: CICCAA 00715, 4 spcms (C&S), Minas Gerais State, Tombos municipality. CICCAA 00710, 51 spcms, Minas Gerais State, Tombos municipality. *H. griemi* Hoedeman, 1957: UFRJ 4496, 7 spcms, Santa Catarina State, Esplanada municipality. *H. haraldschultzi*: CICCAA 00873, 20 spcms, Tocantins State, Ilha do Bananal municipality. *H. itaparicensis* Lima & Costa, 2001: CICCAA 00314, 6 spcms, Sergipe State, Areia Branca municipality. *Pristella maxillaris* (Ulrey, 1894): CICCAA 00850, 2 spcms, aquarium trade. *H. micropterus*: FMNH 57916,

1 spcm, Rio São Francisco at Lagoa do Porto (Photograph of a Holotype). CICCAA 00300, 24 spcms, Bahia; Barras municipality. CICCAA 00699, 8 spcms (C&S), Barras, Bahia municipality. *H. reticulatus* Ellis, 1911: UFRJ 0107, 4 spcms, Rio de Janeiro State, Desengano municipality. *H. sergipanus* Bragança, Ottoni & Rangel-Pereira, 2016: CICCAA 00296, 11 spcms, Sergipe State, Estância municipality. UFRJ 5582, 8 spcms, Mato Grosso State, Poconé municipality. UFRJ 3937, 4 spcms, Mato Grosso State, Cárceres municipality. *H. stegemanni* Géry, 1961: UFRJ 1988, 17 spcms, Tocantins State, Porto Nacional municipality. *H. sweglesi*: CICCAA 00852, 2 spcms, trade aquarium. *H. wernerei*: MUZUSP 42365, 1 spcm, Pará State, Santa Maria do Pará municipality. CICCAA 00751, 1 spcm, Pará State, Paragominas municipality.

DNA extraction, amplification, and sequencing

DNA extraction was carried out with the Wizard Genomic DNA Purification kit (Promega) following manufacturer's protocol. DNA quality was evaluated by agarose gel electrophoresis stained with GelRed (Biotium) and was quantified using Nanodrop 2000 (Thermo Fisher Scientific). DNA was stored at -20 °C until further procedures. Samples (N= 4; Table 1) were amplified using standard PCR (Polymerase Chain Reaction) for partial cytochrome oxidase subunit 1 (COI) gene, with primers designed by Ward et al. (2005) (FISHF1 5'-TCAACCAACCACAAAGACATTGGCAC-3' and FISHR1 5'-TAGACTTCTGGGTGGCCAAAGAATCA-3'). Amplification reactions were performed in a total volume of 15 µl comprising 1× buffer, 1.5 mM MgCl₂, 200 µM dNTP, 0.2 µM of each primer, 1 U of Taq Polymerase (Invitrogen), 100 ng of DNA template, and ultrapure water. The amplification program consisted of a denaturation of 2 min at 94 °C, followed by 35 cycles of 30s at 94 °C, 30s at 54 °C, and 1 min at 72 °C, ending in an extension phase of 10 min at 72 °C. Amplicons were visualized in 1% agarose gel electrophoresis stained with GelRed (Biotium) and purified with Illustra GFX PCR DNA and Gel Purification Kit (GE Healthcare). Samples were sequenced using both forward and reverse primers and BigDye Terminator kit 3.1 Cycle Sequencing kit (Thermo Fisher Scientific) in ABI 3730 DNA Analyser (Thermo Fisher Scientific) Consensus sequences were edited in Geneious 9.0.5 (Kearse et al. 2012) and aligned using ClustalW (Thompson 1994) with those from *Hyphessobrycon* species available in Barcode of Life Database (BOLD) and Genbank (NCBI-National Center for Biotechnology Information) (accession numbers are in Table 1).

Species concept, species delimitation, and diagnoses

The unified species concept (de Queiroz 2005, 2007) is herein adopted by expressing the conceptual definition shared by all traditional species concepts – “species are (segments of) separately evolving metapopulation lineages” – when operational criterion elements to delimit taxa are excluded from the concepts. According to this concept,

Table 1. Sampling sites, specimens and DNA sequence information included in the study.

Species	Locality	Basin/ drainage	Country	GenBank/ BoldSystems	Catalog number
<i>Hyphessobrycon piorskii</i> sp. n.	Anapurus, Maranhão	Munim	Brazil	MF765796	CICCAA00725
<i>Hyphessobrycon piorskii</i> sp. n.	Anapurus, Maranhão	Munim	Brazil	MF765797	CICCAA00726
<i>Hyphessobrycon piorskii</i> sp. n.	Barreirinhas, Maranhão	Preguiças	Brazil	MG791915	CICCAA01650
<i>Hyphessobrycon piorskii</i> sp. n.	Anapurus, Maranhão	Munim	Brazil	MG791914	CICCAA01651
<i>Hyphessobrycon bentosi</i>	Barcelos, Amazonas	Negro	Brazil	HYP097-13	INPA37684-5939
<i>Hyphessobrycon bentosi</i>	Barcelos, Amazonas	Negro	Brazil	HYP098-13	INPA37684-5940
<i>Hyphessobrycon bentosi</i>	Barcelos, Amazonas	Negro	Brazil	HYP099-13	INPA37684-5942
<i>Hyphessobrycon bentosi</i>	Barcelos, Amazonas	Negro	Brazil	HYP100-13	INPA37684-5943
<i>Hyphessobrycon bentosi</i>	Manaus, Amazonas	–	Brazil	HYP116-13	INPA39527-BA1
<i>Hyphessobrycon bentosi</i>	Manaus, Amazonas	–	Brazil	HYP117-13	INPA39527-BA2
<i>Hyphessobrycon bentosi</i>	Manaus, Amazonas	–	Brazil	HYP118-13	INPA39527-BA3
<i>Hyphessobrycon bentosi</i>	Manaus, Amazonas	–	Brazil	HYP119-13	INPA39527-BA4
<i>Hyphessobrycon copelandi</i>	Tabatinga, Amazonas	Solimões	Brazil	HYP094-13	INPA37683-TU1
<i>Hyphessobrycon copelandi</i>	Tabatinga, Amazonas	Solimões	Brazil	HYP095-13	INPA37683-TU1
<i>Hyphessobrycon copelandi</i>	Tabatinga, Amazonas	Solimões	Brazil	HYP096-13	INPA37683-TU1
<i>Hyphessobrycon eques</i>	Santarém, Pará	Amazonas	Brazil	HYP070-13	INPA37678-IC2
<i>Hyphessobrycon eques</i>	Parintins, Amazonas	Amazonas	Brazil	HYP072-13	INPA37680-AL1
<i>Hyphessobrycon erythrostigma</i>	Tabatinga, Amazonas	Solimões	Brazil	HYP073-13	INPA37681-AP1
<i>Hyphessobrycon erythrostigma</i>	Tabatinga, Amazonas	Solimões	Brazil	HYP074-13	INPA37681-AP2
<i>Hyphessobrycon epicharis</i>	São Gabriel da Cachoeira, Amazonas	Negro	Brazil	HYP002-13	INPA37665-JUF1
<i>Hyphessobrycon epicharis</i>	São Gabriel da Cachoeira, Amazonas	Negro	Brazil	HYP003-13	INPA37665-JUF2
<i>Hyphessobrycon megalopterus</i>	–	–	–	FJ749058	–
<i>Hyphessobrycon megalopterus</i>	–	–	–	KU568879.1	–
<i>Hyphessobrycon pyrrhonotus</i>	Santa Isabel do rio Negro, Amazonas	Negro	Brazil	HYP039-13	INPA37672-TRO1
<i>Hyphessobrycon pyrrhonotus</i>	Santa Isabel do rio Negro, Amazonas	Negro	Brazil	HYP040-13	INPA37672-TRO10
<i>Hyphessobrycon pyrrhonotus</i>	Santa Isabel do rio Negro, Amazonas	Negro	Brazil	HYP042-13	INPA37672-TRO2
<i>Hyphessobrycon socolofi</i>	Santa Isabel do rio Negro, Amazonas	Negro	Brazil	HYP020-13	INPA37667-UR1
<i>Hyphessobrycon socolofi</i>	Santa Isabel do rio Negro, Amazonas	Negro	Brazil	HYP022-13	INPA37667-UR7
<i>Hyphessobrycon rosaceus</i>	São Gabriel da Cachoeira, Amazonas	Negro	Brazil	HYP032-13	INPA37669-MAC4
<i>Hyphessobrycon rosaceus</i>	Nova Airão, Amazonas	Negro	Brazil	HYP069-13	INPA37677-FU1
<i>Hyphessobrycon rosaceus</i>	São Gabriel da Cachoeira, Amazonas	Negro	Brazil	HYP082-13	INPA37682-ACA1
<i>Hyphessobrycon sweglesi</i>	São Gabriel da Cachoeira, Amazonas	Negro	Brazil	HYP024-13	INPA37668-JAR1
<i>Hyphessobrycon sweglesi</i>	São Gabriel da Cachoeira, Amazonas	Negro	Brazil	HYP025-13	INPA37668-JAR2
<i>Hyphessobrycon sweglesi</i>	São Gabriel da Cachoeira, Amazonas	Negro	Brazil	HYP028-13	INPA37668-JAR5
<i>Moenkhausia hemigrammoides</i>	Rupununi Road-Guyana	–	Guyana	HYP101-13	INPA38532-PR1

Species	Locality	Basin/ drainage	Country	GenBank/ BoldSystems	Catalog number
<i>Pristella maxillaris</i>	–	–	–	KU568982.1	–
<i>Pristella maxillaris</i>	–	–	–	KU568981.1	–
<i>Hyphessobrycon flammeus</i>	–	–	Brazil	FUPR988-09	LBPV-40464
<i>Hyphessobrycon anisitsi</i>	–	–	Brazil	GBGCA516-10	FJ749040

species are treated as hypothetical and could be tested by the application of distinct criteria (species delimitation methods) (de Queiroz 2005, 2007). It allows for any criteria to separately provide evidence about species limits and identities, independently from other criteria (de Queiroz 2005, 2007). Evidence corroborated from multiple operational criteria is considered to produce stronger hypotheses of lineage separation (de Queiroz 2007, Goldstein and Desalle 2010), a practice called “integrative taxonomy” (Dayrat 2005, Goldstein and Desalle 2010, Padial et al. 2010).

Two distinct operational criteria to delimit species, based on morphological and molecular data, were implemented here. The Population Aggregation Analysis (Davis and Nixon 1992) is a character-based method (hereafter PPA), which consists of an exclusive shared combination of character states assigned to a given population or group of populations. The second method, DNA barcoding, as proposed by Hebert et al. (2003 a, b, 2004 a, b) (hereafter DBC), is a genetic distance-based cut-off method.

Population Aggregation Analysis (PAA)

Only morphological character states were used for this method. The morphological data was based on both examined material (see Comparative material examined) and the literature (e.g., Géry 1977, Géry and Uj 1987, Costa and Géry 1994, Plaquete et al. 1996, Weitzman and Palmer 1997, Zarske 2008, Hein 2009, Carvalho 2011, Lima et al. 2013, Zarske 2014, Carvalho and Malabarba 2015, Carvalho et al. 2017). The data obtained by this method are presented in the diagnosis section of results.

DNA barcoding (DBC)

Pairwise genetic distances between species were calculated using Kimura-2-parameters model (K2P) (Kimura 1980) on the MEGA 7 software (Tamura et al. 2011). Evolutionary relationships among sequences were reconstructed by Bayesian inference using the MrBayes (Huelsenbeck and Ronquist 2001) plugin in Geneious 9.0.5. An independent run with a chain length of 10 million, a burn-in length of 500,000 generations, and subsampling trees every 10,000 generations was carried out under the GTR (generalized time reversible) evolutionary model, which was estimated in jmodeltest (Darriba et al. 2012). *Hyphessobrycon flammeus* Myers, 1924 and *H. anisitsi* (Eigenmann, 1907) were used as outgroup. The ingroup was composed by the remaining terminals.

Results

Hyphessobrycon piorskii sp. n.

<http://zoobank.org/379CFBEA-C3FE-4729-9469-029732DC62BC>

Figures 1, 2

Holotype. CICCAA 00695, 25.9 mm SL, Brazil, Maranhão State: stream at the Anapurus municipality, 03°40'14"S, 43°07'10"W, 05 Feb 2017, Guimarães E. C. and Brito P. S.

Paratypes. All from Brazil, Maranhão State: CICCAA 00430, 15, 18.4–25.2 mm SL; CICCAA 00696, 15, 19.9–24.4 mm SL, CICCAA 00697, 16 (C&S) 19.3–24.5 mm SL; CICCAA 00698, 6, 1 (C&S) 22.0–20.4 mm SL; CICCAA 00750, 9, 20.0–25.3 mm SL; CPUFMA 171664, 15, 19.5–23.1 mm SL; UFRJ 11553, 6, 19.1–22.1 mm SL collected with holotype. CICCAA 00089, 1 (C&S) 25.2 mm SL, stream at Mata de Itamacaoca, Chapadinha municipality; 03°44'50"S, 43°19'21"W, 02 Apr. 2016, Ottoni F. P., Oliveira E., Nascimento I., Fernandes R., Carneiro V. leg. CICCAA 00431, 21, 15.3–19.8 mm SL, stream at the Anapurus municipality, 03°40'53"S, 43°07'23"W, 15 Jan. 2017, W; Aguiar R. leg. CICCAA 00881, 1, 29.4 mm SL, stream at Mata de Itamacaoca, Chapadinha municipality; 03°44'45"S, 45°19'15"W, 15 Jul. 2017, Campos D., Oliveira E., Viana S., Lopes M., Sousa R. leg. CICCAA 01563, 1, 21.6 mm SL, stream at Mata de Itamacaoca, Chapadinha municipality; 03°44'55"S 43°19'55"W, 19 Nov. 2017, Guimarães E. C., Brito P. S., Ottoni F. P., Lucas O., Sousa R. leg. CICCAA01654, 1, 26.9 mm SL, stream at the Anapurus municipality, 03°40'14"S, 43°07'10"W, 17 Jan. 2018, Guimarães E. C. and Brito P. S. leg. CICCAA 01382, 5, 22.7–27.2 mm SL, stream at Mata Fome, Barreirinhas municipality, 02°39'47"S, 42°48'16"W, 15 Jun., 2017, Guimarães E. C., Brito P. S., Ottoni F. P., Ferreira B. R. CICCAA 02008, 12 (C&S), 15.4–18.3 mm SL, stream at Mata Fome, Barreirinhas municipality; 02°39'47"S, 42°48'16"W, 15 Jun., 2017, Guimarães E. C., Brito P. S., Ottoni F. P., Ferreira B. R. leg.

Diagnosis (PAA). The new species *Hyphessobrycon piorskii* sp. n., promptly differs from most congeners except by species of *Hyphessobrycon sensu stricto* by the presence of a dark brown or black blotch on dorsal fin (vs. absence), no midlateral stripe on the body (vs. presence) and Weberian apparatus upward horizontal through dorsal margin of operculum (vs. downward).

The new species herein described differs from all of its congeners from *Hyphessobrycon sensu stricto*, with exception to *H. bentosi* and *H. hasemani*, by possessing an inconspicuous vertically elongated humeral spot [vs. approximately rounded humeral spot in *H. copelandi*, *H. erythrostigma*, *H. jackrobertsi*, *H. minor*, *H. pando*, *H. paepkei*, *H. pyrrhonotus*, *H. roseus*, *H. socolofi*, and *H. sweglesi*; humeral spot horizontally or posteriorly elongated in *H. epicharis*, *H. khardinae*, and *H. wernerii*; conspicuous humeral spot in *H. eques*, *H. haraldschultzi* Travassos, 1960, *H. micropterus*, *H. megalopterus*, *H. simulatus* and *H. takasei*; and absence of humeral spot in *H. compresus*, *H. dorsalis* Zarske, 2014, *H. georgettae*, *H. pulchripinnis*, and *H. rosaceus*].



Figure 1. *Hyphessobrycon piorskii* sp. n. **A** CICCAA 00695, holotype, 25.9 mm SL, Brazil: Maranhão State: Munim River basin **B** CICCAA 00881, paratype, 29.4 mm SL, Brazil: Maranhão State: Munim River basin (photographed by Felipe Ottoni).

The new species differs from *H. bentosi* by the absence of an extended and pointed dorsal and anal-fin tips (Figures 1, 2) [vs. extended and pointed dorsal and anal-fin tips]; and from *H. basemani* by the dorsal-fin black spot shape, which is located approximately at the middle of the fin's depth, not reaching its tip [vs. extended along all the fin, reaching its tip in adults] and by presenting tri to unicuspid teeth in the inner row of premaxillary and dentary [vs. pentacuspid teeth].

Description. Morphometric data of holotype and paratypes are presented in Table 3. Body compressed, moderately deep, greatest body depth slightly anterior to dorsal-fin base. Body profile straight and downward directed from end of dorsal fin to adipose fin, straight or slightly convex between later point and origin of dorsal most procurrent caudal-fin ray. Dorsal profile of head convex from upper lip to vertical through eye; predorsal profile of body roughly straight, dorsal-fin base slightly convex, posteroventrally inclined; ventral profile of head convex from lower jaw to pelvic-fin

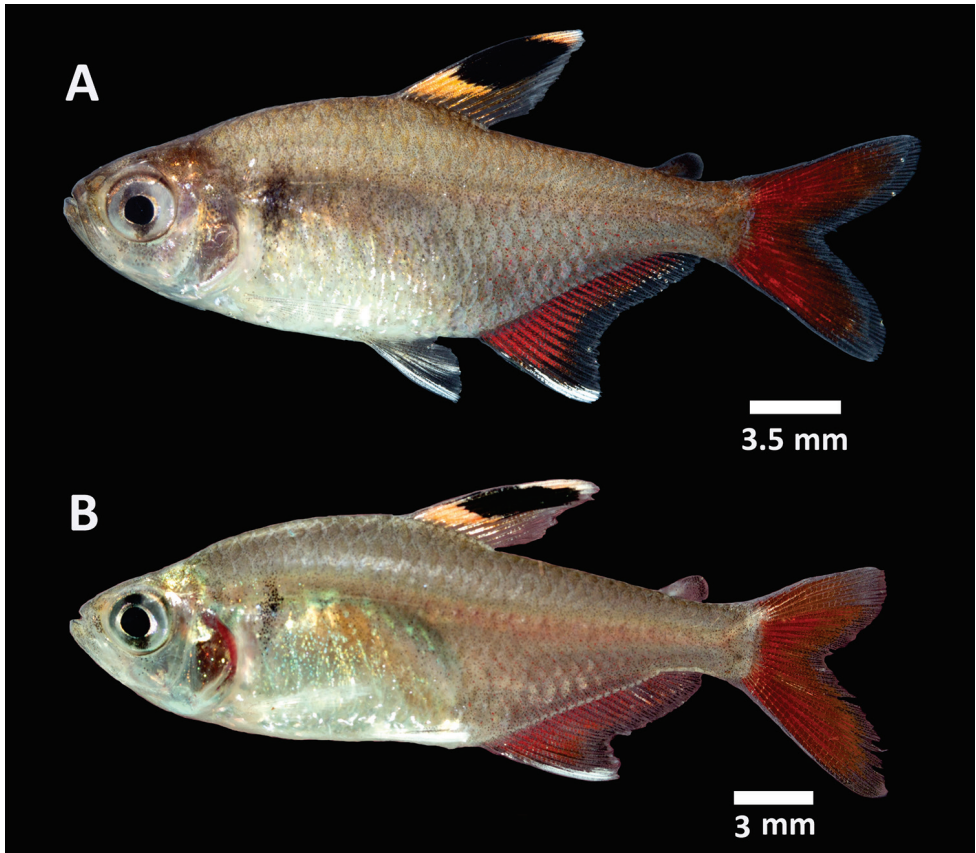


Figure 2. *Hyphessobrycon piorskii* sp. n. **A** CICCAA 00698, paratype, 26.9 mm SL, Brazil: Maranhão State: Munim River basin; living specimen photographed immediately after collection **B** CICCAA 00089, paratype, 25.2 mm SL, Brazil: Maranhão State: Munim River basin; living specimen photographed immediately after collection (photographed by Felipe Ottoni).

origin. Ventral profile of body straight or slightly convex from pelvic-fin origin to anal-fin origin; straight and posterodorsally slanted along anal-fin base; and slightly concave on caudal peduncle. Jaws equal, mouth terminal, anteroventral end of dentary protruding. Maxilla reaching vertical to anterior margin of pupil. Premaxillary teeth in two rows. Outer row with one tricuspid tooth; inner row with 6(6), 7(20) or 8(4) tricuspid teeth and one unicuspid tooth. Maxilla with 3(5), 5(24) or 6(1) tricuspid teeth. Dentary with five (21) or six (9) larger tricuspid teeth followed by one smaller tricuspid teeth 5(2), 6(6), 7(13), 8(5), 9(4) smaller unicuspid teeth (Figure 3). Scales cycloid, three to eight radii strongly marked, *circuli* well-marked anteriorly, weakly-marked posteriorly; lateral line incompletely pored, with 6(19), 7(62) or 8(13) perforated scales. Longitudinal scales series including lateral-line scales 31(9), 32(34), 33(26), 34(17) or 35(3). Longitudinal scales rows between dorsal-fin origin and lateral line 6(49) or 7(41). Horizontal scale

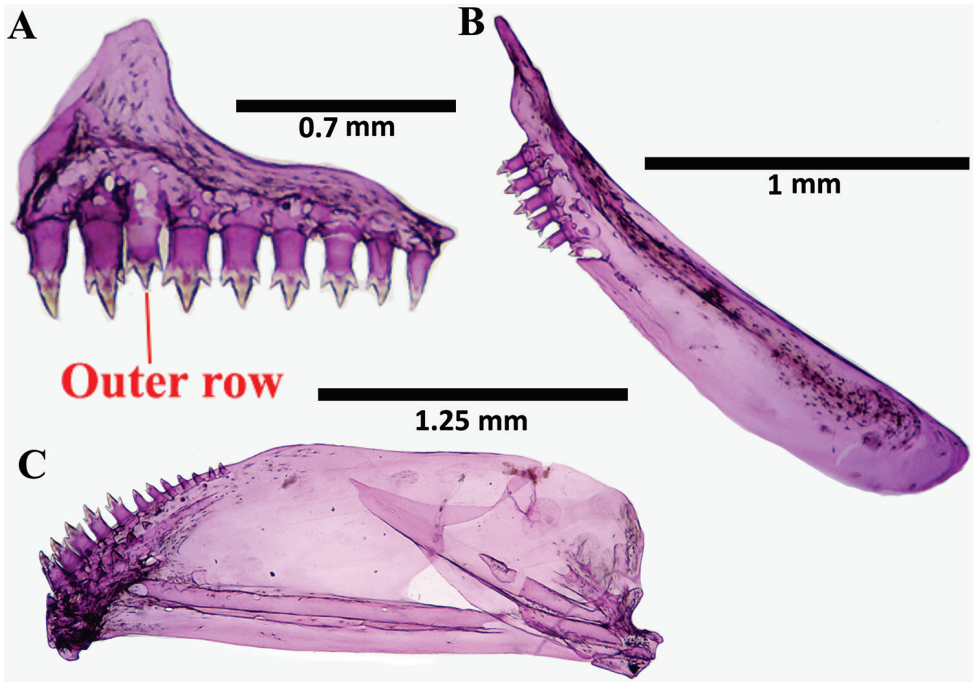


Figure 3. *Hyphessobrycon piorskii* sp. n. CICCAA 00697, 19.3 mm SL; jaw suspensory: **A** Premaxillary. **B** Maxilla **C** Dentary (Photographed by Erick Guimarães).

rows between lateral line and pelvic-fin origin 4(18) or 5(71). Scales in median series between tip of supraoccipital spine and dorsal-fin origin 8(6), 9(14), 10(7) or 11(3). Circumpeduncular scales 11(16), 12(38) or 13(11). Dorsal-fin rays i + 10(105) or ii + 10(18). First dorsal-fin pterygiophore main body located behind neural spine of 4th vertebrae. Adipose fin present. Anteriormost anal-fin pterygiophore inserting posterior to haemal spine of 11th vertebrae. Anal-fin ii+24(3), iii+24(87), ii-25(32) or iii+25(1). Anterior anal-fin margin slightly convex, with anteriormost rays more elongate and slightly more thickened than remaining rays, forming a distinct lobe. Remaining rays smaller with straight distal margin. Anal-fin rays with a sexually dimorphic pattern, which are absent in females (Figure 4). Pectoral fin-rays 12(122) or 13(1) total rays. Tip of pectoral fin usually reaching vertical through pelvic-fin origin. Pelvic-fin rays 8(125) total rays. Pelvic-fin rays with a sexually dimorphic pattern, which are absent in females (Fig. 5). Caudal fin forked, upper and lower lobes similar in size. Principal caudal-fin rays 10+9(121), 10+10(7) or 11+10(17); dorsal procurrent rays 7(1), 9(13), 10(13) or 11(3) and ventral procurrent rays 6(1), 7(8), 8(12) or 9(9). Branchiostegal rays 4(30). First gill arch with 1(1), 2(29) hypobranchial, 11(1), 12(28) or 13(1) ceratobranchial, 1(30) on cartilage between ceratobranchial and epibranchial, and 5(1) or 6(16) epibranchial gill-rakers. Supraneurals 3(2) 4(23) or 5(5). Total vertebrae 29(30).

Color in alcohol Figure 1. Ground coloration light yellowish brown. Humeral region with one inconspicuous vertically elongated spot; more intensely pigmented on its central portion. Flank with chromatophores homogeneously scattered, more concentrated on posterior region to humeral spot, posterior region of dorsal-fin base origin and below mid-portion of trunk, between anal-fin origin and caudal peduncle. Ventral region lacking dark brown chromatophores. Dark brown chromatophores present on head and more concentrated on dorsal portion, becoming sparser on cheek and preopercular regions.

Dorsal fin ground coloration hyaline, with a conspicuous black or dark brown spot located on anterior portion of fin, reaching about sixth ray, approximately between half to two thirds of fin depth. Anal and caudal fins hyaline. Caudal fin with a darker, usually dark brown, posterior margin and on its base. Adipose fin hyaline to light brown, with dark brown or black chromatophores more concentrated on its dorsal portion, depending on the state of preservation of the specimen. Pectoral and pelvic fins hyaline; pelvic fin with variable amounts dark brown pigmentation remaining depending on the state of preservation of the specimen.

Color in life (Figure 2). Pattern similar to coloration of preserved specimens. Ground coloration light yellowish brown to grey, with a reddish-brown pigmentation on vertebrae region, and usually with red chromatophores. Ventral region anterior to anal-fin origin lighter. Humeral spot inconspicuously dark brown or black. Head with same coloration as body, and ventrally lighter.

Conspicuous black spot on dorsal-fin, with yellow or orange pigmentation on dorsal and ventral margins of spot; yellow or orange pigmentation lighter and less evident on dorsal margin, reaching half to two thirds of the spot length and extending to the tip of fin; yellow or orange pigmentation darker and more developed at ventral margin of the spot, reaching entire spot base length, not extended to dorsal fin-base. Rest of dorsal fin hyaline. Anal-fin base with red pigmentation, with different degrees of intensity, with milk white pigmentation on anterior tip of anal fin, which could be extended through entire anterior margin, reaching between second to fourth rays. Posterior margin of anal fin with an inconspicuous dark brown pigmentation. Adipose fin light brown to hyaline at base, with red to black pigmentation at tip. Pectoral and pelvic fins hyaline, with some sparser dark brown chromatophores, more concentrated at pelvic fin base. First ray of pelvic fin with a white pigmentation. Caudal fin with red pigmentation on almost fin, with an inconspicuous light brown, reddish brown or dark brown margin.

Sexual dimorphism. Mature males have hooks on anal-fin and pelvic-fin rays. Hooks absent on females. Anal-fin presenting hooks from 3rd, 4th or 5th rays through last ray. Number of hooks variable, increasing from the first ones to the last rays. Pelvic fin presenting 3rd and 4th rays with 5 smaller hooks (Figures 4, 5).

DNA-based identification. After trimming sequence ends with poor base call quality, the final alignment yielded 446 base pairs with 154 variable sites, and 22 haplotypes. The magnitude of sequence divergence clearly demonstrates the exist-

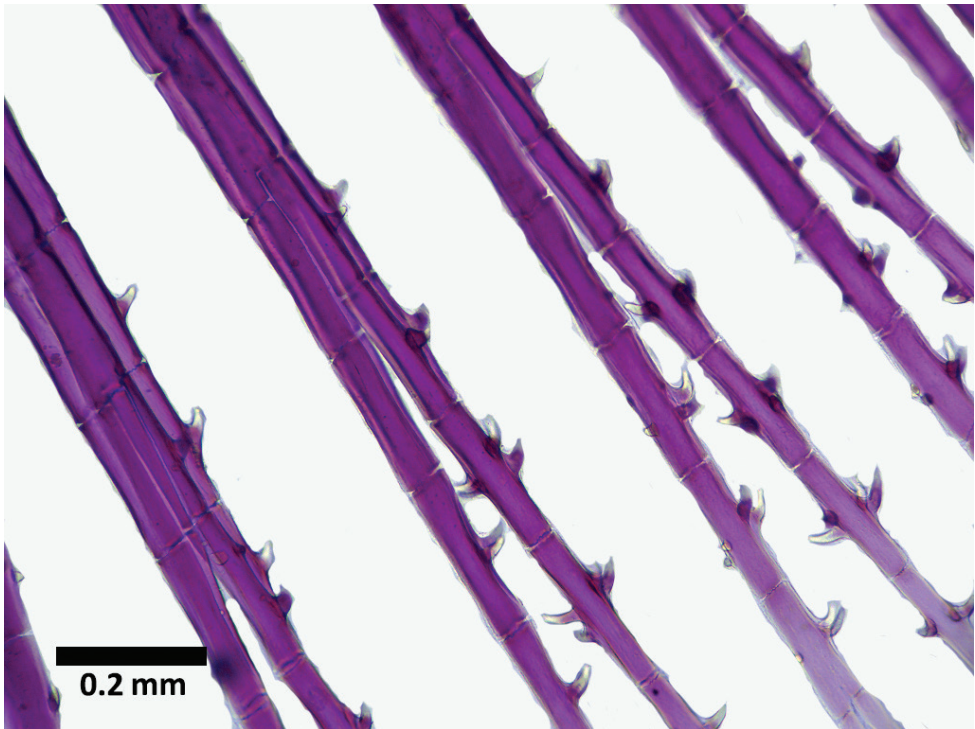


Figure 4. *Hyphessobrycon piorskii* sp. n. CICCAA 00697, male, 19.3 mm SL, bony hooks on anal fin (photographed by Erick Guimarães).

ence of a new species of *Hyphessobrycon* inhabiting the Munim and Preguiças river basins in Maranhão State. Average genetic distances were 14.2%, with the highest values between *H. pyrrhonotus* and *H. epicharis* (19.2%), while the lowest value (2.7%) was between *H. epicharis* and *H. sweglesi* (Table 1). *Hyphessobrycon piorskii* sp. n. has 17% sequence divergent, on average, from the other taxa, with a minimum distance with *H. eques* (13.9%) and a maximum with *H. rosaceus* (18.4%) (Table 2).

Other evidence for the new species is that *H. piorskii* sp. n. formed a single and exclusive clade with maximum posterior probability support (posterior probability = 1) in the Bayesian phylogenetic tree (Figure 7). Furthermore, *H. piorskii* sp. n. clade is located within the *Hyphessobrycon s. str.* group with high support of posterior probability (0.94). *Hyphessobrycon piorskii* sp. n. was recovered as the sister-group of the clade including *H. bentosi*, *H. socolofi*, *H. megalopterus*, *H. erythrostroma* and *H. pyrrhonotus*, with branch support of posterior probability value of 0.55. *Pristella maxillaris* and *Moenkhausia hemigrammoides* formed a clade (posterior probability value = 0.86), and it was recovered as the sister-clade of the *Hyphessobrycon s. str.* group (posterior probability value = 0.6).

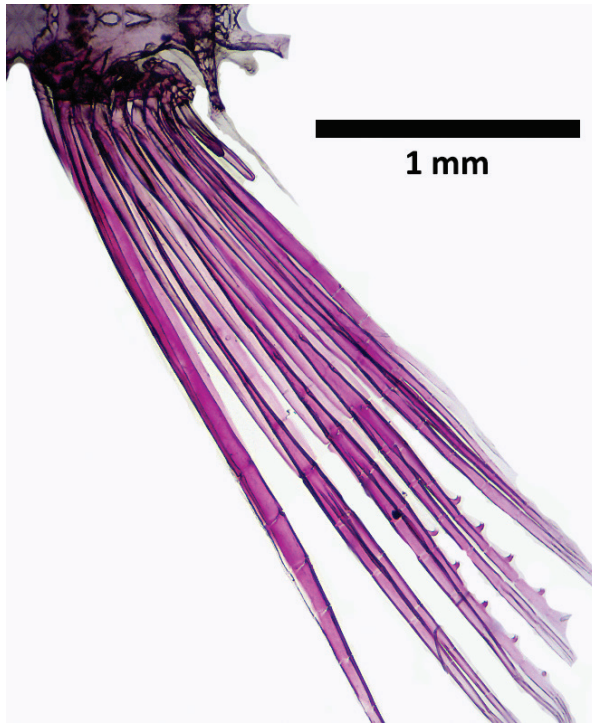


Figure 5. *Hyphessobrycon piorskii* sp. n. CICCAA 00697, male, 19.3 mm SL, bony hooks on pelvic fin (photographed by Erick Guimarães).

Geographical distribution. *Hyphessobrycon piorskii* sp. n. is presently known only from the upper Munim and Preguiças river basins, Maranhão State, northeastern Brazil (Figure 7).

Ecological notes. *Hyphessobrycon piorskii* sp.n. lives in shallow well-oxygenated streams with transparent waters flowing over different types of substrates (Figure 8). The streams where *H. piorskii* sp. n. specimens were collected varied from 0.90 to 10 meters wide, with a maximum depth of 1.60 meters. They possessed moderate water currents (0.1–0.7 m/s), with clear, sandy substrates with pebbles, mud, leaf litter, and submerged logs, often also presenting aquatic macrophytes. *Hyphessobrycon piorskii* sp. n. was found near shore among aquatic vegetation, tree roots and fallen logs. Other species found at both sites were *Anablepsoides vieirai* Nielsen, 2016, *Apistogramma piauiensis* Kullander, 1980, *Astyanax* sp., *Cichlasoma* cf. *zarskei*, *Copella arnoldi* (Regan, 1912), *Crenicichla brasiliensis* (Bloch, 1792), *Hoplias malabaricus* (Bloch, 1794), *Megalechis thoracata* (Valenciennes, 1840), *Nannostomus beckfordi* Günther, 1872, and *Synbranchus marmoratus* Bloch, 1795. Gut contents of C&S specimens contained algae and disarticulated arthropod remains.

Etymology. The name *piorskii* honors the ichthyologist Nivaldo Magalhães Piorski for his contributions to the ichthyologic knowledge of the Maranhão State.

Table 2. Kimura-2 parameters pairwise genetic distances among species. Species names in the upper columns are abbreviated as follows: *H. piorskii* (Hpio), *H. flammeus* (Hfla), *H. anisitsi* (Hani), *H. socolofi* (Hsoc), *H. copelandi* (Hcop), *H. bentosi* (Hben), *H. megalopterus* (Hmeg), *H. eques* (Hequ), *H. erythrostigma* (Hery), *H. pyrrhonotus* (Hpyr), *H. rosaceus* (Hros), *H. sweglesi* (Hswe), *H. epicharis* (Hepi), *M. hemigrammoides* (Mhem), and *P. maxillaris* (Pmax).

Species	Hpio	Hfla	Hani	Hsoc	Hcop	Hben	Hmeg	Hequ	Hery	Hpyr	Hros	Hswe	Hepi	Mhem
Hfla	0.190	-												
Hani	0.194	0.165	-											
Hsoc	0.199	0.193	0.168	-										
Hcop	0.158	0.206	0.162	0.216	-									
Hben	0.207	0.204	0.173	0.008	0.221	-								
Hmeg	0.195	0.209	0.180	0.087	0.213	0.086	-							
Hequ	0.161	0.205	0.186	0.190	0.102	0.194	0.199	-						
Hery	0.196	0.213	0.182	0.114	0.191	0.117	0.131	0.174	-					
Hpyr	0.183	0.206	0.166	0.101	0.191	0.103	0.117	0.181	0.032	-				
Hros	0.218	0.212	0.205	0.224	0.202	0.227	0.204	0.195	0.219	0.221	-			
Hswe	0.205	0.187	0.195	0.224	0.198	0.229	0.192	0.183	0.216	0.211	0.073	-		
Hepi	0.199	0.190	0.198	0.221	0.198	0.226	0.199	0.183	0.233	0.231	0.089	0.028	-	
Mhem	0.185	0.204	0.178	0.214	0.216	0.219	0.234	0.205	0.233	0.222	0.200	0.204	0.208	-
Pmax	0.223	0.212	0.197	0.203	0.219	0.207	0.218	0.200	0.230	0.239	0.202	0.187	0.181	0.169

Table 3. Morphometric data (N = 95) for the holotype and paratypes of *Hyphessobrycon piorskii* sp. n. from the Munim River basin and Preguiças River basin. Abbreviations: SD: Standard deviation.

	Holotype	Paratypes	Mean	SD
Standard length	25.9	18–29.4	20.8	–
Percentages of standard length				
Depth at dorsal-fin origin (body depth)	35.9	28.9–39.4	33.4	1.9
Snout to dorsal-fin origin	49.8	44.2–56.5	52.5	2.1
Snout to pectoral-fin origin	29.1	26.0–35.0	30.8	2.3
Snout to pelvic-fin origin	47.5	39.1–52.2	47.5	1.9
Snout to anal-fin origin	61.9	57.4–66.6	61.7	1.8
Caudal peduncle depth	11.8	9.1–14.1	11.4	0.9
Caudal peduncle length	12.2	8.1–13.6	10.2	1.1
Pectoral-fin length	20.4	16.8–23.7	20.8	1.6
Pelvic-fin length	18.1	13.3–20.4	17.1	1.5
Dorsal-fin base length	15.5	12.9–18.3	15.7	1.2
Dorsal-fin height	28.5	22.1–34.3	29.9	2.4
Anal-fin base length	29.4	26.3–33.9	30.3	1.4
Eye to dorsal-fin origin	35.2	33.6–39.4	36.4	1.4
Dorsal-fin origin to caudal-fin base	50.7	44.9–57.3	51.4	2.3
Head length	26.3	24.2–33.4	29.3	2.1
Percentages of head length				
Horizontal eye diameter	42.8	33.4–43.8	38.2	2.3
Snout length	22.0	16.9–24.4	20.2	1.7
Least interorbital width	25.7	16.4–27.0	20.4	2.2
Upper jaw length	39.6	32.8–41.7	38.1	2.2

Discussion

Despite *Hyphessobrycon*, as defined today, being a non-monophyletic group (Mirande 2010, Oliveira et al. 2011, Carvalho et al. 2017, Ohara et al. 2017, Moreira and Lima 2017), a few putative groups within the genus were proposed in the literature. One such case is the *Hyphessobrycon sensu stricto* as defined by Carvalho (2011) and Cavalho and Malabarba (2015). According to those authors, this group is composed by approximately 25 species.

Among the species considered by Weitzman and Palmer (1997) as possibly related to the “rosy tetra clade”, only *H. hasemani* and *H. pulchripinnis* were considered to belong to *Hyphessobrycon sensu stricto* (Carvalho 2011, Carvalho and Malabarba 2015). *Pristella maxillaris* (Ulrey, 1894) is the sister-group of the *Hyphessobrycon sensu stricto* (Carvalho 2011), and corroborated in our analysis (Figure 6).

Hyphessobrycon piorskii sp. n. exhibits all the diagnostic features that define *Hyphessobrycon sensu stricto* (see introduction and diagnosis section). The new species differs from the other possible species of this assemblage, which also occur near Maranhão (e.g., lower Amazon River basin, Guamá River basin, and São Francisco River basin), such as *H. bentosi*, *H. copelandi*, *H. eques*, *H. dorsalis*, *H. hasemani*, *H. haraldschultzi*, *H. micropterus*, and *H. wernerii*, by a set of features listed below.

Hyphessobrycon piorskii sp. n. possesses an inconspicuous vertically elongated humeral spot, distinguishing it from all the species cited above, except for *H. bentosi* and *H. hasemani* (see morphological diagnosis section). The shape of the dorsal-fin spot is also useful to distinguish *H. piorskii* sp. n. from *H. eques*, *H. hasemani* and *H. micropterus*, which possess dorsal fin spot vertically extended, reaching the tip of the fin, while in *H. piorskii* sp. n. the black spot of dorsal fin never reaches the tip of the fin. The new species also differs from *H. eques* by the color pattern of the anal fin: *H. eques* possess a conspicuous black anal-fin margin on preserved species, while *H. piorskii* sp. n. does not exhibit this feature at the anal fin.

The number of teeth cusps was also revealed to be a useful feature for species discrimination. *Hyphessobrycon piorskii* sp. n. possess all of its teeth with one to three cusps (never pentacuspoid), while *H. eques* possess pentacuspoid teeth on the maxillary and inner row of premaxillary, and *H. copelandi* and *H. hasemani* on the dentary and inner row of the premaxilla (see Lima et al. 2013). The new species differs from *H. bentosi* by not having extended and pointed dorsal and anal-fin tips and by having bone hooks on anal-fin rays of mature males (Figure 3). The dorsal and anal fins of *H. bentosi* have pointed and extended tips, and it has not bony hooks on anal-fin rays (see Carvalho 2011, Zarske 2014). *Hyphessobrycon copelandi* possesses only ten teeth on the dentary, and dorsal-fin black spot reaching to the posterior margin of the fin (see Lima et al. 2013), while *H. piorskii* sp. n. possesses 11–15 teeth on dentary, and dorsal-fin black spot restricted to the anterior half of the fin’s length. In addition, *Hyphessobrycon piorskii* sp. n. is easily distinguished from the sister-species of the clade *Hyphessobrycon sensu stricto*, *P. maxillaris* and *M. hemigrammoides*, by the absence of a black oblique stripe or band on the anterior portion of the anal fin (Figures 1, 2) [vs. presence (Carvalho et al. 2017, figure 7; pers. obs.)].

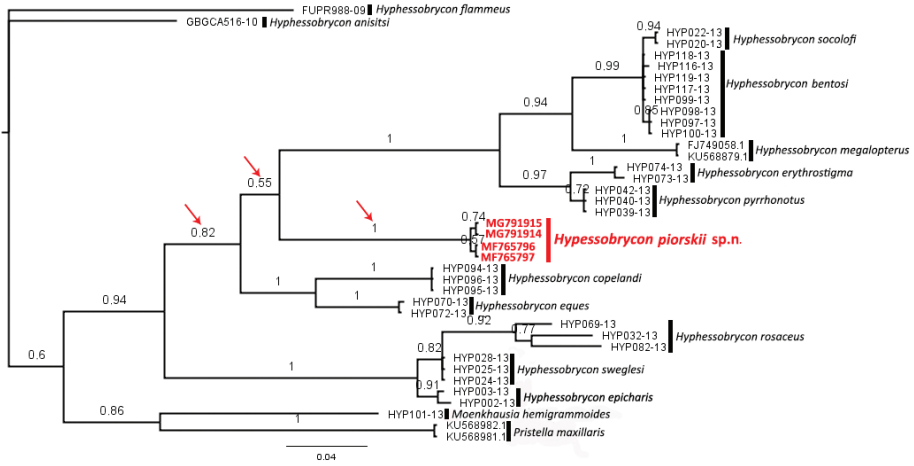


Figure 6. Bayesian phylogenetic tree including *Hyphessobrycon piorskii* sp. n. (in red) and other congeners. Number above branches are posterior probability values.

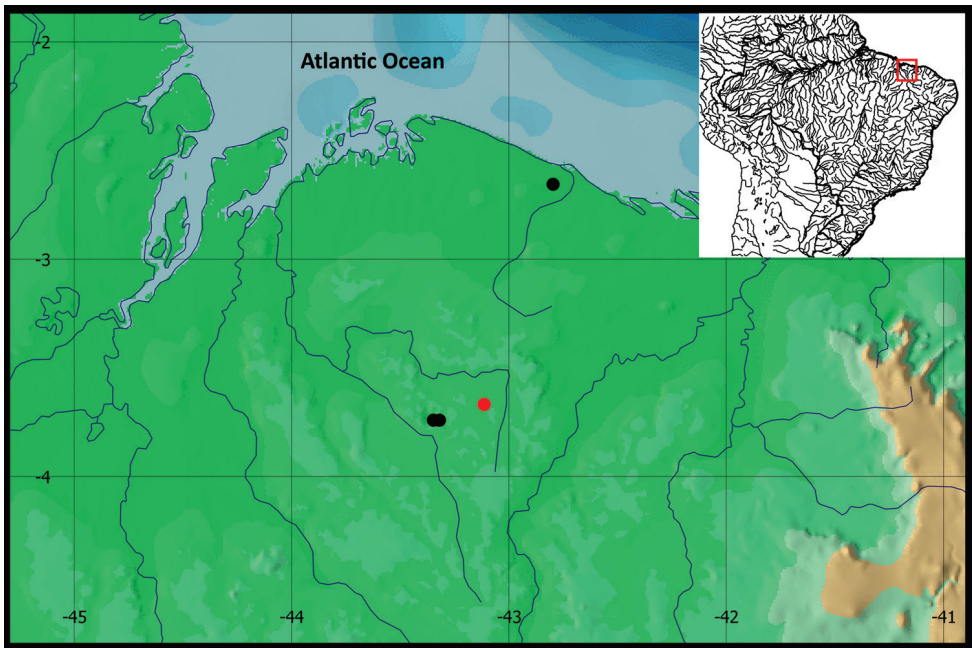


Figure 7. Geographical distribution of *Hyphessobrycon piorskii* sp. n. Red circle denote Holotype and black circle denote paratypes.

The description of *H. piorskii* sp. n. was based on morphological and molecular species delimitation methods, using the congruence of multiple operational criteria for determining species boundaries. As mentioned earlier, evidence corroborated from



Figure 8. Collecting sites of *Hyphessobrycon piorskii* sp. n. **A** stream at the Anapurus municipality **B** stream at Mata de Itamaçoa **C** stream at Mata de Itamaçoa **D** stream at Mata Fome, Barreirinhas municipality (photographed by Felipe Ottoni).

multiple operational criteria is considered to produce stronger hypotheses of lineage divergence (de Queiroz 2007, Goldstein and Desalle 2010), thus congruent to the proposal for an integrative taxonomy (Goldstein and Desalle 2010, Padial et al. 2010). The morphological criteria (PAA) distinguished the new species from all of the other congeners by unambiguous character states (see diagnosis). The DNA barcoding (DBC) criteria also revealed that *H. piorskii* sp. n. is a new species with an average sequence divergence of 17% from the other taxa (Table 2). In addition, *H. piorskii* sp. n. is placed in an exclusive and highly supported clade in the Bayesian tree (Figure 6). Haplotypes clustered as an exclusive and high supported group, with geographical concordance area is evidence of lineage divergence, therefore a good and strong evidence for delimit species, and consequently describe them (Wiens and Penkrot 2002, Costa et al. 2014).

Our Bayesian tree also recovered *H. piorskii* sp. n. within the *Hyphessobrycon sensu stricto* group with high support (posterior probability = 0.94), which fits the morphological evidence, since *H. piorskii* sp. n. exhibits the three main diagnostic character states of the group (see introduction and diagnosis section). *Hyphessobrycon piorskii* sp. n. was recovered as the sister-group of the clade including *H. bentosi*, *H. socolofi*, *H. megalopterus*, *H. erythrostigma*, and *H. pyrrhonotus*, however this relationship was supported by a lower support value (posterior probability value = 0.55). Only posterior probability values about or higher than 0.95 are considered as statistically significant

(Alfaro and Holder 2006). Therefore, any discussion about the relationship and supposed shared morphological features between *H. piorskii* sp. n. and this clade is speculative (Figure 7). To a better understanding of the internal relationships of the group, an analysis including more genes, especially from nuclear genome, is highly recommended. However, this was not the scope of the present paper. *Pristella maxillaris* and *Moenkhausia hemigrammoides* were recovered as the sister-clade of the *Hyphessobrycon sensu stricto* group, corroborating partially the results of Carvalho et al. (2011) and Carvalho and Malabarba (2015), who argue that *P. maxillaris* is the sister-clade of the *Hyphessobrycon sensu stricto* group.

Acknowledgements

We thank Wilson Costa for the loan and donation of material; Riccardo Mugnai for his assistance with osteological photographs; Ingo Schindler for providing useful literature; Vale S.A and Amplo Engenharia for the cession of part of the data analysed in this study; We also thank Pensoft and Clarisse Figueiredo for her English revisions; Elíoenai Oliveira, Ivanilda Nascimento, Rozijane Fernandes, Valquíria Carneiro, Shyrley Viana, Marciara Lopes, Revangivaldo Sousa, Diego Campos, Pedro Bragança, Beldo Ferreira and Lucas Oliveira for collecting the examined material. This paper benefited from suggestions provided by Javier Maldonado and two reviewers: Jorge Enrique García Melo and Carlos García-Alzate. This study was supported by CNPq (National Council for Scientific and Technological Development – Ministry of Science, Technology Innovation and Communication) and FAPEMA (Foundation for Scientific Research and Development of Maranhão). We also thank FACEPE (Fundação de Amparo à Ciência e Tecnologia do Estado de Pernambuco) for providing a scholarship to LMF. All material was collected with permits 51540-3/ from SISBIO (Brazilian Institute of Environment and Natural Resources).

References

- Alfaro ME, Holder MT (2006) The posterior and the prior in Bayesian phylogenetics. *Annual Review of Ecology, Evolution, and Systematics* 37: 19–42. <https://doi.org/10.1146/annurev.ecolsys.37.091305.110021>
- Benzaquem DC, Oliveira C, da Silva Batista J, Zuanon J, Porto JIR (2015) DNA Barcoding in Pencilfishes (Lebiasinidae: *Nannostomus*) Reveals Cryptic Diversity across the Brazilian Amazon. *PLoS ONE* 10(2): e0112217. <https://doi.org/10.1371/journal.pone.0112217>
- Bragança PHN, Ottoni FP, Rangel-Pereira FS (2015) *Hyphessobrycon ellisae*, a new species from northeastern Brazil (Teleostei: Characidae). *Ichthyological Exploration of Freshwaters* 26(3): 255–262. http://pfeil-verlag.de/wp-content/uploads/2016/07/ief26_3_07.pdf
- Carvalho FR (2011) Sistemática de *Hyphessobrycon* Durbin, 1908 (Ostariophysi: Characidae) PhD thesis, Porto Alegre, Brasil: Universidade Federal do Rio Grande do Sul.

- Carvalho FR, Malabarba LR (2015) Redescription and osteology of *Hyphessobrycon compressus* (Meek) (Teleostei: Characidae), type species of the genus. Neotropical Ichthyology 13(3): 513–540. <https://doi.org/10.1590/1982-0224-20140173>
- Carvalho FR, Cabeceira FG, Carvalho LN (2017) New species of *Hyphessobrycon* from the Rio Teles Pires, Rio Tapajós basin, Brazil (Ostariophysi, Characiformes). Journal of Fish Biology 91(3): 750–763. <https://doi.org/10.1111/jfb.13362>
- Castro-Paz FP, Batista JdS, Porto JIR (2014) DNA Barcodes of Rosy Tetras and Allied Species (Characiformes: Characidae: *Hyphessobrycon*) from the Brazilian Amazon Basin. PLoS ONE 9(5): e98603. <https://doi.org/10.1371/journal.pone.0098603>
- Costa WJEM, Amorim PF (2011) A new annual killifish species of the *Hypsolebias flavicaudatus* complex from the São Francisco River basin, Brazilian Caatinga (Cyprinodontiformes: Rivulidae). Vertebrate Zoology 61(1): 99–104.
- Costa WJEM, Amorim PF, Aranha GN (2014) Species limits and DNA barcodes in *Nematolebias*, a genus of seasonal killifishes threatened with extinction from the Atlantic Forest of south-eastern Brazil, with description of a new species (Teleostei: Rivulidae). Ichthyological Exploration of Freshwaters 24(3): 225–236.
- Costa WJEM, Géry J (1994) Two new species of the genus *Hyphessobrycon* (Characiformes: Characidae) from the rio xingú basin, Central Brazil. Revue Française d'Aquariologie Herpétologie 20: 71–76.
- Costa WJEM, Amorim PF, Mattos JLO (2012) Species delimitation in annual killifishes from the Brazilian Caatinga, the *Hypsolebias flavicaudatus* complex (Cyprinodontiformes: Rivulidae): implications for taxonomy and conservation. Systematics and Biodiversity 10(1): 71–91. <https://doi.org/10.1080/14772000.2012.664177>
- Costa WJEM, Cheffe MM, Amorim PF (2017) Two new seasonal killifishes of the *Austrolebias adloffii* group from the Lagoa dos Patos basin, southern Brazil (Cyprinodontiformes: Aplocheilidae). Vertebrate Zoology 67(2): 139–149.
- Darriba D, Taboada GL, Doallo R, Posada D (2012) jModelTest 2: more models, new heuristics and parallel computing. Nature Methods 9(8): 772. <https://doi.org/10.1038/nmeth.2109>
- Davis JJ, Nixon KC (1992) Populations, genetic variation, and the delimitation of phylogenetic species. Systematic Biology 41(4): 421–435. <https://doi.org/10.1093/sysbio/41.4.421>
- Dayrat B (2005) Towards integrative taxonomy. Biological Journal of the Linnean Society 85(3): 407–415. <https://doi.org/10.1111/j.1095-8312.2005.00503.x>
- de Queiroz K (2005) Different species problems and their resolution. BioEssays 27(12): 1263–1269. <https://doi.org/10.1002/bies.20325>
- de Queiroz K (2007) Species concepts and species delimitation. Systematic Biology 56(6): 879–886. <https://doi.org/10.1080/10635150701701083>
- Eigenmann CH (1917) The American Characidae, Part I. Memoirs of the Museum of Comparative Zoology 43(1): 1–102.
- Fink W, Weitzman S (1974) The so called Cheirodontin fishes of Central America with descriptions of two new species (Pisces: Characidae). Smithsonian Contributions to Zoology 172: 1–45. <https://doi.org/10.5479/si.00810282.172>

- García-Alzate CA, Román-Valencia C, Taphorn DC (2008a) *Hyphessobrycon oritoensis* (Characiformes: Characidae), a new species from the Putumayo river drainage, Colombian Amazon. *Zootaxa* 1813: 42–50. <https://doi.org/10.5281/zenodo.182839>
- García-Alzate CA, Román-Valencia C, Taphorn DC (2008b) Revision of the *Hyphessobrycon heterorhabdus* group (Teleostei: Characiformes: Characidae), with description of two new species of Venezuela. *Vertebrate Zoology* 58(2): 139–157.
- García-Alzate CA, Román-Valencia C, Taphorn C (2013) Una nueva especie de *Hyphessobrycon* (Characiformes: Characidae) de la cuenca del río Telembí, vertiente sur del Pacífico, Colombia. *Revista de Biología Tropical* 61(1): 181–192. <https://doi.org/10.15517/rbt.v61i1.10944>
- García-Alzate CA, Urbano-Bonilla A, Taphorn DC (2017) A new species of *Hyphessobrycon* (Characiformes, Characidae) from the upper Guaviare River, Orinoco River Basin, Colombia. *ZooKeys* 668: 123–138. <https://doi.org/10.3897/zookeys.668.11489>
- Géry J (1961). Three new South-American characids. *Tropical Fish Hobbyist* 9(9): 26–46.
- Géry J (1977) Characoids of the world – TFH-publications, Neptune City Inc., 672 pp.
- Géry J, Uj A (1987) Ein neuer tetra (Characoidea, Characidae, Tetragonopterinae) aus dem unteren Amazonasgebiet: *Hyphessobrycon werneri* n. sp. *Aquarien und Terrarien-Zeitschrift* 40(12): 546–550.
- Goldstein PZ, DeSalle R (2010) Integrating DNA barcode data and taxonomic practice: determination, discovery, and description. *BioEssays* 33(2): 135–147. <https://doi.org/10.1002/bies.201000036>
- Hebert PDN, Cywinska A, Ball SL, deWaard JR (2003a) Biological identifications through DNA barcodes. *Proceedings of the Royal Society B* 270(1512): 313–321. <https://doi.org/10.1098/rspb.2002.2218>
- Hebert PDN, Ratnasingham S, Waard JR (2003b) Barcoding animal life: cytochrome c oxidase subunit 1 divergences among closely related species. *Proceedings of the Royal Society B* 270(1): 96–99. <https://doi.org/10.1098/rsbl.2003.0025>
- Hebert PD, Penton EH, Burns JM, Janzen DH, Hallwachs W (2004a) Ten species in one: DNA barcoding reveals cryptic species in the neotropical skipper butterfly *Astraptes fulgerator*. *Proceedings of the National Academy of Sciences* 101(41):14812–14817. <https://doi.org/10.1073/pnas.0406166101>
- Hebert PDN, Stoeckle MY, Zemplak TS, Francis CM (2004b) Identification of birds through DNA barcodes. *PLoS Biology* 2(10): e312. <https://doi.org/10.1371/journal.pbio.0020312>
- Hein G (2009) *Hyphessobrycon pando* sp. n., a new rosy tetra from northern Bolivia (Teleostei, Characiformes, Characidae). *Bulletin of Fish Biology* 10(1/2): 1–10.
- Huelsenbeck JP, Ronquist F (2001) Mr. Bayes: Bayesian inference of phylogenetic trees. *Bioinformatics* 17(8): 754–755. <https://doi.org/10.1093/bioinformatics/17.8.754>
- Kearse M, Moir R, Wilson A, Stones-Havas S, Cheung M, Sturrock S, Buxton S, Cooper A, Markowitz S, Duran C, Thierer T, Ashton B, Meintjes P, Drummond A (2012) Geneious Basic: an integrated and extendable desktop software platform for the organization and analysis of sequence data. *Bioinformatics* 28(12): 1647–1649. <https://doi.org/10.1093/bioinformatics/bts199>
- Kimura M (1980) A simple method for estimating evolutionary rates of base substitutions through comparative studies of nucleotide sequences. *Journal of Molecular Evolution* 16(2): 111–120. <https://doi.org/10.1007/BF01731581>

- Lima FCT, Pires THS, Ohara WM, Jerep FC, Carvalho FR, Marinho MMF, Zuanon J (2013) Characidae. In: Queiroz LJ, Torrente-Vilara G, Ohara WM, Pires THS, Zuanon J, Dória CRC (Eds). Peixes do rio Madeira. 1 ed. São Paulo, Diaeto Latin American Documentary 1: 213–395.
- Marinho MMF, Dagosta FCP, Camelier P, Oyakawa OT (2016) A name for the ‘blueberry tetra’, an aquarium trade popular species of *Hyphessobrycon* Durbin (Characiformes, Characidae), with comments on fish species descriptions lacking accurate type locality. *Journal of Fish Biology* 89(1): 510–521. <https://doi.org/10.1111/jfb.12991>
- Mattos JLO, Costa WJEM, Santos ACA (2015) *Geophagus diamantinensis*, a new species of the *G. brasiliensis* species group from Chapada Diamantina, north-eastern Brazil (Cichlidae: Geophagini). *Ichthyological Exploration of Freshwaters* 26(3): 209–220.
- Miquelarena AM, López HL (2006) *Hyphessobrycon togoi*, a new species from the La Plata basin (Teleostei: Characidae) and comments about the distribution of the genus in Argentina. *Revue Suisse de Zoologie* 113(4): 817–828. <https://doi.org/10.5962/bhl.part.80378>
- Moreira CR, Lima FCT (2017) Two new *Hyphessobrycon* (Characiformes: Characidae) species from Central Amazon basin, Brazil. *Zootaxa* 4318(1): 123–134. <https://doi.org/10.11646/zootaxa.4318.1.5>
- Mirande M (2010) Phylogeny of the family Characidae (Teleostei: Characiformes): from characters to taxonomy. *Neotropical Ichthyology* 8(3): 385–568. <https://doi.org/10.1590/S1679-62252010000300001>
- Ohara WM, Lima FCT, Barros BS (2017) *Hyphessobrycon petricolus*, a new species of tetra (Characiformes: Characidae) from the rio Madeira basin, Mato Grosso, Brazil. *Zootaxa* 4221(2): 242–250. <https://doi.org/10.11646/zootaxa.4221.2.8>
- Oliveira C, Avelino GS, Abe KT, Mariguela TC, Benine RC, Ortí G, Vari RP, Castro RMC (2011) Phylogenetic relationships within the speciose family Characidae (Teleostei: Ostariophysi: Characiformes) based on multilocus analysis and extensive ingroup sampling. *BMC Evolutionary Biology* 11: 275. <https://doi.org/10.1186/1471-2148-11-275>
- Padial JM, Miralles A, De la Riva I, Vences M (2010) The integrative future of taxonomy. *Frontiers in Zoology* 7: 16. <https://doi.org/10.1186/1742-9994-7-16>
- Planquette P, Keith P, Le Bail PY (1996) Atlas des Poissons d’eau douce de Guyane. Tome 1. Collection du patrimoine naturel. Biotope/Publications scientifiques du MNHN, Paris, 421 pp.
- Sabaj-Pérez MH (Ed.) (2016) Standard symbolic codes for institutional resource collections in herpetology and ichthyology, an online reference. Version 6.5 (16 August 2016). American Society of Ichthyologists and Herpetologists, Washington, D.C. Electronically accessible. <http://www.asih.org/> [Accessed 29 jan 2018]
- Tamura K, Peterson D, Peterson N, Stecher G, Nei M, Kumar S (2011) Mega 5: Molecular Evolutionary Genetic Analysis Using Maximum Likelihood. Evolutionary Distance and Maximum Parsimony Methods. *Molecular Biology and Evolution* 28(10): 2731–2739. <https://doi.org/10.1093/molbev/msr121>
- Roxo FF, Oliveira C, Zawadzki, CH (2012) Three new species of *Neoplecostomus* (Teleostei: Siluriformes: Loricariidae) from the Upper Rio Paraná basin of southeastern Brazil. *Zootaxa* 3233: 1–21.

- Taylor W, Van Dyke G (1985) Revised procedures for staining and clearing small fishes and other vertebrates for bone and cartilage study. *Cybiurn* 9: 107–119.
- Teixeira TF, Netto-Ferreira AL, Birindelli JLO, Sousa LM (2015) Two new species of *Hyphessobrycon* (Characiformes: Characidae) from the headwaters of the Tapajós and Xingu River basins, Pará, Brazil. *Journal of Fish Biology* 88(2): 459–476. <https://doi.org/10.1111/jfb.12803>
- Teletchea F (2009) Molecular identification methods of fish species: reassessment and possible applications. *Reviews in Fish Biology and Fisheries* 19: 265–293. <https://doi.org/10.1007/s11160-009-9107-4>
- Thompson JD, Higgins DG, Gibson TJ (1994) CLUSTAL W: improving the sensitivity of progressive multiple sequence alignment through sequence weighting, position-specific gap penalties and weight matrix choice. *Nucleic Acids Research* 22(22): 4673–4680. <https://doi.org/10.1093/nar/22.22.4673>
- Villa-Verde L, Lazzarotto H, Lima SMQ (2012) A new glanapterygine catfish of the genus *Listrura* (Siluriformes: Trichomycteridae) from southeastern Brazil, corroborated by morphological and molecular data. *Neotropical Ichthyology* 10(3): 527–538. <https://doi.org/10.1590/S1679-62252012000300005>
- Ward RD, Zemlak TS, Innes BH, Last PR, Hebert PDN (2005) DNA barcoding Australia's fish species. *Philosophical Transactions of the Royal Society of London B, Biological Sciences* 360(1462): 1847–1857. <https://doi.org/10.1098/rstb.2005.1716>
- Weitzman SH (1962) The osteology of *Brycon meeki*, a generalized characid fish, with an osteological definition of the family. *Stanford Ichthyological Bulletin* 8(1): 3–77.
- Weitzman SH, Palmer L (1997) A new species of *Hyphessobrycon* (Teleostei: Characidae) from the Neblina region of Venezuela and Brazil, with comments on the putative 'rosy tetra clade'. *Ichthyological Exploration of Freshwaters* 7(3): 209–242.
- Wiens JJ, Penkrot TA (2002) Delimiting species using DNA and Morphological variation and discordant limitis in spiny lizards (Sceloporus). *Systematic biology* 51(1): 69–91. <https://doi.org/10.1080/106351502753475880>
- Zarske A (2008) *Hyphessobrycon khardinae* sp. n. – ein neuer Blutsalmler aus Brasilien (Teleostei: Characiformes: Characidae). *Vertebrate Zoology* 58(1): 5–13.
- Zarske A (2014) Zur Systematik einiger Blutsalmler oder "Rosy Tetras" (Teleostei: Ostariophysii: Characidae). *Vertebrate Zoology* 64(2): 139–167.

Molecular data and species diagnosis in *Essigella* Del Guercio, 1909 (Sternorrhyncha, Aphididae, Lachninae)

Thomas Théry¹, Mariusz Kanturski², Colin Favret¹

1 University of Montreal, Department of Biological Sciences, Biodiversity Centre, 4101 E. Sherbrooke Street, Montreal QC, H1X 2B2 Canada **2** Department of Zoology, Faculty of Biology and Environmental Protection, University of Silesia in Katowice, Bankowa 9, 40-007 Katowice, Poland

Corresponding author: Thomas Théry (thomasjcthery@gmail.com)

Academic editor: R. Blackman | Received 31 January 2018 | Accepted 28 April 2018 | Published 7 June 2018

<http://zoobank.org/BD00760D-C946-4110-8C86-8CA2872C7CE3>

Citation: Théry T, Kanturski M, Favret C (2018) Molecular data and species diagnosis in *Essigella* Del Guercio, 1909 (Sternorrhyncha, Aphididae, Lachninae). ZooKeys 765: 103–122. <https://doi.org/10.3897/zookeys.765.24144>

Abstract

Morphological and molecular data are used to describe three new species of *Essigella* (Sternorrhyncha: Aphididae: Lachninae): *Essigella domenechi* **sp. n.**, *Essigella gagnonae* **sp. n.**, and *Essigella sorenseni* **sp. n.**; and to re-establish as valid *Essigella patchae* Hottes, 1957, **stat. n.**, until now considered a synonym of *E. pini* Wilson, 1919. The catalogue of *Essigella* species is updated. This study highlights the need and utility to use discreet DNA characters in aphid species diagnoses.

Keywords

Cryptic species, DNA sequences, Hemiptera, taxonomy

Introduction

Morphological characters remain the commonest way to separate animal species, and they are conspicuously used in diagnoses and descriptions of new taxa. However, in the case of cryptic species, no or few morphological differences are available, and other kinds of taxon-related attributes must be employed as valuable diagnostic characters. DNA sequences permit the discovery of cryptic species and are used to separate them from their relatives (Hebert et al. 2003a, b, Cœur d'acier et al. 2014, Lukhtanov and Dantchenko 2017, Morinière et al. 2017). However, despite their reliability, they are seldom used

specifically in diagnoses of new species, notably because they are not specifically recommended in the International Code of Zoological Nomenclature (Renner 2016).

Essigella (Sternorrhyncha: Aphididae: Lachninae) is an aphid genus found on the needles of various pinaceous hosts. Most species feed on true pines, *Pinus* Linnaeus, but *E. wilsoni* Hottes, 1957, is found only on Douglas firs, *Pseudotsuga* Carrière. *Essigella alyeska* Sorensen, 1988 is recorded on spruce, *Picea* A. Dietrich, although its typical host is *Pinus banksiana* Lamb. (Sorensen 1994). Most species of *Essigella* are considered monophagous except *E. californica* (Essig, 1909) and *E. pini* Wilson, 1919 which are oligophagous on *Pinus* (Sorensen 1994). Although all species are Nearctic in origin, *E. californica* was accidentally introduced in several countries around the world (Théry et al. 2017). *Essigella* currently encompasses 15 valid taxa, with an additional 13 synonyms (Wilson 1919, Gillette and Palmer 1924, Hottes 1957, 1958, Sorensen 1988, 1994). Species are variable and show few diagnostic characters (Sorensen 1994). The genus was revised by Sorensen (1994) using morphometric data and multivariate analyses. Besides the 15 taxa he recognized, Sorensen (1994) notably divided *Essigella* into three subgenera: *Archeoessigella*, *Essigella* and *Lambersella*, two species series, and three species complexes. A recent molecular phylogenetic study did not support the validity of the three subgenera and of one of the species series (Théry et al. in press). Moreover, the phylogenetic results, combined with molecular species delimitation methods, revealed that two species, *Essigella californica* and *E. pini*, actually encompass four and two species, respectively. In the case of *E. pini*, one of the two species is suspected to be *E. patchae* Hottes, 1957, considered a synonym of *E. pini* by Sorensen (1994). Examination of type material of *E. californica* and *E. pini*, as well as that of their respective synonyms and reference specimens, indicates that the three cryptic species found within *E. californica* are new to science and confirms the validity of *E. patchae*.

In the present work, we describe as new the three cryptic species revealed by Théry et al. (in press): *Essigella domenechi* sp. n., *E. gagnonae* sp. n. and *E. sorenseni* sp. n. In addition, we re-establish *E. patchae* stat. n. and provide diagnostic characters to separate it and *E. pini*. Because these four species are difficult to distinguish morphologically, discreet DNA sequence data supplement classical morphological characters in the diagnoses.

Materials and methods

Abbreviations used

- CTT** Private Collection of T. Théry, Fleury les Aubrais, France;
EMEC Essig Museum of Entomology, University of California, Berkeley, CA, USA;
QMOR Ouellet-Robert Entomological Collection, University of Montreal, QC, Canada;
UMSP University of Minnesota Insect Collection, St Paul, MN, USA;
USNM National Aphid Collection, National Museum of Natural History, Beltsville, MD, USA.

Taxon sampling

All *Essigella* specimens published here were collected recently in the USA and Canada (TT and CF), or are found in the Sorensen Collection at EMEC. Specimens studied were mainly viviparous apterae. Some viviparous alatae also were studied in the case of *E. patchae* for which the holotype is an alate. Recently collected specimens were preserved in 95% ethanol after collecting and subsequently kept at -20 °C or -80 °C. DNA extraction of at least one specimen per population was realized. It was non-destructive (Favret 2005), permitting us to keep the specimen as voucher. Those specimens were identified using the keys of Sorensen (1994) and Blackman and Eastop (2017). We compared our material with the type specimens of the valid species, *E. californica* (EMEC) and *E. pini* (UMSP), as well as those of their synonyms *E. claremontiana* Hottes, 1957, *E. cocheta* Hottes, 1957, *E. monelli* Hottes, 1957, *E. pineti* Hottes, 1957, *E. swaini* Hottes, 1957, for *E. californica*, and *E. patchae* for *E. pini* (EMEC, USNM). We also compared specimens of new taxa and of *E. patchae* with other *E. californica* specimens from the Sorensen Collection (EMEC), and of *E. pini* from UMSP and USNM.

Preparation, measurements, and photographs

All new material was slide-mounted in Canada balsam and deposited in QMOR, CTT, and USNM, in the case of holotypes. Preparations were thick to reduce deformation due to compression. As far as possible, appendages were placed so that they be strictly horizontal permitting correct length and width measurements as well as to ascertain the correct location of dorsal and ventral setae of the hind femora and tibiae. Body length was measured from the frontal margin of the head to the posterior margin of the 7th abdominal segment. The abdominal tergum being sclerotized with most segments fused, the cauda and 8th segment sometimes telescope into the 7th, making standardized measurements difficult across specimens. Because of the likely deformation of the body due to a variable number of embryos, width measurements were taken only of the head, between the frontal interior margins of the compound eyes. Lengths of appendages were measured at their longest, including condyles, widths were measured at the widest part of the appendages. The length of the processus terminalis was taken from the distal margin of primary rhinarium to the apex of the antenna. The following abbreviations are applied:

BL	body length;
LAIII	length of third antennal segment;
LAIV	length of fourth antennal segment;
LAV	length of fifth antennal segment;
LPRIV	length of primary rhinarium on fourth antennal segment;
LPRV	length of primary rhinarium on fifth antennal segment;
LPT	length of processus terminalis;
HWE	head width at eyes;

LURS	length of ultimate rostral segment;
LMF	length of metafemur;
WMF	width of metafemur;
LMT	length of metatibia;
WMT	width of metatibia;
WS	width of siphunculus at external edges;
LMB	length of metabasitarsus;
LMD	length of metadistitarsus;
LFS	length of longest frontal seta;
LDMFS	length of longest dorsal metafemoral seta;
LVMFS	length of longest ventral metafemoral seta;
LDMTS	length of longest dorsal metatibial seta;
LVMTS	length of longest ventral metatibial seta.

Entire non-prepared specimens were photographed with a Carl Zeiss Discovery. V20 stereoscope using an AxioCam HRc camera and a Zen 2012 Carl Zeiss Software, version 1.1.1.0. Pictures of slide-mounted specimens were realized using light microscope Nikon Eclipse E600 with differential interference contrast (DIC) and photographed by Nikon DS-Fi camera. Scanning electron microscope (SEM) photos were taken at the University of Silesia in Katowice (Poland) using a Hitachi SU8010 Field Emission Scanning Electron Microscope (FE-SEM) (Hitachi High-Technologies Corporation, Tokyo, Japan) at 5, 10 and 15 kV accelerating voltage with a secondary electron detector (ESD). For specimen preparation for SEM pictures, we followed the protocol of Kanturski et al. (2015). Measurements in diagnoses and descriptions are given in microns (μm) with standard deviation.

Molecular data

The three new species were primarily revealed in the study of Théry et al. (in press) using DNA sequences of the genomes of the mitochondrion (*ATP6*, *COI*) and the obligate bacterial endosymbiont *Buchnera aphidicola* (*Gnd*) within populations of *E. californica* sensu lato. Indeed, *ATP6* and *Gnd* show similar properties as *COI* in species discrimination in barcoding (Hebert et al. 2003a, b, Chen et al. 2013, Lee et al. 2014). Sequence lengths were 663 base pairs (bp), 658 bp and 749 bp for *ATP6*, *COI* and *Gnd*, respectively (see Théry et al. in press, for GenBank accession numbers and other details).

Taxonomy

The following species, including *E. patchae*, belong to the *E. californica* species complex, which also includes *E. hoerneri* Gillette & Palmer, 1924 (Sorensen 1994) (see

discussion). All of these species, as well as *E. pini*, exhibit six dorsal setae at their 3rd and 4th abdominal segments (Sorensen 1994). However, this character is homoplastic within *Essigella* as *E. pini* and the *E. californica* complex are not closely related (Théry et al. in press); it is used here to distinguish the species of the *E. californica* complex and *E. pini* from the other species of the genus. Morphological and ecological (host plant identity) comparisons of specimens of the new species with type material of synonym species of *E. californica* and *E. hoernerii* permitted to reject the possibility that our new species correspond to one of those synonyms.

***Essigella domenechi* sp. n.**

<http://zoobank.org/390343A7-D620-4578-93A8-A5BBBBF7FE00F>

Figure 1d

Holotype. viviparous aptera, USA, California, Alpine Co., 38.328°N 119.637°W, 10.vii.2013, on *Pinus albicaulis*, T. Théry & C. Favret leg. (USNM). **Paratypes.** 8 viviparous apterae, same data as holotype (QMOR, CTT).

Diagnosis. Like species of the *E. californica* complex and *E. pini*, *E. domenechi* sp. n. has its 3rd and 4th abdominal dorsal terga usually bearing six setae. The species can be distinguished from *E. patchae* by the presence of rows of spinules on the URS (absent or faint in *E. patchae*; Fig. 2b, d); from *E. pini* by a relatively elongate URS with sub-parallel lateral margins (URS with margins rounded and convergent at base in *E. pini*; Fig. 2a, c); from *E. gagnonae* sp. n. and *E. sorenseni* sp. n. with the following characters: tibiae and femora more or less concolorous showing almost or same color as that of body (pro- and metatibiae and metafemora conspicuously darkened in *E. sorenseni* sp. n., pro- and metatibiae sometimes slightly darkened in *E. gagnonae* sp. n.), dorsal tegument thick; width of head between eyes = 300.7 ± 14.2 (289.0 ± 13.3 for *E. gagnonae* sp. n., and 353.6 ± 15.3 for *E. sorenseni* sp. n.); ratio of 3rd / 5th antennal segments < 1.6 (< 1.6 for *E. gagnonae* sp. n. but > 1.6 in *E. sorenseni* sp. n.); overall pubescence short or medium-sized with average length of the longest dorsal seta of metafemora = 29.7 ± 4.2 (59.8 ± 9.8 for *E. gagnonae* sp. n., and 51.2 ± 10.7 for *E. sorenseni* sp. n.; average length of the longest ventral seta of metafemora = 32.6 ± 4.5 (43.1 ± 5.4 for *E. gagnonae* sp. n., and 54.4 ± 5.6 for *E. sorenseni* sp. n.); average length of the longest dorsal seta of metatibiae = 44.0 ± 8.1 (85.7 ± 10.8 for *E. gagnonae* sp. n., and 76.4 ± 15.8 for *E. sorenseni* sp. n.); average length of the longest ventral seta of metatibiae = 37.5 ± 7.0 (49.4 ± 9.5 for *E. gagnonae* sp. n., and 67.7 ± 12.0 for *E. sorenseni* sp. n.); average length of the longest frontal seta = 32.6 ± 7.5 (58.7 ± 8.3 for *E. gagnonae* sp. n., and 53.4 ± 11.9 for *E. sorenseni* sp. n.); average number of setae of the genital plate = 22.0 ± 2.1 (23.6 ± 2.1 for *E. gagnonae* sp. n., and 31.6 ± 1.7 for *E. sorenseni* sp. n.). *Essigella domenechi* sp. n. is morphologically not distinguishable from *E. californica*, the latter being highly variable, nor from *E. hoernerii*. *Essigella domenechi* sp. n. can be separated from *E. californica*, *E. gagnonae* sp. n., *E. hoernerii* and *E. sorenseni* sp. n. with the DNA characters shown in Table 1.

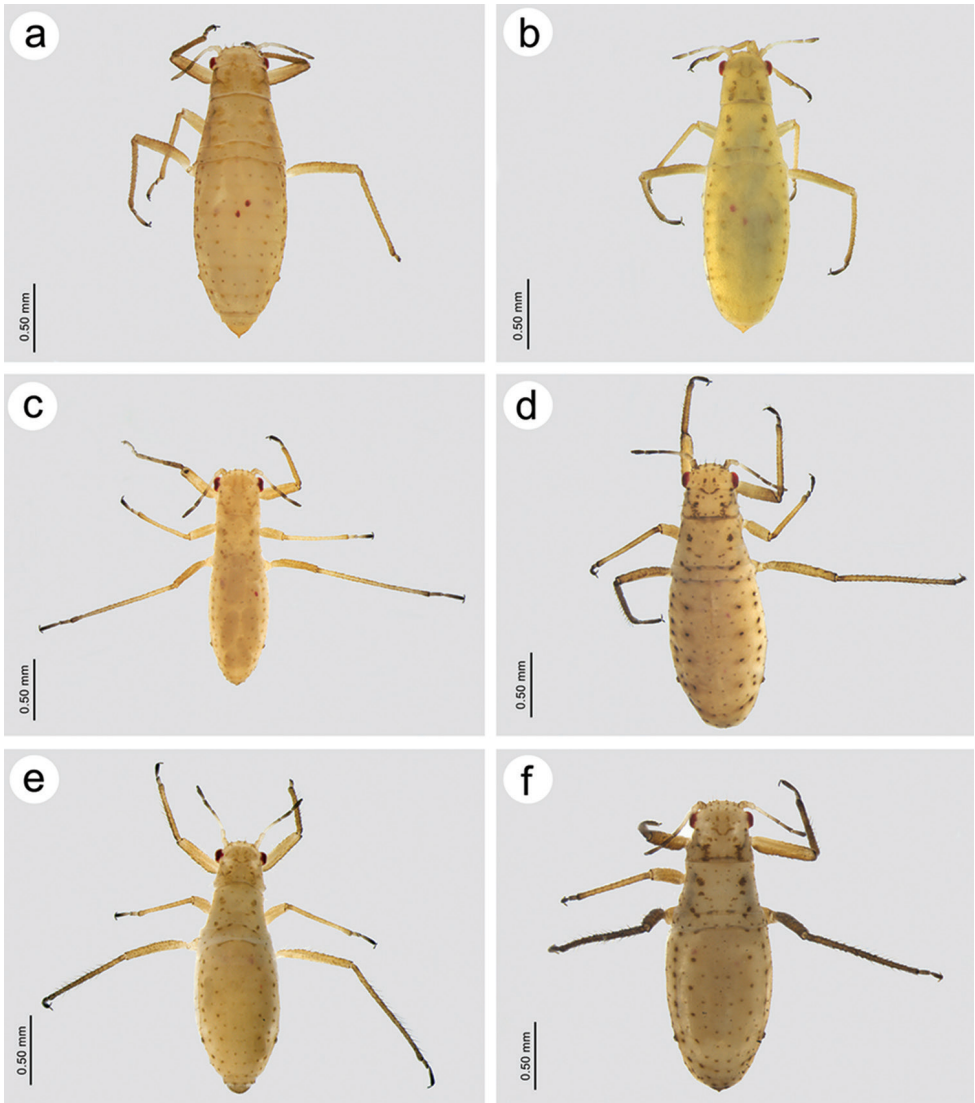


Figure 1. Habitus of viviparous apterae of **a** *Essigella pini* **b** *E. patchae* **c** *E. californica* **d** *E. domenechi* sp. n. **e** *E. gagnonae* sp. n. **f** *E. sorenseni* sp. n.

Description. Viviparous apterae (prepared specimens): body with pale tegument, with visible pigmented scleroites; dorsal tegument visibly thicker, sclerotized. Legs quite pale, concolorous, more or less the same color than that of body. Antennae pale, the 5th, the 4th and the apical third part of the 3rd segment of antennae darkened. URS elongated, with lateral margins subparallel, bearing rows of spinules. Overall pubescence short to medium-sized, dorsal setae of appendages incrassate, ventral ones acute. Terga of abdominal segments 3 and 4 with six dorsal setae. Genital plate with 19–25 setae (22.0 ± 2.1) ($n = 6$). Cauda obvious but not too protruding, apically rounded,

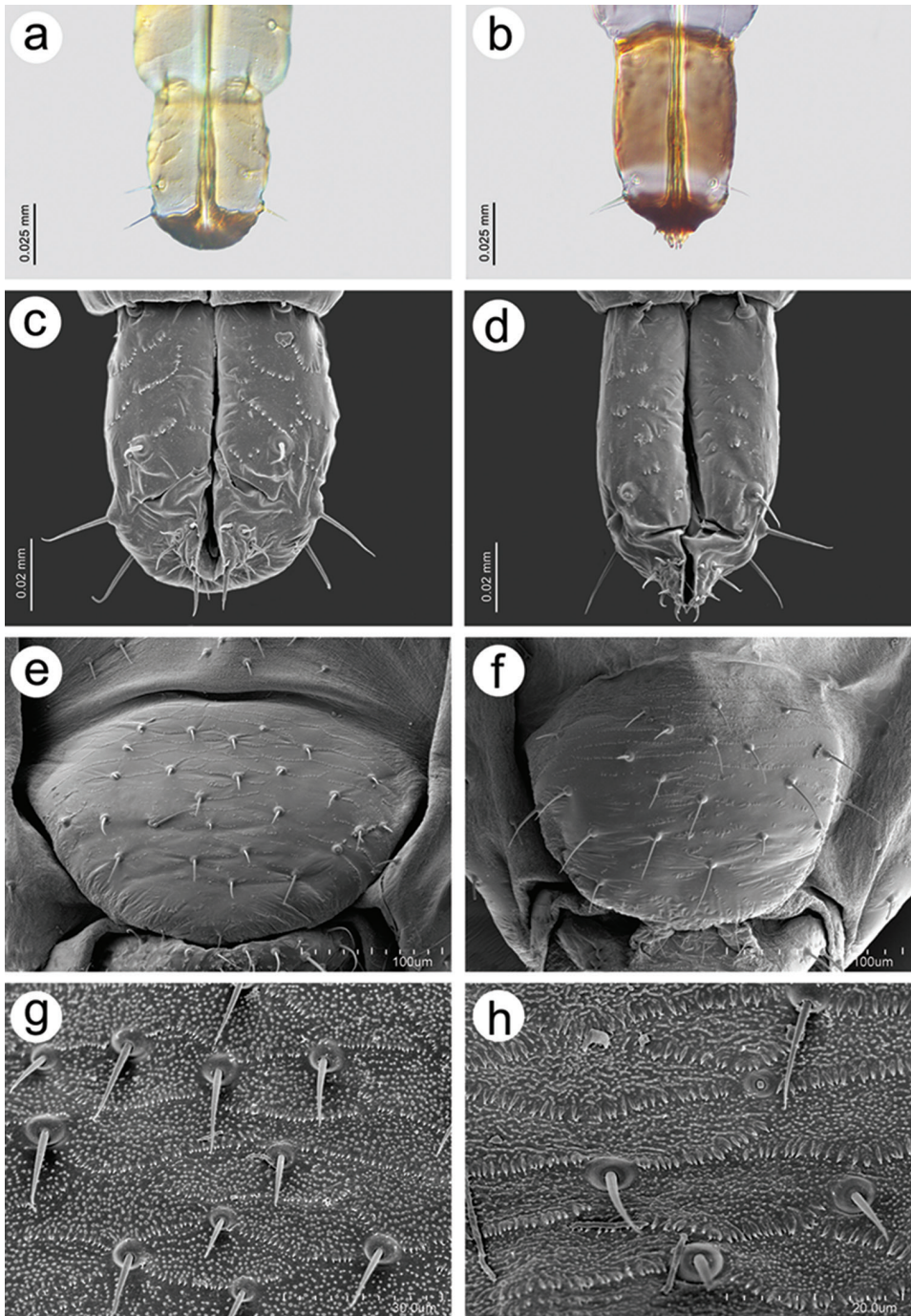


Figure 2. Morphological structures in *Essigella pini* and in *E. patchae*: **a** URS in *E. pini* (slide-mounted specimen) **b** URS in *E. patchae* (slide-mounted specimen) **c** URS in *E. pini* (SEM) **d** URS in *E. patchae* (SEM) **e** genital plate in *E. pini* (SEM) **f** genital plate in *E. patchae* (SEM) **g** details in genital plate in *E. pini* (SEM) **h** details in genital plate in *E. patchae* (SEM).

Table 1. Diagnostic nucleotide differences between *E. domenechi* sp. n. and *E. californica*, *E. gagnonae* sp. n., *E. hoerneri*, and *E. sorenseni* sp. n. for *ATP6*, *COI*, and *Gnd*.

Gene	ATP6 (663 bp)				COI (658 bp)								Gnd (749 bp)	
	4	71	227	324	190	229	334	386	418	565	619	625	219	621
<i>E. domenechi</i> sp. n.	C	C	C	G	G	G	A	G	C	G	G	G	C	C
<i>E. gagnonae</i> sp. n.	T	T	T	A	A	A	T	A	T	A	A	A	A	A
<i>E. sorenseni</i> sp. n.	T	T	T	A	A	A	T	A	T	A	A	A	A	A
<i>E. californica</i>	T	T	T	A	A	A	T	A	T	A	A	A	A	A
<i>E. hoerneri</i>	T	T	T	A	A	A	T	A	T	A	A	A	A	A

slightly turned upward. BL: 1600–2100 (1800 ± 170) (n = 7). HWE: 283.2–326.0 (300.7 ± 14.2) (n = 7), LAIII: 162.2–184.6 (171.8 ± 6.5) (n = 13), LAIV: 96.4–106.7 (101.0 ± 4.1) (n = 9), LAV: 113.7–124.4 (120.2 ± 4.1) (n = 5), LPRIV: 20.8–25.8 (23.0 ± 1.6) (n = 9), LPRV: 17.6–21.9 (19.6 ± 1.4) (n = 9), LPT: 8.5–14.5 (11.9 ± 1.9) (n = 9), LURS: 71.4–79.2 (75.2 ± 2.8) (n = 6), LMF: 675.7–728.8 (708.3 ± 24.2) (n = 6), WMF: 68.2–77.3 (74.9 ± 2.9) (n = 11), LMT: 975.1–1074.4 (1027.8 ± 38.2) (n = 9), WMT: 36.8–43.9 (41.4 ± 2.2) (n = 12), WS: 36.7–43.5 (40.4 ± 2.2) (n = 9), LMB: 107.2–114.4 (110.9 ± 2.3) (n = 11), LMD: 189.4–206.4 (194.9 ± 6.9) (n = 11), LFS: 18.7–39.5 (32.6 ± 7.5) (n = 7), LDMFS: 25.2–36.8 (29.7 ± 4.2) (n = 12), LVMFS: 26.1–44.0 (32.6 ± 4.5) (n = 12), LDMTS: 33.7–61.8 (44.0 ± 8.1) (n = 12), LVMTS: 24.7–48.1 (37.5 ± 7.0) (n = 12).

Comments. USA, California, on *Pinus albicaulis* Engelmann, known from Stanislaus National Forest at high elevation (type series). The species probably occurs in other high mountains where *P. albicaulis* is present. This species corresponds to the *E. californica* population living on *P. albicaulis* (cluster H3) shown in Théry et al. (in press).

Etymology. This species is dedicated to Boris Domenech, PhD student at the University of Montreal (QC, Canada) for his comments in genetic analyses with which the species was discovered.

Essigella gagnonae sp. n.

<http://zoobank.org/53A36CBB-AE8E-42FD-B792-C431EE48BBD4>

Figs 1e, 3b

Holotype. viviparous aptera, USA, Nevada, Douglas Co., 38.999°N 119.896°W, 10.vii.2013, on *Pinus monticola*, T. Théry & C. Favret *leg.* (USNM). **Paratypes.** 1 viviparous aptera, same data as holotype (QMOR); 12 viviparous apterae, California, El Dorado Co., 38.834°N 120.042°W, 09.vii.2013, on *Pinus monticola*, T. Théry & C. Favret *leg.*, specimens on 10 slides (QMOR, CTT); 5 viviparous apterae, California, Lassen Co., HWY 89, 6 km N Jct HWY 36 & 89, 6600', S of Lassen Nat'l Park (77G20), 10.vii.1977, on *Pinus monticola*, J. T. Sorensen *leg.*, specimens on 1 slide (EMEC); 5 viviparous apterae, California, Alpine Co., E side Ebbett's Pass, HWY 4, 3 km E summit (77G41), 17.vii.1977, on *Pinus monticola*, J. T. Sorensen *leg.*, speci-

mens on 1 slide (EMEC); 13 viviparous apterae, Washington, Kitsap Co., 8 km S Hood Canal Bridge, HWY 3 (78G49), 09.vii.1978, on *Pinus monticola*, J. T. Sorensen leg., specimens on 3 slides (4 + 4 + 5) (EMEC); 8 viviparous apterae, Washington, Grays Harbor Co., 16 km W Amanda Park, HWY 101 (78G54), 10.vii.1978, on *Pinus monticola*, J. T. Sorensen leg., specimens on 2 slides (4 + 4) (EMEC); 5 viviparous apterae, Nevada, Washoe Co., Mt Rose, Summit, Cmpgd, Toiyabe Nat'l Forest (78H9), 02.viii.1978, on *Pinus monticola*, J. T. Sorensen leg., specimens on 2 slides (2 + 3) (EMEC).

Diagnosis. Like species of the *E. californica* complex and *E. pini*, *E. gagnonae* sp. n. has its 3rd and 4th abdominal dorsal terga usually bearing six setae. It can be distinguished from *E. patchae* by the presence of spinules on the URS (absent or faint in *E. patchae*; Fig. 2b, d); from *E. pini* by a relatively elongate URS with subparallel lateral margins (URS with margins rounded and convergent at base in *E. pini*; Fig 2a, c); from *E. domenechi* sp. n. and *E. sorenseni* sp. n. with the following characters: legs ranging from concolorous and slightly darker than body, to pro- and metatibiae slightly darkened with mesotibiae lighter and metafemora pale (tibiae concolorous in *E. domenechi* sp. n., pro- and metatibiae, and metafemora conspicuously darkened in *E. sorenseni* sp. n.); width of head between eyes = 289.0 ± 13.3 (300.7 ± 14.2 for *E. domenechi* sp. n., and 353.6 ± 15.3 for *E. sorenseni* sp. n.); ratio of 3rd / 5th antennal segments < 1.6 (< 1.6 for *E. domenechi* sp. n. but > 1.6 in *E. sorenseni* sp. n.); overall pubescence medium-sized to long with average length of the longest dorsal setae of metafemora = 59.8 ± 9.8 (29.7 ± 4.2 for *E. domenechi* sp. n., and 51.2 ± 10.7 for *E. sorenseni* sp. n.); average length of the longest ventral seta of metafemora = 43.1 ± 5.4 (32.6 ± 4.5 for *E. domenechi* sp. n., and 54.4 ± 5.6 for *E. sorenseni* sp. n.); average length of the longest dorsal seta of metatibiae = 85.7 ± 10.8 (44.0 ± 8.1 for *E. domenechi* sp. n., and 76.4 ± 15.8 for *E. sorenseni* sp. n.); average length of the longest ventral seta of metatibiae = 49.4 ± 9.5 (37.5 ± 7.0 for *E. domenechi* sp. n., and 67.7 ± 12.0 for *E. sorenseni* sp. n.); average length of the longest frontal seta = 58.7 ± 8.3 (32.6 ± 7.5 for *E. domenechi* sp. n., and 53.4 ± 11.9 for *E. sorenseni* sp. n.); average number of setae of the genital plate = 23.6 ± 2.1 (22.0 ± 2.1 for *E. domenechi* sp. n., and 31.6 ± 1.7 for *E. sorenseni* sp. n.). *Essigella gagnonae* sp. n. is for now morphologically not distinguishable from *E. californica*, the latter being highly variable, nor from *E. hoernerii*. *Essigella gagnonae* sp. n. can be separated from *E. californica*, *E. domenechi* sp. n., *E. hoernerii*, and *E. sorenseni* sp. n. with the DNA characters shown in Table 2.

Description. Viviparous apterae (prepared specimens): body with pale tegument sometimes slightly yellowish, with visible pigmented scleroites. Legs ranging from concolorous, slightly darker than body, to pro- and metatibiae slightly darkened, darker than body and mesotibiae. Antennae pale, the 5th, the 4th and the apical third part of the 3rd segment darkened. URS elongated, with lateral margins subparallel, bearing rows of spinules. Overall pubescence medium-sized to long, dorsal setae of appendages incrassate, ventral ones acute, in specimens with very long dorsal setae in metafemora and metatibiae (> 100 μ m), these setae almost acute to acute (Fig. 3b), straight to sinuated. Terga of abdominal segments 3 and 4 with six dorsal setae. Genital

Table 2. Diagnostic nucleotide differences between *E. gagnonae* sp. n. and *E. californica*, *E. domenechi* sp. n., *E. boernerii* and *E. sorenseni* sp. n. for *ATP6*, *COI*, and *Gnd*.

Gene	<i>ATP6</i> (663 bp)	<i>COI</i> (658 bp)			<i>Gnd</i> (749 bp)
Site	260	28	235	271	665
<i>E. gagnonae</i> sp. n.	G	G	C	C	C
<i>E. domenechi</i> sp. n.	A	A	T	A	T
<i>E. sorenseni</i> sp. n.	A	A	T	A	A
<i>E. californica</i>	A	A	T	A	A
<i>E. boernerii</i>	A	A	T	A	T

plate with 21–26 setae (23.6 ± 2.1) ($n = 9$). Cauda obvious but not too protruding, apically rounded, slightly turned upward. BL: 1600–2000 (1800 ± 130) ($n = 19$). HWE: 271.0–311.9 (289.0 ± 13.3) ($n = 13$), LAIII: 157.6–197.4 (178.1 ± 11.1) ($n = 29$), LAIV: 90.2–111.6 (99.7 ± 6.3) ($n = 33$), LAV: 116.0–141.6 (125.4 ± 5.8) ($n = 20$), LPRIV: 21.5–29.1 (24.3 ± 1.8) ($n = 21$), LPRV: 18.5–22.6 (20.6 ± 1.2) ($n = 18$), LPT: 7.6–16.8 (12.1 ± 2.5) ($n = 23$), LURS: 64.5–79.8 (72.0 ± 3.8) ($n = 18$), LMF: 650.3–798.5 (707.3 ± 38.6) ($n = 22$), WMF: 69.5–104.6 (87.0 ± 10.8) ($n = 29$), LMT: 876.1–1104.2 (999.9 ± 67.4) ($n = 25$), WMT: 33.8–52.5 (42.3 ± 4.1) ($n = 40$), WS: 34.4–42.6 (38.9 ± 2.5) ($n = 18$), LMB: 101.8–131.0 (116.1 ± 8.0) ($n = 36$), LMD: 180.3–209.9 (195.0 ± 8.6) ($n = 34$), LFS: 44.4–80.2 (58.7 ± 8.3) ($n = 26$), LD-MFS: 42.0–82.9 (59.8 ± 9.8) ($n = 43$), LVMFS: 31.5–52.6 (43.1 ± 5.4) ($n = 42$), LD-MTS: 60.9–107.7 (85.7 ± 10.8) ($n = 46$), LVMTS: 30.5–74.5 (49.4 ± 9.5) ($n = 46$).

Comments. USA, California, Nevada, and Washington, on *Pinus monticola* Douglas ex D. Don. The species occurs in elevated places where *P. monticola* is present. This species corresponds to the *E. californica* population living on *P. monticola* (cluster H2) shown in Théry et al. (in press).

Etymology. This species is dedicated to Édeline Gagnon, PhD student at the University of Montreal (QC, Canada) for her help in genetic analyses with which the species was discovered.

Essigella sorenseni sp. n.

<http://zoobank.org/4C35698B-A28C-4794-8AE8-C9A6BA84541F>

Figs 1f, 3a

Holotype. viviparous aptera, USA, California, Sonoma Co., 38.534°N 123.276°W , 02.vii.2013, on *Pinus muricata*, T. Théry & C. Favret leg. (QMOR). **Paratypes.** 14 viviparous apterae, same data than holotype, specimens on 14 slides (QMOR, CTT); 3 viviparous apterae, California, Mendocino Co., 38.984°N 123.696°W , 03.vii.2013, on *Pinus muricata*, T. Théry & C. Favret leg., specimens on 3 slides (QMOR, CTT); 6 viviparous apterae, California, Mendocino Co., HWY 1, 5 km of Albion, Little River Road, 23.vii.1977, on *Pinus muricata*, 77G52, J. T. Sorensen leg., specimens on 3

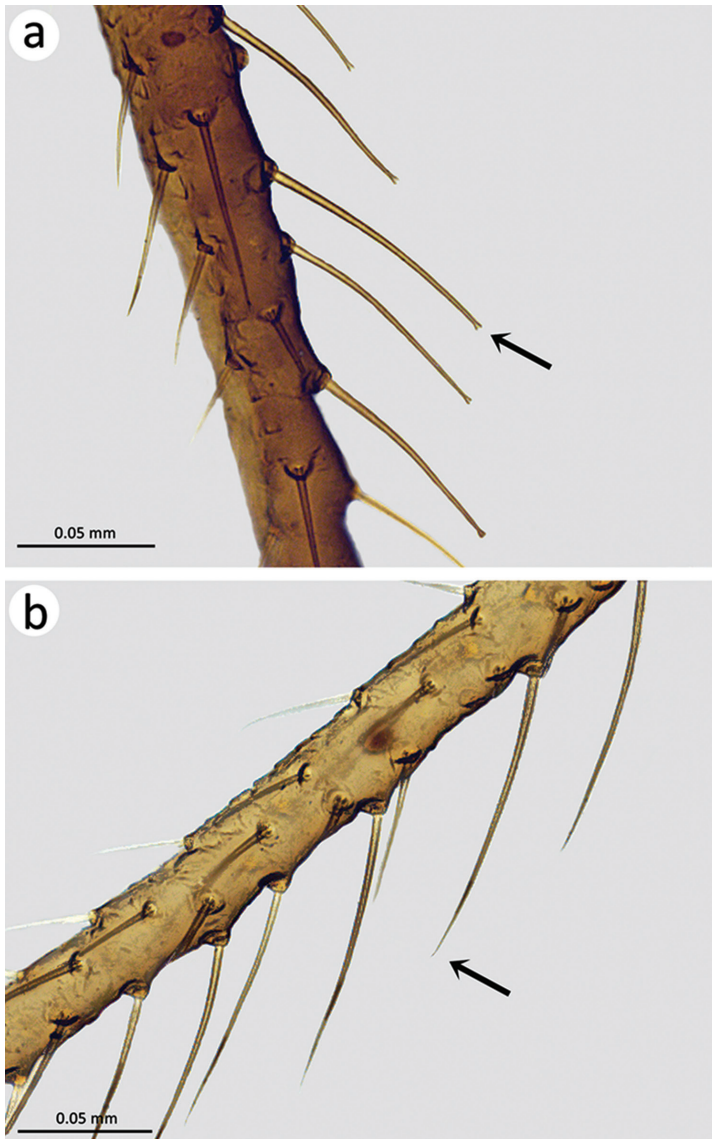


Figure 3. Details of dorsal setae of metatibia in **a** *E. sorenseni* sp. n. (slide-mounted specimen) **b** *E. gagnonae* sp. n. (slide-mounted specimen).

slides (2 + 2 + 2) EMEC); 13 viviparous apterae, California, Humboldt Co., nr Little River State Beach, 17 km N Arcata, HWY 101, 04.vii.1978, on *Pinus muricata*, 78G3, J. T. Sorensen *leg.*, specimens on 4 slides (4 + 4 + 4 + 1) (EMEC).

Diagnosis. Like species of the *E. californica* complex and *E. pini*, *E. sorenseni* sp. n. has its 3rd and 4th abdominal dorsal terga usually bearing six setae. It can be distinguished from *E. patchae* by the presence of spinules on the URS (absent or faint in *E. patchae*; Fig 2b, d); from *E. pini* by a relatively elongate URS with subparallel

lateral margins (URS with margins rounded and convergent at base in *E. pini*; Fig 2a, c); from *E. domenechi* sp. n. and *E. gagnonae* sp. n. with the following characters: usually pro- and metatibiae conspicuously darkened with mesotibiae always lighter, metafemora darkened (tibiae concolorous, metafemora pale in *E. domenechi* sp. n., concolorous or with pro- and metatibiae slightly darkened with mesotibiae lighter, metafemora pale in *E. gagnonae* sp. n.); width of head between eyes = 353.6 ± 15.3 (300.7 ± 14.2 for *E. domenechi* sp. n., and 289.0 ± 13.3 for *E. gagnonae* sp. n.); ratio of 3rd / 5th antennal segments > 1.6 (< 1.6 for *E. domenechi* sp. n. and *E. gagnonae* sp. n.); overall pubescence medium-sized to long with average length of the longest dorsal setae of metafemora = 51.2 ± 10.7 (29.7 ± 4.2 for *E. domenechi* sp. n., and 59.8 ± 9.8 for *E. gagnonae* sp. n.); average length of the longest ventral seta of metafemora = 54.4 ± 5.6 (32.6 ± 4.5 for *E. domenechi* sp. n., and for 43.1 ± 5.4 for *E. gagnonae* sp. n.); average length of the longest dorsal seta of metatibiae = 76.4 ± 15.8 (44.0 ± 8.1 for *E. domenechi* sp. n., and 85.7 ± 10.8 for *E. gagnonae* sp. n.); average length of the longest ventral seta of metatibiae = 67.7 ± 12.0 (37.5 ± 7.0 for *E. domenechi* sp. n., and 49.4 ± 9.5 for *E. gagnonae* sp. n.); average length of the longest frontal setae = 53.4 ± 11.9 (32.6 ± 7.5 for *E. domenechi* sp. n., and for 58.7 ± 8.3 *E. gagnonae* sp. n.); average number of setae of the genital plate = 31.6 ± 1.7 (22.0 ± 2.1 for *E. domenechi* sp. n., and 23.6 ± 2.1 for *E. gagnonae* sp. n.). *Essigella sorenseni* sp. n. is for now morphologically not distinguishable from *E. californica*, the latter being highly variable, nor from *E. hoernerii*. *E. sorenseni* sp. n. can be separated from *E. californica*, *E. domenechi* sp. n., *E. gagnonae* sp. n., and *E. hoernerii* with the DNA characters shown in Table 3.

Description. Viviparous apterae (prepared specimens): body with a yellowish tement more or less darkened at joints depending on the specimens, with conspicuous and pigmented scleroites. Legs usually with pro- and metatibiae conspicuously darkened, much darker than body and mesotibiae. Antennae pale, the 5th, the 4th and the apical third part of the 3rd segment darkened. URS elongated, with lateral margins subparallel, bearing rows of spinules. Overall pubescence medium-sized to long, dorsal setae of appendages incrassate, ventral ones acute, in specimens with very long dorsal setae on metafemora and metatibiae (> 100 μ m), these setae not acute or seemingly acute but still incrassate (Fig 3a), the setae sometimes curved at base. Terga of abdominal segments 3 and 4 with six dorsal setae. Genital plate with 29–34 setae (31.6 ± 1.7) (n = 10). Cauda obvious but not protruding, apically rounded, slightly turned upward. BL: 1900–2300 (2200 ± 110) (n = 21). HWE: 322.3–376.1 (353.6 ± 15.3) (n = 17), LAIII: 207.5–256.3 (233.6 ± 12.8) (n = 25), LAIV: 98.3–130.0 (112.2 ± 7.1) (n = 34), LAV: 120.1–139.8 (127.9 ± 4.7) (n = 23), LPRIV: 19.9–27.8 (24.1 ± 1.8) (n = 28), LPRV: 17.4–23.4 (19.5 ± 1.5) (n = 21), LPT: 11.6–15.7 (13.8 ± 1.4) (n = 21), LURS: 74.1–86.4 (80.5 ± 3.2) (n = 21), LMF: 702.3–927.8 (810.8 ± 58.9) (n = 26), WMF: 87.5–128.9 (103.1 ± 11.3) (n = 36), LMT: 1064.2–1450.4 (1233.4 ± 95.1) (n = 26), WMT: 49.5–76.0 (55.1 ± 5.1) (n = 37), WS: 39.0–44.6 (41.4 ± 1.7) (n = 22), LMB: 118.5–140.3 (130.3 ± 6.4) (n = 38), LMD: 183.4–212.5 (198.1 ± 7.9) (n

Table 3. Diagnostic nucleotide differences between *E. sorenseni* sp. n. and *E. californica*, *E. domenechi* sp. n., *E. gagnonae* sp. n., and *E. hoernerii* for *ATP6*, *COI*, and *Gnd*.

Gene	<i>ATP6</i> (663 bp)		<i>COI</i> (658 bp)	<i>Gnd</i> (749 bp)		
	110	399	247	198	407	431
<i>E. sorenseni</i> sp. n.	C	C	T	T	C	G
<i>E. domenechi</i> sp. n.	T	T	C	C	T	T
<i>E. gagnonae</i> sp. n.	T	T	C	C	T	T
<i>E. californica</i>	T	T	C	C	T	T
<i>E. hoernerii</i>	T	T	C	C	T	T

= 34), LFS: 31.9–82.7 (53.4 ± 11.9) (n = 25), LDMFS: 34.2–79.4 (51.2 ± 10.7) (n = 45), LVMFS: 43.4–66.0 (54.4 ± 5.6) (n = 44), LDMTS: 47.7–113.8 (76.4 ± 15.8) (n = 46), LVMTS: 45.9–92.2 (67.7 ± 12.0) (n = 45).

Comments. USA, California, on *Pinus muricata* D. Don, known from Humboldt, Mendocino, and Sonoma counties (type series), but probably present everywhere on the coastal range in California where *P. muricata* occurs. This species corresponds to the *E. californica* population living on *P. muricata* (cluster H1) shown in Théry et al. (in press).

Etymology. This species is dedicated to John T. Sorensen, aphid specialist who eminently revised the genus *Essigella* in 1994, for his advice and hospitality accorded to the authors (TT and CF) in California.

Essigella patchae Hottes, 1957, stat. n.

Figs 1b, 2b, d, f, h

Essigella patchae Hottes, 1957: 98 (Type locality: “Stillwater, Maine”). Holotype viviparous alate in USNM. Sorensen 1994: 49 [synonymy with *E. pini* Wilson].

Status re-established.

Other examined material. 1 viviparous alate and 1 viviparous aptera, Canada, Québec, Saint-Hippolyte, N45.991 - W74.009, ix.2015, on *Pinus strobus*, C. Favret leg. (QMOR); 1 viviparous aptera, Saint-Hippolyte, N45.989 - W74.005, ix.2016, on *Pinus strobus*, T. Théry leg. (QMOR); 1 viviparous aptera, Saint-Hippolyte, N45.989 - W74.005, ix.2017, on *Pinus strobus*, T. Théry leg. (QMOR).

Diagnosis. Like species of the *E. californica* complex and *E. pini*, *E. patchae* has its 3rd and 4th dorsal abdominal terga usually with six setae. *Essigella patchae* can be distinguished from the other species of the *E. californica* complex species and from *E. pini* by its ultimate rostral segment (URS) exhibiting no or barely visible rows of spinules (Fig. 2b, d), which are clearly visible in other species of the *E. californica* complex and also in *E. pini* (Fig. 2a, c). *Essigella patchae* can also be differentiated from *E. pini* by having the general shape of the URS more elongated with lateral margins almost

parallel (Fig. 2b, d) (margins more rounded and convergent at base in *E. pini*; Fig. 2a, c); shorter cauda than that of *E. pini* which can be elongated and acute; genital plate with fewer setae (15–20 vs 26–30 in *E. pini*), longer in *E. patchae* in comparison with *E. pini* (Fig. 2e, f), with spinules of the genital plate tegument more developed in *E. patchae* (Fig. 2g, h).

Host plant and distribution. The species is currently known from its type locality in Maine (USA) and from one locality in Quebec (Canada) on *Pinus strobus* Linnaeus (see discussion).

Simplified key to species of the *Essigella californica* complex, for viviparous apterae

Due to the variability of preparation, notably cover slip-induced deformations, teneral specimens, and general morphological variability, several specimens and the identity of the host plant are required to best use this key.

- 1 Dorsal terga 3 and 4 usually with six setae.....***E. californica* complex, *E. pini*...2**
- Dorsal terga 3 and 4 usually with more than six setae**other *Essigella* species** (see Sorensen 1994)
- 2 Western North American species**3**
- Eastern North American species.....**7**
- 3 On pinyon pines (*Pinus cembroides*, *P. edulis*, *P. monophylla*, *P. quadrifolia*) ...***E. hoerneri***
- Not on pinyon pines.....**4**
- 4 On *Pinus albicaulis*, *P. monticola*, or *P. muricata***5**
- On other pine species***E. californica***
- 5 Ratio of LAIII / LAV > 1.6 (1.66–1.94), number of setae on genital plate > 27 (29–34), on *P. muricata****E. sorenseni* sp. n.**
- Ratio of LAIII / LAV < 1.6 (1.29–1.54), number of setae on genital plate < 27 (19–26)**6**
- 6 Dorsal setae of metafemora (25.2–36.8 µm) and of metatibiae (33.7–61.8 µm) short, on *P. albicaulis*.....***E. domenechi* sp. n.**
- Dorsal setae of metafemora (42.0–82.9 µm) and of metatibiae (60.9–107.7 µm) long, on *P. monticola*.....***E. gagnonae* sp. n.**
- 7 Ultimate Rostral Segment (URS) with rows of spinules; sides of URS convex, convergent at base (Fig 2a, c), number of setae on genital plate > 24 (26–30)***E. pini***
- Ultimate Rostral Segment (URS) without or with barely visible rows of spinules (Fig 2b, d); sides of URS subparallel, not convergent at base, number of setae on genital plate < 24 (15–20)***E. patchae***

Catalogue of *Essigella* species

Genus *Essigella* del Guercio, 1909: 329

Type species : *Lachnus californicus* Essig, 1909: 1

= *Archeoessigella* Sorensen, 1994: 21; [new synonym]

= *Lambersella* Sorensen, 1994: 29; [new synonym]

Essigella alyeska Sorensen, 1988: 118; Sorensen 1994: 72

Essigella californica (Essig), 1909: 1; Sorensen 1994: 53

= *Lachnus californicus* Essig, 1909: 1

= *Essigella claremontiana* Hottes, 1957: 79 [synonymy by Sorensen 1994: 53]

= *Essigella cocheta* Hottes, 1957: 82 [synonymy by Sorensen 1994: 53]

= *Essigella monelli* Hottes, 1957: 95 [synonymy by Sorensen 1994: 53]

= *Essigella pineti* Hottes, 1957: 101 [synonymy by Sorensen 1994: 53]

= *Essigella swaini* Hottes, 1957: 105 [synonymy by Sorensen 1994: 53]

Essigella critchfieldi Sorensen, 1994: 75

Essigella domenechi sp. n.

Essigella eastopi Sorensen, 1994: 30

Essigella essigi Hottes, 1957: 84; Sorensen 1994: 45

Essigella fusca fusca Gillette & Palmer, 1924: 6 ; Sorensen 1994: 34

= *Essigella fusca* Gillette & Palmer, 1924: 6

= *Essigella agilis* Hottes, 1957: 71 [synonymy by Sorensen 1994: 34]

= *Essigella palmerae* Hottes, 1957: 96 [synonymy by Sorensen 1994: 34]

Essigella fusca voegtlini Sorensen, 1994: 39

Essigella gagnonae sp. n.

Essigella hillerislambersi Sorensen, 1994: 41

Essigella hoerneri Gillette & Palmer, 1924: 5; Sorensen 1994: 62

= *Essigella gillettei* Hottes, 1957: 88 [synonymy by Sorensen 1994: 62]

= *Essigella maculata* Hottes, 1957: 93 [synonymy by Sorensen 1994: 62]

Essigella kathleenae Sorensen, 1988: 115; Sorensen 1994: 26

Essigella kirki Sorensen, 1988: 121; Sorensen 1994: 22

Essigella knowltoni braggi Hottes, 1957: 73; Sorensen 1994: 84

= *Essigella braggi* Hottes, 1957: 73 [new status by Sorensen 1994: 84]

= *Essigella robusta* Hottes, 1957: 103 [synonymy by Sorensen 1994: 84]

Essigella knowltoni knowltoni Hottes, 1957: 92 [new status by Sorensen 1994: 78]

= *Essigella knowltoni* Hottes, 1957: 92

Essigella patchae Hottes, 1957: 98; Sorensen 1994: 49; [stat. n.]

Essigella pini Wilson, 1919: 2; Sorensen 1994: 49

Essigella sorenseni sp. n.

Essigella wilsoni Hottes, 1957: 106; Sorensen 1994: 67

= *Essigella pergandei* Hottes, 1957: 100 [synonymy by Sorensen 1994: 67]

= *Essigella oregonensis* Hottes, 1958: 155 [synonymy by Sorensen 1994: 67]

Discussion

Essigella californica

Sorensen, in his revision of the genus *Essigella* (1994) had already documented the existence of different host-associated groups within *E. californica*. He notably mentioned populations living on *Pinus flexilis* E. James and *P. lambertiana* Douglas, populations that he nevertheless considered as exhibiting intraspecific variation (Sorensen 1983, 1994). Populations from those two pine species were not considered in the study of Théry et al. (in press) and it is possible that they correspond to yet two more cryptic species. *Essigella californica* is known to live on at least 34 *Pinus* species (Kimber et al. 2013) and it is likely that other cryptic species await discovery. We are unable to fully evaluate the species complex here due to a lack of material. The taxonomic nature of *Essigella californica* continues to be a complex issue meriting further study. Such a study would require substantial material of representative populations from as many known host plants as possible. A redescription of this species and the members of its complex would require morphometric data and multivariate analyses as per Sorensen (1994), combined with molecular phylogenetic and species delimitation methods as per Théry et al. (in press).

Essigella patchae and *E. pini*

Essigella pini is known to be oligophagous on *Pinus* and according to Sorensen (1994), it can be found on pine species of the subgenus *Pinus*, section *Trifoliae*, subsection *Contortae* (notably on *P. virginiana* Miller), subsection *Australes* (notably on *P. taeda* Linnaeus), and on pine species of the subgenus *Strobus*, section *Quinquefoliae*, subsection *Strobus* (notably on *P. strobus*). It may be also found on species of subsection *Sylvestres* (Sorensen 1994). The type specimen of *E. pini* was collected in Maryland on *P. virginiana* (Wilson 1919; Sorensen 1994) whereas that of *E. patchae* was collected in Maine on *P. strobus* (Hottes 1957; Sorensen 1994). Genetic material analysed by Théry et al. (in press) came from a Canadian specimen of *E. patchae* collected on *P. strobus* and a US specimen of *E. pini* collected on *P. rigida* (subsection *Australes*). Our first suspicions are that *E. patchae* could be a more northern species that would feed on pines of subsection *Strobus* whereas *E. pini* would be more southern developing on pines of both subsections *Australes* and *Contortae*. It could appear curious that Sorensen did not discriminate both species, even though they are morphologically very close. Actually, Sorensen himself collected only species occurring in the western part of USA. Because *E. pini* and *E. patchae* are the only species occurring in the East, all *E. pini* and *E. patchae* specimens that Sorensen studied came from other collections and represented a smaller specimen sample in comparison with other species. Considering the list of specimens Sorensen (1994) studied and those we verified from both USNM and UMSP collections, it is likely that he studied no more than two specimens identified as *E. patchae*, notably the type specimen in poor condition. Those conditions made revelation of significant differences between the two species difficult.

Molecular data in aphid diagnoses

Aphids represent a relatively well-studied insect group mostly because of their economic importance. Molecular data are most often used in population genetics (Wongsa et al. 2017; Medina et al. 2017). They are used also in works linked with species recognition using barcodes because of their small size and their difficult systematics (Cœur d'acier et al. 2014; Lee et al. 2011). As in other animal groups, new aphid species can be discovered or confirmed using DNA analyses (Depa et al. 2012; Chen et al. 2015; Jiang et al. 2015). The present paper represents the first time that DNA sequence characters have been used in an aphid species diagnosis. Indeed, use of this kind of data and especially substitutions of nucleotides as characters is rare in animal diagnoses (Renner 2016), and rarer in insects. The precedent was established 8 years ago (Brower 2010). The International Code of Zoological Nomenclature does not explicitly recommend DNA sequence data to establish animal taxa, yet nor does it forbid it (ICZN 1999). Other kinds of non-morphological characters are commonly used in other groups. For example, songs or acoustic signals are used to differentiate species in several animal groups and can be considered good diagnostic characters in frogs (Brown and Richards 2008) or in Orthopteran insects (Hertach et al. 2015; Iorgu et al. 2017). In consequence, we judge that the absence, the presence, or the identity of a nucleotide or of a DNA sequence fragment are the molecular equivalent to the absence, the presence, or the shape of a seta, a puncture, or of any other morphological character. We thus support that this kind of DNA character can be used unambiguously in a diagnosis.

Acknowledgments

We are grateful to G. L. Miller (USDA Systematic Entomology Laboratory, Beltsville, MD), P. T. Oboyski (Essig Museum of Entomology, University of California, Berkeley, CA), and R. E. Thomson (University of Minnesota, St Paul, MN) for specimen loans. We extend our thanks to J. T. Sorensen for his advice and assistance in the field. We also thank the two reviewers, Susan Halbert and Roger Blackman, for the helpful comments on previous versions of the manuscript. Mariusz Kanturski gratefully acknowledges the Scholarship for Outstanding Young Scientists from the Ministry of Science and Higher Education of Poland (1165/E-340/STYP/12/2017).

References

- Blackman RL, Eastop VF (2017) Aphids on the world's plants: An online identification and information guide. <http://www.aphidinwordsplants.info/> [accessed on 2017-11-01]
- Brower AV (2010) Alleviating the taxonomic impediment of DNA barcoding and setting a bad precedent: names for ten species of '*Astraptus fulgerator*' (Lepidoptera: Hesperidae:

- Eudaminae) with DNA-based diagnoses. *Systematics and Biodiversity* 8(4): 485–491. <https://doi.org/10.1080/14772000.2010.534512>
- Brown RM, Richards SJ (2008) Two new frogs of the genus *Platymantis* (Anura: Ceratobatrachidae) from the Isabel Island group, Solomon Islands. *Zootaxa* 1888(1): 47–68.
- Chen R, Jiang LY, Liu L, Liu QH, Wen J, Zhang RL, Li XY, Wang Y, Lei FM, Qiao GX (2013) The *gnd* gene of *Buchnera* as a new, effective DNA barcode for aphid identification. *Systematic Entomology* 38: 615–625. <https://doi.org/10.1111/syen.12018>
- Chen J, Zhang B, Zhu X, Jiang L, Qiao GX (2015) Review of the aphid genus *Aspidophorodon* Verma, 1967 with descriptions of three new species from China (Hemiptera: Aphididae: Aphidinae). *Zootaxa* 4028(4): 551–576. <https://doi.org/10.11646/zootaxa.4028.4.6>
- Cœur d'acier A, Cruaud A, Artige E, Genson G, Clamens AL, Pierre É, Hudaverdian S, Simon JC, Jousset E, Rasplus JY (2014) DNA barcoding and the associated PhylAphidB@se website for the identification of European aphids (Insecta: Hemiptera: Aphididae). *PLoS ONE* 9 (6): e97620.
- Del Guercio G (1909) Intorno a due nuovi generi e a tre specie nuove di afidi di California. *Rivista di Patologia Vegetale* 3: 328–332.
- Depa Ł, Mróz E, Szawaryn K (2012) Molecular identity of *Stomaphis quercus* (Hemiptera: Aphidoidea: Lachnidae) and description of a new species. *European Journal of Entomology* 109: 435–444. <https://doi.org/10.14411/eje.2012.056>
- Essig EO (1909) Aphididae of southern California I. *Pomona College Journal of Entomology* 11–10.
- Favret C (2005) A new non-destructive DNA extraction and specimen clearing technique for aphids (Hemiptera). *Proceedings of the Entomological Society of Washington* 107: 469–470.
- Gillette CP, Palmer MA (1924) New Colorado Lachnini. *Annals of the Entomological Society of America* 17(1): 1–57. <https://doi.org/10.1093/aesa/17.1.1>
- Hebert PDN, Cywinska A, Ball SL, de Waard JR (2003a) Biological identifications through DNA barcodes. *Proceedings of the Royal Society of London. Series B* 270 (1512): 313–321. <https://doi.org/10.1098/rspb.2002.2218>
- Hebert PDN, Ratnasingham S, de Waard JR (2003b) Barcoding animal life: cytochrome *c* oxidase subunit I divergences among closely related species. *Proceedings of the Royal Society of London. Series B* 270 (Suppl 1): S96–S99. <https://doi.org/10.1098/rsbl.2003.0025>
- Hertach T, Trilar T, Wade EJ, Simon C, Nagel P (2015) Songs, genetics, and morphology: revealing the taxonomic units in the European *Cicadetta cerdaniensis* cicada group, with a description of new taxa (Hemiptera: Cicadidae). *Zoological Journal of the Linnean Society* 173(2): 320–351. <https://doi.org/10.1111/zoj.12212>
- Hottes FC (1957) A synopsis of the genus *Essigella* (Aphidae). *Proceedings of the Biological Society of Washington* 70: 69–109.
- Hottes FC (1958) A new species of *Essigella* from Oregon (Aphidae). *Proceedings of the Biological Society of Washington* 71: 155–156.
- ICZN (1999). *International Code of Zoological Nomenclature*. 4th ed. London, UK: The International Trust for Zoological Nomenclature. 306 pp. <http://iczn.org/iczn/index.jsp> [accessed on 2017-11-01]
- Iorgu IŞ, Iorgu EI, Szövényi G, Orci KM (2017) A new, morphologically cryptic bush-cricket discovered on the basis of its song in the Carpathian Mountains (Insecta, Orthoptera, Tettigoniidae). *ZooKeys* 680: 57–72. <https://doi.org/10.3897/zookeys.680.12835>

- Jiang L, Chen J, Guo K, Qiao GX (2015) Review of the genus *Ceratovacuna* (Hemiptera: Aphididae) with descriptions of five new species from China. *Zootaxa* 3986(1): 35–60. <https://doi.org/10.11646/zootaxa.3986.1.2>
- Kanturski M, Karcz J, Wiczorek K (2015) Morphology of the European species of the aphid genus *Eulachmus* (Hemiptera: Aphididae: Lachninae) – a SEM comparative and integrative study. *Micron* 76: 23–36. <https://doi.org/10.1016/j.micron.2015.05.004>
- Kimber W, Glatz R, Shaw S (2013) Introduction of the wasp *Diaeretus essigellae*, for biological control of Monterey Pine Aphid *Essigella californica*, in Australia. Final Report. Forest & Wood Products Australia, Resources. Project Number PNC063-0607, Melbourne, Vic, 72 pp.
- Lee W, Kim H, Lim J, Choi HR, Kim Y, Kim YS, Ji JY, Footitt RG, Lee S (2011) Barcoding aphids (Hemiptera: Aphididae) of the Korean Peninsula: updating the global data set. *Molecular Ecology Resources* 11: 32–37. <https://doi.org/10.1111/j.1755-0998.2010.02877.x>
- Lee W, Lee Y, Kim H, Akimoto SI, Lee S (2014) Developing a new molecular marker for aphid species identification: Evaluation of eleven candidate genes with species-level sampling. *Journal of Asia-Pacific Entomology* 17: 617–627. <https://doi.org/10.1016/j.aspen.2014.06.008>
- Lukhtanov VA, Dantchenko AV (2017) A new butterfly species from south Russia revealed through chromosomal and molecular analysis of the *Polyommatus (Agrodiaetus) damonides* complex (Lepidoptera, Lycaenidae). *Comparative Cytogenetics* 11(4): 769–795. <https://doi.org/10.3897/compcytogen.v11i4.20072>
- Medina RF, Armstrong SJ, Harrison K (2017) Genetic population structure of sugarcane aphid, *Melanaphis sacchari*, in sorghum, sugarcane, and Johnsongrass in the continental USA. *Entomologia Experimentalis et Applicata* 162(3): 358–365. <https://doi.org/10.1111/eea.12547>
- Morinière J, Hendrich L, Balke M, Beermann AJ, König T, Hess M, Koch S, Müller R, Leese F, Hebert PDN, Hausmann A, Schubart CD, Haszprunar G (2017) A DNA barcode library for Germany's mayflies, stoneflies and caddisflies (Ephemeroptera, Plecoptera & Trichoptera). *Molecular Ecology Resources* 17(6): 1293–1307. <https://doi.org/10.1111/1755-0998.12683>
- Renner SS (2016) A return to Linnaeus's focus on diagnosis, not description: the use of DNA characters in the formal naming of species. *Systematic biology* 65(6): 1085–1095. <https://doi.org/10.1093/sysbio/syw032>
- Sorensen JT (1983) Cladistic and phenetic analysis of *Essigella* aphids: systematics and phylogeny in relation to their Pinaceae host plants (Homoptera: Aphididae, Lachninae). Ph.D. dissertation, University of California, Berkeley.
- Sorensen JT (1988) Three new species of *Essigella* (Homoptera: Aphididae). *Pan-Pacific Entomologist* 64 (2): 115–125.
- Sorensen JT (1994) A revision of the aphid genus *Essigella* (Homoptera: Aphididae: Lachninae): its ecological associations with, and evolution on, Pinaceae hosts. *Pan-Pacific Entomologist* 70(1): 1–102.
- Théry T, Brockerhoff EG, Carnegie AJ, Chen R, Elms SR, Hullé M, Glatz R, Ortego J, Qiao GX, Turpeau É, Favret C (2017) *EF-1a* DNA Sequences Indicate Multiple origins of introduced populations of *Essigella californica* (Hemiptera: Aphididae). *Journal of economic entomology* 110(3): 1269–1274. <https://doi.org/10.1093/jee/tox026>

- Théry T, Kanturski M, Favret C (in press) Molecular phylogenetic analysis and species delimitation in the pine needle-feeding aphid genus *Essigella* (Hemiptera, Sternorrhyncha, Aphididae). *Insect Systematics and Diversity*.
- Wilson HF (1919) Three new lachnids with comparative notes on three others (Homop.). *Entomological News* 30(1): 1–7.
- Wongsa K, Duangphakdee O, Rattanawanee A (2017) Genetic structure of the *Aphis craccivora* (Hemiptera: Aphididae) from Thailand inferred from mitochondrial *COI* gene sequence. *Journal of Insect Science* 17(4): 84. <https://doi.org/10.1093/jisesa/iex058>

Odontonia plurellicola sp. n. and *Odontonia bagginsi* sp. n., two new ascidian-associated shrimp from Ternate and Tidore, Indonesia, with a phylogenetic reconstruction of the genus (Crustacea, Decapoda, Palaemonidae)

Werner de Gier¹, Charles H.J.M. Fransen¹

¹ Research group Taxonomy & Systematics, Naturalis Biodiversity Center, Vondellaan 55, 2332 AA Leiden, The Netherlands

Corresponding author: Charles H.J.M. Fransen (charles.fransen@naturalis.nl)

Academic editor: S. De Grave | Received 26 March 2018 | Accepted 30 April 2018 | Published 7 June 2018

<http://zoobank.org/03763455-6AB1-4B50-AD65-C2DF38F6136F>

Citation: de Gier W, Fransen CHJM (2018) *Odontonia plurellicola* sp. n. and *Odontonia bagginsi* sp. n., two new ascidian-associated shrimp from Ternate and Tidore, Indonesia, with a phylogenetic reconstruction of the genus (Crustacea, Decapoda, Palaemonidae). ZooKeys 765: 123–160. <https://doi.org/10.3897/zookeys.765.25277>

Abstract

Two new species of palaemonid shrimp associated with ascidian hosts, *Odontonia bagginsi* sp. n. from Tidore and *Odontonia plurellicola* sp. n., from Ternate, Indonesia are described and figured. Through phylogenetic analyses based on both morphological and molecular datasets (mitochondrial Cytochrome c oxidase subunit I gene and the 16S mitochondrial ribosomal gene) of the genus *Odontonia*, the phylogenetic positions of the new species have been reconstructed. Scanning Electron Microscopy has been used to observe additional characters on dactyli of the ambulatory pereopods. *Odontonia plurellicola* sp. n. appears to be more closely related to *O. simplicipes* and *O. seychellensis*, but it differs most notably in the morphology of the rostrum and mouthparts. *Odontonia plurellicola* sp. n. appears to be the only *Odontonia* species living inside a phlebobranch ascidian *Plurella* sp. *Odontonia bagginsi* sp. n. is closely related to *O. sibogae*, but differs markedly in the abundance of setae on the propodi of the ambulatory pereopods. In the present paper, *O. maldivensis* Fransen, 2006 is regarded as a junior synonym of *O. rufopunctata* Fransen, 2002 based on both morphological and molecular aspects.

Keywords

Ascidians, Caridea, new species, *Odontonia*, Palaemonidae, symbiosis, Ternate, Tidore

Introduction

The palaemonid genus *Odontonia* Fransen, 2002, currently contains 7 species (Fransen 2002, De Grave and Fransen 2011): *O. compacta* (Bruce, 1996); *O. katoi* (Kubo, 1940); *O. maldivensis* Fransen, 2006; *O. rufopunctata* Fransen, 2002; *O. seychellensis* Fransen, 2002, *O. sibogae* (Bruce, 1972); and *O. simplicipes* (Bruce, 1996). As far as is known these species are endosymbionts of solitary ascidians (Fransen 2002) and are distributed in the Indo-West Pacific.

In 2009 an expedition was organised by the Naturalis Biodiversity Center (Leiden, the Netherlands) and the Research Center of Oceanography, Indonesian Institute of Sciences (RCO-LIPI) (Jakarta, Indonesia), to the Indonesian islands of Ternate and Tidore (Hoeksema and van der Meij 2010). During the expedition, two *Odontonia* species new to science were collected from ascidian hosts. The species are described and figured. Their phylogenetic relationships with other members of the genus are analysed using both morphological as well as molecular datasets. The host preference is analysed in relation to the phylogenetic relationships within the genus. A key to the species in the genus is provided.

The following abbreviations are used: COI, mitochondrial gene cytochrome c oxidase subunit I; 16S, 16S mitochondrial ribosomal gene; PoCL, post orbital carapace length; RMNH, Naturalis Biodiversity Center, Leiden (formerly Rijksmuseum van Natuurlijke Historie); MZB, Museum Zoologicum Bogoriense, Research Center for Biology, Indonesian Institute of Sciences, Cibinong, Indonesia.

Materials and methods

Specimens were gathered around Ternate, in the northern Moluccas during an expedition organised from 23 October to 18 November 2009, by the Research Center of Oceanography, Indonesian Institute of Sciences (RCO-LIPI) (Jakarta, Indonesia) and Naturalis Biodiversity Center (NBC) (Leiden, the Netherlands). This expedition was part of the Ekspedisi Widya Nusantara project (E-Win expeditions). Specimens were collected using SCUBA equipment. Live specimens were photographed with a Nikon D80 digital camera and preserved in 70% ethanol.

Specimens were studied and drawn using a dissecting stereomicroscope (Zeiss Discovery.V8) and a compound microscope (Olympus BX53) both provided with a drawing tube. Sketches were traced using 2.5 to 3 mm Sakura Pigma Micron-pens and scanned (Canon Canoscan 9000F) with a resolution of 600 dpi. Details of the third pereopods were photographed with a Scanning Electron Microscope. Pereopods were dried using Critical Point Drying-methods (CPD) in a Leica EM CPD300 (located in Biopartner, Leiden, the Netherlands) with the following parameters (standard protocol preservation insects): CO₂ intake: Auto, Speed slow, Delay 120s; Exchange: Speed 5, Cycles 18; Gas output: Heat medium, Speed slow 100%. The pereopods were placed on stubs/mounts in pairs of two species, and coated with 20 nm Pt/Pd using a

Table 1. Specimens used for SEM photography and 16S & COI DNA analyses (roman numerals can be linked back to the phylogenetic trees (Figs 20, 21)).

Species	Sample location	Host organism	Registration number	GenBank 16S	GenBank COI	SEM
<i>Odontonia bagginsi</i> sp. n.	Indonesia, Halmahera, Tidore	Unid. ascidian	MZB Cru 4733		MH257316	×
<i>Odontonia katoii</i> (Kubo, 1940)	Indonesia, Bali, Tulamben beach	<i>Polycarpa aurata</i>	RMNH. CRUS.D.48689	MH251614		
	Indonesia, SW Sulawesi, Spermonde Archipelago	<i>Polycarpa aurata</i>	RMNH. CRUS.D.46701			×
	Indonesia, NE Sulawesi, Bitung	<i>Polycarpa aurata</i>	RMNH. CRUS.D. 57295	MH251615		
<i>Odontonia maldivensis</i> Fransen, 2006	Maldives, S Malé Atoll	<i>Polycarpa cryptocarpa</i>	RMNH. CRUS.D.51001			×
	Maldives, Faafu Atoll, Magoodhoo Island	<i>Polycarpa cryptocarpa</i>	RMNH. CRUS.D. 57296	MH251616		
	Maldives, Faafu Atoll, Magoodhoo Island	<i>Herdmania momus</i> (?)	RMNH. CRUS.D. 57297	MH251617		
<i>Odontonia plurellicola</i> sp. n.	Indonesia, W Halmahera, Ternate	<i>Plurella</i> sp.	RMNH.MZB Cru 4734			×
<i>Odontonia rufopunctata</i> Fransen, 2002	Indonesia, Halmahera mainland, Tanjung Ratemu	Unid. ascidian	RMNH. CRUS.D.53601		MH257314	
	Indonesia, NE Sulawesi, Bitung	<i>Polycarpa</i> sp.	RMNH. CRUS.D. 57298	MH251618	MH257313	
	Indonesia, NE Sulawesi, Bitung	<i>Polycarpa</i> sp.	RMNH. CRUS.D. 57299	MH251619		
	Indonesia, NE Sulawesi, Bitung	<i>Polycarpa</i> sp.	RMNH.CRUS. D57300	MH251620		
	Indonesia, SW Sulawesi, Spermonde Archipelago	Unid. ascidian	RMNH. CRUS.D.48694			×
<i>Odontonia seychellensis</i> Fransen, 2002	Seychelles, E of Mahé	Unid. stolidobranch ascidian *	RMNH. CRUS.D.42762			×
<i>Odontonia sibogae</i> (Bruce, 1972)	Indonesia, Bali, Sanur	<i>Polycarpa</i> sp.	RMNH. CRUS.D.48691	MH251621		
	Indonesia, Halmahera, Tidore	Unid. ascidian	RMNH. CRUS.D.53558		MH257315	
	Indonesia, Borneo, Sabah	<i>Polycarpa argentata</i>	RMNH. CRUS.D.53964		JX185703	
	Indonesia, Ambon, E coast	<i>Polycarpa</i> sp.	RMNH. CRUS.D.47581			×
Outgroup species:						
<i>Pontonia panamica</i> Marin & Anker, 2008	Panama, Playa Venao	<i>Ascidia</i> sp.	RMNH. CRUS.D.51825	MH251622	MH257312	
<i>Pontonia pinnophylax</i> (Otto, 1821)	Cape Verde Islands, S coast of São Vicente	<i>Pinna rudis</i>	RMNH. CRUS.D.42607	KU170692		
	Cape verde Island, São Nicocau	<i>Pinna rudis</i>	RMNH. CRUS.D.42608	MH251623		
<i>Dactyлонia ascidicola</i> (Borradaile, 1898)	Indonesia, Bali, Tulamben area	<i>Ascidia</i> sp.	RMNH. CRUS.D.48678	KU170688		
	Indonesia, Borneo, Sabah	<i>Ascidia</i> sp.	RMNH. CRUS.D.53793		MH257317	

* The host of *Odontonia seychellensis* was identified by the authors as an ascidian from the order of the Stolidobranchia, using the collected ascidian specimens from RMNH.CRUS.D.42762 and basic identification guides (Rocha 2011).

Quorum Q150T S. The dactyli were photographed using a JEOL JSM-S480LV Scanning Electron Microscope (located in the Naturalis Biodiversity Center, Leiden, the Netherlands). Drawings and photographs were edited in Adobe Photoshop (CS6) for better contrast and brightness.

Morphological character state analysis (Appendix I) was based on specimens in the RMNH collection (Table 1) and literature (Bruce 1996, Fransen 2002, Marin and Anker 2008). Two species of the closely related genera *Pontonia* Latreille, 1829 (*P. panamica* Marin & Anker, 2008; *P. pinnophylax* (Otto, 1821) and *Dactylonia* Fransen, 2002 (*D. ascidicola* (Borradaile, 1898)) were included as outgroup in the analyses. A datamatrix was constructed with ordered (Fitch 1971) and unordered (Farris 1970) characters states (Table 2). The analysis was performed using exhaustive search in PAUP 4.0 (Swofford 2003). Trees were viewed in FigTree 1.4.2 (Rambaut 2009).

Mitochondrial COI (7 sequences) and 16S (12 sequences) were available for a partial molecular phylogenetic reconstruction of the genus *Odontonia* (Table 1). For extraction and sequencing see Brinkmann and Fransen (2016). The available sequences were edited and aligned using the alignment tools BioEdit 7.0.0 (Hall 1999) and ClustalX 2.1 (Larkin et al. 2007). The best-fitted model was found using JModelTest (Posada 2008) (using both the Akaike Information Criterion and Bayesian Information Criterion). The datasets were analysed using PAUP 4.0 (Swofford 2003) and MrBayes (Ronquist and Huelsenbeck 2003). Trees were made visible and edited in FigTree 1.4.2 (Rambaut 2009) and Adobe Illustrator (CS6).

Host records for *Odontonia* species were assembled from the literature (Fransen 2002, 2006) and the present material. Ascidian host classification is based on Tzagkogeorga et al. (2009).

Systematics

Superfamily Palaemonoidea Rafinesque, 1815

Family Palaemonidae Rafinesque, 1815

Genus *Odontonia* Fransen, 2002

Generic diagnosis. (modified from Fransen 2002). Small sized shrimp of subcylindrical body form. Rostrum well developed, short, depressed; dorsally unarmed; dorsal carina formed by shallow broad central elevation, bordered by lateral depressions; lateral carinae well developed; ventral margin with or without small subdistal tooth. Carapace smooth; inferior orbital angles broadly rounded; orbit feebly developed; supraorbital, epigastric and hepatic spines absent; antennal spine blunt, rounded, not separated from the inferior orbital angle; anterolateral angle of branchiostegite rounded, not strongly produced. Eye normal, with hemispherical cornea. Antennula normal, ventromedial tooth on basal segment usually large; distolateral tooth of basal segment well developed, reaching distal margin of intermediate segment, anterior margin oblique, not ex-

Table 2. Data matrix of morphological characters used for phylogenetic analysis. Ordered characters in bold face, other characters unordered.

		Species												
		Outgroup species			Odontonia species									
		<i>Dacylonia ascidicola</i>	<i>Pontonia pinnophylax</i>	<i>Pontonia panamica</i>	<i>Odontonia bagginsi</i> sp. n.	<i>Odontonia compacta</i>	<i>Odontonia katoii</i>	<i>Odontonia multivensis</i>	<i>Odontonia rufopunctata</i>	<i>Odontonia seychellensis</i>	<i>Odontonia sibogae</i>	<i>Odontonia simplicipes</i>	<i>Odontonia plurellicola</i> sp. n.	
Characters	1	0	1	1	2	2	2	0	2	2	2	0	2	
	2	0	0	0	1	2	2	2	2	1	1	2	1	
	3	0	0	0	0	0	0	0	0	0	0	1	0	
	4	1	0	0	1	1	1	1	1	2	1	2	2	
	5	0	0	0	0	1	1	1	0	1	1	1	1	
	6	0	0	0	1	1	1	1	1	1	1	0	1	
	7	0	0	0	0	0	0	0	0	1	0	1	1	
	8	0	0	2	1	0	2	1	0	0	0	2	1	
	9	1	0	0	1	0	0	0	2	0	0	0	0	
	10	1	0	0	0	1	1	2	1	1	0	1	2	
	11	0	0	0	1	1	1	0	0	1	1	1	1	
	12	0	0	0	0	1	1	1	1	1	0	1	2	
	13	0	0	0	0	1	0	0	0	0	0	1	2	
	14	1	0	0	1	0	0	0	1	0	0	0	0	
	15	2	0	0	1	1	1	1	1	0	1	1	1	
	16	1	0	0	2	2	2	2	2	0	2	2	2	
	17	1	0	0	0	1	1	2	2	0	1	0	0	
	18	0	1	0	1	1	1	1	1	0	1	1	1	
	19	0	0	0	0	0	0	1	0	1	0	1	1	
	20	0	0	0	0	0	0	0	0	0	0	1	1	
	21	0	0	0	1	1	1	0	0	0	1	0	0	
	22	0	1	1	0	2	1	1	1	1	?	1	1	
	23	1	0	0	?	1	1	1	1	1	1	?	2	
	24	0	0	0	1	?	1	1	1	1	0	2	2	

tending beyond distolateral tooth; flagella short, composed of few segments. Antenna with basicerite unarmed; scaphocerite well developed, with distolateral tooth strongly developed, bent inward, more than 0.2 times length of scaphocerite. Epistome unarmed. Corpus of paragnaths with two submedian, oblique non-setose carinae. Second thoracic sternite with anterior margin broadly rounded, not produced. Fourth thoracic sternite with medially developed centrally slightly notched or completely fused lateral plates. Fifth thoracic sternite with broad rectangular, medially blunt, partly fused lateral plates. Mandible robust, without palp, molar process stout, incisor process simple, with or without row of denticles along medioventral border. Maxillula with bilobed palp, lower lacinia small, slender with few simple setae. Maxilla with simple palp; bilobed endite; scaphognathite broad; basal endite with many simple setae on upper

and lower lacinia, both laciniae well developed; basal endite shorter than palp. First maxilliped with slender palp, basal and coxal endites partly fused, with few short setae along median margin, not forming basket; exopod with caridean lobe; flagellum broad, densely setose distally; epipod large, oval. Second maxilliped with distinct angle in median margin of basis of endopod; exopod with flagellum well developed, plumose setae distally; epipod a small rounded, curled lobe; without podobranch. Third maxilliped with ischiomerus of endopod partly fused to basis, as broad as penultimate segment; exopod well developed, with plumose setae distally; coxa with oval, lateral plate, without median process, arthrobranch absent. First pereopods with chela simple. Chelae unequal in size, subequal in form; major and minor chelae with one proximal tooth on dactylus and two on fixed finger, dactylus without median carina; fixed finger without median fossa to receive dactylar tooth when fingers closed; fingers not gaping. Ambulatory pereopods stout, dactylus simple or biunguiculate, with or without accessory teeth on flexor margin of corpus; flexor margin with scattered setae; unguis with or without distal scales. Abdomen smooth; posterior margins of pleura rounded, posterolateral angle of sixth segment blunt or rounded. Uropod with protopodite feebly acute distally, exopod with distolateral margin with mobile spinule, feebly armed. Telson with two pairs of large submarginal dorsal spines, and two pairs of cuspidate setae, and submedian pair of plumose setae at posterior margin.

Type species. The type species: *Pontonia katoi* Kubo, 1940, by original designation, gender feminine.

Generic distribution. Known from shallow coastal waters of the Indo-West Pacific.

Hosts. Associated with Ascidiacea.

Odontonia plurellicola sp. n.

<http://zoobank.org/CEB25096-4C73-48F3-B4CE-7A207E890B4A>

Figs 1–7, 15A–D, 16F, 17E

Material examined. Type series. 1 ovigerous female (**holotype**), PoCL 1.55 mm (MZB Cru 4734), Tarau, W Halmahera, Ternate, Indonesia, 0°50'30"N, 127°22'38.5"E, shallow area with coral followed by sandy slope with coral gardens, 9 m depth, scuba diving, 2-11-2009; in ascidian *Plurella* sp. (Asc. 68), leg. C.H.J.M. Fransen, photo TER.17.0049 – 76; 1 male, PoCL 1.30 mm, 1 ovigerous female, PoCL. 1.50 mm, 2 non-ovigerous females PoCL 0.90–1.05 mm (paratypes) (RMNH.CRUS.D.53554), same data as holotype.

Diagnosis. Rostrum as long as antennular peduncle, with distoventral tooth. Pterygostomial angle produced. Basal segment of antennular peduncle with distolateral tooth minute, medioventral tooth strong, acute. Distolateral tooth of scaphocerite robust, 0.3 length of lamina. Dactylus of ambulatory pereopods with flexor margin of corpus with few (usually 3) short teeth but without accessory tooth; unguis without terminal scales. Telson with two pairs of medium sized (approx. 0.17 of telson length) submarginal dorsal spines at 0.20 and 0.54 of telson length.

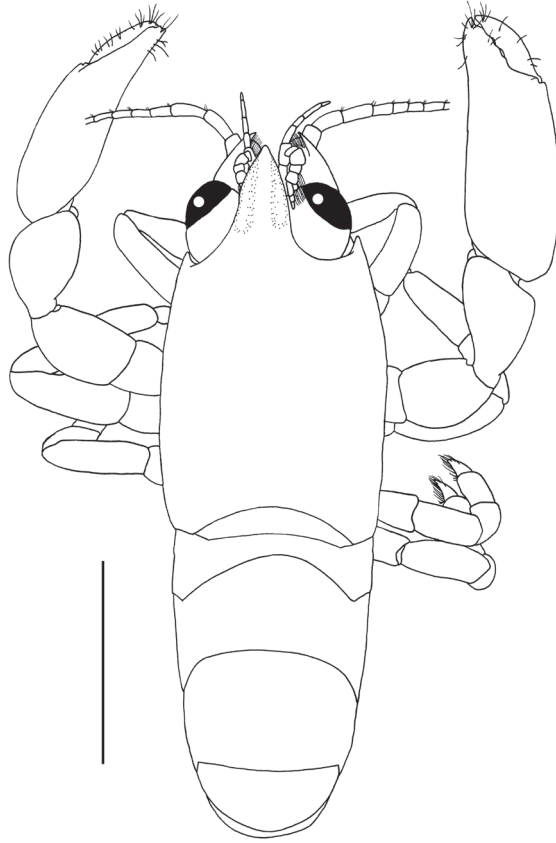


Figure 1. *Odontonia plurellicola* sp. n., habitus, dorsal aspect. Ovigerous female PoCL 1.50 mm (RMNH. CRUS.D.53554). Scale bar: 1 mm.

Description. Body (Figs 1, 2A) subcylindrical, depressed. Carapace smooth. Rostrum well developed, approx. 0.45 of post-orbital carapace length, as long as antennular peduncle, falling short of distal margin of scaphocerite, approximately 1.8 times longer than diameter of hemispherical cornea, with broad shallow indistinct dorsal carina, with acute lateral carinae, with straight ventral carina; with distal ventral tooth, with distal setae, bluntly acute in dorsal view, broadened at base. Inferior orbital angle not produced, straight. Antennal spine reduced to blunt process. Pterygostomial of carapace straight, anterolateral angle slightly produced, rounded.

Abdomen smooth, sixth segment 1.4 times longer than fifth, 1.4 times wider than long, posterolateral angle blunt, slightly produced, posteroventral angle blunt, not produced; pleura of first five segments broadly rounded.

Telson (Fig. 2B–D) 1.6 times as long as sixth abdominal segment, 2.3 times longer than proximal width; lateral margins almost straight, slightly tapering posteriorly; posterior border without median process; two pairs of medium-sized submarginal dorsal spines at 0.20 and 0.54 of telson length; distal and proximal pair of spines of equal

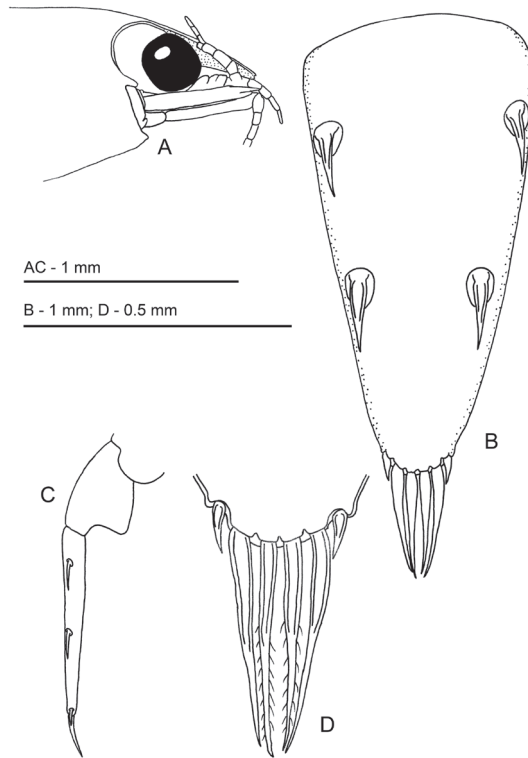


Figure 2. *Odontonia pluellicola* sp. n. ovigerous female PoCL 1.50 mm (RMNH.CRUS.D.53554). **A** anterior appendages, lateral view, setae omitted **B** telson, dorsal view **C** distal part of abdomen, lateral view **D** telson, dorsal view, detail of apex.

length, 0.17 of telson length; posterior margin with three pairs of spines, lateral spines small, marginal, 0.06 times telson length; submedian spines about as long as intermediate spines, lateral spines 0.23 of submedian and intermediate spines; both intermediate and submedian spines approx. 0.75 of dorsal spine length, but more slender.

Eyestalk short, broader than long, slightly broader than diameter of hemispherical cornea.

Antennula (Fig. 3B) with peduncle and flagella short. Basal segment as long as proximal width, with feebly produced distolateral tooth just reaching beyond proximal margin of intermediate segment, anterior margin not developed, oblique; medioventral tooth strongly developed, acute, submarginal, situated halfway basal segment; stylocerite short, reaching halfway basal segment, with acute tip, lateral margin with few plumose setae. Intermediate segment short, broader than long, medial margin with single long distal plumose seta. Distal segment broader than long, upper flagellum short, biramous, with three fused segments; short free ramus one-segmented; longer free ramus with three or four segments. Lower flagellum with four segments; upper ramus carried reflexed beneath lateral rostral carina.

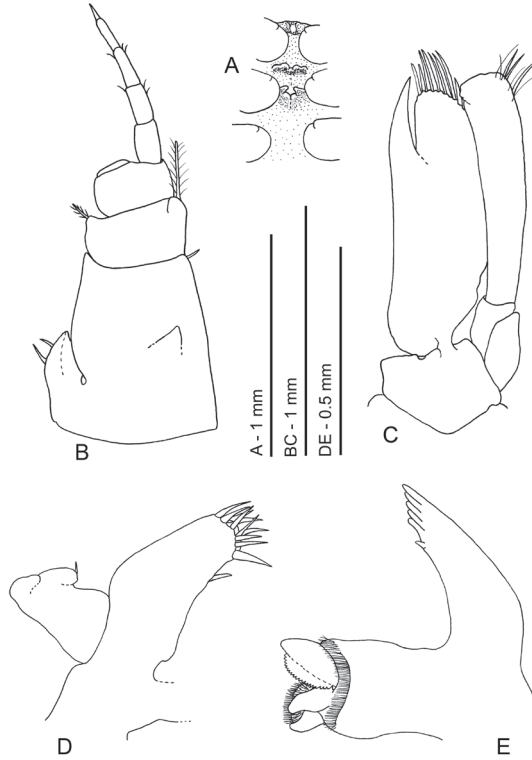


Figure 3. *Odontonia plurellicola* sp. n., ovigerous female PoCL 1.50 mm (RMNH.CRUS.D.53554). **A** second to fifth thoracic sternites **B** antennula, ventral view **C** antenna, ventral view **D** maxillula, ventral view **E** mandible, ventral view.

Antenna (Fig. 3C) with basicerite short, laterally unarmed, with large gland tubercle medially; ischiocerite and merocerite normal; carpo-cerite extending to distal end of distolateral tooth of scaphocerite, rather slender, 4.5 times longer than distal width; flagellum short, slender, nearly as long as postorbital carapace length; scaphocerite with lamina almost twice as long as wide, anterior margin small, rounded, lateral margin broadly convex; distolateral tooth robust, 0.3 length of lamina, reaching beyond lamina, curved medially.

Epistome with rather sharp anterior carina; labrum normal.

Paragnath well developed, alae with broad transverse more or less rectangular distal lobes, and small rounded more or less triangular ventromedial lobes; corpus very short, with shallow median excavation, bordered laterally by non-setose, small, oblique, carinae.

Second thoracic sternite (Fig. 3A) with anterior margin broadly rounded; without median process.

Third thoracic sternite with indistinct shallow lateral carinae.

Fourth thoracic sternite with shallowly developed, medially notched plate formed by the lateral carinae.

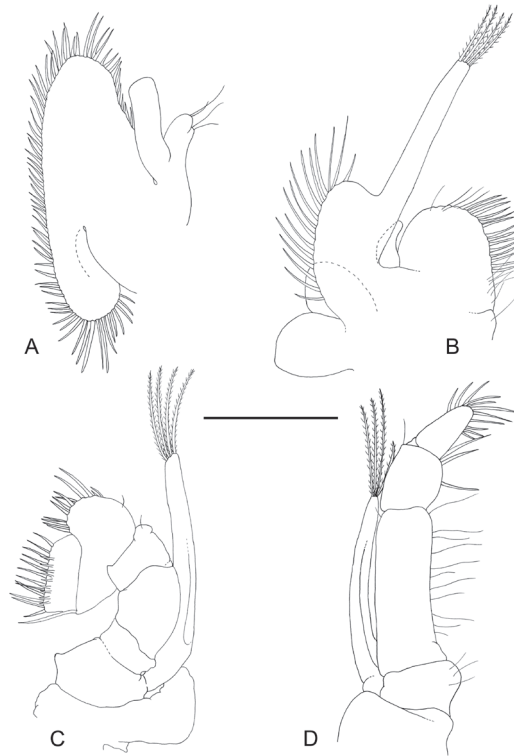


Figure 4. *Odontonia plurellicola* sp. n., ovigerous female PoCL 1.50 mm (RMNH.CRUS.D.53554). **A** maxilla, ventral view **B** first maxilliped, ventral view **C** second maxilliped, dorsal view **D** third maxilliped, ventral view. Scale bar: 1 mm.

Fifth thoracic sternite with well-developed lateral plates with medial broadened deep slit, posteromedial to second pereopod coxae.

Sixth to eight thoracic sternites unarmed, broadening posteriorly.

Mandible (Fig. 3E) with incisor process with five terminal teeth and one large teeth-like ventromedial denticle; molar process robust, with several blunt teeth, some fringed with setal brushes.

Maxillula (Fig. 3D) with upper lacinia rather small, rectangular with about nine distal spines in two rows, with only few simple setae in distal part; lower lacinia lost in dissection; palp feebly bilobed, larger lobe with small ventral tubercle with single short recurved simple seta.

Maxilla (Fig. 4A) with basal endite well developed, bilobate, distal and proximal lobe short, distal lobe with two distal seta of unequal length, proximal lobe with two distal setae; coxal endite obsolete, median margin convex, without setae, scaphognathite large, 2.3 times longer than wide, posterior lobe large, 2.3 as long as anterior width, anterior lobe 1.4 times longer than proximal width; palp simple, subquadrate distally, longer than basal endite, not expanding proximally, without row of plumose setae along lateral margin.

First maxilliped (Fig. 4B) with coxal and basal endite partly fused, broad; basal endite fringed with scattered, rather short simple and finely serrulate setae along median and distal margins; coxal endite convex, separated from basal endite, with few simple setae medially; exopod well developed, flagellum with four plumose setae distally; caridean lobe rather small, narrow; epipod bilobate, lobes rounded; palp simple, rather short, non-setose.

Second maxilliped (Fig. 4C) with endopod short, compact; dactylar segment 2.4 times longer than broad, fringed with short, coarsely serrulate, spiniform, and longer curled, finely serrulate setae medially; propodal segment with row of robust spines and few simple setae along expanded distomedian margin; one seta in distal part of ventrolateral margin; carpal segment short, broader than long, unarmed; meral segment without setae, ischial and basal segments partly fused, without setae, basal part angular produced medially; exopod long, with four long plumose setae distally; coxal segment not medially produced, without setae, with proximally expanded epipod laterally.

Third maxilliped (Fig. 4D) short; with ischiomerus distinct from basis, 2.5 times as long as broad, not tapered distally, somewhat flattened, with row of long simple setae along median margin, lateral margin with few simple setae; basal segment medially convex with few simple setae on medial margin; exopod well developed, reaching just beyond distal margin of ischiomerus, with about four long plumose setae in distal part; coxal segment with small median process, with large lateral plate without setae; without arthrobranch; penultimate segment 1.3 times longer than broad, somewhat flattened, with few long finely serrulate setae ventromedially; ultimate segment slightly shorter than penultimate segment, more slender, with groups of long coarsely serrulate setae ventromedially and distally.

First pereopod (Fig. 5C) stout, exceeding carpocerite with chela and carpus, chela 2.8 times longer than deep, subcylindrical, slightly compressed; fingers as long as palm, stout, with lateral entire cutting edges, with groups of many serrulate setae, tips slightly hooked, suture of unguis visible; carpo-propodal brush present, serrulate setae in distal part of carpus, no setae in proximal part of palm; carpus 1.2 length of chela, 3.7 times longer than distal width, tapering proximally, unarmed, with medially and laterally few simple setae; merus as long as carpus, 3.7 times longer than central width, somewhat bowed, with few simple setae medially; ischium 0.5 times merus length, slightly expanded medially, with few simple setae medially; basis slightly smaller than ischium, with few simple setae medially; coxa with small ventral lobe with few short simple setae.

Second pereopods (Fig. 5A–B) subequal, similar. Chela 0.8 times postorbital carapace length in females, major chela about as long as the postorbital carapace length in females, palm smooth, compressed, without carinae, non-setose; fingers with few simple setae in distal part; dactylus 0.39 of palm length, 3.2 times longer than deep, with low, triangular tooth halfway of cutting edge, distal part of cutting edge entire, tip strongly hooked; fixed finger 1.7 times as long as deep, with broad flattened tooth, separated by shallow notch from triangular, small acute tooth at around midpoint of cutting edge, distal part of cutting edge entire, straight, tip strongly hooked; carpus 0.5 of palm length, 1.5 times longer than distal width, strongly tapering proximally;

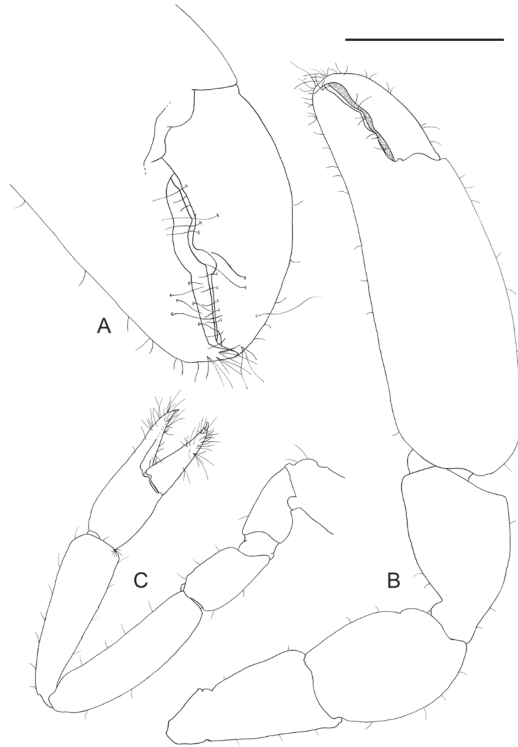


Figure 5. *Odontonia phurellicola* sp. n., ovigerous female PoCL 1.50 mm (RMNH.CRUS.D.53554). **A** major second pereiopod, chela **B** major second pereiopod **C** first pereiopod. Scale bars: 0.5 mm (**A**); 1 mm (**B, C**).

merus as long as carpus, 1.5 times longer than central width, distomedially excavate; ischium slightly shorter than merus, somewhat tapering proximally, with slightly protruded distomedial angle; basis and coxa without special features. Minor cheliped similar, dactylus slightly longer in relation to palm than in major chela; palm less swollen than in major chela.

Ambulatory pereiopods short, stout. Dactylus of third pereiopod (Fig. 6A, B, 16F, 17E) with corpus compressed, 2.2 times longer than proximal width, with about three small proximal ventrally directing teeth, without accessory tooth, with few simple setae along dorsal margin, with row of simple short setae along flexor margin; unguis long and slender, acute, 0.45 of corpus length, without terminal scales; propodus stout, compressed, 3.7 times length of dactylus, 3.7 times longer than deep, with minute lateral distoventral spinules, and distal ventral spinule with sparse simple setae and one plumose distodorsal setae, carpus 0.6 of propodus length, unarmed, merus subequal to propodus length, 2.2 times longer than central depth, unarmed; ischium 0.6 of merus length, slightly tapering proximally; basis and coxa without special features. Fourth and fifth pereiopods similar, but fifth pereiopod (Fig. 6C) with slightly bigger dactylus, with single lateral pectinate spine.

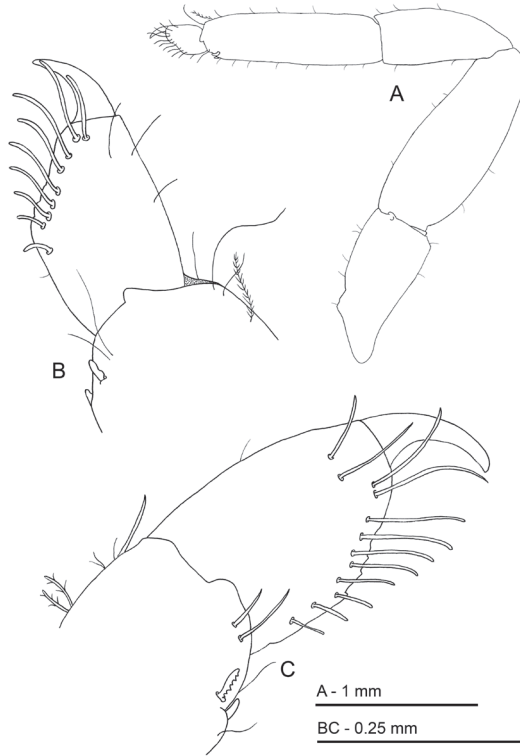


Figure 6. *Odontonia plurellicola* sp. n., ovigerous female PoCL 1.50 mm (RMNH.CRUS.D.53554). **A** third pereiopod **B** dactylus third pereiopod **C** dactylus fifth pereiopod.

First pleopod of female (Fig. 7A) with endopod, more than $1/3$ as long as exopod, with two long plumose distal setae when ovigerous, with two lateral simple setae. Male first pleopod (Fig. 7B) with endopod about three times as long as proximal width, distinctly tapering distally; median margin straight with single simple setae, with few plumose long setae along lateral and distal margin.

Endopod of second pleopod (Fig. 7C) with appendix masculina about $2/3$ length of appendix interna, with three very long setulose setae distally. Uropods (Fig. 7D), with short unarmed protopodite; exopod broad, 2.2 times longer than central width, lateral margin feebly convex, without distolateral tooth, with minute spinule distolaterally; endopod exceeding exopod, about as long as telson, 2.8 times longer than wide.

Number of eggs approximately 11.

Size. This is a small sized species. The maximum PoCL is 1.55 mm in adult females, 1.30 mm in adult males. The minimal PoCL in ovigerous females is 1.50 mm.

Colour in life (Fig. 15A–D). Body with small white chromatophores and scattered larger white spots. Carapace with white chromatophores at base of rostrum and in posterior part, central part without white spots or chromatophores. Laterally covered with white chromatophores and big large white spots. Eyestalks with some big dorsal white

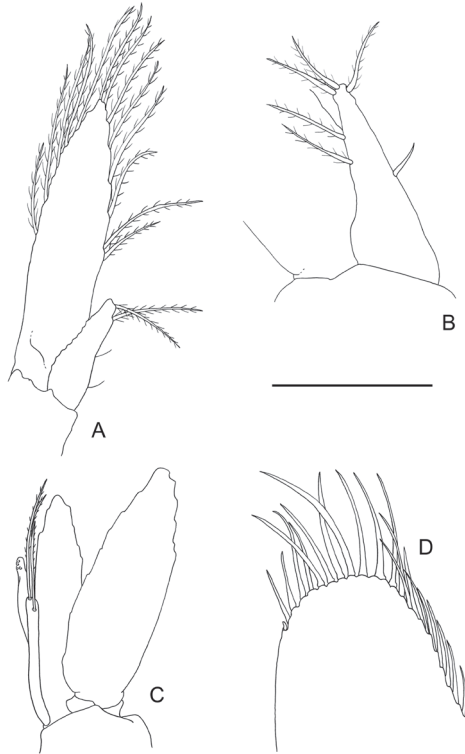


Figure 7. *Odontonia plurellicola* sp. n., ovigerous female PoCL 1.50 mm (**A, D**), male PoCL 1.30 mm (**B, C**) (RMNH.CRUS.D.53554). **A** first pleopod of female with endopod **B** male first pleopod with endopod **C** endopod of second pleopod with appendix masculina and appendix interna **D** detail of left uropod. Scale bars: 1 mm (**A, C, D**); 0.5 mm (**B**).

spots, cornea with white spots. Antennular peduncle with large white spots distally. Pereiopods without small white chromatophores, with white spots at joints. Palm of chela of second pereiopods with scattered white spots. Abdominal pleura with many small white chromatophores and large white spots dorsally and laterally at fixed distances; in dorsal view, each tergum with a transverse row of white spots anteriorly. First abdominal segment covered with large white spots as fixed distances. Tailfan without chromatophores. Thoracical appendages and tailfan appear to be translucent; carapace, eyestalks, corneas and abdominal segments appear to be darker in colour.

Host. Specimens were found inside a colonial ascidian of the genus *Plurella* Kott, 1973 (Plurellidae, Phlebobranchia).

Distribution. Only known from the type locality.

Etymology. The species is named *plurellicola* after the colonial ascidian genus *Plurella* Kott, 1973 in which it was found.

Remarks. The species resembles *O. simplicipes*, known only by the holotype, in morphological characters. It differs from this species in the length and shape of the

rostrum (most notably, *O. simplicipes* has no distal tooth on its rostrum, while *O. plurellicola* bears a small distal tooth), in the size of the ventromedial tooth on the basal segment of the antennular peduncle which is larger in *O. seychellensis* than in the new species, in the distolateral tooth of the basal segment of the antennular peduncle which is well developed in *O. seychellensis* while minute in the new species, in the amount of plumose setae on the three maxillipedes and the antennular peduncle.

Thus far this is the only species of *Odontonia* living inside a colonial ascidian. The ascidian genus *Plurella* has also been recorded as host for *Dactyлонia holthuisi* Fransen, 2002, another symbiotic palaemonid shrimp (Fransen 2002, 2006).

***Odontonia bagginsi* sp. n.**

<http://zoobank.org/2AF91392-9595-4D14-9F1B-C9BDB3BDB954>

Figs 8–14, 15E, 16A, 17A

Material examined. (i) Indo-West Pacific: Indonesia. –1 ovigerous female (**holotype**) PoCL 3.4 mm (MZB Cru 4733, ex RMNH.CRUS.D.53559), N of Desa Rum, Tidore, Ternate, Indonesia, 0°44'35.8"N 127°23'6.3"E, 27 m depth, scuba diving, reef consisting primarily of boulders and soft corals; 4-11-2009; in solitary ascidian (Asc. 67), leg. A. Gittenberger, photo TER.17.0136–39.

Diagnosis. Rostrum as long as antennular peduncle, with strong distoventral tooth. Pterygostomial angle broadly rounded, produced. Basal segment of antennular peduncle with strong, acute medioventral tooth. Distolateral tooth of scaphocerite robust, 0.4 length of lamina. Dactylus of ambulatory pereopods with blunt accessory tooth, perpendicular to flexor margin; flexor margin of corpus with strong, acute forward directed proximal tooth and two small denticles between this tooth and accessory tooth; unguis without terminal scales. Telson with two pairs of medium sized (0.13 of telson length) submarginal dorsal spines at 0.15 and 0.48 of telson length.

Description. Body (Figs 8, 15E) subcylindrical, depressed. Carapace smooth. Rostrum well developed, 0.38 of post-orbital carapace length, without dorsal teeth, as long as antennular peduncle, reaching distal margin of scaphocerite, approximately 2.6 times longer than diameter of hemispherical cornea, with broad shallow indistinct dorsal carina, with acute lateral carinae, with straight ventral carina; with strong distal ventral tooth just extending beyond apex, with few distal setae, bluntly acute in dorsal view, broadened at base. Inferior orbital angle not produced, straight. Antennal spine reduced to blunt protruding process, not separated by notch from inferior orbital angle. Pterygostomial angle of carapace strongly produced, rounded.

Abdomen smooth, sixth segment 1.3 times longer than fifth, 1.4 times wider than long, posterolateral angle blunt, slightly produced, posteroventral angle blunt, not produced; pleura of first five segments broadly rounded.

Telson (Fig. 10A–B) 1.8 times as long as sixth abdominal segment, 2.0 times longer than proximal width; lateral margins almost straight, slightly convex; posterior border without median process; two pairs of medium-sized submarginal dorsal spines



Figure 8. *Odontonia bagginsi* sp. n., ovigerous female PoCL 3.40 mm (MZB Cru 4733). Dorsal aspect. Scale bar: 3 mm.

at 0.15 and 0.48 of telson length; distal and proximal pair of dorsal spines of equal length, 0.13 of telson length; posterior margin with three pairs of spines, lateral spines small, submarginal, 0.06 times telson length; submedian spines slightly longer than intermediate spines, lateral spines 0.20 of submedian and intermediate spines; both intermediate and submedian spines 0.7 of dorsal spine length, but more slender.

Eyestalk short, about as long as broad, as broad as diameter of hemispherical cornea.

Antennula (Fig. 9A–B) with peduncle and flagella short. Basal segment as long as proximal width, with acute produced distolateral tooth just falling short of distal margin of intermediate segment, anterior margin not developed, oblique; medioventral tooth strongly developed, acute, submarginal, situated halfway basal segment; stylocerite short, reaching proximal third of basal segment, distally bluntly acute, lateral margin with few plumose setae. Intermediate segment short, broader than long, medial margin with single long distal plumose seta. Distal segment broader than long, upper flagellum short, biramous, with four fused segments; short free ramus one-segmented; longer free ramus with five segments. Lower flagellum with six or seven segments.

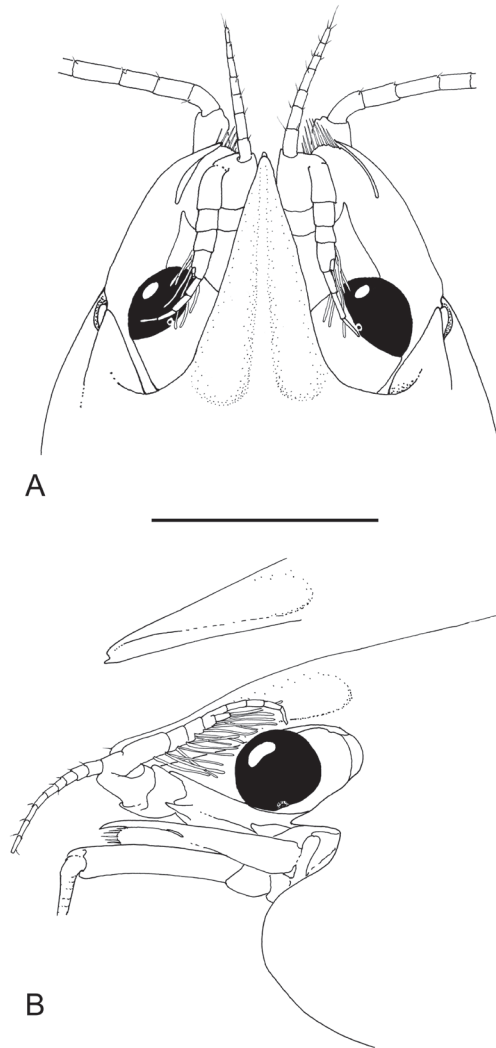


Figure 9. *Odontonia bagginsi* sp. n., ovigerous female PoCL 3.40 mm (MZB Cru 4733). **A** anterior appendages, dorsal view **B** anterior appendages, lateral view. Scale bar: 1 mm.

Antenna (Fig. 9A–B) with basicerite short, laterally unarmed, with large gland tubercle medially; ischiocerite and merocerite normal; carpocerite extending just beyond distal end of distolateral tooth of scaphocerite, rather slender, 4.2 times longer than distal width; flagellum short, slender, about as long as postorbital carapace length; scaphocerite with lamina about twice as long as wide, anterior margin small, rounded, lateral margin broadly convex; distolateral tooth robust, 0.4 length of lamina (incl. distolateral tooth) reaching beyond lamina, curved medially; incision between distolateral tooth and lamina deep.

Epistome anteriorly broadly rounded; labrum normal, oval.

Paragnath well developed, alae with broad transverse more or less rectangular distal lobes, and small rounded more or less triangular ventromesial lobes; corpus very short, with shallow median excavation, bordered laterally by non-setose, small, oblique, carinae.

Second thoracic sternite with anterior margin broadly rounded; without median process forming round tubercle.

Third thoracic sternite with indistinct shallow lateral carinae.

Fourth thoracic sternite with developed, bluntly triangular medial plate without median notch.

Fifth thoracic sternite with well-developed lateral plates with medial broadened deep slit, posteromedial to second pereopod coxae.

Sixth to eight thoracic sternites unarmed, broadening posteriorly.

Mandible (Fig. 10C) with incisor process with five terminal teeth of which larger distalmost is bifid, without ventromedial denticle; molar process robust, with several blunt teeth, some fringed with setal brushed.

Maxillula (Fig. 10D) with upper lacinia broad, rectangular with about 30 spines in two rows in distal half, with many simple setae along entire median margin; lower lacinia slender, acutely pointed upward, with many serrate and simple setae; palp present, but lost in dissection.

Maxilla (Fig. 11A) with basal endite well developed, bilobed, distal lobe broad with about 11 short simple distal setae of unequal length, proximal lobe small with 3 distal setae; coxal endite obsolete, median margin convex, without setae; scaphognathite large, 2.5 times longer than wide; palp simple, longer than basal endite, not expanding proximally, with row of about 4 plumose setae along proximolateral margin.

First maxilliped (Fig. 11B) with coxal and basal endite partly fused, broad; basal endite fringed with dense cover of, long simple and finely serrulate setae along median and distal margins; coxal endite convex, feebly demarcated from basal endite, with few simple setae medially; exopod well developed, flagellum with 6 plumose setae distally; caridean lobe rather small, narrow; epipod bilobate, lobes rounded; palp simple, rather short, non-setose.

Second maxilliped (Fig. 11C) with endopod short, compact; dactylar segment 2.6 times times longer than broad, fringed with short, coarsely serrulate, spiniform, and longer curled, finely serrulate setae medially; propodal segment with row of robust spines and few simple setae along expanded distomedian margin; one seta in distal part of ventrolateral margin; carpal segment short, broader than long, unarmed; meral segment without setae, ischial and basal segments almost completely fused, with few short setae, basal part produced medially; exopod long, with 12 long plumose setae in distal part; coxal segment medially produced, with few simple setae, with proximally expanded epipod laterally.

Third maxilliped (Fig. 11D) short; with ischiomerus distinct from basis, 3.2 times as long as broad, not tapered distally, somewhat flattened, with row of long simple setae along median margin, lateral margin with few simple setae; basal segment medially convex with long simple setae on medial margin; exopod well developed, reaching just halfway penultimate segment, with about 16 long plumose setae in distal part; coxal segment with small median process, with large lateral plate with few short setae;

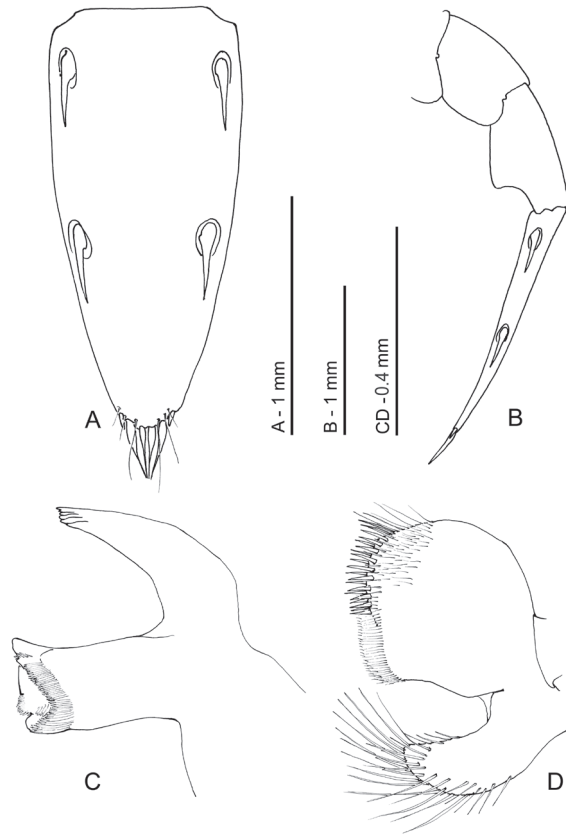


Figure 10. *Odontonia bagginsi* sp. n., ovigerous female PoCL 3.40 mm (MZB Cru 4733). **A** telson, dorsal view **B** telson, lateral view **C** mandible, ventral view **D** maxillula, ventral view.

without arthrobranch; penultimate segment 2.0 times longer than broad, somewhat flattened, with many finely serrulate setae ventromedially; ultimate segment slightly shorter than penultimate segment, more slender, with groups of long coarsely serrulate setae ventromedially and distally.

First pereiopod (Fig. 12A) stout, exceeding carpopocrite with chela and carpus, chela 3.2 times longer than deep, subcylindrical, slightly compressed; fingers as long as palm, stout, with lateral entire cutting edges, with groups of many serrulate setae, tips slightly hooked, suture of unguis distinct; carpo-propodal brush present, serrulate setae in distal part of carpus, and proximal part of palm; carpus 1.2 length of chela, 3.9 times longer than distal width, tapering proximally, unarmed, with simple setae medially and laterally; merus as long as carpus, 4.0 times longer than central width, somewhat bowed, with simple setae medially, short sparse setae dorsally; ischium 0.5 times merus length, slightly expanded medially, with few simple setae medially; basis slightly smaller than ischium, with few simple setae medially; coxa with small ventral lobe with few short simple setae.

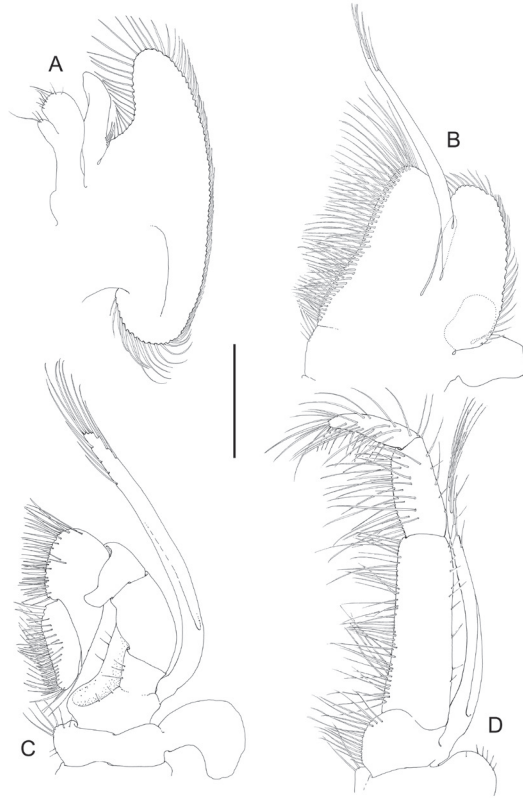


Figure 11. *Odontonia bagginsi* sp. n., ovigerous female PoCL 3.40 mm (MZB Cru 4733). **A** maxilla, ventral view **B** first maxilliped, ventral view **C** second maxilliped, ventral view **D** third maxilliped, ventral view. Scale bar: 0.4 mm.

Second pereiopods (Fig. 12B–C) similar in form, unequal in length. Major right chela 1.8 times postorbital carapace length, palm smooth, compressed, without carinae, with few scattered simple short setae; fingers with few simple setae in distal part; dactylus 0.5 of palm length, 3.3 times longer than deep, with large broad flattened tooth with row denticles at almost halfway of cutting edge, distal part of cutting edge entire, tip strongly hooked; fixed finger 1.9 times as long as deep, with broad flattened tooth in proximal part, separated by shallow notch from acute triangular tooth at about distal third of cutting edge, distal part of cutting edge entire, straight, tip strongly hooked; carpus 0.4 of palm length, about as long as distal width, strongly tapering proximally; merus 1.4 times as long as carpus, 1.2 times longer than central width, distomedially excavate; ischium much shorter than merus, tapering proximally, with slightly protruded distomedial angle; basis and coxa without special features. Minor left cheliped with chela 1.2 times postorbital carapace length, dactylus slightly longer in relation to palm than in major chela; palm less swollen than in major chela.

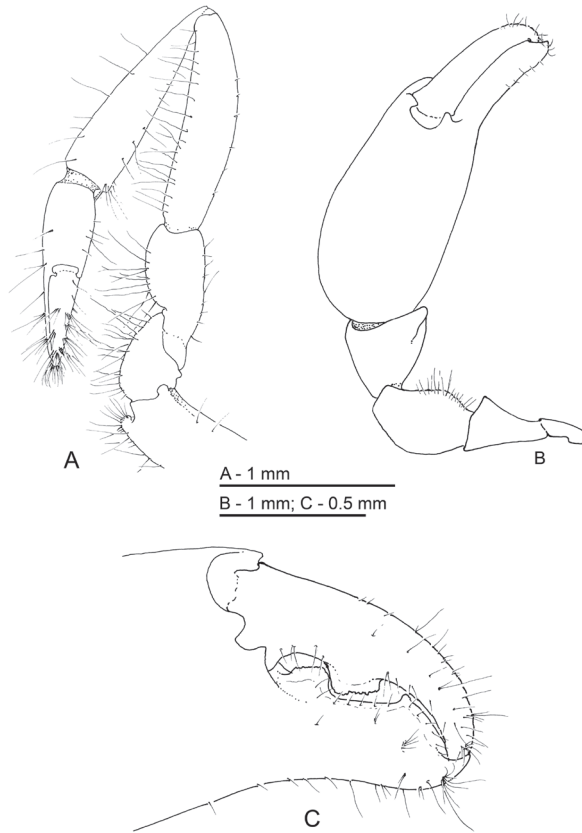


Figure 12. *Odontonia bagginsi* sp. n., ovigerous female PoCL 3.40 mm (MZB Cru 4733). **A** first pereopod **B** major second pereopod **C** major second pereopod, chela.

Ambulatory pereopods short, stout. Dactylus of third pereopod (Figs 13A, 14A–B, 16A, 17A) with corpus compressed, 1.8 times longer than proximal width, accessory tooth terminal, blunt, perpendicular to flexor margin, flexor margin with one large acute forward directed tooth at proximal third, with two small denticles in between proximal tooth and accessory tooth, with few simple setae at distolateral surface, with row of simple short setae along flexor margin; unguis longer than accessory tooth, acute, 0.43 of corpus length, without terminal scales, with faint proximal transverse grooves; propodus stout, compressed, 4.0 times length of dactylus, 4.0 times longer than deep, with minute lateral distoventral spine, and distal ventral spine, with many long simple setae on lateral margin; carpus 0.7 of propodus length, unarmed; merus 1.3 times propodus length, 3.7 times longer than central depth, unarmed; ischium 0.7 of merus length, slightly tapering proximally; basis and coxa without special features. Fourth and fifth (Fig. 13B) pereopods similar.

First pleopod with endopod almost half as long as exopod, with plumose setae laterally and distally, with long simple setae distomedially.

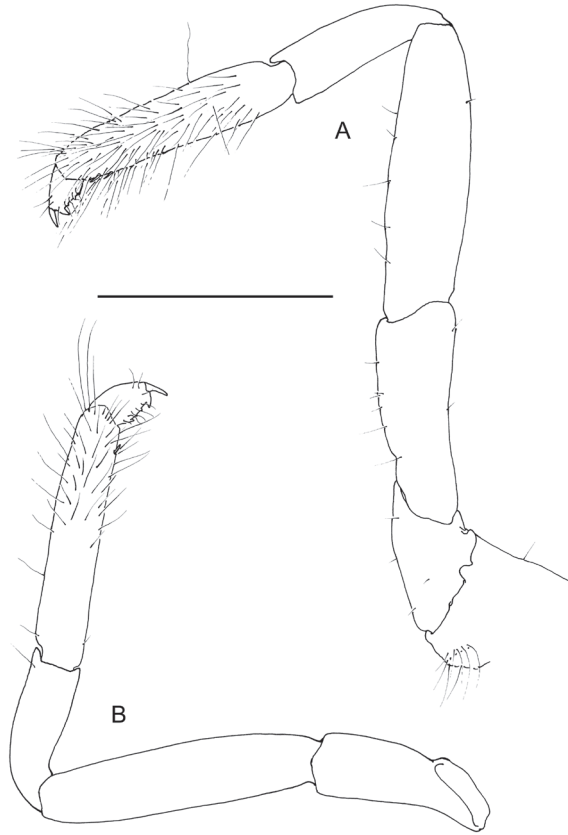


Figure 13. *Odontonia bagginsi* sp. n., ovigerous female PoCL 3.40 mm (MZB Cru 4733). **A** third pereopod **B** fifth pereopod. Scale bar: 1 mm.

Uropods, with short unarmed protopodite; exopod broad, 2.2 times longer than central width, lateral margin feebly convex, without distolateral tooth, with minute spinule distolaterally; endopod exceeding exopod, about as long as telson, 2.8 times longer than wide.

Ovigerous female with about 100 eggs of 0.05 mm in diameter.

Colour in life (Fig. 15E). Body and chelipeds generally semitransparent, with small red chromatophores and scattered larger white spots. Carapace with larger white chromatophores at base of rostrum and scattered in a bilaterally symmetrical pattern. Eyestalks reddish with some big dorsal white spots, cornea with white spots as well. Antennular peduncle and scaphocerite reddish. Ambulatory pereopods translucent with white chromatophores at joints. Abdomen reddish with many small white chromatophores and large white spots dorsally and laterally at fixed distances. Tailfan with red and white chromatophores. Eggs dark red.

Host. Solitary ascidian (A. Gittenberger Asc. 67).

Distribution. Only known from its type locality at Tidore, Indonesia.

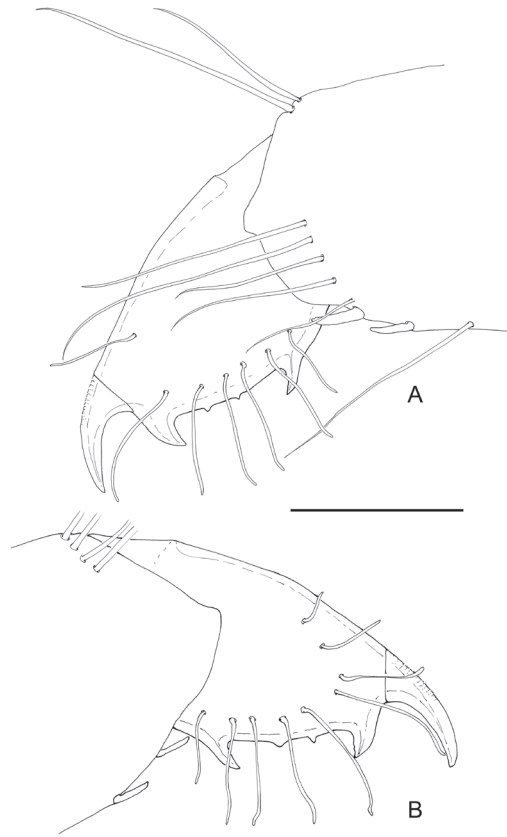


Figure 14. *Odontonia bagginsi* sp. n., ovigerous female PoCL 3.40 mm (MZB Cru 4733). **A** dactylus third pereiopod, medial view **B** dactylus third pereiopod, ventral view. Scale bar: 0.25 mm.

Etymology. The species is named “bagginsi”, inspired by the famous Hobbit family name “Baggins” featured in the “The Hobbit” and “The Lord of the Rings” books. The fictional characters called “Hobbits” possess hairy feet comparable to this species.

Remarks. The species bears resemblance to *O. sibogae* in its morphological characters. It differs in having a strongly developed ventral tooth on the rostrum; a strongly produced pterygostomial margin of the carapace; two pairs of dorsal spines on the telson and a broad upper lacinia of the maxillula. In addition, the pereiopods bear some notable differences: the segments of the first pereiopods are stouter and the cutting edge of the major cheliped bears a broad flattened tooth. The dactyli of the ambulatory pereiopods bear two denticles on the flexor margin. The unguis is devoid of distal scales. Most characteristic is the dense cover of simple setae on the propodi of the ambulatory pereiopods. Life colour patterns of the new species is similar to that of *O. sibogae* (see Levitt & Shenkar 2018: fig. 2B) with scattered white chromatophores of various sizes scattered over body and appendages. The new species has a reddish overall appearance while *O. sibogae* is paler.

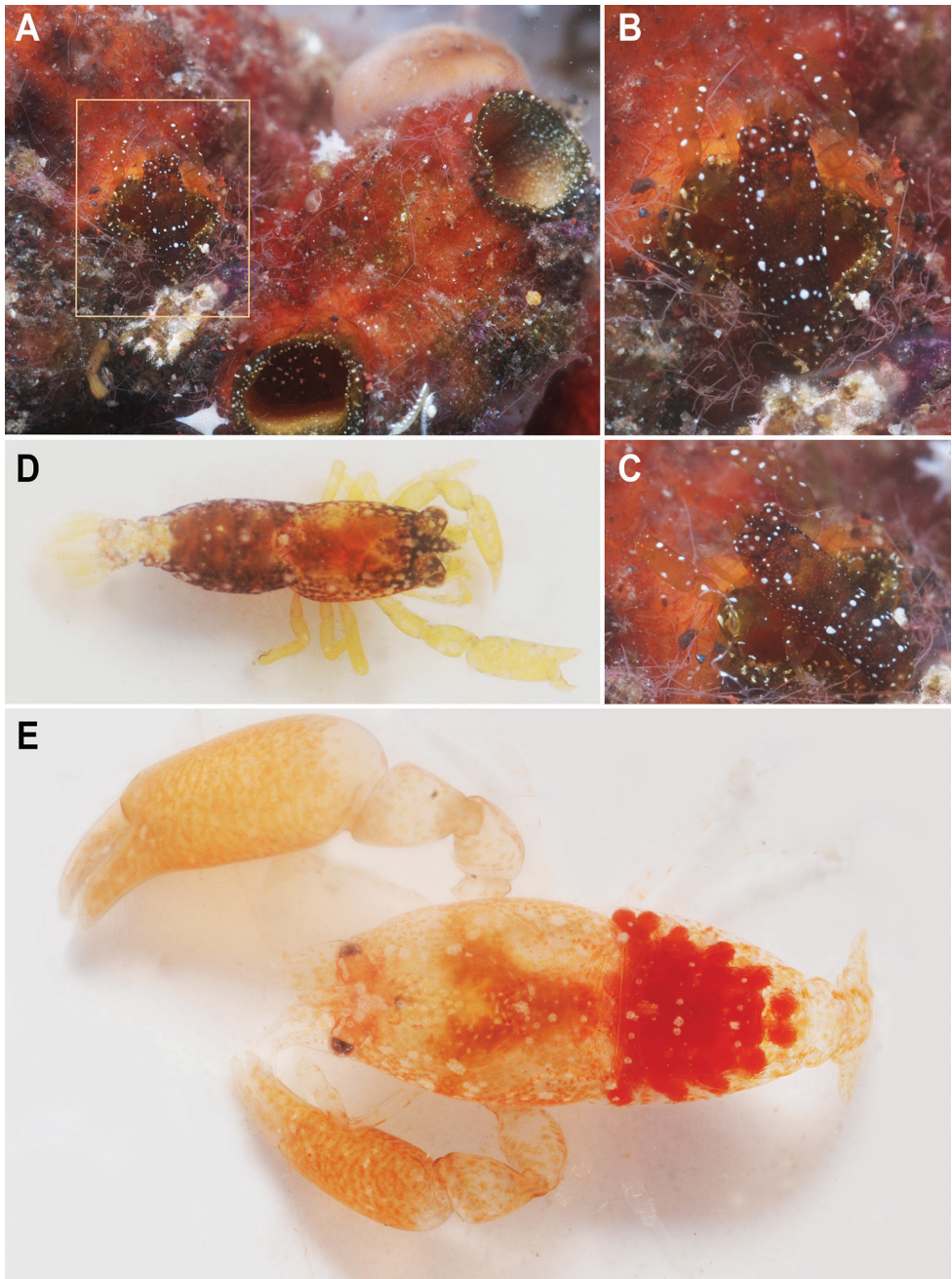


Figure 15. Colour patterns. **A–D** *Odontonia plurillicola* sp. n. (RMNH.CRUS.D.53554). **A–C** individuals inside *Plurella* sp. **D** outside host **E** *Odontonia bagginsi* sp. n. (MZB Cru 4733), outside host.

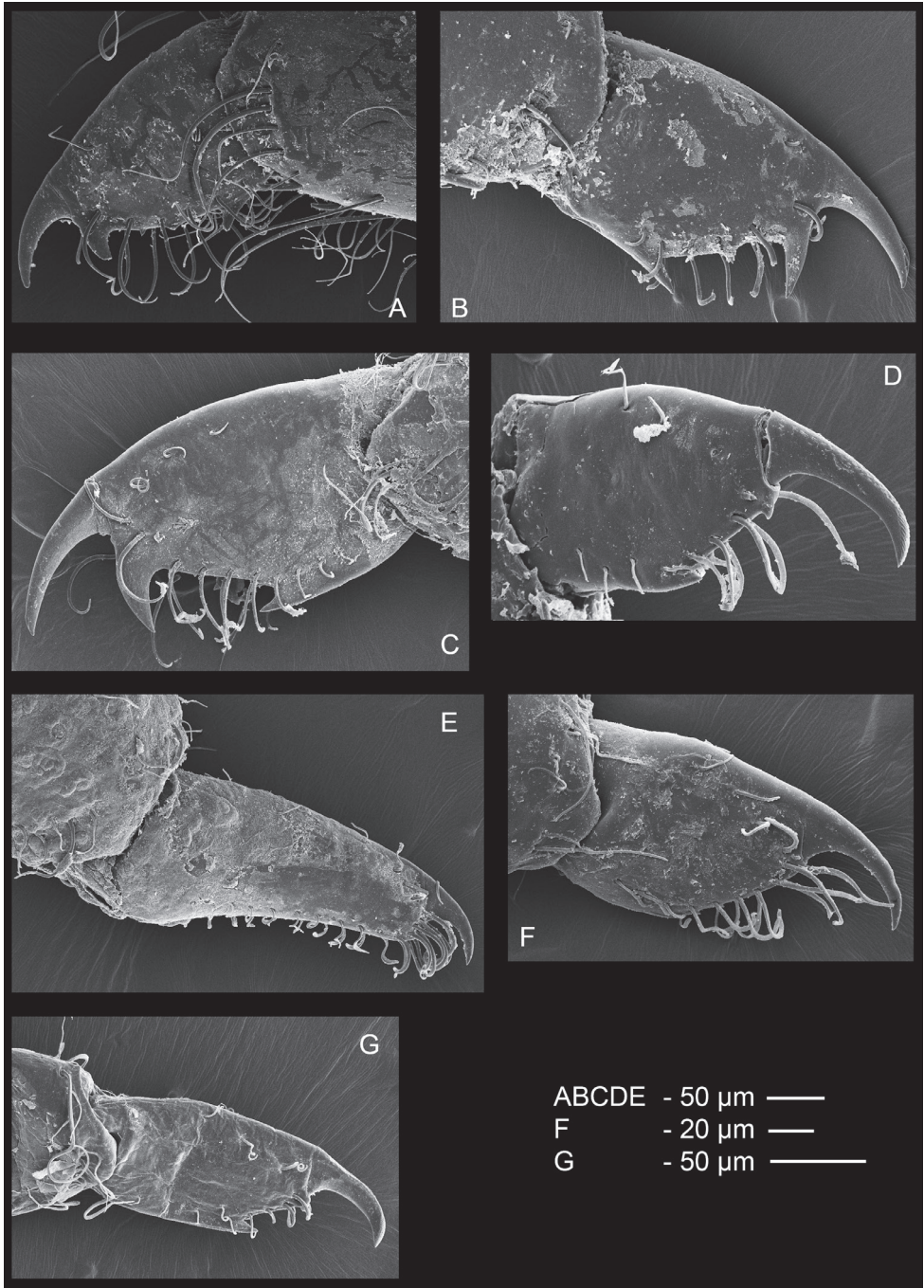


Figure 16. SEM photos dactylus third pereiopod. **A** *Odontonia bagginsi* sp. n. **B** *O. sibogae* (Bruce, 1972) **C** *O. katoi* (Kubo, 1940) **D** *O. rufopunctata* Fransen, 2002 **E** *O. seychellensis* Fransen, 2002 **F** *O. plurellicola* sp. n. **G** *O. maldivensis* Fransen, 2006.

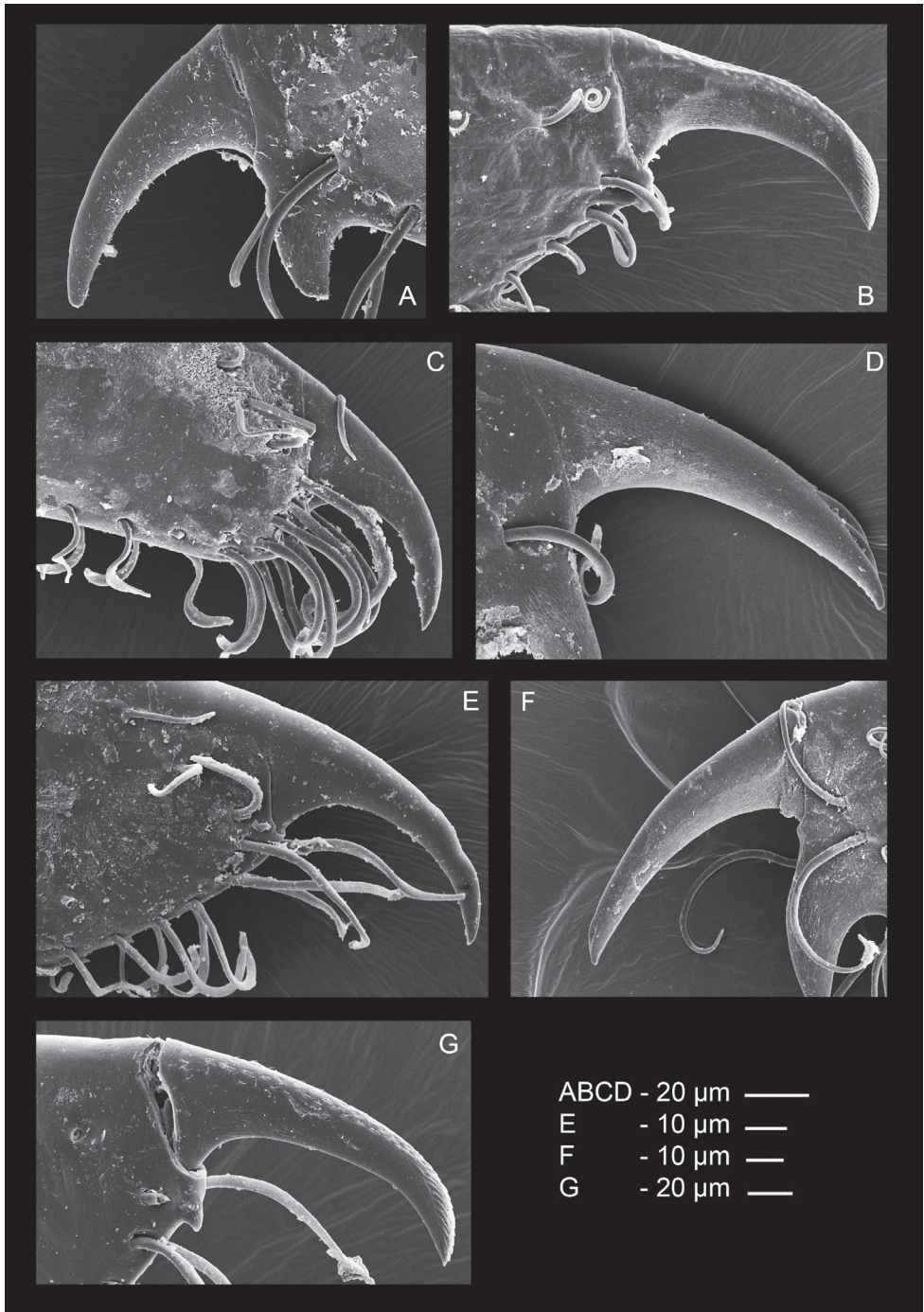


Figure 17. SEM photos unguis of third pereiopod. **A** *Odontonia bagginsi* sp. n. **B** *O. maldivensis* Fransen, 2006 **C** *O. seychellensis* Fransen, 2002 **D** *O. sibogae* (Bruce, 1972) **E** *O. plurellicola* sp. n. **F** *O. katoi* (Kubo, 1940) **G** *O. rufopunctata* Fransen, 2002.

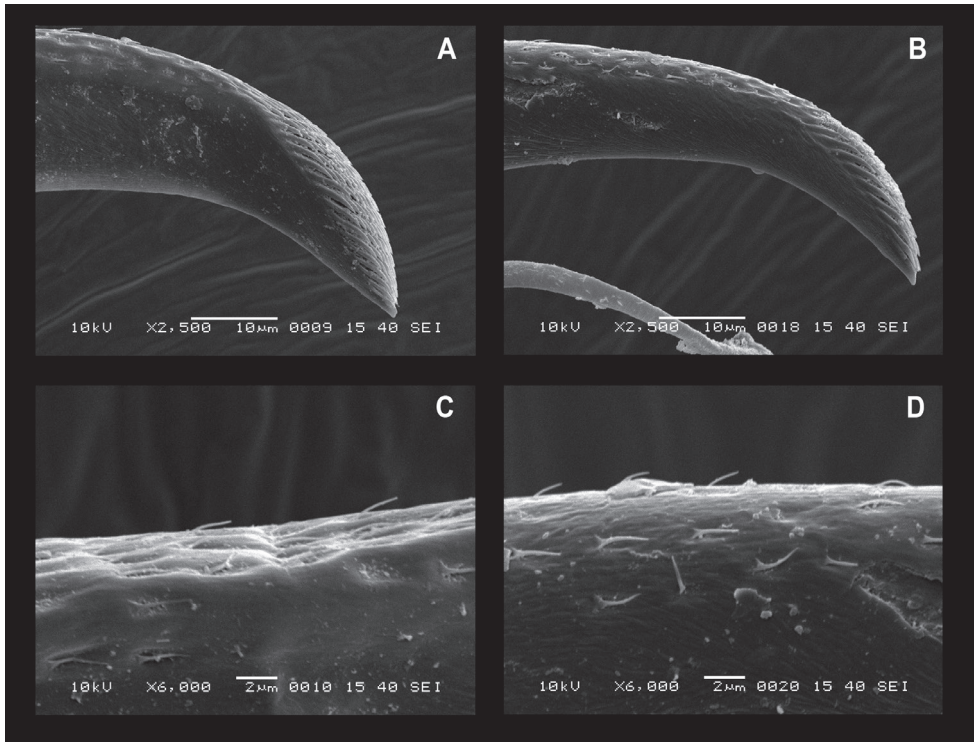


Figure 18. SEM photos details unguis. **A** *Odontonia maldivensis* Fransen, 2002, tip. **B** *O. rufopunctata* Fransen, 2002, tip **C** *O. maldivensis*, dorsal surface **D** *O. rufopunctata*, dorsal surface.

Phylogeny

The morphological phylogenetic analysis (Fig. 19), with *O. maldivensis* not yet synonymised with *O. rufopunctata*, indicates the sister position of *Odontonia plurellicola* sp. n. to *O. simplicipes* as well as the sister position of *O. bagginsi* to *O. sibogae*. *Odontonia maldivensis* and *O. rufopunctata* end up as sister species as well. The resolution in the basal part of the tree is low resulting in a polytomy.

The resulting tree from the incomplete COI dataset (Fig. 20) indicates the sister position of *O. bagginsi* to *O. sibogae* although support values are low. Bootstrap and posterior probability support values in the basal part of the tree are low in the morphological phylogenetic reconstruction.

The resulting tree of the incomplete 16S dataset (Fig. 21) is in line with the COI and morphological phylogenetic reconstructions. The basal branch within the *Odontonia* clade is not well supported. The 16S sequences of *O. maldivensis* and *O. rufopunctata* are similar (genetic distance between 0.012 and 0.092) and end up in the same clade. The genetic distance between the sister species *O. sibogae* and *O. katoi*, for instance, is 0.142.

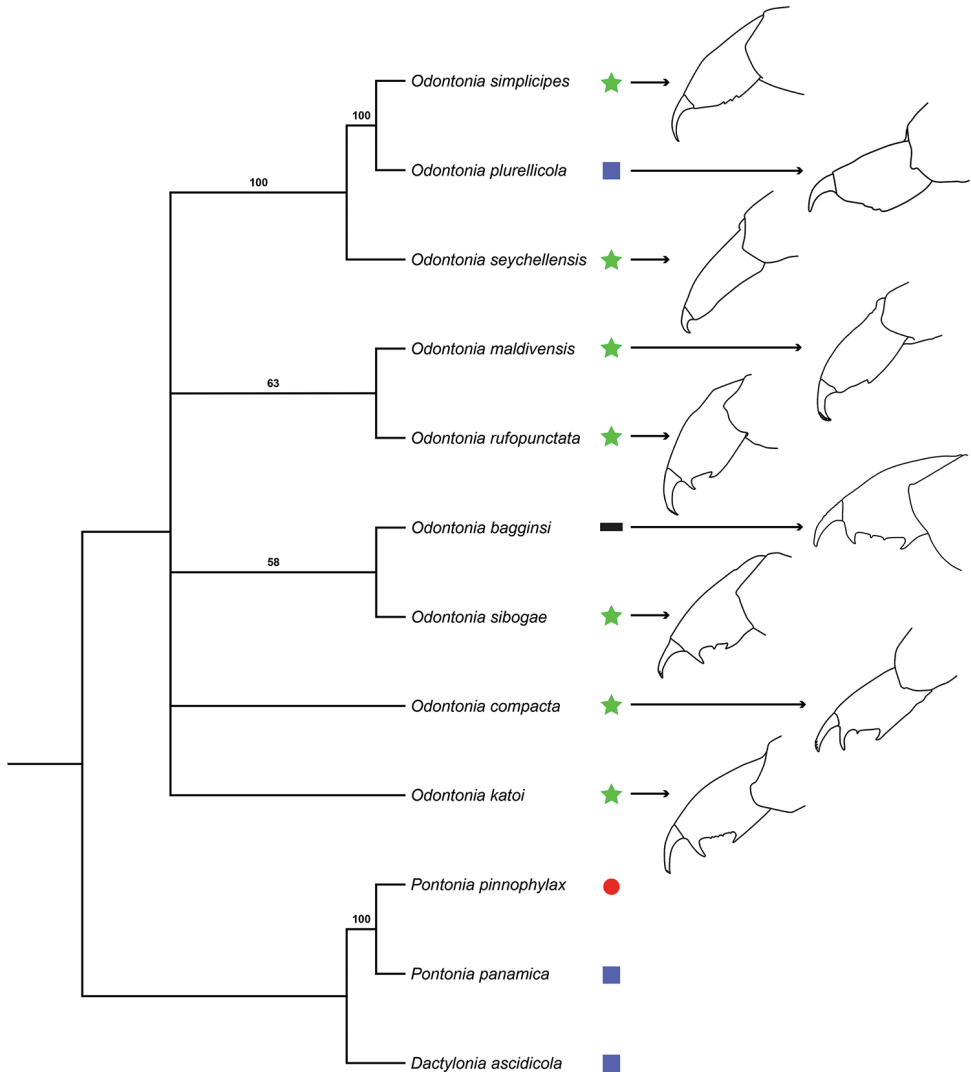


Figure 19. Phylogenetic analysis based on morphological dataset (Table 2). 50% majority-rule tree, CI=0.58. Dactyli of third pereiopods shown for *Odontonia* species, and host group (★: Stolidobranchia, ■: Phlebobranchia, ●: Mollusca, Bivalvia, —: solitary ascidian).

Hosts

Most *Odontonia* species live as endosymbionts in ascidian species in the order Stolidobranchia (Fig. 19). An exception is a single record of *O. sibogae* in the phlebobranch *Rhopalaea* (Fransen 2002). All other records of *O. sibogae* are from stolidobranch hosts (Fransen 2002). The other exception is *O. plurellicola* sp. n., which was found in the phlebobranch *Plurella* species.

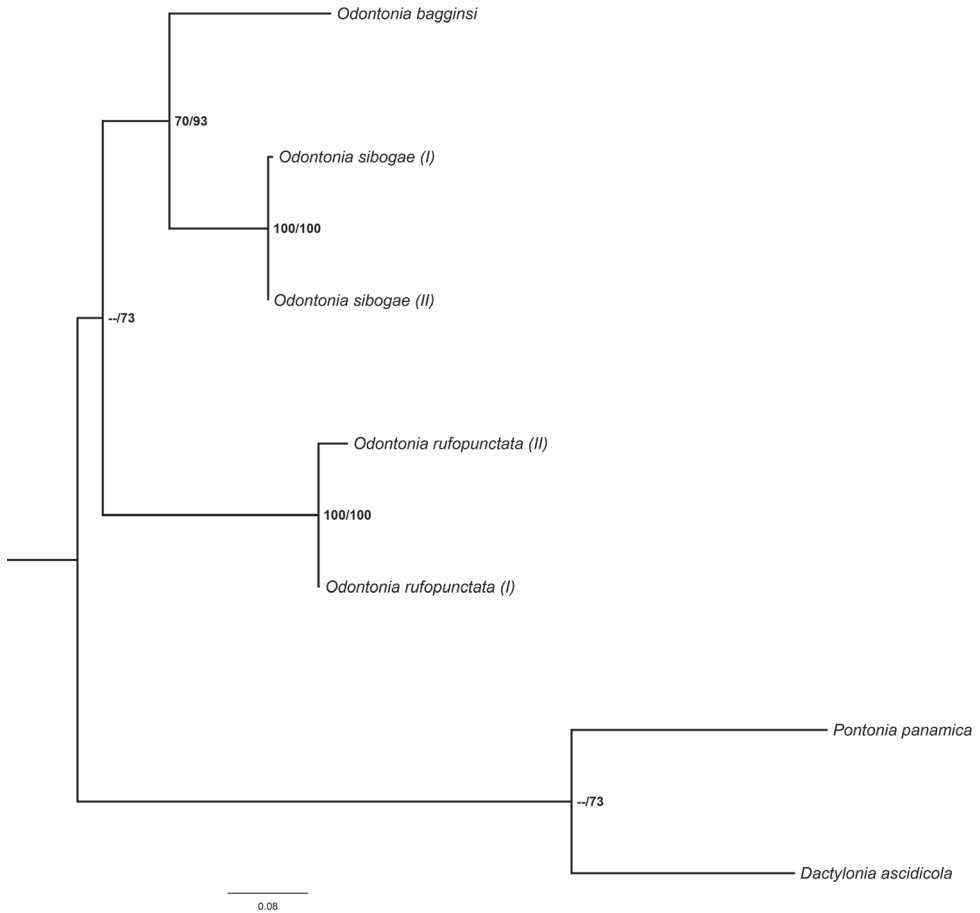


Figure 20. Phylogenetic analysis based on the COI barcoding gene of a subset of *Odontonia* species (Table 1). Maximum likelihood tree with Bootstrap values and Bayesian posterior possibility values respectively.

Discussion and conclusions

Both molecular and morphological phylogenetic analyses show good resolution in the distal part of the tree while basal support is low. The sister position of the species pair *O. sibogae* – *O. bagginsi* in the morphological tree is confirmed by the COI phylogeny. Low support in the basal nodes of the molecular phylogenies might be an effect of the chosen markers. More conservative markers might give better resolution in the basal part of the tree. However, the low support of the basal branches in the molecular trees and the basal polytomy in the morphological phylogeny could also be an indication of a rapid radiation over the host species as was shown for Caribbean sponge-dwelling snapping shrimps *Synalpheus* (Morrison et al. 2004).

The similar 16S sequences of *O. rufopunctata* and *O. maldivensis* as well as their highly similar morphology, indicate that these nominal species actually form one spe-

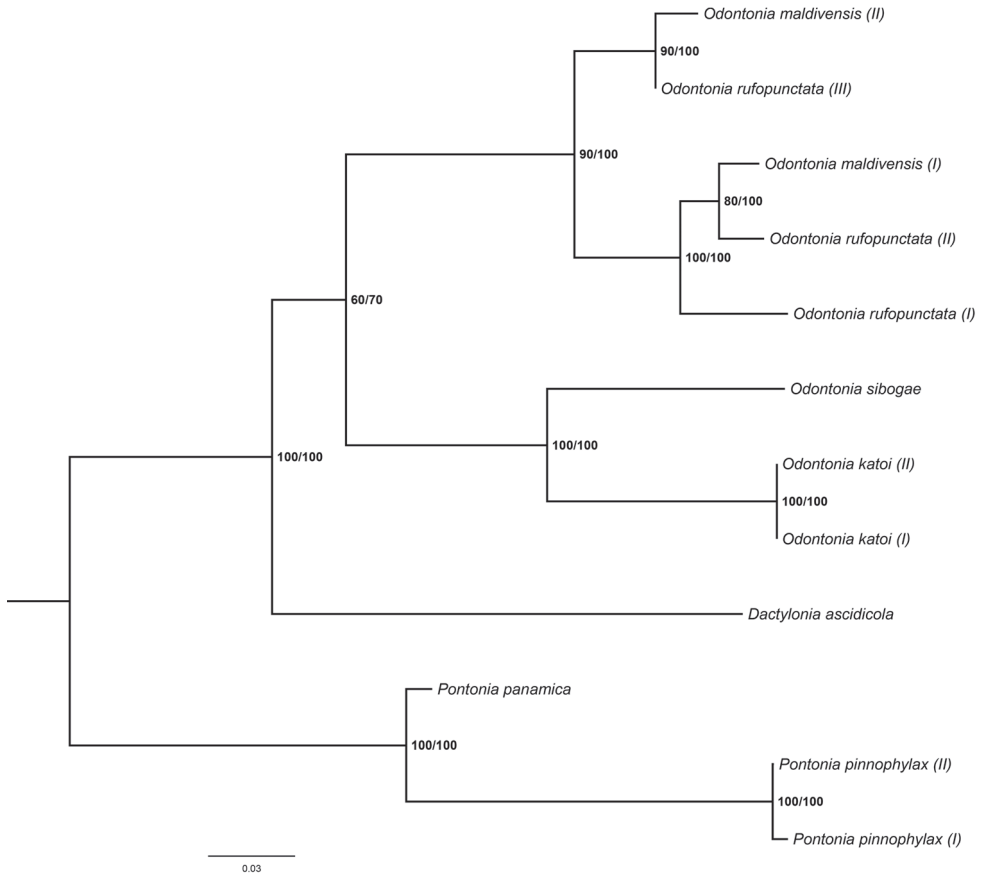


Figure 21. Phylogenetic analysis based on the 16S mitochondrial ribosomal gene of a subset of *Odontonia* species (Table I). Maximum likelihood tree with Bootstrap values (first value) and Bayesian posterior possibility values (second value).

cies. Differences indicated by Fransen (2006) are: 1) the ventral subdistal tooth of the rostrum being absent in *O. maldivensis* while present in *O. rufopunctata*, 2) the unguis of the ambulatory pereopods of *O. maldivensis* (Fig. 18A) has a distal patch with more transverse rows of scales compared to *O. rufopunctata* (Fig. 18B), 3) the distal accessory tooth on the corpus of the dactylus is absent in *O. maldivensis* while present in *O. rufopunctata*, and 4) the dactyli of the second chelipeds have a pile of long simple setae on the dorsal surface in *O. maldivensis* while less setae are present in *O. rufopunctata*. In some specimens of *O. maldivensis*, however, a very small accessory tooth is present on the dactylus of the ambulatory legs (Fig. 17G). A striking character which was observed in both nominal species is the presence of simple short setae implanted in pits on the dorsal surface of the unguis of the ambulatory dactyli (Fig. 18C, D). It seems the morphological differences initially observed by Fransen (2006) might be mere intraspecific variation. *Odontonia maldivensis* Fransen, 2006 is therefore synonymised with *O. rufopunctata* Fransen, 2002.

Several *Odontonia* species (*O. simplicipes*, *O. compacta*, and *O. bagginsi* sp. n.) are only known from a single or few type specimens. Therefore, intraspecific morphological variation is not known and molecular data are not available (except for *O. bagginsi* sp. n.) which hampers the present phylogenetic analyses. When more material of these rare species comes available a more comprehensive phylogenetic analysis can be performed.

Most *Odontonia* species live as endosymbionts in ascidian species in the order Stolidobranchia (Fig. 19) (Fransen 2002). Taxa in this order are characterised by having folded internal structures (branchial sacs). These folded structures probably limit the amount of space the shrimp have inside the ascidian, which could be an explanation for the compact and spineless body of *Odontonia* species. The ascidian associated outgroup species have members of the order Phlebobranchia as their host. The phlebobranch ascidians do not have the stolidobranchial folded branchial sac, which might explain the larger and somewhat less smooth, rounded bodies of these outgroup species. Members of the genus *Plurella* are colonial ascidians, but they do not share a common branchial sac. Shrimp living inside *Plurella* would not be able to move internally from ascidian to ascidian. From the phylogenetic reconstruction of *Odontonia* it can be deduced that *O. plurellicola* switched from a stolidobranch host to a phlebobranch host. Species of *Plurella* have also been recorded as host for the palaemonid shrimp *Dactylonia holthuisi*.

Key to the species of the genus *Odontonia*

- 1 Dactylus of ambulatory pereopods without proximal teeth on flexor margin or with row of few shallow, forward directed teeth; unguis glabrous.....2
- Dactylus of ambulatory pereopods with single large forward directed proximal tooth on flexor margin; distodorsal scales on unguis (except in *O. bagginsi*)..... 4
- 2 Dactylus of ambulatory pereopods with row of few shallow, forward directed teeth on flexor margin.....3
- Dactylus of ambulatory pereopods with flexor margin entire *O. seychellensis*
- 3 Rostrum with distal ventral tooth; distolateral tooth of antennular basal segment slightly exceeding distal margin of segment *O. plurellicola* sp. n.
- Rostrum without distal ventral tooth; distolateral tooth of antennular basal segment reaching distal margin of intermediate segment..... *O. simplicipes*
- 4 Unguis of dactylus of ambulatory pereopods without or with few distal scales (not more than 5); small denticles between accessory and proximalmost tooth 5
- Unguis of dactylus of ambulatory pereopods with patch with many distal scales; no denticles between accessory and proximalmost tooth *O. rufopunctata*
- 5 Rostrum not overreaching antennular peduncle 6
- Rostrum overreaching antennular peduncle 7

- 6 Telson with 2 pairs of dorsal spines; unguis without scales; propodi of ambulatory pereopods with many long simple setae *O. bagginsi* sp. n.
- Telson with 5 pairs of dorsal spines; unguis with few distodorsal scales; propodi of ambulatory pereopods almost devoid of setae *O. sibogae*
- 7 Unguis of dactylus of ambulatory pereopods with two distal scales, and one denticle between accessory and proximalmost tooth *O. compacta*
- Unguis of dactylus of ambulatory pereopods with one distal scale, and (with or without) five small denticles between accessory and proximalmost tooth....
..... *O. katoi*

Acknowledgements

The authors would like to thank Bastian T. Reijnen for his assistance with the SEM, Bertie-Joan van Heuven for her help preparing and coating the pereopods for the SEM, and Livia Oliveira for her help with the ascidian phylogeny.

References

- Brinkmann BW, Fransen CHJM (2016) Identification of a new stony coral host for the anemone shrimp *Periclimenes rathbunae* Schmitt, 1924 with notes on the host-use pattern. *Contributions to Zoology* 85(4): 437–456.
- Bruce AJ (1972) Notes on some Indo-Pacific Pontoniinae, XX. *Pontonia sibogae* sp. nov., a new species of *Pontonia* from eastern Australia and Indonesia (Decapoda Natantia, Palaemonidae). *Crustaceana* 23: 182–186. <https://doi.org/10.1163/156854072X00354>
- Bruce AJ (1996) Crustacea Decapoda: Palaemonoid shrimps from the Indo-West Pacific region mainly from New Caledonia. In: Crosnier A. (Ed.) *Résultats des Campagnes Musorstom*, Vol. 15. *Mémoires du Muséum national d'Histoire naturelle* 168: 197–267.
- De Grave S, Fransen CHJM (2011) Carideorum catalogus: the recent species of the dendrobranchiate, stenopodidean, procarididean and caridean shrimps (Crustacea: Decapoda). *Zoologische Mededelingen* 85: 195–589.
- Farris JS (1970) Methods for Computing Wagner Trees. *Systematic Biology* 19: 83–92. <https://doi.org/10.1093/sysbio/19.1.83>
- Fitch WM (1971) Toward defining the course of evolution: Minimum change for a specific tree topology. *Systematic Biology* 20: 406–416. <https://doi.org/10.1093/sysbio/20.4.406>
- Fransen CHJM (2002) Taxonomy, phylogeny, historical biogeography, and historical ecology of the genus *Pontonia* Latreille (Crustacea: Decapoda: Caridea: Palaemonidae). *Zoologische Verhandlungen* 336: 1–433. <https://doi.org/10.1163/156854008784513483>
- Fransen CHJM (2006) On Pontoniinae (Crustacea, Decapoda, Palaemonidae) collected from ascidians. *Zoosystema* 28: 713–746.
- Hall T (1999) BioEdit: a user-friendly biological sequence alignment editor and analysis program for Windows 95/98/NT. *Nucleic Acids Symposium Series* 41: 95–98.

- Hoeksema BW, Van der Meij SET (2010) Crossing marine lines at Ternate (expedition 2009). Naturalis Biodiversity Center, Leiden, 85 pp.
- Kubo I (1940) Studies on Japanese palaemonoid shrimps. II. Pontoniinae. Journal of the Imperial Fisheries Institute, Tokyo 34: 31–75.
- Larkin MA, Blackshields G, Brown NP, Chenna R, McGettigan PA, McWilliam H, Valentin F, Wallace IM, Wilm A, Lopez R, Thompson JD, Gibson TJ, Higgins DG (2007) Clustal W and Clustal X version 2.0. Bioinformatics, 23: 2947–2948. <http://bioinformatics.oxford-journals.org/content/23/21/2947>. <https://doi.org/10.1093/bioinformatics/btm404>
- Levitt-Barmats Y, Shenkar N (2018) Observations on the symbiotic relationship between the caridean shrimp *Odontonia sibogae* (Bruce, 1972) and its ascidian host *Herdmania momus* (Savigny, 1816). PLoS ONE 13(2): e0192045. <https://doi.org/10.1371/journal.pone.0192045>
- Marin I, Anker A (2008) A new species of *Pontonia* Latreille, 1829 (Crustacea, Decapoda, Palaemonidae) associated with sea squirts (Tunicata, Ascidiacea) from the Pacific coast of Panama. Zoosystema 30: 501–515.
- Morrison CL, Rios R, Duffy JE (2004) Phylogenetic evidence for an ancient rapid radiation of Caribbean sponge-dwelling snapping shrimps (*Synalpheus*). Molecular Phylogenetics and Evolution 30: 563–581. [https://doi.org/10.1016/S1055-7903\(03\)00252-5](https://doi.org/10.1016/S1055-7903(03)00252-5)
- Posada D (2008) jModelTest: Phylogenetic model averaging. Molecular Biology and Evolution 25: 1253–1256. <https://doi.org/10.1093/molbev/msn083>
- Rambaut A (2009) FigTree, a graphical viewer of phylogenetic trees. Institute of Evolutionary Biology University of Edinburgh. <http://tree.bio.ed.ac.uk/software/figtree/>
- Rocha R (2011) Glossary of Tunicate Terminology. Available from: https://www.stri.si.edu/sites/taxonomy_training/future_courses/Biological_glossary_Tunicates.html
- Ronquist F, Huelsenbeck JP (2003) MrBayes 3: Bayesian phylogenetic inference under mixed models. Bioinformatics 19: 1572–1574. <https://doi.org/10.1093/bioinformatics/btg180>
- Swofford DL (2003) Phylogenetic Analysis Using Parsimony. Options 42: 294–307. <https://doi.org/10.1007/BF02198856>
- Tsagkogeorga G, Turon X, Hopcroft RR, Tilak M-K, Feldstein T, Shenkar N, Loya Y, Huchon D, Douzery EJ, Delsuc F (2009) An updated 18S rRNA phylogeny of tunicates based on mixture and secondary structure models. BMC evolutionary biology 9: 187. <https://doi.org/10.1186/1471-2148-9-187>

Appendix I

Character state analysis

Rostrum

1. Ventral teeth: 0, absent; 1, one subdistal; 2, one apical. Character states 0 and 1 are found in the outgroups. An apical tooth (often accompanied by some distal setae) is found in most *Odontonia* species, while a subdistal tooth is found only in the *Pontonia* members of the outgroup. No tooth is found in the outgroup *Dactylonia ascidicola*, in *O. simplicipes* and *O. maldivensis*. (Fig. A1).

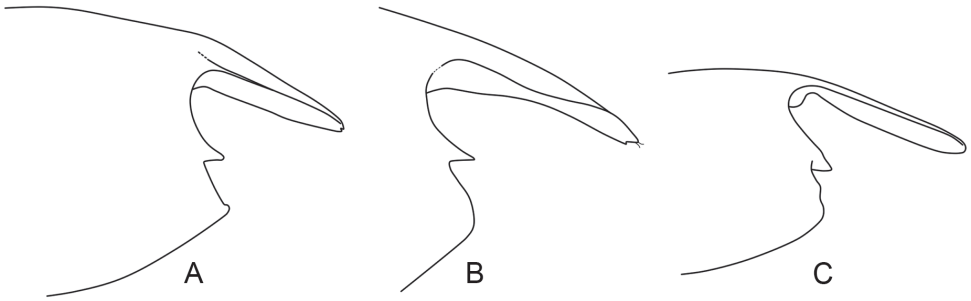


Figure A1. Variety in rostrum morphology and anterolateral angle variety in three *Odontonia* species. Note that A and B have a terminal tooth on the rostrum, while C has no teeth. **A** *O. katoi* (Kubo, 1940) **B** *O. rufopunctata* Fransen, 2002 **C** *O. simplicipes* (Bruce, 1996).

2. Length of rostrum: 0, falling short of antennular peduncle; 1, around the same length as antennular peduncle; 2, overreaching antennular peduncle. A small rostrum is found in all outgroups, while in most *Odontonia* species the rostrum is overreaching, or as long as, the antennular peduncle.
3. Relative size rostrum to post-orbital carapace length: 0, around 0.15 to 0.45 times the PoCL; 1, around 0.75 times the PoCL. All outgroup species, as well as most *Odontonia* species possess a small rostrum-PoCL ratio, while only *O. simplicipes* has a rostrum-PoCL ratio of 0.75.
4. Relative size rostrum to hemispherical diameter of cornea: 0, around 4.0 times the cornea size; 1, around 2.5 to 3.0 times the cornea size; 2, around 2.0 times the cornea size. A rostrum-cornea ratio of 4.0 is found in the outgroup species *Pontonia pinnophylax* (Otto, 1821) and *P. panamica*, while most *Odontonia* species and the other outgroup species have a smaller ratio.

Carapace

5. Anterolateral angle: 0, absent; 1, present. No angle is found in the outgroup species, as well as in *O. rufopunctata* Fransen, 2002 and *O. bagginsi* sp. n. (Fig.A1).

Antennulae

6. Ventromedial tooth basal segment: 0, small; 1, strongly developed; A strongly developed tooth is found in almost all *Odontonia* species (hence the name of the genus), while a small tooth is found in the three outgroup species, and in *O. simplicipes* (Fig. A2).
7. Dimensions of intermediate segment: 0, about as long as wide or slightly broader than long; 1, about twice as long as wide. Most *Odontonia* species share character state 0 with the outgroups. *Odontonia plurellicola* sp. n., *O. simplicipes*, and

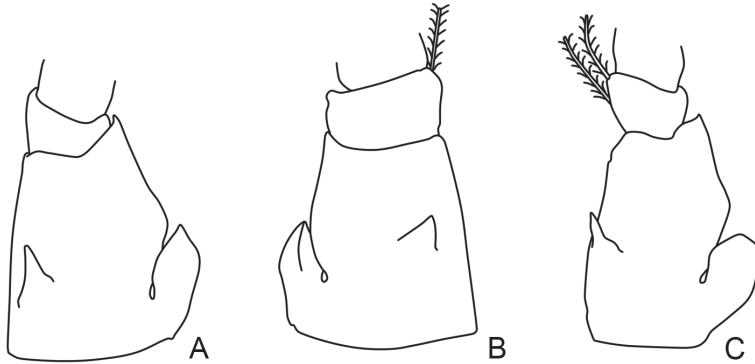


Figure A2. Variety in antennular peduncle. Note the well-developed ventromedial tooth in **A, B, C** and the amount of plumose hairs in **B** and **C**. **A** *O. katoii* (Kubo, 1940) **B** *O. plurellicola* sp. n. **C** *O. sibogae* (Bruce, 1972).

O. seychellensis Fransen, 2002 have a longer intermediate segment. The character is treated ordered in the analysis.

8. Plumose setae on median margin of intermediate segment: 0, two or more setae; 1, one setae; 2, no setae. The specific setae are absent in *Pontonia panamica*, as well as in *O. katoii* (Kubo, 1940) and *O. simplicipes*. The other two outgroup species have two or more setae, and most *Odontonia* species share this trait (Fig. A2).

Mouthparts

9. Maxilla: 0, upper lacinia and lower lacinia both well developed; 1, upper lacinia well-developed, lower reduced; 2, both lacinia almost completely fused. *Dactyлонia ascidicola* is the only species in the analysis with an uneven development of the two lacinia. The other outgroups share both developed lacinia with almost all *Odontonia* species. *Odontonia rufopunctata* has no more distinguishable lacinia, both are almost completely fused.
10. First maxilliped; amount of distal setae on exopod: 0, eight or more setae; 1, five or six setae; 2, four setae. This character is treated as ordered; it is believed that the number of setae decreases in the exopods of *Odontonia* species due to their symbiotic lifestyle in ascidians.
11. Second maxilliped; angle in median margin of basis: 0, absent; 1, distinct angle. Character state 1 is found in two outgroup species, except for *Pontonia panamica*. Most *Odontonia* species do have an angle in the basis, with the exception of *O. maldivensis* and *O. rufopunctata*.
12. Second maxilliped; amount of distal setae on exopod: 0, eight or more setae; 1, five or six setae; 2, four setae. This character is treated as ordered (see character 10).
13. Third maxilliped; amount of distal setae on exopod: 0, eight or more setae; 1, five or six setae; 2, four setae. This character is treated as ordered (see character 10).

Pereiopods

14. First pereiopod; ratio merus/carpus: 0, merus as long as carpus; 1, carpus shorter than merus. Character state 1 is present in outgroup species *Dactylonia ascidicola*, *O. rufopunctata* and *O. bagginsi* sp. n.
15. Third pereiopod; dactylus; teeth on flexor margin: 0, teeth absent; 1, dactylus with simple teeth; 2, dactylus with minutely spinulate blunt tubercles. Character state 2 is only found in *Dactylonia ascidicola*, and character state 0 is found in the two *Pontonia* outgroup species, and in *O. seychellensis* (Fig. A3).
16. Third pereiopod; dactylus; teeth on flexor margin: 0, teeth absent; 1, teeth similar, increasing in size; 2, proximalmost tooth strong, large, directed forward. The teeth of *Dactylonia ascidicola* are very different from the *Odontonia* and *Pontonia* species, hence character state 1. All *Odontonia* with teeth on their flexor margin have one large proximalmost tooth, with or without more teeth following (Fig. A3).
17. Third pereiopod; dactylus, unguis: 0, distal scales absent; 1, unguis with fewer than five distal scales; 2, unguis with more than five distal scales. Scales are absent in the two *Pontonia* outgroup species, as well as in *O. seychellensis*, *O. simplicipes*, *O. plurellicola* sp. n., and *O. bagginsi* sp. n. The species *O. maldivensis* and *O. rufopunctata* have more than five distal scales (Fig. A3). This character is treated as ordered, the amount of distal scales is believed to increase the further a species is located from the outgroups.
18. Third pereiopod; dactylus; dimensions of corpus: 0, more than 2.0 times as long as broad; 1, less than 2.0 times as long as broad. *Dactylonia ascidicola*, *Pontonia panamica* and *O. seychellensis* all share a dactylus that is more than 2.0 times as long as broad (Fig. A3).
19. Third pereiopod; dactylus; accessory tooth: 0, present; 1, absent. Most *Odontonia* species, as well as the outgroup species, possess an accessory tooth on the distal flexor margin. *Odontonia seychellensis*, *O. simplicipes*, *O. maldivensis* and *O. plurellicola* sp. n. all have no accessory tooth (Fig. A3).
20. Third pereiopod; dactylus; additional forward-pointing teeth distal from proximalmost tooth: 0, absent; 1, two additional forward-pointing teeth. Only *O. simplicipes* and *O. plurellicola* sp. n. possess the two additional teeth (Fig. A3).
21. Third pereiopod; dactylus; denticles between accessory and proximalmost tooth: 0, absent; 1, one, two or five denticles in flexor margin. *Odontonia sibogae* and *O. compacta* are the only ones with one denticle. *Odontonia bagginsi* sp. n. has two denticles. *Odontonia katoi* is the only species with accounts of there being a row of five denticles on the flexor margin, but often these denticles are not visible or not present. The outgroup *Dactylonia ascidicola* has broad denticles considered not homologous with the ones from *Odontonia* (Fig. A3). This character is treated as ordered.

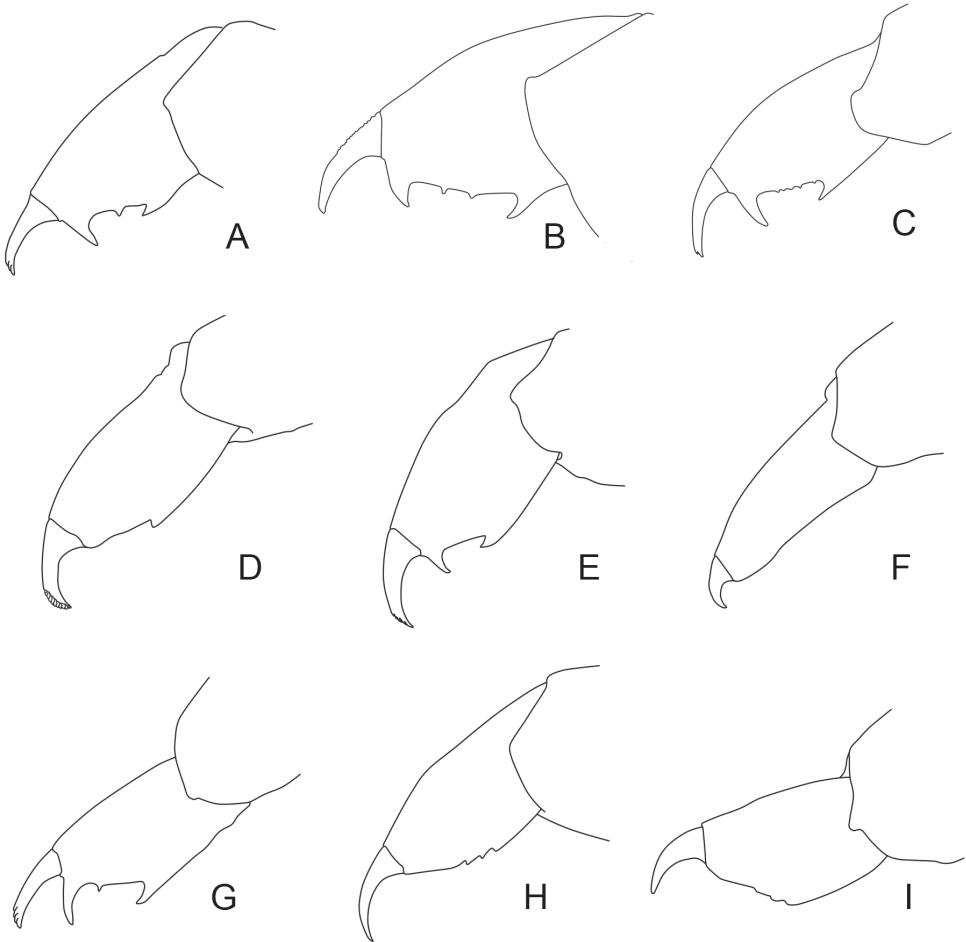


Figure A3. Variety in dactylar morphology of all currently known *Odontonia* species (setae omitted). Note the amount of distal scales, presence of an additional and accessory tooth, size of the dactylus, and the presence of denticles. **A** *O. compacta* (Bruce, 1996) **B** *O. bagginsi* sp. n. **C** *O. katoi* (Kubo, 1940) **D** *O. maldivensis* Fransen, 2006 **E** *O. rufopunctata* Fransen, 2002 **F** *O. seychellensis* Fransen, 2002 **G** *O. sibogae* (Bruce, 1972) **H** *O. simplicipes* (Bruce, 1996) **I** *O. plurellicola* sp. n.

Telson

22. Position of distal pair of dorsal spines over telson length: 0, at about 1/2; 1, at about 2/3; 2, in distal 1/4. Character state 0 is present in *Dactyлонia ascidicola* and in *O. bagginsi* sp. n. The species *O. compacta* has the distal spines implanted in the most distal 1/4th of the telson length. In *O. sibogae* there are more than four spines implanted in the dorsal telson side. It is not sure which spines are homologous with the

four spines in other species, hence the “?” in the dataset. This character is treated as ordered; it is believed the spines migrate more distally in the evolution of the shrimp.

Length of post-orbital carapace length

23. Maximum PoCL of male specimens: 0, PoCL longer than 5.5 mm; 1, PoCL between 5.5 and 2.0 mm; 2, between 2.0 and 0.5 mm. Depending on the availability of the specimens a “?” may be given to missing character states.
24. Maximum length of female specimens: 0, PoCL longer than 5.5 mm; 1, between 5.5 and 2.0 mm; 2, between 2.0 and 0.5 mm. Depending on the availability of the specimens a “?” may be given to missing character states.